

UNIVERSIDADE DE BRASÍLIA
FACULDADE DE MEDICINA
PROGRAMA DE PÓS-GRADUAÇÃO EM PATOLOGIA TROPICAL

TESE DE DOUTORADO

Caracterização e análise da expressão de microRNAs-like
de *Paracoccidioides brasiliensis*

JULIANA SANTANA DE CURCIO

Brasília-DF
2018



UNIVERSIDADE DE BRASÍLIA
FACULDADE DE MEDICINA
PROGRAMA DE PÓS-GRADUAÇÃO EM PATOLOGIA MOLECULAR

Juliana Santana de Curcio

CARACTERIZAÇÃO E ANÁLISE DA EXPRESSÃO DE microRNAs-like *DE*
Paracoccidioides brasiliensis

Tese apresentada ao Programa de Pós-Graduação em Patologia Molecular da Universidade de Brasília como requisito para obtenção do Título de doutor em Patologia Molecular.

Orientadora: Prof. Dra. Célia Maria de Almeida Soares

Brasília-DF
2018

Banca examinadora

Titulares:

Dra. Célia Maria de Almeida Soares- Presidente da banca.
Instituto de Ciências Biológicas-UFG

Dra. Maristela Pereira
Instituto de Ciências Biológicas-UFG

Dra. Isabela Marques Dourado
Instituto de Ciências biológicas-UNB

Drº André Correa Amaral-UFG
Instituto de Patologia Tropicã e Saúde Pública-IPTSP

Suplente: Drº Sébastien Olivier Charneau
Instituto de Ciências biológicas-UNB

Data: 02/04/2018

Até aqui nos ajudou o Senhor!
1 Samuel 7:12

Agradecimentos

A Deus, pela oportunidade que me foi dada, pelo dom da minha vida e por toda força durante minhas batalhas!

À professora Dra. Célia Maria de Almeida Soares, pela paciência e confiança durante os quatro anos de desenvolvimento da tese de doutorado, agradeço infinitamente as oportunidades que a senhora me concedeu. Além do grande desenvolvimento profissional e pessoal. Admiro muito sua competência e profissionalismo!

Aos professores Juliano D. Paccez e Evandro Novaes, por toda contribuição científica para o desenvolvimento da tese, ambos contribuíram imensamente para execução deste projeto.

Aos professores do Laboratório de Biologia Molecular, da Universidade Federal de Goiás, Maristela Pereira, Alexandre Bailão, Clayton Borges, Juliana Parente por trabalharem em conjunto com o objetivo de manter um laboratório de pesquisa funcional frente a condições tão adversas de trabalho.

Aos professores da pós-graduação em Patologia Molecular da Universidade de Brasília, por fornecer um curso tão estruturado, além de ministrar disciplinas extremamente interessantes em diferentes áreas da pesquisa. Muito obrigado por toda a contribuição profissional e para o meu desenvolvimento como uma estudante de doutorado. Agradeço também aos funcionários da secretária de pós-graduação em Patologia Molecular.

Agradeço infinitamente aos meus pais por todo apoio em minha vida pessoal e profissional, as lutas durante os meus estudos culminaram agora na realização de nossos sonhos: Finalizar minha tese de doutorado!

Ao meu Marido Vitor Magalhães Rezende, por ser um grande apoio e conforto durante essa minha jornada. Sua presença foi essencial para realização dos meus sonhos.

Agradeço também as minhas irmãs Wanessa e Alessandra, vocês foram fundamentais durante os meus estudos de mestrado e doutorado, o apoio de vocês foram essenciais para vencer todas as dificuldades durante essa jornada. Além delas agradeço toda felicidade proporcionada pelos meus sobrinhos Maria Eduarda, Rafael e Tiago. E pelo apoio dos meus cunhados Rodrigo e Eric.

Agradeço os amigos UNB together Danielle Araújo, Lucas Nojosa e Marielle Garcia, as dificuldades enfrentadas durante as idas e vindas de Brasília foram muito mais suave devido a pela presença de vocês. Todos os meus momentos de desânimo, cansaço só foram

superados devido ao apoio que vocês me deram. Então a minha vitória também é de vocês. Agradeço muito a Deus por ter colocados amigos tão especiais em minha vida!

Também agradeço infinitamente aos amigos do LBM Lívia do Carmo, por todas as risadas, brincadeiras, ajuda e por toda amizade durante todos os anos que estive no LBM. A Mariana Pedrosa pela ajuda e amizade. Também agradeço aos amigos Igor, Guilherme Petito, Kleber Santiago, Amanda, Raisal, Edilânia, André, Santiago por todos os bons momentos passados juntos e a todos os meus outros amigos e companheiros do LBM.

A Luciana Casaletti, Patrícia Lima, Mirelle Garcia e Elisa Flávia, por todo conhecimento profissional e amizade.

À CAPES pelo importante financiamento do meu doutorado.

Aos órgãos financiadores, MCTI/CNPq (Ministério da Ciência e Tecnologia/Conselho Nacional de Desenvolvimento Científico e Tecnológico), FNDCT (Fundo Nacional de Desenvolvimento Científico e Tecnológico), FAPEG (Fundação de Amparo à Pesquisa do Estado de Goiás) e FINEP (Financiadora de Estudos e Projetos) pelo apoio financeiro para o desenvolvimento dos projetos.

SUMÁRIO

CAPÍTULO 1	
1. INTRODUÇÃO	17
1.1 Características dos microRNAs e Biogênese	17
1.2 Descrição e função de microRNAs-like em fungos	22
1.3 MicroRNAs e interação patógeno-hospedeiro	23
1.4 <i>Paracoccidioides</i> spp.	25
1.5 Classificação filogenética de fungos do complexo <i>Paracoccidioides</i>	27
1.6 Paracoccidioidomicoses (PCM)	29
1.7 Transição dimórfica no complexo <i>Paracoccidioides</i>	32
2. JUSTIFICATIVA	37
3. OBJETIVO	38
3.1 Objetivo geral	38
3.2 Objetivos específicos	38
CAPÍTULO 2	
Artigo submetido na revista GMB: In silico characterization of microRNAs-like sequences in the genome of <i>Paracoccidioides brasiliensis</i> Pb18	39
CAPÍTULO 3	
Regulation of the morphogenesis, cell wall synthesis and energy production, mediated by microRNAs-like produced in yeast, mycelium and during the dimorphic transition in <i>Paracoccidioides brasiliensis</i> .	150
CAPÍTULO 4	
DISCUSSÃO	192
CONCLUSÃO	199
PERSPECTIVAS	200
REFERÊNCIAS	201
ANEXO: COLABORAÇÃO EM ARTIGO	210

LISTA DE FIGURAS E TABELAS

CAPÍTULO 1

Figura 1- Via canônica para produção de microRNAs em plantas e mamíferos.

Figura 2-Diagrama representativo das quatro vias de produção de microRNAs-like em *N. crassa*.

Figura 3-Características microscópicas de *Paracoccidioides* spp.

Figura 4-Ciclo biológico hipotético de *Paracoccidioides* spp.

Figura 5-Distribuição geográfica de espécies filogenéticas do gênero *Paracoccidioides*.

Figura 6-Manifestações clínicas da Paracoccidioidomicose (PCM).

CAPÍTULO 2

Table 1. *In silico* prediction of proteins potentially involved in post-transcriptional gene silencing machinery in *Paracoccidioides* spp.

Figure 1- Domains identified in proteins involved post-transcriptional gene silencing pathway.

Figure 2-Genes involved in the processing of microRNAs-like are induced in the parasite phase of *Pb18*

Table 2. Potential miRNAs-like identified in the genome of *P. brasiliensis* *Pb18*.

Figure 3- Representation of the newly-identified potential pre-miRNAs in *P. brasiliensis*.

Table 3. Characteristics of miRNAs-like predicted in this study.

Figure 4- Qualitative RT-PCR of microRNAs-like predicted by bioinformatics tools.

Supplementary table 1. Access number of the proteins used to construct the phylogenetic trees.

Supplementary table 2. Oligonucleotide sequences used in the present study.

Supplementary table 3. Identified miRNAs-like homologues to other fungi species, in the genome of *Paracoccidioides brasiliensis* Pb18.

Supplementary table 4. Identification of miRNAs-like described in fungi vesicles with identity in the genome of *P. brasiliensis* Pb18.

CAPÍTULO: 3

Figure 1- Analysis of expression of genes involved in post-transcriptional gene silencing.

Figure 2- Heat map of differentially expressed microRNAs-like. The differentially expressed miRNAs-like are those with values of $p_{adj} < 0.05$.

Figure 3- Predicted targets for microRNAs-like, that were induced in the yeast phase.

Table 1- MicroRNAs-like identified in all the libraries.

Table 2- MicroRNAs-like with the highest values in the yeast libraries.

Table 3- Biological process regulated by microRNAs-like induced in yeast cells.

Supplementary Figure 1- Work flow chart. Stages for characterization of microRNAs-like in mycelial, dimorphic transition and yeast cDNA libraries.

Supplementary Figure 2- Yeast cells appearing at the transitional times of *Paracoccidioides brasiliensis* Pb18. Mycelia was transferred from 22°C to 36°C and aliquots were taken at different times to count the number of yeast cells in the culture

Supplementary figure 3- Distribution of Phred quality score of sequences from the library M1_raw.fg. The majority of the sequences presented Phred score > 30 .

Supplementary Figure 4- Secondary structure of microRNAs-like identified among **libraries**. The secondary structure of the microRNAs-like and the negative free energy values were predicted by the RNA fold tool.

Supplementary Figure 5- Biological processes regulated by microRNAs-like of *P. brasiliensis* Pb18

Supplementary Table 1- Number of sequences obtained and percentage of sequences eliminated after removal of the adapters with the Trimmomatic program.

Supplementary table 2- Differentially expressed microRNAs-like between the mycelial and transition libraries.

Supplementary table 3- Differentially expressed microRNAs-like between the mycelium and yeast libraries.

Supplementary table 4- Differentially expressed microRNAs-like between the transition and yeast libraries.

LISTA DE ABREVIATURAS

AGO: Proteína Argonauta

DCL: Proteína Dicer

miRISC: Complexo de silenciamento induzido pelo microRNA maduro

miRNA*: microRNA estrela

ncRNA: RNA não codificador

miR ou miRNA: (microRNA) maduro

DNA: ácido desoxirribonucleico

RNA: Ácido ribonucleico

pre-miRNA: microRNA precursor

pri-miRNA: microRNA primário

piRNA: RNA de interação com a proteína Piwi

RdRP: RNA polimerase dependente de RNA

3'-UTR: região 3' não traduzida do RNAm

5'-UTR: região 5' não traduzida do RNAm

***Pb/P.lutzi* (01,03,18):** Isolados (01,03 e 18) de *Paracoccidioides* spp.

cDNA: DNA complementar

Exp-5: Exportina 5

MFE: Energia mínima livre

MFEI: Índice de energia livre mínima

AMFE: Menor energia mínima ajustada

D-bodies: corpúsculos (nucleares de processamento)

dsRNA: RNA dupla fita

g: aceleração da gravidade

g: grama

µg: micrograma

mM: Milimolar

M: molar

h: horas

Poli-A: polímero de adenosina monofosfato

RT: Transcrição reversa

RT-PCR: Transcrição reversa seguida pela reação em cadeia da DNA polimerase

RT-qPCR: Transcrição reversa seguida pela reação em cadeia da (DNA) polimerase, de natureza quantitativa

NGS: Sequenciamento de ultima geração

mRNA: RNA mensageiro

siRNA: RNAs de interferência

tRNA: RNA transportador

rRNA: RNA ribossomal

QDE: defectivo para repressão

NCBI: National Center of Biotechnology Information

nt: nucleotídeos

°C: graus Celsius

RNAi: RNA de interferência

ATP: Adenosina trifosfato

PCM: Paracoccidioidomicose

RESUMO

Fungos do gênero *Paracoccidioides* compreendem os agentes etiológicos da Paracoccidioidomicose (PCM), a micose sistêmica mais prevalente na América latina. Estes patógenos apresentam como característica o dimorfismo térmico. Em temperaturas entre 22°C à 26°C *Paracoccidioides* spp. crescem como micélio; já no hospedeiro à 36°C estes fungos apresentam-se como levedura. A transição morfológica da fase de micélio ou conídios para levedura é essencial para o desenvolvimento da doença no hospedeiro. Em vários fungos, pequenos RNAs regulatórios denominados microRNAs-like tem sido descritos durante as diferentes fases morfológicas, sugerindo um possível papel regulatório em etapas essenciais para o desenvolvimento fúngico no ambiente e no hospedeiro. Desta forma o presente trabalho tem como objetivos a descrição *in silico* das proteínas envolvidas na via de silenciamento gênico pós-transcricional mediado por microRNAs-like em *Paracoccidioides* spp., a identificação *in silico* de microRNAs-like no genoma deste fungo e a caracterização dessa classe de RNAs presentes nas diferentes fases e na transição dimórfica através de RNAseq, além da categorização dos possíveis processos biológicos regulados por microRNAs-like. Análises *in silico* revelaram a presença de proteínas homólogas a dicers e argonautas em *P. brasiliensis* (*Pb18* e *Pb03*) e *P. lutzii*. Além disso, os transcritos que codificam para estas proteínas são induzidos na fase parasitaria. Através de ferramentas de bioinformática, baseado em similaridade de sequências detectou-se 18 potenciais microRNAs-like conservados no genoma deste fungo e destes 5 microRNAs-like com os maiores e menores valores de MFE foram validados por PCR qualitativa, demonstrando assim que este patógeno retém em seu genoma regiões de gênese de microRNAs-like. Posteriormente a esta etapa, os transcritos que codificam para dicers e argonautas foram analisados em estádios morfológicos de *P. brasiliensis* *Pb18*, através de qRT-PCR. Os dados de expressão gênica relevaram que a maquinaria de silenciamento mediado por microRNAs-like é diferencialmente expressa entre os estádios morfológicos deste fungo. Os dados do sequenciamento das bibliotecas de pequenos RNAs nas fases de micélio, transição e levedura, permitiram a identificação de 48 microRNAs-like e deste 44 foram diferencialmente expressos. Análises dos microRNAs-like com maior expressão na fase de levedura, demonstram que estas moléculas regulam processos essenciais para a sobrevivência do patógeno, como a via para produção de energia, resposta a agentes

oxidativos, determinação de polissacarídeos na parede celular, além de influenciaram nos processos de divisão celular e morfogênese. De modo geral os dados apontam para conservação de um mecanismo de regulação gênica pós-transcricional neste patógeno e tal fenômeno pode influenciar no desenvolvimento deste fungo durante a fase miceliana, na forma parasitária e durante a transição dimórfica.

Palavras-chave: microRNAs-like, *Paracoccidioides brasiliensis*, micose, transição dimórfica, levedura.

ABSTRACT

Fungi of the genus *Paracoccidioides* comprise etiologic agents of Paracoccidioidomycosis (PCM) the main systemic mycoses in Latin America. These pathogens presents thermal dimorphism. At temperatures from 22°C to 26°C *Paracoccidioides* spp. grow as mycelium and in the host or at 36°C they are yeast cells. The morphological transition from mycelium or conidia to the yeast phase is essential for development of disease in the host. In fungi small regulatory RNAs have been described during different morphological phases suggesting a possible regulatory role of those microRNAs in steps essential for fungal growth on the environment and host. In this way, the present work aims to perform *in silico* description of proteins involved in the post-transcriptional gene silencing pathway mediated by microRNAs-like in *Paracoccidioides* spp., *in silico* identification of microRNAs-like in the genome and the characterization of this class of RNAs in the different phases and in the dimorphic transition through RNAseq, besides the categorization of possible biological processes regulated by microRNAs-like. *In silico* analyzes revealed the presence of homologous proteins to dicers and argonauts in *P. brasiliensis* (*Pb18* and *Pb03*) and *P. lutzii*. In addition, the transcripts encoding these proteins are induced in the parasitic phase. Through bioinformatics tools based on sequence similarity, we detected 18 potential microRNAs-like conserved in the genome of those fungi and of these, 5 microRNAs-like with the higher and lower MFE values were validated by qualitative PCR, thus demonstrating that this pathogen retains in its genome regions of microRNAs-like genes. Subsequently to this step the transcripts coding for dicers and argonauts were analyzed in morphological stages of *P. brasiliensis* *Pb18*, through qRT-PCR. Gene expression data showed that the microRNAs-like mediated silencing machinery is differentially expressed between the morphological stages of this fungus. Sequencing data of the microRNA-like libraries in mycelium, transition and yeast phases allowed the identification of 48 microRNAs-like and 44 of these were differentially expressed. Analysis of the microRNAs-like with higher expression in the yeast phase, demonstrated that these molecules regulate processes essential for the survival of the pathogen, such as the pathways for energy production, response to oxidative agents, determination of polysaccharide in the cell wall,

besides influencing in the processes, of cell division and morphogenesis. In synthesis, , the data point to the conservation of a mechanism of post-transcriptional gene regulation in this pathogen and such phenomenon may influence the development of this fungus in mycelia, as well as, in the parasitic form and during the dimorphic transition.

Keywords: microRNAs-like, *Paracoccidioides brasiliensis*, mycose, dimorphic transition, yeast.



Capítulo 1

1. INTRODUÇÃO

1.1 Características dos microRNAs e Biogênese

Pequenos RNAs de eucariotos com possível função regulatória são classificados em três tipos: microRNAs (microRNAs), RNAs de interferência (siRNA) e RNAs associados às proteínas Piwi (piRNAs). Pequenos RNAs já foram descritos em animais, plantas e fungos como moléculas efetoras do silenciamento gênico. São moléculas sequência-específicas, sendo o mecanismo de silenciamento efetuado em resposta a um RNA dupla fita (dsRNA). A diferença entre as três classes de pequenos RNAs é devida ao seu mecanismo de biogênese, processamento e função dentro da célula (GROSSHAN; FILIPOWICZ, 2008).

MicroRNAs (microRNAs) são uma classe de pequenos RNAs não codificantes de proteínas ou peptídeos (npcRNAs), conservados evolutivamente. Possuem em torno de 20-25 nucleotídeos e atuam como silenciadores pós-transcricionais regulando vários processos biológicos por interferirem na tradução do RNA mensageiro (mRNA), (GROßHANS; FILIPOWICZ, 2008). Descrito pela primeira vez por Lee e colaboradores (1993), o microRNA *lin-4* demonstrou ser essencial nas primeiras etapas do desenvolvimento larval de *Caenorhabditis elegans*, regulando a tradução do gene *lin-14* por um mecanismo antisentido entre o microRNA e a região não traduzida (3' UTR) do mRNA alvo. Em 2000 Reinhart e colaboradores, descreveram um segundo microRNA presente em *C. elegans* denominado *let-7*, sendo este pequeno RNA capaz de promover a regulação da expressão de outros genes incluindo *lin-14*, *lin-28*, *lin-41*, *lin-42* e *daf-12*.

Posteriormente, microRNAs foram identificados em organismos invertebrados como *Drosophila melanogaster* e em órgãos de vertebrados. Embora, alguns microRNAs foram comuns a ambos animais e insetos, o perfil de expressão destes pequenos RNAs foi diretamente relacionado ao tipo de tecido e ao estágio de desenvolvimento analisado. Dessa maneira, foi demonstrado que microRNAs podem possuir um papel regulatório não apenas no tempo de desenvolvimento larval como visto em *C. elegans* mas também apresentar funções regulatórias em tecidos específicos (LAGOS-QUINTANA et al., 2001).

Genes de microRNAs são frequentemente localizados em regiões intergênicas e transcritos similarmente a genes codificantes de proteínas (NOZAWA; MIURA; NEI,

2011) em alguns casos genes codificantes de microRNAs são localizados em regiões de íntrons ou éxons (YANG et al., 2013). A regulação da biogênese de microRNAs envolve fatores transcricionais e fatores acessórios. Trabalhos revelam que a abundância de um microRNA é controlada através da transcrição, estabilidade e processamento dos pri-microRNAs (XIE, 2015). Proteínas acessórias DDX5 e DDX17, juntamente com Drosha e DGCR8 são envolvidas na formação do complexo microprocessador nuclear de pri-microRNAs. Essas proteínas acessórias atuam de duas formas: Primeiro estabilizando este complexo para o correto processamento do pri-microRNAs e também servem como mediadores de sinal que conectam a atividade do microprocessador nuclear com outras vias de sinalização sob várias circunstâncias, como em casos de dano ao DNA ou durante a formação de microRNAs com função de supressão tumoral, aumento a atividade do complexo com intuito de inibir o crescimento do tumor. Além disto, a estabilidade e o processamento dos pri-microRNAs no núcleo são regulados pela edição desta molécula. Proteínas ADARs 1 e 2 editam moléculas de RNA trocando a adenosina pela inosina, esta mudança na estrutura do pri-microRNA, suprime a atividade de Drosha e reduz a estabilidade da molécula de pri-microRNA, favorecendo o reconhecimento e degradação desta molécula por nuclease. A concentração das proteínas envolvidas no processamento de microRNAs como argonautas também variam entre os diferentes tecidos e células, por exemplo em células tronco embrionários, a proteína argonauta 2 sofre ubiquitinação e degradação no proteassoma, tal evento bloqueia o silenciamento gênico pós-transcricional mediado por microRNAs (revisado por SHEN & HUNG, 2015).

A via de biogênese de microRNAs em plantas (VOINNET, 2009) e mamíferos é bem elucidada. Em plantas como *Arabidopsis thaliana* a produção de um microRNA envolve duas etapas de clivagem do microRNA primário e do pre-microRNA, no núcleo, pela enzima dicer-1 (REINHART et al., 2002), posteriormente a esta etapa a enzima (HEN1) adiciona um grupo metil à extremidade 3' do duplex microRNA/microRNA*, estabilizando a molécula. O duplex é então transportado do núcleo para o citoplasma através de Hasty (HST), uma proteína homóloga à exportina 5 (PARK et al., 2005). Em *A. thaliana* a principal proteína efetora de silenciamento mediado por microRNAs é argonauta 1, a qual possui atividade de endonuclease e é capaz de suprimir a expressão de genes alvos por clivagem do RNAm ou inibição da tradução (BAUMBERGER; BAULCOMBE, 2005). Estudos mostram que o

crescimento normal da planta e suas funções fisiológicas requerem um controle rigoroso dos níveis e da atividade dos microRNAs (XIE, 2015) (Figura-1A).

Sabe-se que em mamíferos microRNAs são originados de um precursor de RNA codificado no genoma (GROßHANS; FILIPOWICZ, 2008). A transcrição destas regiões pela RNA polimerase II (Pol II) (VOINNET, 2009) produz longas fitas simples de RNAs que, por complementariedade de bases, formam RNA dupla fita (dsRNA) com estrutura semelhante a grampos, chamados de microRNAs primários (pri-microRNAs) (GROßHANS, FILIPOWICZ, 2008). No núcleo, a enzima do tipo ribonuclease III Drosha e seu cofator DGCR8 são responsáveis por processar os microRNAs (primários) e produzir estruturas em dupla fita, também em forma de grampo (*hairpin*) com aproximadamente 70 nucleotídeos denominados precursores de microRNAs (pre-microRNAs) (HE; HANNON, 2004). Tais moléculas são transportadas para o citoplasma através da exportina 5 (YI et al., 2005), onde são processados pela enzima Dicer. A clivagem por esta enzima gera os microRNAs maduros que variam entre 21 a 25 nucleotídeos, constituídos por moléculas de RNA dupla fita microRNA/microRNA* (HE; HANNON, 2004). Um das fitas do duplex, o microRNA*, é degradada, enquanto a outra é associada ao complexo de indução do silenciamento (RISC) (HE; HANNON, 2004). Membros da família das proteínas argonautas constituem o núcleo central do RISC e são associadas aos microRNAs antes e após o reconhecimento do mRNA alvo (BARTEL; LEE; FEINBAUM, 2004). Em muitos casos, os microRNAs ligam-se à região 3' UTR do mRNA por um mecanismo de complementariedade de bases imperfeita, causando repressão da tradução do mRNA, sem degradação de sua fita (HE; HANNON, 2004) (Figura-1B).

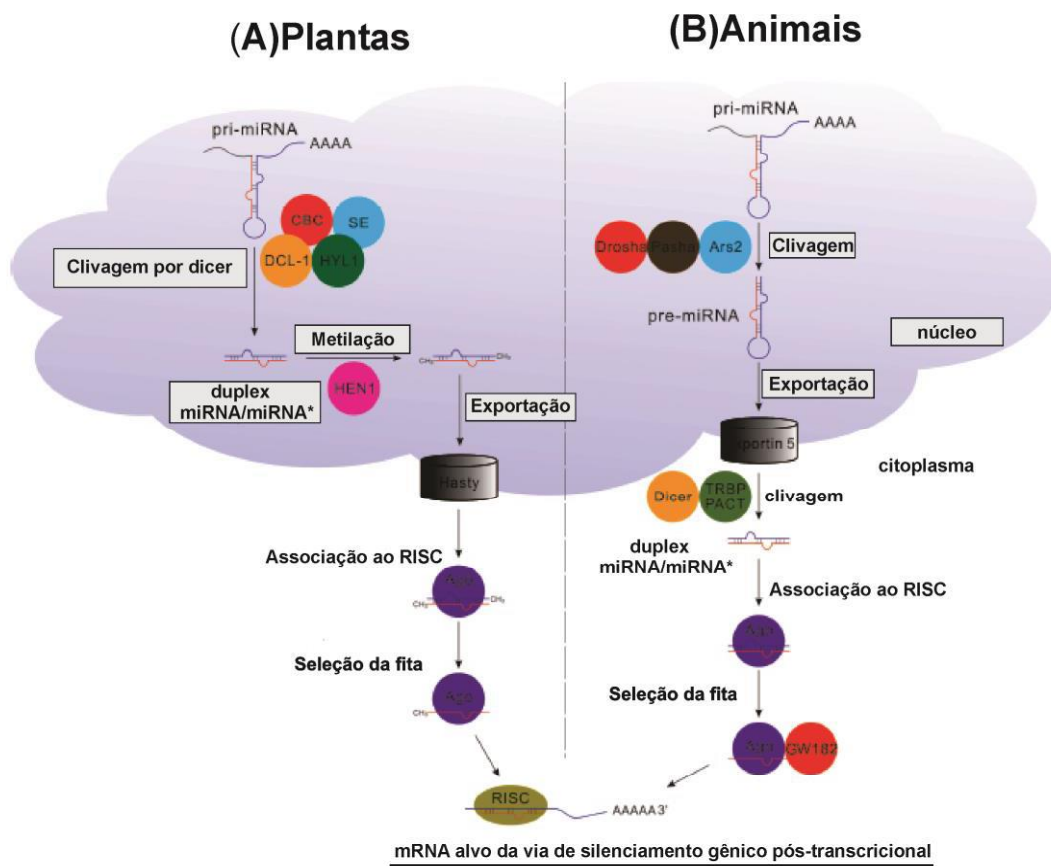


Figura-1 Via canônica para produção de microRNAs em plantas e mamíferos. Homólogos com funções similares são representados pela mesma cor (Adaptado de Zhang et al., 2018).

Já em fungos como *Neurospora crassa* o mecanismo de produção de microRNAs-like é parcialmente semelhante ao realizado por plantas e mamíferos. Quatro vias distintas para a produção de microRNAs-like neste fungo foram descritas por (Lee e colaboradores, 2010). O milR-1 é produzido através de um longo miRNA primário (pri-milRNA) onde proteínas dicers dcr1/dcr2p clivam o pri-milRNA formando um RNA dupla fita (dsRNA) denominado precursor de milRNAs. Após esta etapa o precursor de milRNAs, liga-se à argonauta qde-2p e esta proteína recruta a exonuclease QPIp para processamento do pré-microRNA e formação do microRNA maduro. Além disso, análises de linhagens mutantes para qde-1p (RNA-Polimerase-dependente de RNA) e qde-3p (RecQ helicase) revelaram que estas proteínas não são necessárias para a biossíntese de milR-1, o qual é processado por enzimas dicers e argonauta.

Ainda em *N. crassa*, o mecanismo para a produção de milR-3 requer a presença de dicers (dcr1p/dcr2p). Para a síntese de milR-4 o mecanismo é parcialmente dependente de dicers indicando possivelmente a presença de outra nuclease envolvida

no processamento de milR-4. Ao contrário de milR-1 a produção do milR-3 e milR-4 não requer a presença de qde-2p evidenciando um mecanismo independente de qde-2p para síntese deste dois microRNAs. A biogênese de milR-2 é independente de dicers, embora a proteína argonauta qde-2p, com seu sítio catalítico, seja necessária para a produção de pre-milRNA e milR-2 maduro, entretanto para a síntese de milR-2 a proteína QPIp, não é empregada. Desta forma, o pri-milR (milR-2) é processado por uma nuclease desconhecida e o pre-milR associa-se com qde-2p, que através da sua atividade catalítica é envolvida na geração do microRNA-like maduro. Em *N. crassa* a proteína mitocondrial MRPL3p contendo um domínio de Ribonuclease III poderia atuar na biogênese de microRNAs-like que não são dependentes do processamento por dicers (LEE et al., 2010) (Figura-2).

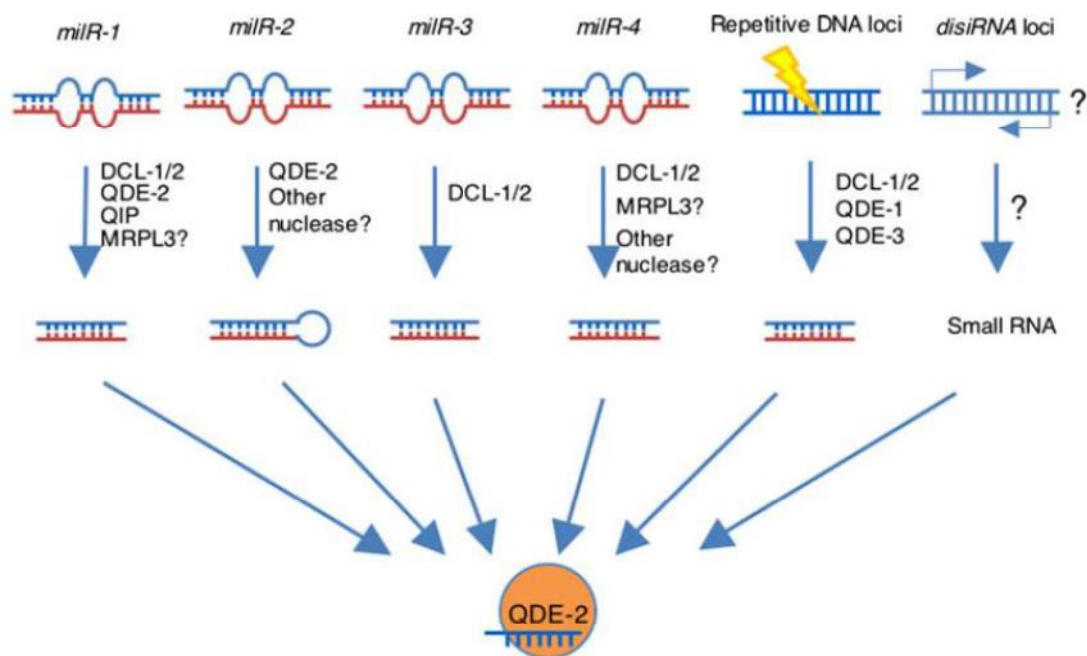


Figura 2- Diagrama representativo das quatro vias de produção de microRNAs-like em *N. crassa* (Lee et al., 2010).

Assim como em *N. crassa*, em *Mucor circinelloides* diferentes vias para produção de pequenos RNAs são presentes, empregando proteínas dicers, argonautas e RNA polimerase dependente de RNA. Além disso, uma via não canônica, dependente de argonautas e RNA polimerase dependente de RNA, porém independente de dicers é presente neste fungo, sendo envolvida no processo de degradação de RNAs mensageiros endógenos (TRIEU et al., 2015).

MicroRNAs-like produzidos por fungos apresentam semelhanças com microRNAs de plantas e animais, tais quais, todos são processados a partir de um

precursor de RNA em forma de braço e alça (*stem-loop*). Muitos microRNAs-like de fungos requerem proteínas dicers e argonauta durante as etapas de processamento (LEE et al., 2010) e atuam também como reguladores da expressão gênica. MicroRNAs-like produzidos por *N. crassa* (LEE et al., 2010) e *Cryptococcus neoformans* (JIANG et al., 2012) induzem o silenciamento de genes alvo e componentes centrais da via são conservados entre diferentes espécies de fungos (DRINNENBERG et al., 2009).

1.2 Descrição e função de microRNAs-like em fungos

Após a descoberta de microRNAs em *C. elegans* (LEE et al., 1993) pequenos RNAs foram identificados em animais, plantas e algas (GRIMSON et al., 2008, ZHAO et al., 2007). Os primeiros microRNAs-like identificados em fungos foram descritos em *N. crassa* (LEE et al., 2010) e *C. neoformans* (JIANG et al., 2012). Posteriormente microRNAs-like foram identificados em outros fungos, em *Aspergillus flavus* microRNAs-like foram regulados em resposta à mudanças de temperatura (BAI et al., 2015). Em *Penicillium marneffei* microRNAs-like foram identificados nas fases de micélio e levedura, tais microRNAs-like foram mais abundantes na fase filamentosa deste fungo (LAU et al., 2013). Em *Metarhizium anisopliae* um perfil de expressão diferencial de microRNAs-like foi detectado nas fases de micélio e conídio, sugerindo um possível papel regulatório dos microRNAs-like nas diferentes fases de crescimento deste fungo (ZHOU et al., 2012).

Diferentes microRNAs-like foram identificados em *Penicillium chrysogenum*, análises *in silico* revelaram genes alvo silenciados por microRNAs-like produzidos por este fungo (DAHLMANN, KÜCK, 2015). MicroRNAs-like foram ainda descritos em *Fusarium oxysporum* (CHEN et al., 2014), *Trichoderma reesei* (KANG et al., 2013) *Sclerotinia sclerotiorum* (ZHOU et al., 2012), demonstrando assim a presença dessas moléculas em diferentes espécies de fungos. Análises do perfil de RNAs contidos em vesículas secretadas por *C. neoformans*, *Paracoccidioides brasiliensis* (Pb18), *Candida albicans* e *Saccharomyces cerevisiae* identificaram a presença de mRNA, ncRNA incluindo pequenos RNAs com tamanhos de até 250 nt. A busca por homologia entre estas sequências de pequenos RNAs e microRNAs de outros organismos depositados no mirBASE (<http://www.mirbase.org/>) permitiram a identificação de 145 sequências em *P. brasiliensis*, 344 em *C. neoformans*, 423 em *C. albicans* e 532 sequências em *S. cerevisiae* que apresentaram homologia com microRNAs de outros organismos (PERES

DA SILVA et al., 2015). Assim como em células de mamíferos e plantas, a presença de microRNAs-like em fungos evidencia um mecanismo conservado entre diferentes eucariotos (KANG et al., 2013).

Mutações de genes envolvidos no fenômeno de RNA por interferência em *Mucor circinelloides* alteraram a função de vários processos biológicos incluindo esporulação, crescimento em diferentes variações de pH e autólise. Além disso, um conjunto extenso de genes foi regulado entre as linhagens mutantes e selvagens (NICOLÁS et al., 2015). Neste fungo a via de RNA por interferência também atua de forma não-canônica, promovendo mutações epigenéticas em determinadas linhagens e conferindo resistência a antifúngicos, favorecendo assim uma rápida adaptação do patógeno a condições de estresse (TRIEU et al., 2015).

Elementos essenciais da via de biogênese de pequenos RNAs de interferência como a proteína Argonauta e a enzima dicer foram descritos em vários fungos pertencentes a diferentes filos, entre eles *Aspergillus nidulans*, *N. crassa*, *C. neoformans*, *Schizosaccharomyces pombe* entre outros (DRINNENBERG et al., 2009). Análises do transcriptoma de *Paracoccidioides* sp. revelaram que este fungo possui genes ortólogos aos de *N. crassa*, os quais codificam as proteínas RNA polimerase dependente de RNA, argonauta e dicers, elementos chave da via de biossíntese de pequenos RNAs de interferência (ALBUQUERQUE et al., 2005). Análises dos genomas de *Paracoccidioides* spp. revelaram proteínas homólogas às de *N. crassa*, *C. neoformans*, *Aspergillus* spp. e *Histoplasma capsulatum* envolvidas na via de silenciamento gênico pós-transcricional (de CURCIO 2018 submetido).

1.3 MicroRNAs e interação patógeno-hospedeiro

Pequenos RNAs de interferência como os microRNAs, atuam em vários processos biológicos através de um mecanismo de regulação pós-transcricional, alterando a expressão de genes envolvidos em eventos de diferenciação e proliferação celular, tumorigênese, imunidade celular, atuando também durante o processo de interação patógeno-hospedeiro. Weiberg e colaboradores, 2013 demonstraram que o fungo fitopatogênico *Botrytis cinerea*, durante a infecção em *Arabidopsis thaliana* e tomate produz pequenos RNAs capazes de silenciar genes do hospedeiro relacionados com a imunidade, desta forma favorecendo a infecção do patógeno em plantas.

A estratégia de uso de microRNAs produzidos pelo hospedeiro a favor do processo infeccioso também tem sido descrita em patógenos humanos. A bactéria

intracelular *Mycobacterium avium*, após contato com macrófagos do hospedeiro induz a expressão de dois microRNAs produzidos por estas células, o microRNA let 7 e mir-29. Tais microRNAs possuem como alvos as proteínas Casp3 e Casp7 respectivamente, estas proteínas são membros da família BCL2, as quais são envolvidas na ativação da via de apoptose celular. Desta forma a indução destes dois microRNAs inibe a apoptose celular, mecanismo utilizado pelo hospedeiro para combater patógenos intracelulares, favorecendo assim a infecção por *M. avium* (SHARBATI et al., 2011). *Mycobacterium tuberculosis* outro patógeno intracelular, regula positivamente a expressão de miR-106b produzido por macrófagos esse microRNA possui como alvo a enzima lisossomal degradativa catepsina. A indução da expressão deste microRNA manipula as respostas do hospedeiro com o intuito de evitar a exposição da bactéria às enzimas degradativas produzidas por macrófagos (PIRES et al., 2017).

O parasita *Leishmania donovani*, agente etiológico da leishmaniose visceral, altera o perfil de expressão de microRNAs hepáticos envolvidos no metabolismo lipídico, através da clivagem da proteína dicer 1 do hospedeiro. Este processo desregula a homeostase lipídica, favorecendo a infecção, visto que pacientes com hipolipidemia são mais susceptíveis à doença causada por este parasita (GHOSH et al., 2013). Nos estágios iniciais da infecção por *Schistosoma* spp. a expressão de miR-351 é reduzida nos tecidos hepáticos do hospedeiro, entretanto nos estágios mais tardios da infecção ocorre a indução da expressão de miR-351 e conseqüente aumento da fibrose hepática esquistossomótica. O uso de um antagonista de miR-351 promoveu a redução da fibrose hepática protegendo parcialmente o hospedeiro da esquistossomose letal (HE et al., 2018).

Estudos de interação entre macrófagos derivados de medula óssea e *Listeria monocytogenes* demonstram que esta bactéria é capaz de modular a expressão de inúmeros microRNAs contidos nos macrófagos, sugerindo que microRNAs podem fazer parte de uma resposta imune inata do hospedeiro contra a infecção por este patógeno (SCHNITGER et al., 2011). Análises do padrão de expressão de microRNAs produzidos por células dendríticas, após o contato com *Aspergillus fumigatus* e *Candida albicans* revelaram uma resposta específica de microRNAs à infecção causada por estes fungos, sendo que alguns dos microRNAs induzidos após o contato com estes patógenos foram miR-212 e miR-132. Possivelmente a indução da expressão destes microRNAs é associada à resposta antifúngica medida por células dendríticas, visto que

alvos destes pequenos RNAs são associados a genes envolvidos na resposta imune durante o processo de infecção no hospedeiro (DIX et al., 2017).

Em infecções sistêmicas a presença de um agente patogênico frequentemente induz uma significativa mudança no perfil de expressão de microRNAs circulantes do hospedeiro. Neste contexto Singulani e colaboradores 2017, analisaram o perfil de expressão de microRNAs produzidos por pacientes com Paracoccidioidomicose (PCM) e indivíduos saudáveis. Os dados do trabalho apontaram para uma indução da expressão de oito microRNAs entre os indivíduos com PCM. Apoptose, resposta imune e adesão do fungo as células do hospedeiro são possíveis processos regulados pelos microRNAs diferencialmente expressos, demonstrando assim a influência destas moléculas no processo de interação patógeno-hospedeiro. Além disso, segundo os autores, a presença de microRNAs circulantes no soro de pacientes com PCM pode ser uma possível alternativa para a obtenção de biomarcadores da infecção. Em um modelo de infecção pulmonar por *P. brasiliensis*, microRNAs produzidos pelas células do pulmão do hospedeiro foram diferencialmente expressos em 28 e 56 dias após a infecção, sugerindo um papel putativo destes pequenos RNAs durante o curso da micose nos pulmões (MARIOTO et al., 2017).

1.4 *Paracoccidioides* spp.

Fungos pertencentes ao complexo *Paracoccidioides* foram descritos pela primeira vez por Adolpho Lutz em 1908, sendo este patógeno isolado de um paciente que apresentava lesões na mucosa oral. *Paracoccidioides* spp. são fungos termodimórficos, que quando cultivados em temperaturas entre 22 à 25° C, ou no solo, apresentam-se na forma miceliana. Quando cultivados em temperaturas de 36° a 37°C *in vitro* ou no hospedeiro, desenvolvem-se na sua forma parasitária caracterizada como leveduras (RESTREPO, 1985, BOCCA et al., 2013). Nesta fase morfológica ocorre a presença de múltiplos brotamentos originados de uma célula grande e central, com aspecto de roda de leme de navio (Figura-3A). Quando em meio de cultura, as leveduras apresentam-se como colônias enrugadas e de cor creme, formadas por células de tamanho variado (4 a 30 μ m). Já a forma miceliana, apresenta septos formados por conídios terminais ou intercalares (Figura-3B), (BRUMMER et al., 1993). Após 15 dias de cultivo a 25°C, observa-se na fase filamentosa a presença de colônias brancas, tornando-se aveludadas e acastanhadas, sendo possível observar-se a presença de hifas hialinas septadas, com ramificações (Figura-3B) (MENDES et al., 2017).

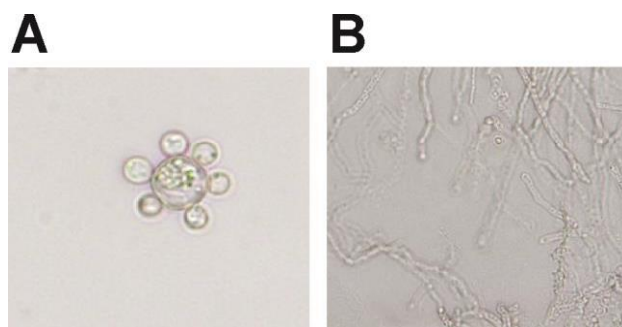


Figura 3- Características microscópicas de *Paracoccidioides* spp. (3A) Uma célula grande e central, rodeada por brotamentos periféricos, típico da fase parasitária ou de levedura (3B). Emaranhado de hifas hialinas, septadas característica de micélio. Aumento de 40x: Fonte Laboratório de Biologia Molecular-UFG.

Os fungos do complexo *Paracoccidioides* possuem, ao menos, dois nichos ecológicos conhecidos, sendo um correspondente à forma miceliana, encontrada no solo e outro à sua forma parasitária ou leveduriforme, associada ao hospedeiro. Durante a fase leveduriforme estes fungos adaptam-se a um habitat diferente, podendo ocupar variados nichos em órgãos internos do hospedeiro, dependendo da sua tolerância à mudanças na temperatura, influência hormonal e às respostas do sistema imune do hospedeiro. Durante a fase saprobiótica ou miceliana o fungo encontra-se sobre a influência de fatores ambientais como umidade do solo, mudança na temperatura e competição com outros microorganismos (Figura-4) (BAGAGLI et al., 2008). A dispersão e crescimento destes patógenos parecem ser influenciados por alterações climáticas. Por exemplo, períodos com altas taxas de umidade favorecem o crescimento fúngico e manutenção no solo. Entretanto um breve período de seca remove água da camada mais superficial da terra, favorecendo a disseminação dos propágulos infectantes (YAMAMOTO et al., 2012).

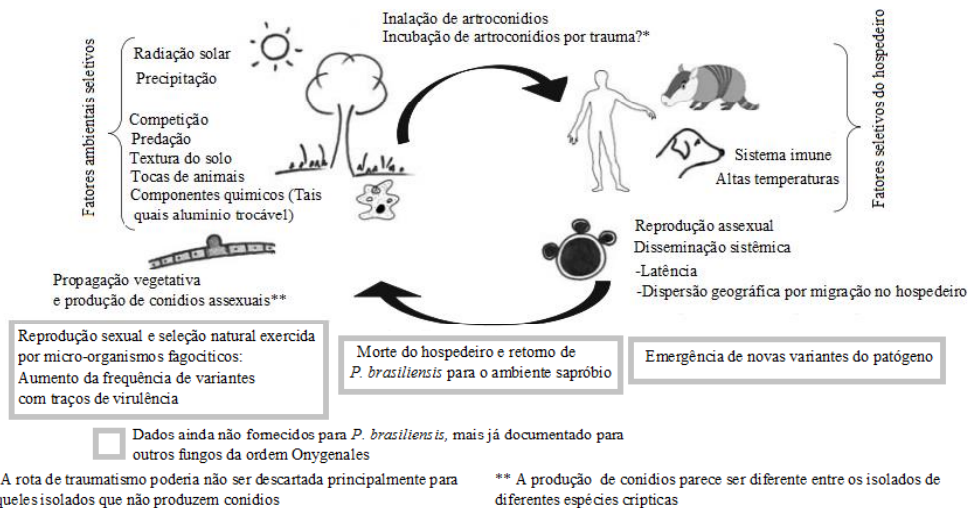


Figura 4- Ciclo biológico hipotético de *Paracoccidioides* spp. São descritas algumas forças seletivas que podem atuar sobre seu suposto nicho ecológico no ambiente saprobiótico e no hospedeiro (adaptado de BAGAGLI et al., 2008).

Acreditava-se que os humanos eram os únicos hospedeiros infectados por espécies do gênero *Paracoccidioides*. Entretanto, vários trabalhos têm mostrado que animais podem ser infectados como, por exemplo, cachorros, cavalos (MENDES et al., 2017) e coelhos (BELITARDO et al., 2014). Além destes, animais selvagens como roedores que vivem em áreas endêmicas da PCM são infectados por este fungo e tais achados podem ser utilizados como valiosos marcadores epidemiológicos da presença destes patógenos no meio ambiente (SBEGHEN et al., 2015). Espécies do complexo *Paracoccidioides* também tem sido isoladas de amostras de solo e aerossóis de áreas endêmicas da doença como os estado de Goiás e Minas Gerais (ARANTES et al., 2016).

1.5 Classificação filogenética de fungos do complexo *Paracoccidioides*

Fungos do complexo *Paracoccidioides* são classificados como pertencentes ao filo Ascomycota ordem Onygenales e família Ajellomycetaceae, que incluem fungos anamorfos como *Blastomyces dermatitidis*, *Histoplasma capsulatum*, *Emmonsia parva*, *Emmonsia crescens* e *Lacazia loboi* (UNTEREINER et al., 2004, DUKIK et al., 2017). Durante muitos anos vários trabalhos foram realizados no intuito de caracterizar as espécies filogenéticas pertencentes ao gênero *Paracoccidioides*. Em 2006, Matute e colaboradores, empregando técnicas de polimorfismo genético, descreveram três espécies filogenéticas distintas dentro do complexo *Paracoccidioides brasiliensis*. Essas espécies foram classificadas como espécie filogenética S1 (contendo 38 isolados pertencentes ao Brasil, Venezuela, Peru e Argentina), PS2 (com 6 isolados sendo 5

brasileiros e 1 venezuelano) e PS3 (contendo 21 isolados colombianos). Posteriormente análises de diferentes isolados de *Paracoccidioides brasiliensis* revelaram que *Pb01* difere filogeneticamente dos outros isolados pertencentes às espécies S1, PS2 e PS3 (CARRERO et al., 2008).

Em 2009 Teixeira e colaboradores, empregando o método de reconhecimento de espécies filogenéticas por concordância genealógica descreveram uma possível nova espécie dentro do gênero *Paracoccidioides*, sendo esta denominada como *Pb01-like* ou *P. lutzii* uma homenagem a Adolpho Lutz, o qual descreveu *P. brasiliensis*, em 1908. Através de análises de dados moleculares foi proposta a divisão do gênero *Paracoccidioides* em duas espécies biológicas, *P. brasiliensis* e *P. lutzii* (TEIXEIRA et al., 2009, SALGADO-SALAZAR et al., 2010, THEODORO et al., 2012 e BOCCA et al., 2013). Isolados pertencentes à espécie *P. lutzii* são endêmicos da região Centro-Oeste mais especificamente nos estados de Goiás e Mato Grosso. Uma sobreposição geográfica é observada entre a espécie filogenética S1 de *P. brasiliensis* e *P. lutzii* sugerindo que as espécies sejam simpátricas (TEIXEIRA et al., 2009) (Figura-5).



Figura 5- Distribuição geográfica de espécies filogenéticas do gênero *Paracoccidioides*. Os isolados *Pb01-like* são encontrados quase que exclusivamente na Região Centro-Oeste do Brasil, principalmente nos estados de Mato Grosso e Goiás. A espécie filogenética S1 sobrepõe parcialmente na mesma região (Teixeira et al., 2009).

Posteriormente outra nova espécie filogenética dentro do complexo *P. brasiliensis* foi sugerida, sendo esta denominada como PS4, sendo os isolados clínicos recuperados de pacientes da Venezuela (BOCCA et al., 2013, TEIXEIRA et al., 2014 Turissini e colaboradores, 2017 empregando análises morfológicas e moleculares, sugeririam uma nova classificação para as espécies filogenéticas do complexo *P. brasiliensis*, como se segue: *P. americana* para PS2, *P. restrepiensis* para PS3, *P. venezuelensis* para PS4 e *P. brasiliensis* sendo usada apenas para S1, além da espécie já descrita como *P. lutzii* (TEIXEIRA et al., 2009).

1.6 Paracoccidioidomicose (PCM)

Paracoccidioidomicose (PCM) anteriormente conhecida como blastomicose sul americana é uma micose sistêmica endêmica causada por fungos do gênero *Paracoccidioides* (RESTREPO, 1985, CATAN, MORALES, 2015, TURISSINI et al., 2017). A rota de infecção por estes fungos ocorre através da inalação de conídios ou propágulos micelianos, que ao atingirem os alvéolos pulmonares realizam a transição dimórfica para a fase leveduriforme, a qual pode disseminar-se pelas vias linfática e/ou hematogênica para outros locais do organismo hospedeiro (MCEWEN et al., 1987, (SHIKANAI-YASUDA et al., 2006).

Esta micose pode ser classificada em: Paracoccidioidomicose infecção e Paracoccidioidomicose doença (Forma: Aguda/subaguda) e (Forma: Crônica). A PCM infecção é contraída quando o indivíduo saudável entra em contato com *Paracoccidioides* spp. e se torna positivo para o antígeno paracoccidioidina. Entretanto, não ocorrem manifestações dos sintomas da doença (FRANCO et al., 1987, MARQUES, 2013, SHIKANAI-YASUDA et al., 2017). A forma crônica da doença acomete principalmente indivíduos do gênero masculino, relacionados à atividade rural, com faixa etária entre 30 a 60 anos de idade, sendo responsável por 90% dos casos da doença. A doença crônica é caracterizada como unifocal quando é restrita a apenas um órgão, geralmente pulmão e multifocal acometendo mais de um órgão simultaneamente, sendo pulmão e mucosa os sítios mais comuns (Figura 6A). Dependendo das condições gerais do paciente e dos achados clínicos, a forma crônica da doença pode ser subdividida em leve, moderada ou grave. Os pacientes podem morrer ou se recuperar da infecção e muitas vezes as lesões pulmonares podem deixar sequelas resultando em insuficiência respiratória (FRANCO et al., 1987, MARQUES 2013, SHIKANAI-YASUDA et al., 2006, SHIKANAI-YASUDA et al., 2017).

A forma aguda/subaguda (tipo juvenil) é caracterizada por evolução rápida dos sintomas e sinais da doença, ocorrendo a presença de linfadenomegalia, hepatoesplenomegalia, manifestações digestivas, envolvimento ósseo-articular e lesões cutâneas (Figura 6B). Esta forma clínica é responsável por 5 a 25% dos casos da doença, podendo ser mais frequente em certas regiões endêmicas. No Brasil os maiores relatos desta forma da micose são dos estados do Maranhão, Minas Gerais, Pará, Goiás e São Paulo. A distribuição da doença é igual entre crianças e adolescentes dos gêneros feminino e masculino (FRANCO et al., 1987, SHIKANAI-YASUDA et al., 2006, SHIKANAI-YASUDA et al., 2017).

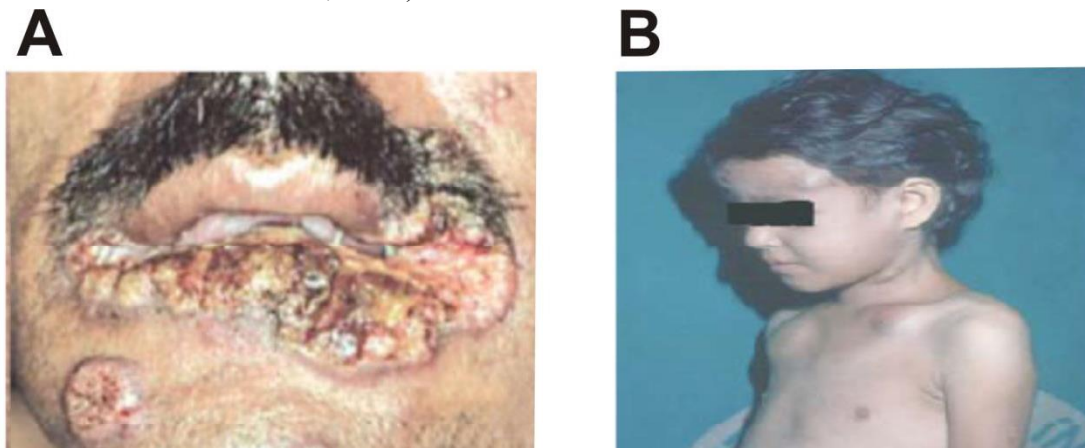


Figura 6-Manifestações clínicas da Paracoccidioidomicose (PCM). Aspectos clínicos da forma crônica da doença com acometimento peri-oral (3A), Forma aguda da PCM com abscessos em regiões frontal e clavicular, resultantes do acometimento ósseo-articular (3B) (Fonte: SHIKANAI-YASUDA et al., 2006 e SHIKANAI-YASUDA et al., 2017).

A PCM não é uma doença de notificação compulsória, sendo que a prevalência, incidência e morbidade da doença são estimadas com base em análises epidemiológicas, dados de internação hospitalar e dados de mortalidade (SHIKANAI-YASUDA et al., 2017). Estima-se que cerca de 80% dos pacientes que adquirem esta doença são brasileiros, o restante dos casos ocorre principalmente na Colômbia, Venezuela, Argentina e Equador. A taxa de letalidade desta doença é de 3% a 5% e o número de casos no Brasil, por ano, varia de 3360 a 5600. Análises dos dados epidemiológicos das cinco principais regiões do Brasil revelaram que as regiões Centro-Oeste e Norte do Brasil têm as taxas mais altas de hospitalização e mortalidade, sugerindo que estas regiões são importantes áreas endêmicas da paracoccidioidomicose (MARTINEZ, 2017). A PCM tem grande impacto médico e social em áreas endêmicas da doença, não apenas pelo elevado número de casos, mas também por causa da cronicidade da doença, longo período de tratamento e sequelas que frequentemente causam incapacidade para o

trabalho e baixa qualidade de vida. Entre as doenças crônicas granulomatosa no Brasil a PCM é menos comum que a tuberculose, porém com maiores índices que a histoplasmose. Entretanto a histoplasmose associada a pacientes com HIV é mais prevalente do que a PCM (MARTINEZ, 2015). No Rio de Janeiro após o término da rodovia Raphael de Almeida Magalhães, foi detectado um surto de PCM na sua forma aguda, com uma incidência de 8,25 por milhão de pessoas. Possivelmente este fato relaciona-se a uma grande área desmatada e maciça quantidade de terra removida, expondo a população aos propágulos infectantes deste patógeno, presentes no solo (VALLE et al., 2017)

O padrão ouro do diagnóstico da PCM é presença de elementos fúngicos sugestivos de *Paracoccidioides* spp. em amostras provenientes de escarro, raspado de lesão, aspirado de linfonodos e ou fragmentos de fungo em biopsia de órgãos possivelmente acometidos por esta micose. Como esta micose é uma doença sistêmica, o diagnóstico também deve observar os principais órgãos acometidos em cada forma da infecção (aguda/crônica), além do estado geral de saúde do paciente. (SHIKANAI-YASUDA et al., 2006, BOCCA et al., 2013 e SHIKANAI-YASUDA et al., 2017). Além disso, testes sorológicos com o antígeno gp-43 são utilizados para diagnósticos da PCM, embora alguns espécies dentro do gênero apresentem menor reatividade a este exame (CAPELLA MACHADO et al., 2013).

Diferentes de outros fungos, as espécies do gênero *Paracoccidioides* são susceptíveis ao tratamento com a maioria dos antifúngicos. Vários medicamentos tem se mostrado eficazes no tratamento da doença incluindo derivados azólicos (cetoconazol, fluconazol, itraconazol, voriconazol), derivados de sulfonamida (cotrimoxazol, sulfadiazina, trimetoprima) e anfotericina B. O antifúngico itraconazol na concentração de 200 mg tem sido empregado para o tratamento da infecção nas formas leve e moderada, com altas taxas de eficácia. A duração do tratamento pode variar de 9 a 18 meses, com tempo médio de 12 meses, sendo que o paciente deve sempre passar por exames clínicos, imunológicos e radiológicos. Os pacientes com a forma grave da doença devem fazer uso de anfotericina B em ambiente hospitalar ou de solução intravenosa de sulfametoxazol/trimetoprim até a melhora, para o posterior tratamento com outros antifúngicos orais (SHIKANAI-YASUDA et al., 2006, BOCCA et al., 2013 e SHIKANAI-YASUDA et al., 2017).

A resistência feminina à paracoccidioidomicose provavelmente está relacionada aos eventos iniciais após a infecção e possivelmente estes processos sejam modulados

por hormônios (ARISTIZABAL et al., 1998). A presença do hormônio β -estradiol em mulheres confere resistência à infecção, devido ao fato que este hormônio inibe o processo de transição dimórfica de conídio ou micélio para levedura (SALAZAR; RESTREPO; STEVENS, 1988, SHANKAR et al., 2011). Análises das respostas imunológicas entre camundongos machos e fêmeas com PCM, revelaram um perfil de ativação de células do sistema imune diferente entre os dois grupos, macrófagos derivados de camundongos fêmeas são mais potentes em produzir óxido nítrico, além de induzir a expressão do fator transcricional T-bet e a produção de citocinas do tipo Th1. De fato o hormônio sexual feminino estradiol confere proteção ao desenvolvimento da PCM por influenciar na ativação das respostas imunológicas do hospedeiro (PINZAN et al., 2010).

1.7 Transição dimórfica no complexo *Paracoccidioides*

A virulência de um patógeno não pode ser definida como uma propriedade microbiana independente, visto que este mecanismo resulta do processo de interação entre o patógeno e hospedeiro. O patógeno possui estruturas como enzimas e componentes, presentes na parede celular, capazes de induzir danos ao tecido do hospedeiro ou mascarar a resposta imune (CASADEVALL; PIROFSKI, 2009). No intuito de eliminar o patógeno, o hospedeiro produz células de defesa como macrófagos e células dendríticas, assim como citocinas, como interferon gama e fator de necrose tumoral, além de estimular a produção de espécies reativas de oxigênio e nitrogênio por macrófagos (THIND; TABORDA; NOSANCHUK, 2015). Espécies do complexo *Paracoccidioides* utilizam de vários mecanismos para colonizar o hospedeiro e escapar da resposta imune (BOCCA et al., 2013). A temperatura é o único fator que desencadeia o processo de alteração morfológica em fungos do complexo *Paracoccidioides* e portanto a capacidade de sobreviver em temperaturas mais elevadas e o dimorfismo térmico são etapas essenciais para a sobrevivência destes fungos no hospedeiro (RESTREPO 1985, revisado por TEIXEIRA et al., 2014).

Vários trabalhos têm caracterizado as respostas em nível transcricional destes patógenos durante o processo de transição dimórfica. Nunes e colaboradores, 2005 analisando o perfil de expressão de genes em diferentes tempos da transição dimórfica de micélio a levedura em *P. brasiliensis* Pb18 detectaram 2.583 genes diferencialmente expressos. Vários processos celulares foram regulados durante a transição morfológica, incluindo aumento da síntese de componentes ribossomais, indução de genes

codificadores de proteínas de vias de sinalização como os da MAPK, calmodulina, proteínas G. Foi detectado também a indução de genes envolvidos em resposta ao estresse oxidativo, provável alteração da composição dos polissacarídeos presentes na parede celular, através da indução da expressão de genes envolvidos em síntese de quitina e repressão de enzimas envolvida na degradação deste polímero, bem como, diminuição da expressão de genes codificadores de histonas nos pontos finais da transição dimórfica e indução de genes envolvidos na via de catabolismo de aminoácidos. O tratamento com Nitisinona, um inibidor de 4-hidroxifenilpiruvato dioxigenase, uma enzima envolvida na segunda etapa de catabolismo de aminoácidos aromáticos, bloqueou o processo de transição dimórfica de micélio para levedura. Avaliação do nível de transcritos durante a morfogênese, de micélio para levedura em *P. brasiliensis* Pb18 revelou um perfil de expressão diferencial de genes. Transcritos com maior indução durante este processos incluem aqueles codificadores de ubiquitina, HSP70, HSP82, HSP104 e delta-9-dessaturase. A indução destes transcritos durante a transição dimórfica relaciona-se aos processos de estabilização de proteínas, adaptação ao aumento de temperatura e fluidez da membrana plasmática, respectivamente (GOLDMAN et al., 2003).

Análises do transcriptoma de *P. lutzii* nos estágios iniciais da morfogênese, de micélio para levedura, revelaram a indução de genes envolvidos no remodelamento da parede celular incluindo genes de biossíntese de quitina e α -glucana, além de vários transportadores como a permease de aminoácidos DIP5p envolvida na captação de glutamato, um precursor requerido para a síntese de quitina. Genes envolvidos na síntese de ergosterol e fosfolipídios presentes na membrana plasmática de células fúngicas também foram induzidos. Transcritos codificadores de proteínas envolvidas em vias de sinalização celular foram induzidos, incluindo MAPK, proteína histidina quinase, calcineurina, RhoGTPase e a proteína PKC, tais proteínas são envolvidas na biossíntese de parede celular, captação de estímulos ambientais e resposta ao estresse (BASTOS et al., 2007). Durante o processo de transição dimórfica em *P. lutzii* também ocorre um aumento da síntese proteica e de modificações pós transcricionais de proteínas como ubiquitinação e degradação proteossomal, além da indução de glicosiltransferases, proteínas envolvidas na biossíntese de inúmeras moléculas dentro das células fúngicas, incluindo os componentes da parede celular (PARENTE et al., 2008).

Dados de expressão gênica durante a transição de micélio para levedura e durante o processo de germinação de levedura para micélio revelaram indução de genes envolvidos na resposta ao estresse, sinalização celular, síntese de parede celular, captação de estímulos ambientais e modificação de proteínas (HERNÁNDEZ et al., 2011). De fato as alterações na parede celular, demonstrado por análises transcricionais, corroboram com os dados já descritos na literatura, visto que na fase filamentosa o principal polissacarídeo é o β -1,3-glucana, enquanto o α -1,3-glucana é o principal polissacarídeo da parede celular, constituinte da fase de levedura (KANETSUNA, CARBONELL, 1970 revisado por MENDES et al., 2017).

O gene da histidina quinase *drk1* é envolvido no processo de dimorfismo térmico de fungos como *Histoplasma capsulatum* e *Blastomyces dermatitidis* (NEMECEK et al., 2006). Em *P. brasiliensis* o gene da histidina quinase *drk1* é altamente expresso em diferentes pontos da transição dimórfica e linhagens deste fungo submetidas ao crescimento com o inibidor de *drk1* apresentam um atraso no processo de transição dimórfica de micélio para levedura (CHAVES et al., 2016). Outros genes envolvidos no processo de morfogênese destes fungos são *Ras-1* e *2* e o bloqueio do processo de farnesilação das proteínas prejudica o crescimento de células leveduriformes e favorece o crescimento da forma miceliana (FERNANDES et al., 2008). As proteínas Hsp-90 e calcineurina de *Paracoccidioides* spp. são envolvidas no processo de transição dimórfica de micélio para levedura e a Hsp-90 também é envolvida na resposta ao estresse devido à elevação de temperatura (MATOS; MORAIS; CAMPOS, 2013). A transição morfológica de membros do complexo *Paracoccidioides* é controlada pelos níveis de Adenosina Monofosfato Cíclico (AMP-cíclico). Durante o início da transição ocorre um aumento dos níveis de AMP-cíclico. A expressão do gene *cyr1* que codifica adenilato ciclase (AC) correlaciona-se com os níveis de AMP cíclico e a atividade de AC é diferencialmente modulada pelas proteínas Gpa1p e Gpb1p, com o intuito de manter a ativação da via de sinalização mediada por AMP-cíclico ao longo da mudança morfológica (CHEN et al., 2007).

A enzima oxidase alternativa de *P. brasiliensis* influencia o processo de transição dimórfica de conídio para levedura, de fato o silenciamento deste gene reduziu a quantidade de células em transição e a viabilidade celular, possivelmente por alterar a homeostase celular, devido ao desequilíbrio do potencial redox intracelular (HERNÁNDEZ et al., 2015). A proteína paracoccina presente na parede celular, é envolvida no processo de crescimento e transição dimórfica, esta proteína é localizada

em regiões de brotamento em células de levedura e mutações neste gene acarretam na diminuição da segregação de células filhas a partir de células mãe (OLIVEIRA et al., 2017).

Além das mudanças celulares desencadeadas pela troca de temperatura em espécies do complexo *Paracoccidioides*, os dados transcricionais também demonstraram que diferentes genes são expressos em cada estágio específico destes patógenos. Análises do transcriptoma de células de levedura e micélio de *P. lutzii* permitiram a categorização de diferentes classes de genes neste patógeno. Processos biológicos realizados pelos transcritos presentes nas bibliotecas de cDNAs incluem metabolismo celular, transcrição, divisão celular, além de genes envolvidos em vias de sinalização celular relacionadas com o processo de transição dimórfica, gene codificadores de MAPK, calmodulina e cAMP/PKA foram anotados. Alguns genes foram altamente expressos em uma das bibliotecas, por exemplo, os genes codificadores de hidrofobinas presentes na biblioteca de micélio (FELIPE et al., 2003). O metabolismo entre as fases de micélio e levedura também é diferente sendo que o micélio possui um metabolismo preferencialmente aeróbio com a indução de genes envolvidos no ciclo do ácido cítrico como, por exemplo: isocitrato desidrogenase e succinil-CoA sintetase. Em contraste, as células leveduriformes induzem genes envolvidos no metabolismo anaeróbico tais quais: álcool desidrogenase I e piruvato desidrogenase, e enzimas do ciclo do glioxilato, como isocitrato liase. De forma geral, a produção de ATP pela fermentação alcoólica e cadeia respiratória tende a ocorrer preferencialmente em células leveduriformes e micélio, respectivamente. Além da expressão de genes envolvidos em vias metabólicas, células leveduriformes induzem a expressão de genes relacionados à resposta ao choque térmico como *Hsps*, genes que codificam proteínas envolvidas na detoxificação de agentes oxidantes e genes envolvidos na síntese de quitina (FELIPE et al., 2005). Além disso, transcritos que codificam proteínas como β -1,3-glucosidase, Hex1p e bglp foram induzidos na biblioteca de micélio, tais proteínas são envolvidas na manutenção e integridade da parede celular. Transcritos que codificam proteínas envolvidas no transporte de ferro também foram induzidos na biblioteca de cDNAs de micélio. Na biblioteca de levedura os transcritos mais expressos codificam para proteínas envolvidas na síntese ou modificações na molécula de quitina, como α -1,3-glucana sintase e quitina desacetilase, respectivamente. Enzimas da via de biossíntese de cisteína foram induzidas nesta

condição, possivelmente porque na forma parasitária ocorre a síntese de cisteína, a partir de sulfato inorgânico (ANDRADE et al., 2006).

Dados proteômicos das fases de micélio, transição dimórfica e levedura corroboram com os dados obtidos do transcriptoma destes fungos. De modo geral os dados apontam para maior expressão de proteínas da via glicolítica, enzimas do ciclo do glioxilato e do metabolismo de lipídeos na fase de levedura. Já em micélio as proteínas induzidas são relacionadas ao processo de produção de energia, como aldeído desidrogenases, além de proteínas envolvidas na defesa celular contra agentes oxidantes como a peroxiredoxina mitocondrial e superóxido dismutase dependente de Manganês. No período de 22 horas de transição dimórfica de micélio para levedura ocorre a indução de proteínas da via da pentose fosfato, possivelmente para produzir substrato para a glicólise que é induzida na fase de levedura, além da indução de proteínas de resposta ao choque térmico (REZENDE et al., 2011).

2. JUSTIFICATIVA

A paracoccidiodomicose é a micose sistêmica mais prevalente em países como Brasil, Venezuela, Equador e Colômbia, com altas taxas de mortalidade, constituindo-se em um problema de saúde pública. Vários trabalhos têm demonstrado a plasticidade que espécies pertencentes ao complexo *Paracoccidioides* possuem em adaptarem-se a diferentes nichos do hospedeiro. De modo geral, os membros do complexo alteram vias metabólicas para sobreviver em um ambiente hostil, como aquele encontrado durante o processo infeccioso. Também, alteram a constituição da parede celular para evadir das respostas do sistema imune e ativam vias de sinalização para induzir o processo de transição dimórfica, essencial para o estabelecimento da doença. Apesar do avanço no conhecimento de genes e processos relacionados com a transição dimórfica, os mecanismos que controlam esse processo ainda não estão elucidados em membros do complexo *Paracoccidioides*.

Pequenos RNAs com funções regulatórias como microRNAs têm sido identificados em muitos microorganismos patogênicos e não patogênicos. Tais moléculas desempenham papel importante no processo infeccioso, favorecendo ou inibindo o desenvolvimento de doenças. Em muitos fungos, microRNAs-like são associados a respostas a mudanças ambientais, assim como ao desenvolvimento fúngico, em diferentes fases de crescimento. Estudos revelaram que membros do complexo *Paracoccidioides* possuem todos os genes que codificam as proteínas chave para produção de miRNAs e que possivelmente uma via de RNA de interferência seja ativa nestes patógenos. Além disso, microRNAs foram identificados em vesículas secretadas por esses fungos. Portanto, visto a relevância do conhecimento de mecanismos desenvolvidos por este fungo para sobrevivência e regulação de processos biológicos, estudar o papel de microRNAs-like é relevante. Além disso, a possível presença de microRNAs-like em diferentes estádios de desenvolvimento do fungo, abre perspectivas para investigações da função destas moléculas durante o processo infeccioso no hospedeiro.

3. OBJETIVO

3.1 Objetivo geral

O presente trabalho tem como objetivo geral identificar e caracterizar microRNAs-like produzidos por *P. brasiliensis* nas formas miceliana e leveduriforme e durante a transição dimórfica, micélio-levedura, a qual precede o processo infeccioso no hospedeiro.

3.2 Objetivos específicos

- Analisar *in silico* proteínas homólogas em *Paracoccidioides* spp. envolvidas na via de silenciamento gênico pós-transcricional;
- Identificar *in silico* possíveis microRNAs-like através de ferramentas de bioinformática;
- Confirmar a predição *in silico* dos possíveis microRNAs-like por reação de RT-PCR qualitativa;
- Quantificar a expressão relativa dos genes que codificam para as proteínas dicers e argonautas, em diferentes fases de crescimento deste fungo;
- Avaliar o conjunto de microRNAs-like produzidos por micélio, micélio em transição para leveduras e células leveduriformes;
- Determinar o nível de expressão dos microRNAs-like entre as diferentes fases de *P. brasiliensis*;
- Identificar os possíveis alvos dos microRNAs-like entre os estágios específicos e inferir os possíveis processos biológicos realizados.



Capítulo 2

***In silico* characterization of microRNAs-like sequences in the genome of
Paracoccidioides brasiliensis Pb18**

**Juliana S. de Curcio^{1,2}; Mariana P. Batista¹; Juliano D. Paccez¹; Evandro Novaes³;
Célia Maria de Almeida Soares^{1*}.**

1-Laboratório de Biologia Molecular, Instituto de Ciências Biológicas, Universidade Federal de Goiás, Brasil, Campus II Samambaia, CEP: 74690-900.

2-Programa de Pós-Graduação em Patologia Molecular, Faculdade de Medicina, Universidade de Brasília, Brasil, CEP:70910-900.

3-Universidade Federal de Goiás, Escola de Agronomia, Setor de Melhoramento de Plantas, Campus II Samambaia, Rodovia Goiânia a Nova Veneza, CEP: 74.690-900.

Short running title: MicroRNAs-like in *P. brasiliensis*.

Keywords: fungi; mycoses; dicer; argonaute; microRNAs

julianadecurcio1@gmail.com

marianabiomed@gmail.com

julianopaccez@gmail.com

evnovaes@gmail.com

*Correspondence and reprints: Tel +55 62 35211736; cmasoares@gmail.com

Abstract

Eukaryotic cells have different mechanisms of post-transcriptional regulation. Within these mechanisms exist the microRNAs, such molecules promote regulation of the target by cleavage or degradation of the mRNA. Fungi of the complex *Paracoccidioides* are the etiological agents of the main systemic mycosis of Latin America. These fungi present a plasticity to adapt and survive in different conditions, so the presence of microRNAs-like could be part of one of the mechanisms that influence this process. In fact, microRNAs produced by the host influence the progression of this mycosis in the lungs besides regulating targets involved in apoptosis and immune response. Therefore this work analyzes the presence of regions in the genome of this fungus with potential to be regions encoding microRNAs-like. Here we show that by analysis of sequence similarity the presence of 18 potencies regions for microRNAs-like in *Pb18* genome. We have too described the conservation of dicers and argonauts proteins and the transcripts encoding these proteins are induced in the parasitic phase. Therefore, we predict that this work will be a starting point for the analysis of the presence of these molecules between the different morphological stages of this fungus and its influence on fungal development.

Introduction

MiRNAs were originally identified in *Caenorhabditis. elegans* (Lee *et al.*, 1993), and since then have been described in animals, plants and algae (Zhao *et al.*, 2007; Grimson *et al.*, 2008). In fungi, the first identified miRNAs-like were described in *Neurospora crassa* and *Cryptococcus neoformans* (Lee *et al.*, 2010; Jiang *et al.*, 2012). Subsequently, several studies demonstrated the presence of miRNA-like structures in different species of fungi such as *Metarhizium anisopliae*, *Sclerotinia sclerotiorum*, *Penicillium marneffeii*, *Trichoderma reesei*, *Fusarium oxysporum*, *Aspergillus flavus* and *Penicillium chrysogenum* (Zhou *et al.*, 2012 ; Zhou *et al.*, 2012; Lau *et al.*, 2013; Kang *et al.*, 2013; Chen *et al.*, 2014; Bai *et al.*, 2015), Dahlmann and Kück 2015). In fungi such as *Neurospora crassa* different pathways are involved in the production of a microRNAs-like, for example the milR-1 are produced dependent on protein dicers and argonauts qde-2p, unlike the biogenesis of milR-2 is independent of dicers, although protein argonaut qde-2p, with its catalytic site, is required for the production of pre-milRNA and mature milR-2 (Lee *et al.*, 2010).

MicroRNAs act in pathways of cellular differentiation, tumorigenesis, heart disease and cellular signalling. Furthermore, several studies have demonstrated how fungi can alter the expression profile of host microRNAs. Process regulated by microRNA from host during the development mycoses includes cell cycle, macrophage polarization, chemokine expression, granulocyte production (Croston *et al.*, 2018). For example, analyzes of profile microRNAs produced by lungs, during the process of germination of *A. fumigatus*, characterized different levels of expression of the microRNA and mRNA between viable and non-viable conidia. In this sense, repressed microRNAs in lungs infected with viable conidia include miR-29a-3p, miR-30c-5p targeted of these microRNAs include genes involved in the inflammatory response such as *Clec7*, *SMAD2/3* and *TGF-β*. The genes *Clec7a* elicit an inflammatory response due to the recognition of β -glucan on the hyphal cell wall. The TGF- β

signaling pathway includes the transcription factors MDES, in these sense microRNAs that regulate these transcripts have been repressed in macrophages. In fact, the process of germination of conidia induces in of allergic inflammation in the lungs (Croston et al., 2016).

Analysis of the expression pattern of microRNAs produced by dendritic cells after contact with *Aspergillus fumigatus* and *Candida albicans* revealed a specific response of microRNAs to the infection caused by these fungi, and some of the microRNAs induced after contact with these pathogens were miR-212 and miR-132. The expression of these microRNAs is associated with the antifungal response measured by dendritic cells, since targets of these small RNAs are associated with genes involved in the immune response during the host infection process (Dix et al., 2017).

In systemic infections the presence of a pathogen often induces a significant change in the expression profile of circulating microRNAs in the host. In this context Singulani and collaborators 2017, analysed the expression profile of microRNAs produced by patients with Paracoccidioidomycosis (PCM) and healthy individuals. The data of the work pointed to an induction of the expression of eight microRNAs among the individuals with PCM. Apoptosis, immune response and adhesion of the fungus host cells are possible processes regulated by differentially expressed microRNAs, thus demonstrating the influence of these molecules on the pathogen-host interaction process. In addition, according to the authors, the presence of circulating microRNAs in the serum of PCM patients may be a possible alternative for obtaining biomarkers of the infection.

The comparison of the histopathological changes observed in the lungs of mice infected with *P. brasiliensis* at 28 and 56 days after infection correlates with the level of expression of the microRNAs produced by this organ. In fact, within 28 days of infection, the lungs shown the presence of granulomas with infiltrates of giant cells, bordering the fungal cells, and the presence of phagocytic cells, however in 56 after the infection the lungs

presented a low number of yeasts, characteristic of resolution of the infection. In parallel, the analyzes of 84 microRNAs involved in inflammatory responses were differentially regulated between the two periods of mycosis development. In this sense, microRNAs induced at 56 days after lung infection could act to reduce damage to lung tissues, as for example the MiRNA-26b-5p, this molecule negatively regulates the expression of IL-6 and the presence of this interleukin increases in the population of regulatory T cells, in this way this microRNA could influence the amount of T cells after 56 infection (Marioto et al., 2017).

Paracoccidioidomycosis (PCM) is an endemic systemic mycosis caused by fungi of the genus *Paracoccidioides* (Restrepo, 1985, Turissini et al., 2017). It is estimated that approximately 80% of the patients who acquire this disease are Brazilian, the rest of the cases occur mainly in Colombia, Venezuela, Argentina and Ecuador. The lethality rate of this disease is 3% to 5% and the number of cases in Brazil per year varies from 3360 to 5600 (Martinez, 2017)

Although miRNAs-like have already been described in pathogenic microorganisms, and microRNAs produced by the host, are modulated in response to fungal infections, the information about the presence of microRNAs-like in *Paracoccidioides* spp. is limited. In this work, we sought to identify, in the genomes of members of the *Paracoccidioides* genus, proteins involved in the post-transcriptional gene silencing pathway mediated by miRNAs, and we evaluated the level of expression of transcripts encoding these proteins in the parasitic phase of *P. brasiliensis* Pb18. Using miRNA-like sequences identified in other fungi such as (*Neurospora crassa*, *Cryptococcus neoformans* and *Penicillium marneffei*) we performed *in silico* identification of sequences of miRNAs-like in the genome of *P. brasiliensis* Pb18. In general, we identified dicers and argonaut proteins conserved in species of the *Paracoccidioides* complex and identified sequences in the genome of *P. brasiliensis* Pb18 with potential to be regions of microRNAs-like genes To our knowledge, this work it is

indeed that is an in-dept in *silico analysis* added of experimental results of the presence of microRNA-like coding regions in this important human pathogen.

Materials and methods

In *silico analysis* of homologous proteins in *Paracoccidioides* spp. involved in the post-transcriptional gene silencing pathway

The sequences of dicer and argonaute proteins, present in the UNIPROT database, were used for searching homologous proteins in *Paracoccidioides* spp. We compared these sequences with those described for other fungi species: *N. crassa*, *C. neoformans* H99, *Histoplasma capsulatum*, *Aspergillus nidulans* and *A. fumigatus* (Galagan *et al.*, 2003; Nakayashiki *et al.*, 2006; Janbon *et al.*, 2010). Prediction of similarity and identity among homologous proteins was performed using the BLASTp tool from the NCBI database. Sequences alignment and protein domain prediction were performed using the CLUSTALX2 and PFAM databases respectively (Larkin *et al.*, 2007; Finn *et al.*, 2015).

Phylogenetic analysis of RNA-induced silencing complex proteins in fungi

RNA-induced silencing complex proteins, dicer and argonaute, from *Paracoccidioides* spp., *N. crassa*, *C. neoformans* H99, *H. capsulatum*, *A. nidulans*, *A. fumigatus* and other fungi, were used for phylogenetic analysis. A phylogenetic tree was constructed by multiple sequence alignments using CLUSTALX2. The tree was generated by neighbor-joining method and visualized by TreeView software (Saitou and Nei 1987; Thompson *et al.*, 1997). Robustness of branches was estimated using 10.000 bootstrapped replicates. The accession numbers for each gene used in this comparison are described in supplementary table 1.

Culture and maintenance of *P. brasiliensis* and RNA extraction

Yeast cells from *P. brasiliensis* Pb18 (ATCC 32069) were cultivated in Sabouraud media at 36°C (Sharma *et al.*, 2010). After five days growing in solid media, yeast cells were

inoculated in liquid media and cultivated for 18 h at 36°C at 150 rpm, as previously described (Silva-Bailão *et al.*, 2014).

Detection of genes from the RNA-induced silencing complex in *P. brasiliensis*

Detection of genes involved in the post-transcriptional gene silencing pathway was performed by qRT-PCR. The primer sequences for amplification of Dicer 1 (*dcr 1*), Dicer 2 (*dcr 2*), Argonaute 1 (*ago-1*), Argonaute 2 (*ago-2*) and Actina (*act*) are described in (Table S2). In brief, total RNA extracted from *P. brasiliensis* was treated with DNase (RQ1 RNase-free DNase, Promega) and subjected to *in vitro* reverse transcription (SuperScript III First-Strand Synthesis SuperMix; Invitrogen, Life Technologies) following the manufacturer's recommendation. cDNA were used in the qRT-PCR reaction in the Step OnePlus platform (Applied Biosystems), using a mixture of SYBR green PCR master mix (Applied Biosystems, Foster City, CA). Normalization of the values was performed using the gene encoding the actin protein (GenBank XP_010761942). The standard curves were generated by dilution of the cDNA at 1:5 and the relative expression levels of the transcripts were calculated using the standard curve method for relative quantification (Bookout *et al.*, 2006).

***In silico* prediction of miRNAs-like molecules in *P. brasiliensis* genome**

For *in silico* prediction of miRNAs-like molecules in the genome of *P. brasiliensis*, search in the literature was performed in order to obtain sequences of mature miRNAs-like described in other fungi, including *Fusarium oxysporum*, *P. marneffei*, *Aspergillus flavus*, *Trichoderma reesei*, *Metarhizium anisopliae*, *C. neoformans*, *N. crassa* and in extracellular vesicles of *C. neoformans*, *Candida albicans*, *Saccharomyces cerevisiae* and *P. brasiliensis* (Lee *et al.*, 2010; Jiang *et al.*, 2012; Zhou *et al.*, 2012; Lau *et al.*, 2013; Kang *et al.*, 2013; Chen *et al.*, 2014; Peres da Silva *et al.*, 2015; Bai *et al.*, 2015).

Data of miRNA-like described in the literature were subjected to Blastn against the *P. brasiliensis* Pb18 genome, using the task blastn-short option of the Blastn program (Camacho

et al., 2009). Using a threshold with E-value <0.10, the alignments were obtained with at least 16 bp, and identities above 95%. The results were converted into GFF files, through a custom script written in Perl. The GFF file contains information about the position of genes, or any other element in the reference genome. The InrsectBED tool from package BEDTools (Quinlan and Hall 2010) was employed for identifying the position of the blast hits in relation to the annotation of the *P. brasiliensis* genome. Only the sequences of mature miRNAs-like which were not recorded in gene regions were considered for further analysis. After these steps, one Fasta file containing the sequences of the mature miRNAs-like that aligned to the genome of *Pb18* in non-gene regions was generated. The data in Fasta file format was obtained considering 35 pb or 50bp above or below the alignment region.

These sequences were analyzed for their secondary structure, seeking to identify those that form secondary hairpin structures, similar to those of known pre-miRNA. The sequences in the Fasta file were submitted for analysis in the RNAFold database. The sequences of potential miRNAs were manually revised using the following parameters: (A) The minimum size of the pre-miRNA could not be less than 45 nucleotides; (B) The pre-miRNA folded into the perfect stem-loop hairpin secondary structure; (C) The values of the minimum free energy (MFE) of folding should be at least -7 kcal/mol; (D) Maximum mismatch of six between the miRNA/miRNA* duplex, (*) the similar-sized fragment derived from the opposing arm of the pre-microRNA. These criteria were adopted to predict the true microRNAs-like (Dehury *et al.*, 2013). As the size of the pre-miRNA is variable and, in our study, unknown, in some cases, we adjusted the size of the retrieved regions upstream and downstream (35-50 bp) of the alignment to search for a typical miRNA hairpin structure with RNAfold (Lorenz *et al.*, 2011a, Lorenz *et al.*, 2016b). Manual checking of real pre-microRNAs has already been used in other bioinformatics works, such as the work of Dehury *et al.*, 2013. All MFEs were expressed as negative kcal/mol. Adjusted MFE (AMFE) represented the MFE of 100

nucleotides. It was calculated by $(\text{MFE} \div \text{length of RNA sequence}) \times 100$. The minimal folding free energy index (MFEI) was calculated by the equation: $\text{MFEI} = \text{AMFE} / (\text{G+C}\%)$ (Zhang *et al.*, 2006).

Polyadenylation, Reverse Transcription and Poly(T) adaptor RT-PCR

After the *in silico* prediction of similar microRNAs-like in the genome of *P. brasiliensis* *Pb18*, five potential candidates were chosen for the validation experiments. This choice was based on the MFE values. We chose the predicted microRNAs-like between the highest MFE values: *Pb-milR-11/Superconting_2.3:1128222-1128358(-)*; *Pb-milR-7/Superconting_2.6:955763_955879(+)*; *Pb-milR-6/Superconting_2.5:587199-587317(-)* and *Pb-milR-1/Superconting_2.14:171583_171670(+)*. We also chose a candidate with the lowest MFE value *Pb-milR-4/Superconting_2.12:21200_21275(-)*. Validation experiments of microRNAs-like employed the the poly a tail method (Balcells *et al.*, 2011). Initially, yeast and mycelium cells of *Pb18* were cultured in Sabouraud medium (Sharma *et al.*, 2010) for 18 h and the RNA of both conditions was extracted by the method of TRIzol® reagent (Sigma). Total extracted RNA was treated with DNase (RQ1 RNase-free DNase, Promega). The treated total RNA (3 µg) was polyadenylated with ATP by poly(A) polymerase (Biolabs); for polyadenylation reaction the following reagents were used: 4 µl of 10 x PolyA buffer; 4 µl of 10 mM ATP; 0.4 µl of PoliA polymerase corresponding to 2 units and 3 µg of RNA. Water was used to complete the reaction to a final volume of 20 µl. The reaction of polyadenylation was performed with the following steps: 37°C for 75 min, 65°C for 25 min according to manufacturer's instructions. After this step, the polyadenylated RNAs were submitted to the reverse transcription with SuperScript™ II Reverse Transcriptase (Invitrogen). For the synthesis of cDNA the following reagents were used: 0.8 µl of 20 nM of poly(T) adaptor; 4 µl of 10 mM dNTPS; 8 µl of 5 x buffer; 1.5 µl of 25 mM MgCl₂; 0.5 µl of RNase inhibitors; 1.25 µl of Reverse transcriptase and 5 µl of Polyadenylated RNA. The conditions for the cDNA

synthesis were: 42°C for 2 h and 15 min and 85°C for 10 min. The qualitative RT-PCR was performed under the following conditions: 2 min at 94°C, followed by 40 cycles each of 95°C for 15 sec, 57°C or 57.6°C for 5 sec, and 72°C for 20 sec and a final elongation step at 72°C for 5 min. After, this step the products from reaction were visualized on 3% agarose gel, and the size of the bands of the potential microRNAs-like present on the agarose gel were calculated by linear regression. The primers used for the amplification of microRNAs-like were described in Table S2.

Results

***In silico* analysis indicates the presence of proteins involved in post-transcriptional gene silencing in *Paracoccidioides* spp.**

The steps for *in silico* prediction of proteins involved in gene silencing by RNA interference as well as potential miRNAs-like are shown in the flowchart of the overall study depicted in (Figure S1). Our analysis allowed the identification of dicers and argonaute proteins in *Paracoccidioides* spp. (Table 1). We observed that *P. brasiliensis* (Pb18), *P. americana* (Pb03) and *P. lutzii* (Pb01) present two dicers (Dcr-1p and Dcr-2p) and two argonaute (Ago-1 and Ago-2) proteins. *C. neoformans* Serotype D presents two paralogous genes for argonaute (*ago1* and *ago2*) and dicer (*dcr1* and *dcr2*). On the other hand, *C. neoformans* serotype A (H99) contains single genes for argonaute (*ago1*) and two paralogous genes for dicers (*dcr1* and *dcr2*) (Janbon *et al.*, 2010). Studies with *N. crassa* demonstrated the presence of two genes that encode for dicer (*qde-2* and *dcr*) and two that code for argonaute (*Sms-2* and *Sms-3*) (Galagan *et al.*, 2003). Analysis demonstrated that *A. nidulans* genome has only one gene that codes for dicer (ANID_10380) and one that codes for argonaute (ANID_01519), while *A. fumigatus* contains homologue genes that encode for two dicers (AFUA_5G11790/AFUA_4G02930) and two argonaute proteins (AFUA_3G11010/AFUA_8G05280) (Nakayashiki *et al.*, 2006; Janbon *et al.*, 2010). The

comparison of the amount of proteins involved in post transcriptional gene silencing in fungi of the *Paracoccidioides* complex are similar to that seen in other fungi. Furthermore, analysis of identity indicates major similarity amongst proteins from *Paracoccidioides* spp., *H. capsulatum* and *A. fumigatus* (Table 1).

Table 1. *In silico* prediction of proteins potentially involved in post-transcriptional gene silencing machinery in *Paracoccidioides* spp.

Proteins ^a	Identity/e-value ^b	Identity/e-value ^b	Identity/e-value ^b	Identity/e-value ^b	Identity/e-value ^b	Identity/e-value ^b
Argonaut 1 ^c	<i>C. neoformans</i> (H99) CNAG_04609	<i>N. crassa</i> NCU09434	<i>A. fumigatus</i> Af230 Afu3g11010	<i>A. nidulans</i>	<i>H. capsulatum</i> H143 HCDG_08528	<i>H. capsulatum</i> G186AR HCBG_06692
<i>P. brasiliensis</i> (Pb18) PADG_00716	28%/2 e-81	40%/0.0	54%/0.0	ND	76%/0.0	76%/0.0
<i>P. americana</i> (Pb03) PABG_02302	28%/2 e-82	40%/0.0	54%/0.0	ND	74%/0.0	74%/0.0
<i>P. lutzii</i> PAAG_11422	28%/2e-80	40%/9e-179	54%/0.0	ND	74%/0.0	74%/0.0
Argonaut 2 ^c	<i>C. neoformans</i>	<i>N. crassa</i> NCU04730	<i>A. fumigatus</i> Af230 Afu8g05280	<i>A. nidulans</i> ANID_01519	<i>H. capsulatum</i> H143 HCDG_00823	<i>H. capsulatum</i> G186AR HCBG_03944
<i>P. brasiliensis</i> (Pb18) PADG_03108	ND	37%/2 e-177	50%/0.0	49%/0.0	78%/0.0	76%/0.0
<i>P. americana</i> (Pb03) PABG_00673	ND	37%/7e-175	50%/0.0	49%/0.0	78/00	76%/0.0
<i>P. lutzii</i> PAAG_03231	ND	37%/7e-175	50%/0.0	49%/0.0	78%/0.0	77%/0.0
Dicer 1 ^c	<i>C. neoformans</i> CNAG_02745	<i>N. crassa</i> NCU08270	<i>A. fumigatus</i> Afu5g11790	<i>A. nidulans</i>	<i>H. capsulatum</i> H143 HCDG_06891	<i>H. capsulatum</i> G186AR HCBG_01751
<i>P. brasiliensis</i> (Pb18) PADG_11946	29%/2 e-38	39%/0.0	53%/0.0	ND	62%/0.0	72%/0.0
<i>P. americana</i> (Pb03) PABG_04917	24%/4e-37	40%/0.0	54%/0.0	ND	67%/0.0	70%/0.0
<i>P. lutzii</i> PAAG_11489	24%/3e-33	38%/0.0	53%/0.0	ND	65%/0.0	71%/0.0
Dicer 2 ^c	<i>C. neoformans</i>	<i>N. crassa</i> NCU06766	<i>A. fumigatus</i> Afu4g02930	<i>A. nidulans</i> ANID_10380	<i>H. capsulatum</i> H143 HCDG_06620	<i>H. capsulatum</i> G186AR HCBG_01136
<i>P. brasiliensis</i> (Pb18) PADG_07189	ND	32%/0.0	38%/0.0	37%/0.0	70%/0.0	68%/0.0

<i>P. americana</i> (Pb03) PABG_05105	ND	32%/0.0	38%/0.0	37%/0.0	70%/0.0	68%/0.0
<i>P. lutzii</i> PAAG_00072	ND	34%/0.0	39%/0.0	37%/0.0	70%/0.0	69%/0.0

a) Predicted name of the protein involved in the post-transcriptional gene silencing mediated by miRNAs;

b) The sequence identity values and e-value were obtained through the BLASTp tools of the NCBI database;
(http://blast.ncbi.nlm.nih.gov/Blast.cgi?PROGRAM=blastp&PAGE_TYPE=BlastSearch&LINK_LOC=blasthome)

c) Proteins of *Paracoccidioides* spp. homologous to *C. neoformans* (H99), *N. crassa*, *A. fumigatus*, *A. nidulans*, *H. capsulatum* G186AR and H143 strains.
N.D. (non described).

Phylogenetic analysis of Ago-1p and Ago-2p, Dcl-1p and Dcl-2p showed that the corresponding sequences present in *Paracoccidioides* spp. are closely related to *Blastomyces dermatitidis*, *H. capsulatum*, *P. chrysogenum* and *Aspergillus* spp. (Supplemental Fig S2). With phylogenetic distances of 0.98 to 1 from this homology found in phylogenetic analysis, we can infer that the proteins are orthologous, possibly having a similar function between different fungi. In fact, a study by Lau and colleagues (2013) shows that Dcl-2p from *P. marneffei* is more closely related to those of the thermal dimorphic pathogenic fungi *H. capsulatum*, *B. dermatitidis*, *P. brasiliensis* and *C. immitis* than to *P. chrysogenum* and *Aspergillus* spp.

Post-transcriptional gene silencing machinery is highly conserved in *Paracoccidioides* spp. and other fungi species.

Prediction of protein domains performed using the PFAM database allowed the identification of conserved domains in dicers and argonautes (Figure 1). It is important to highlight that the main components involved in miRNAs processing and gene silencing includes RNA polymerase (Pol II), dicer and the silencing complex induced by RNA (Bartel *et al.*, 2004). Studies analyzing domains from the canonical dicer of *N. crassa* Dcr-2p demonstrated the presence of DEAD box, Helicase C, ribonuclease 3 and dicer dimerization domains. Dicer 1 from *N. crassa* contains at its N-terminal region a RESIII domain instead of DEAD box. The homologue from *C. neoformans* has only the ribonuclease 3 and dicer dimerization domains (Janbon *et al.*, 2010). Analysis of Dcr-1p protein from *Pb18* and *P. lutzii* (*Pb01*) indicates similarity to the homologue protein found in *C. neoformans*, since it possesses just dicer dimerization and Ribonuclease III domains (Figure 1A). On the other hand, analysis of the same homologue in *Pb03* demonstrated higher similarity to dicer dimerization, Ribonuclease III and RESIII domains found in the *N. crassa* homologue (Figure

1A). Therefore, we can conclude that the general domain arrangement in of this protein is not fully conserved in members of the complex *Paracoccidioides*.

Furthermore, analysis of protein domains from *Paracoccidioides* spp. demonstrated that Dcr-2p contains the Dicer dimerization, DEAD/DEAH box, Helicase C, and Ribonuclease domains similar to those present in other dimorphic and filamentous fungi, except *H. capsulatum* (H143) (Figure 1B). Comparing the members of the *Paracoccidioides* complex, depicted in (Figure 1), it is evident that Dcr-2p is conserved among members of those organisms.

Previous studies described the dicer dimerization domain as being similar to the binding domain of dsRNA (Dlakić 2006), while the DEAD/DEAH box helicase domain interacts with the pre-miRNA loop, helping the alignment of this molecule to the RNase III domain for precise cleavage of pre-miRNA (Tsutsumi *et al.*, 2011). Additionally, the Helicase C domain binds to the dsRNA loop region and checks the size. Furthermore, this domain also measures the distance between two adjacent nucleotides in the region of the 3' mRNA molecule, with the loop region verifying the pre-miRNA sequence before cutting (Tsutsumi *et al.*, 2011). Dicers proteins have a Ribonuclease III domain responsible for the cleavage of pre-miRNA, generating a duplex of small RNAs with two adjacent nucleotides in the 3' end (Zhang *et al.*, 2004). In this regard, our data suggest that these proteins are able to process double-stranded RNA, since we identified conserved domains among dicers from *Paracoccidioides* spp.

Our data also indicate that Ago-1p from *Paracoccidioides* spp. contains PIWI, PAZ, ArgoL1, ArgoL2, ArgoMid2 and ArgoN domains (Figure 1C), while Ago-2p contains PIWI, PAZ, ArgoL1, ArgoL2 and ArgoN domains (Figure 1D). Analysis of argonaute proteins from *N. crassa*, *P. chrysogenum*, *P. marneffeii* and *C. neoformans* indicates the presence of PAZ and PIWI domains that are conserved among different species of fungi and that play a role in

RNA interference processes (Nakayashiki 2005; Joshua-Tor 2006; Janbon *et al.*, 2010; Lau *et al.*, 2013; Dahlmann and Kück 2015). Interestingly, the PIWI domain present in argonaute shows a tertiary structure similar to the RNase H family and has been described as being involved in targeting mRNA cleavage, while the PAZ domain is responsible for the binding and transfer of small RNAs for the RISC complex (Lingel *et al.*, 2003; Yan *et al.*, 2003; Song *et al.*, 2004).

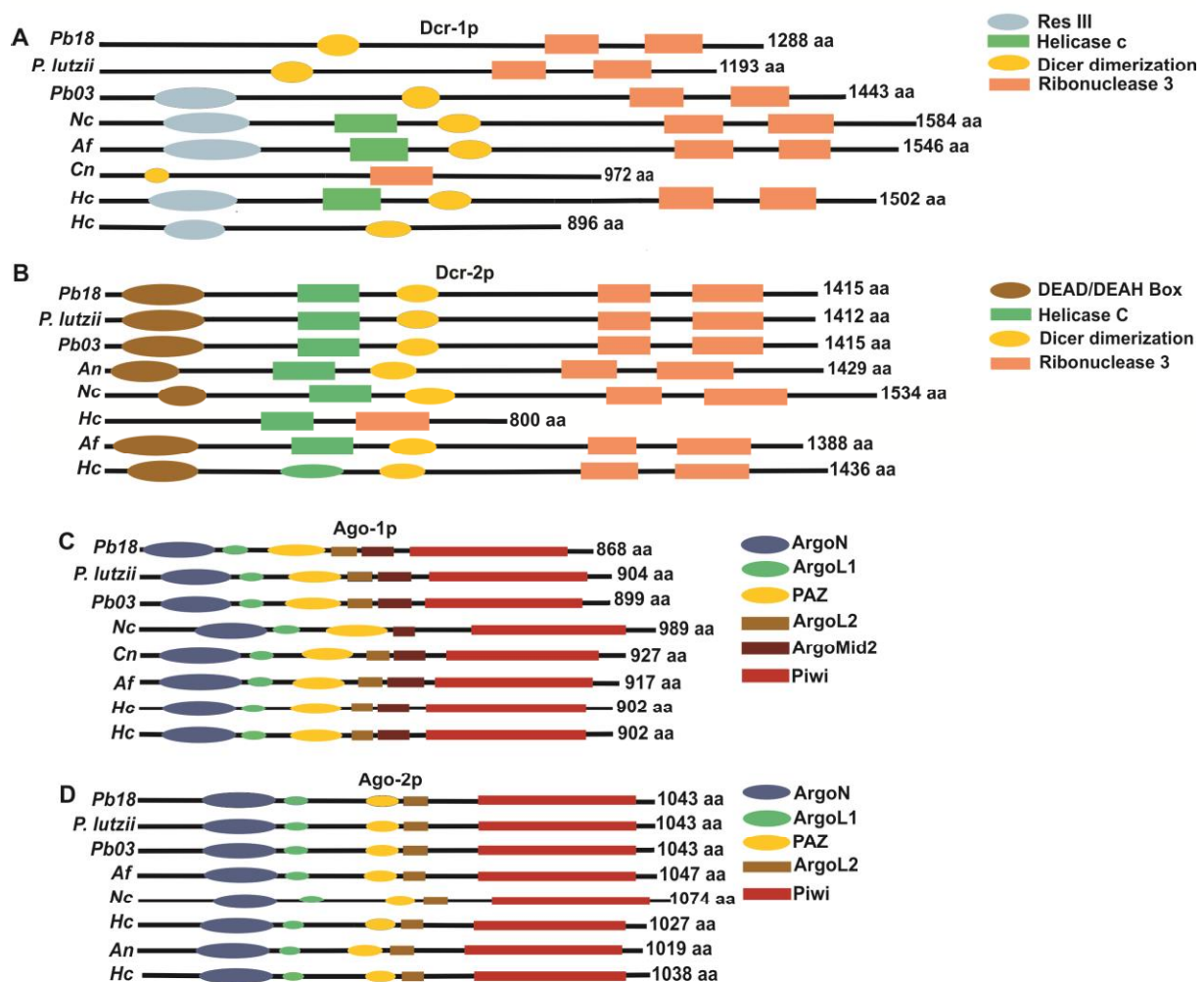


Figure 1- Domains identified in proteins involved post-transcriptional gene silencing pathway. (A-D) Domains present in dicers and Argonaute proteins from *Pb18*, *P. lutzii* (01) and *Pb03*. The access numbers of the proteins are as follows. **Dicer 1:** (PADG_11946; PABG_04917; PAAG_11489; NCU08270; Afu5g11790; CNAG_02745; HCBG_01751; HCDG_06891), **Dicer 2:** (PADG_07189; PAAG_00072; PABG_05105; ANID_10380; NCU06766; HCDG_06620; Afu4g02930; HCBG_01136) **Ago1:** (PADG_00716; PAAG_11422; PABG_02302; NCU09434; CNAG_04609; Afu3g11010; HCBG_06692; HCDG_08528) **Ago2:** (PADG_03108; PAAG_03231; PABG_00673; Afu8g05280; NCU04730; HCBG_03944; ANID_01519; HCDG_00823).

After *in silico* prediction of proteins involved in gene silencing mediated by miRNAs-like, the identification of transcripts encoding these proteins was performed by qRT-PCR. We performed this study in *Pb18*, a highly investigated species in the *Paracoccidioides* complex. The transcripts were assessed in yeast cells cultivated at 18 h of growth. As observed in (Figure 2), transcription of dicers and argonautes are clearly detected in yeast cells after 18 h of growth. Detection of the transcripts encoding argonaute and dicer proteins reinforce our *in silico* data, depicting the active pattern of transcription of the cognate genes.

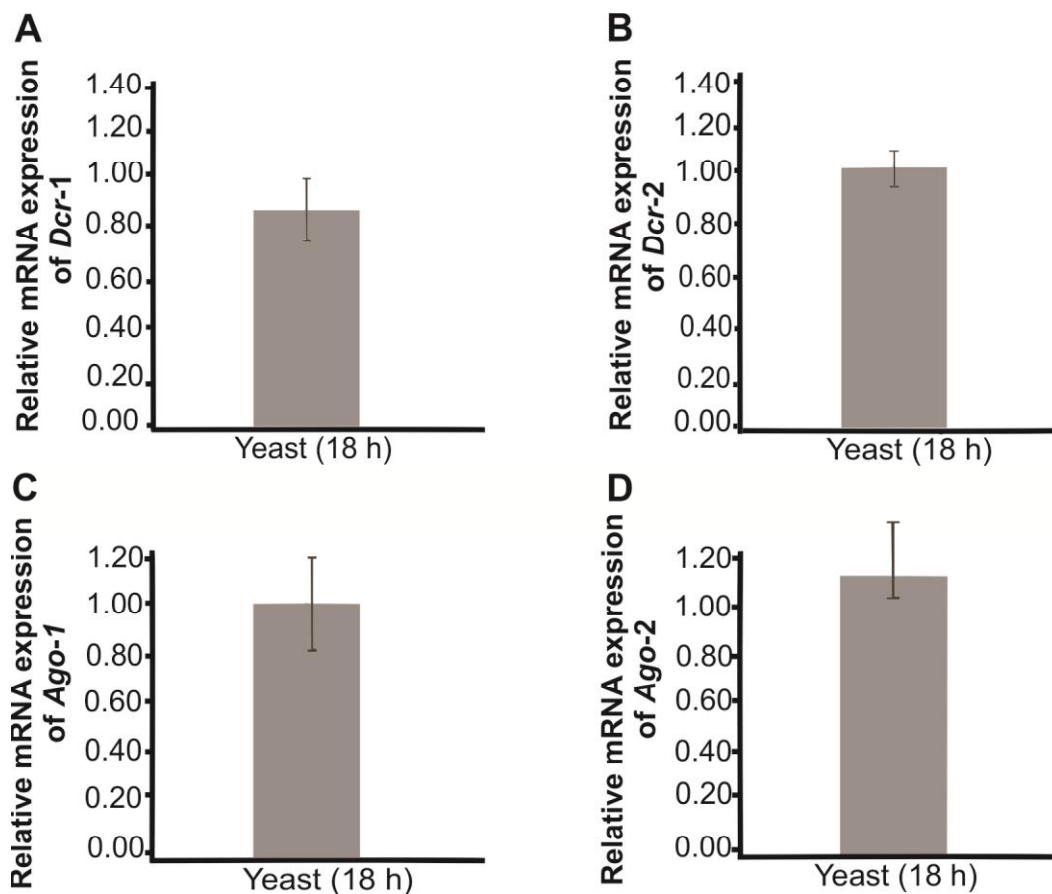


Figure 2-Genes involved in the processing of microRNAs-like are induced in the parasite phase of *Pb18*. Quantitative RT-PCR was performed with transcripts of *Pb18* yeast cells cultivated in liquid sabouraud medium for 18 hours. Expression values of genes involved in the processing of microRNAs (*dcr-1*, *dcr-2*, *ago-1*, *ago-2*) were calculated using actin as endogenous control. Data are expressed as mean \pm standard deviation from triplicates. Statistically significant difference was determined by Student's t-test (*p.0.05).

Identification of miRNAs-like sequences in *P. brasiliensis Pb18* genome

In order to identify putative miRNAs-like in the genome of *P. brasiliensis (Pb18)* we analyzed similarity between microRNA-like sequences characterized in fungi or present in

vesicles secreted by these microorganism with regions of the genome of *P. brasiliensis Pb18*. The sequences of miRNAs-like were obtained from literature as described in Materials and Methods. In the first group we analyzed the microRNAs-like ones characterized in other fungi, from this analysis we obtained the following results. We identified 134 potential miRNAs-like sequences, as demonstrated in (Table S3). Remarkably, amongst these miRNA-like sequences, our analysis demonstrated that 20 sequences aligned in the genome of *P. brasiliensis* with identity higher than 95% (Tables S3). Moreover, the analyzed sequences demonstrated a higher percentage of alignment with *A. flavus* (7.5%) and *N. crassa* (5%) genomes (Figure S3). Furthermore, we observed that seven sequences of the miRNAs-like matched all the criteria as described in the methodology (Dehury *et al.*, 2013) to be considered mature miRNA-like in *P. brasiliensis* (*Pb18*)'s genome (Table 2).

d) Name of miRNAs-like described in other fungi in the genome or in vesicles/ Minimum Free Energy predicted by RNAfold.

* a small variation in the position of the supercontings occurred in some cases due to the removal of some bases after alignment for better prediction of the secondary structure.

+ The microRNAs with similarity to *P. brasiliensis*, *C. albicans*, *C. neoformans* and *S. cerevisiae* were described in secreted vesicles and classified by the authors Silva et al., 2015 based only on similar sequences present in mirBase.

Analysis of the predicted secondary structure of those sequences corroborate with the features of a pre-miRNA hairpin and free energy folding (Table 2 and Figure 3A). In fact, all the Fasta sequences were analyzed in relation to these two characteristics by RNAFold. Additional analysis was performed using miRNAs-like sequences previously described to be present in secreted vesicles (Peres da Silva *et al.*, 2015). From a total number of 1477 miRNA sequences described in vesicles of other fungi species only 100 sequences aligned in the genome of *P. brasiliensis* with identity higher than 95% (Table S4). It is important to note that in many cases, the same miRNAs-like aligned in more than one region in the *P. brasiliensis* genome. From the total of 100 sequences that aligned in the genome of *P. brasiliensis*, only 11 presented all the criteria to be considered potential miRNAs-like (Dehury *et al.*, 2013) (Table 2 and Figure 3B). The microRNAs-like predicted *in silico* in *P. brasiliensis* Pb18 already described in other fungi are listed in (Figure 3A), whereas the microRNAs present in vesicles with similarity are demonstrated in (Figure 3B).

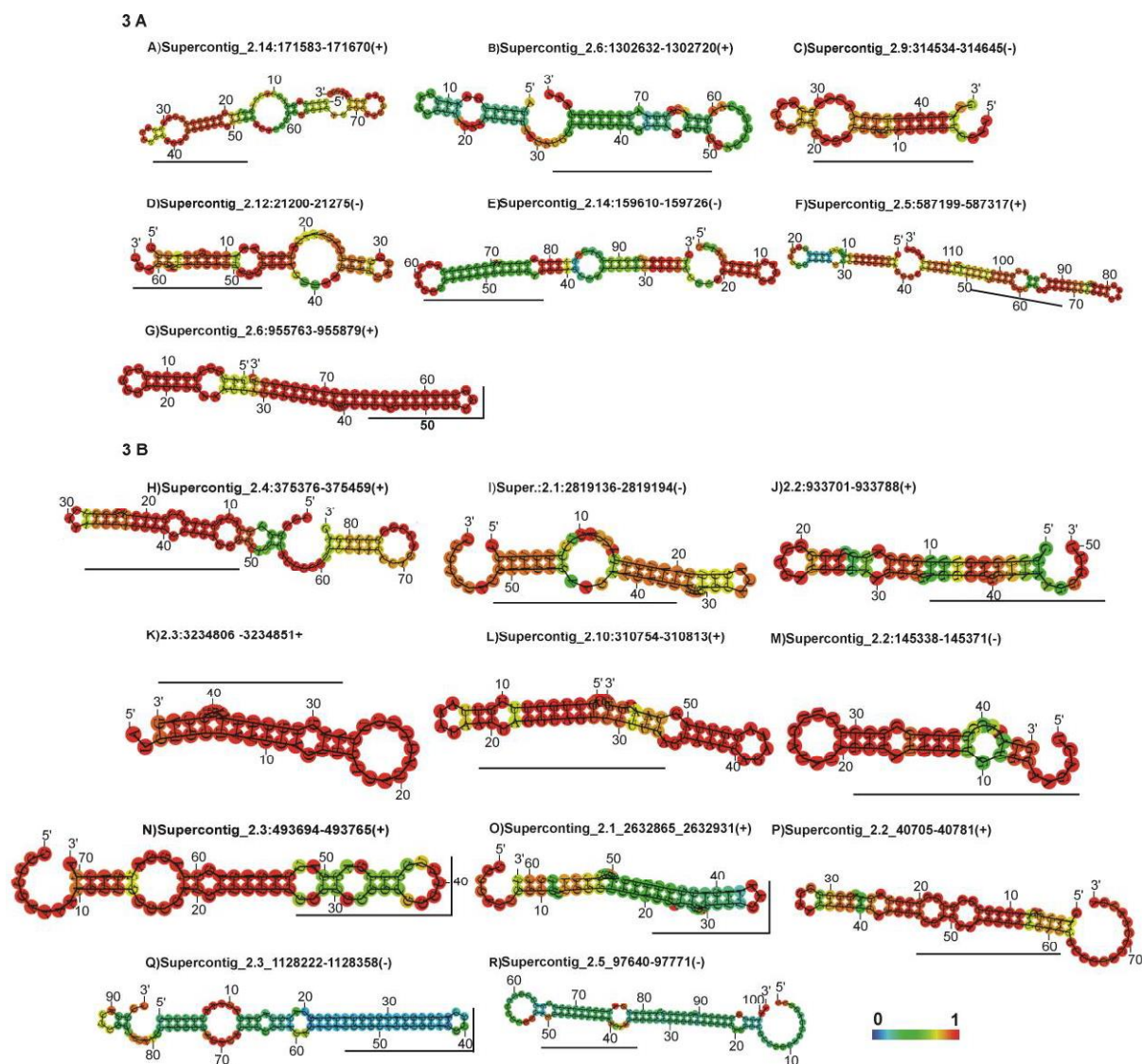


Figure 3- Representation of the newly-identified potential pre-miRNAs in *P. brasiliensis*. The matured miRNA portion is highlighted in the black bar. The structures were generated using the RFOLD program. The actual size of the precursors may be slightly shorter or longer than shown in the figures. The structures are colored according to the base pairing probabilities, the red color denotes high probability and the purple color demonstrates the low probability of a given base being paired or not, as represented in the color bar.

Here, *in silico* prediction approach based on the comparison with miRNAs-like data described in other fungi or present in secreted vesicles allowed the characterization of 18 potential miRNA-like sequences in the genome of *P. brasiliensis* (*Pb18*), with identity values above 95%, values of negative folding free energies between -7.60 kcal/mol and -33.30 kcal/mol (Tables 2 and 3) and hairpin formation. Previous reports have evaluated the Minimal folding Free Energy Index (MFEI) and the calculation of the Adjusted Minimal folding Free Energy (AMFE) (Zhang *et al.*, 2006). It is noteworthy that MFEI values found in plants vary

between 0.81 and 0.96, while their AMFE values are between 26 and 44 kcal/mol (Mishra *et al.*, 2015). In this work, we observed lower MFEI and similar AMFE values when compared to those described in plants (Table 3). We also evaluated other features of miRNA precursors such as the amount of uracil and adenine in their sequences. In fact, previous reports demonstrated that miRNA precursors have a higher percentage of these bases in their sequences (Zhang *et al.*, 2006). As demonstrated in (Table 3), the majority of the miRNAs precursors described in *P. brasiliensis* have high proportion of uracil and adenine in their sequence.

Table 3. Characteristics of miRNAs-like predicted in this study.

Number of microRNA ^a	Superconting ^b	Length ^c	MFE ^d	AMFE ^e	MFEI ^f	(G+C)% ^g	(A+U)% ^h
<i>Pb-milR-1*</i>	Super.:2.14:171583-171670(+)	17	-26.50	30.45	0.48	63.2%	36.80%
<i>Pb-milR-2</i>	Super.:2.6:1302632-1302720(+)	18	-14.10	17.62	0.42	41.25%	58.75%
<i>Pb-milR-3</i>	Super.:2.9:314534-314645(-)	18	-10.10	22.44	0.40	55.6%	44.44%
<i>Pb-milR-4*</i>	Super.:2.12:21200-21275(-)	16	-7.60	12.06	0.31	38.1%	61.9%
<i>Pb-milR-5</i>	Super.:2.14:159610-159726(-)	16	-18.90	18.9	0.55	34%	66%
<i>Pb-milR-6*</i>	Super.:2.5:587199-587317(+)	18	-26.70	22.62	0.58	39%	61%
<i>Pb-milR-7*</i>	Super.:2.6:955763-955879(+)	16	-28.56	36.61	0.69	52.56%	47.43%
<i>Pb-milR-8</i>	Super.:2.4:375376-375459(+)	17	-16.90	20.36	0.41	49.50%	50.60%
<i>Pb-milR-9</i>	Super.:2.1:2819136-2819194(-)	16	-10.50	20.19	0.56	35.8%	64.2%
<i>Pb-milR-10</i>	Super.:2.2:933701-933788(+)	16	-10.10	19.80	0.4	49.00%	51.00%
<i>Pb-milR-11*</i>	Super.:2.3:1128222-1128358(-)	16	-33.30	35.42	0.73	47.87%	51.06%
<i>Pb-milR-12</i>	Super.:2.10:310754-310813(+)	16	-15.19	25.74	0.63	40.67%	59.32%
<i>Pb-milR-13</i>	Super.:2.2:145338-145371(-)	17	-9.60	22.32	0.50	44.2%	55.8%
<i>Pb-milR-14</i>	Super.:2.3:493694-493765(+)	16	-15.20	21.4	0.41	52.11%	47.88%
<i>Pb-milR-15</i>	Super.:2.1:2632865-2632931(+)	16	-25.80	42.29	0.73	57.40%	42.60%
<i>Pb-milR-16</i>	Super.:2.2:40705-40781(+)	16	-26.30	34.60	0.71	48.60%	51.40%
<i>Pb-milR-17</i>	Super.:2.3:3234806-3234851(+)	17	-14.30	32.5	0.79	40.90%	59.1%

Pb-milR-18	Super.:2.5:97640-97771(-)	17	-27.80	27.52	0.58	47%	54%
------------	---------------------------	----	--------	-------	------	-----	-----

-
- a) Name of predicted microRNA-like in the genome of *P. brasiliensis* (Pb18);
 - b) Region of alignment;
 - c) Size of mature microRNA-like;
 - d) Minimum free energy predicted by RNA fold;
 - e) AMFE: adjust minimal folding free energy (kcal/mol);
 - f) MFEI: minimal folding free energy index;
 - g) Percentage of nucleotides (G/C) present in the pre-microRNA sequence;
 - h) Percentage of nucleotides(A/U) present in the pre-microRNA sequence. A small variation in the position of the supercontings occurred in some cases due to the removal of some bases after alignment for better prediction of the secondary structure.
- * microRNAs-like used for the validation experiments.

In general, the *in silico* analyzes, based on similarity of sequences allowed the identification of 18 potential microRNA-like coding regions, such sequences exhibited microRNAs-like characteristics such as hairpin structure, MFE values similar to those already described for microRNAs-like from other microorganisms, large amount of uracil, demonstrating that possibly these coding regions of microRNAs-like were conserved in the genome of this fungus.

Experimental validation of predictions of bioinformatics

The validation of our prediction data of bioinformatics were performed by qualitative RT-PCR, as depicted in (Figure 4), in which are presented the amplification of five potential microRNAs-like based on the highest and lowest MFE values. It is possible to detect the presence of three amplification products, putatively, the pri-microRNA, pre-microRNA and mature microRNA-like. Some articles in the literature have used this method to detect microRNAs in different cell types (He *et al.*, 2005; CHIBA *et al.*, 2012). Therefore, the presence of these amplification products suggests potential microRNAs-like conserved in the genome of this human pathogen, confirming the data predicted by bioinformatics.

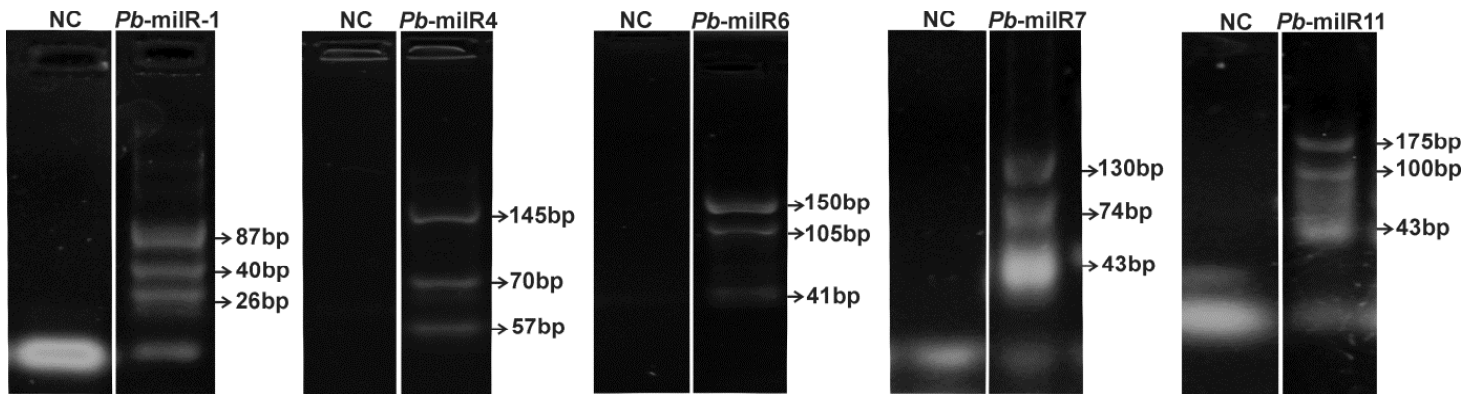


Figure 4- Qualitative RT-PCR of microRNAs-like predicted by bioinformatics tools. Five potential microRNAs-like based on the highest and lowest MFE values were used for the validation experiments, each sample ran individually on agarose gel 3%, the band sizes were predicted by the linear regression calculation. The RNA was obtained from *P. brasiliensis* Pb18.

Discussion

Proteins involved in the machinery of genetic silencing by RNA interference (dicers and argonautes) are conserved in fungi of different phyla including Ascomycota, Basidiomycota and Zygomycota (Drinnenberg *et al.*, 2009). Our analysis demonstrated that the number of proteins involved in the post-transcriptional gene silencing pathway in *Paracoccidioides* spp. are in line with data described in literature for other fungi such as *C. neoformans*, *A. fumigatus* and *N. crassa* that also present two paralogous genes for dicer and argonaute in their genomes (Galagan *et al.*, 2003; Nakayashiki *et al.*, 2006; Janbon *et al.*, 2010). In this regard, the conservation of domains in proteins involved in RNA interference in *Paracoccidioides* spp. demonstrates that these organisms retains components involved in the processing of miRNAs-like, as seen in other fungi (Lee *et al.*, 2010; Jiang *et al.*, 2012). In addition, after the phylogenetic analysis of our data, proteins involved in the processing of microRNAs-like in *Paracoccidioides* spp. were phylogenetically related to dimorphic fungi, and possibly dimorphic fungi would have conserved such proteins to perform similar functions (Lau *et al.*, 2013). The gene expression data reinforces the information, which in addition to retaining the complement of the microRNA-like processing in fungi of the

Paracoccidioides complex, support the concept that these genes are active in the parasitic form of the pathogen.

Different dicers and argonats proteins are required to produce microRNAs-like in fungi such as *N. crassa*. These proteins are specifically involved in the production of microRNAs-like between mycelium and yeast. For example, the dicer 2 protein is specifically involved in the production of two microRNAs-like exclusive of the mycelium phase from *P. marneffeii* (Lau et al., 2013). In addition, microRNAs-like too can be processed in canonical form using both dicers and argonats proteins (Lau et al., 2013). In fact our data demonstrate the expression of dicers and argonats in the yeast phase of this pathogen and in this same condition five microRNAs-like were identified, therefore possibly the expression of the transcripts encoding the proteins involved in the microRNAs process, correlates with the identification of these small RNAs. However which proteins are specifically involved in the production of these microRNAs-like is still not elucidated, and such question will be investigated.

The analysis of *in silico* prediction of microRNAs-like in *P. brasiliensis* Pb18 suggesting that this fungus retains regions in the genome responsible for the genesis of mature miRNAs. It has already been described in the literature that mature sequences of miRNAs are conserved in different kingdoms, demonstrating the importance of the conservation of those post-transcriptional gene regulation mechanisms (Lee et al., 1993; Chen et al., 2014). In fact, Peres da Silva and colleagues 2015 predicted possible miRNAs-like present in vesicles secreted by *P. brasiliensis* (Pb18), using a strategy based on similarity of sequences (Peres da Silva et al., 2015). Furthermore, 22 miRNA-like sequences were identified in the genome of *Humulus lupulus* employing *in silico* prediction of miRNAs based on similar sequences present in the miRBase database (Mishra et al., 2015).

The potential miRNAs-like predicted in this work originated from precursors which forms hairpin structures. During the formation of a mature miRNA, precursor molecules generate hairpins which are subsequently processed by dicer to form miRNA/miRNA* duplex (Bartel *et al.*, 2004). Previous reports demonstrated negative folding free energies of the precursors of PM-milR-M1 and PM-milR-M2 from *P. marneffeii* of -17.86 kcal/mol and -23.88 kcal/mol respectively (Lau *et al.*, 2013). In *A. flavus* values vary between -19.4 kcal/mol and -140.2 kcal/mol, and in *M. anisopliae* they vary between -20 kcal/mol and -105.32 kcal/mol (Bai *et al.*, 2015; Zhou *et al.*, 2012). In this context, values of negative folding free energies described in the present work are in agreement to those described in fungi, although in some cases the free energy values were lower. Interestingly, we obtained sequences of microRNA-like precursors of size similar to those described for other fungi (Zhou *et al.*, 2012). For example, in *C. neoformans* the sizes of the precursors of the miR1 and miR2 are approximately 70 nucleotides (Jiang *et al.*, 2012).

Additionally we found low MFEI and similar AMFE values in the sequences of the microRNA-like precursors. Although those indexes have not been described for miRNA-like precursors present in fungi, we hypothesize that the observed differences may be a result of the lower base complementarity between the precursor sequences present in fungi genome when compared to plants, where the complementarity of bases could be greater (Mishra *et al.*, 2015). In general, the data also demonstrate a higher amount of uracil in microRNA-like precursors as already described in the literature (Zhang *et al.*, 2006).

The experimental validation of some like microRNAs-like in this work allowed the characterization of sequences ranging in size from 26 to 57 bp. In other fungi, smaller sizes for mature microRNAs-like were seen as for example *N. crassa* (Lee *et al.*, 2010) and *C. neoformans* (Jiang *et al.*, 2012), *P. marneffeii* (Lau *et al.*, 2013), where detection of microRNAs-like was performed by Northern Blot. In this work the Poly(T) adaptor RT-PCR

method (Balcells *et al.*, 2011) adds a Poly A tail in the microRNA-like molecule, and possibly this process confers a larger size to the mature microRNA-like.

In brief the data of the work, demonstrate the conservation of proteins involved in the mechanism of gene regulation post-transcriptional in different species of the complex *Paracoccidioides*. The transcript that coding this protein were detected in the parasitic phases of one of the most prevalent species in Latin America and sequences of microRNAs-like were conserved in region of the genome from *P. brasiliensis Pb18*. Furthermore, five sequences beyond of the conserved in the genome were expresses. Therefore, our results point to the ability of species of the complex *Paracoccidioides* to produce microRNAs-like. In fact, several works demonstrate the plasticity that these fungi possess in surviving in different conditions, such as those found in the environment or in the host and during the transition from mycelium to yeast, stage that preceding the infectious process. For example, these pathogens alter the constitution of the cell wall and plasma membrane, change the metabolic pathways for energy production besides altering the cellular morphology (Nunes *et al.*, 2005, Felipe *et al.*, 2005, Bastos *et al.*, 2007, Rezende *et al.*, 2011). However the molecular mechanisms that control these processes are still not fully elucidated and the confirmation of the capacity of these fungi to produce microRNAs-like, opens door to the function of these molecules in the regulation of biological processes essential for the survival of these pathogens under different conditions such as those found in the host or between the different morphological stages.

Acknowledgments

This work was supported by grants from Conselho Nacional de Desenvolvimento Científico e Tecnológico (CNPq) and Fundação de Amparo à Pesquisa do Estado de Goiás (FAPEG)- Instituto Nacional de Ciência e Tecnologia (INCT) de Estratégias de Interação

Patógeno-Hospedeiro and Fundo Newton. JSC and MPB are fellows from Coordenação de Aperfeiçoamento de Pessoal de Nível Superior.

References

- Bai Y, Lan F, Yang W, Zhang F, Yang K, Li Z, Gao P and Wang S (2015) sRNA profiling in *Aspergillus flavus* reveals differentially expressed miRNA-like RNAs response to water activity and temperature. *Fungal Genet Biol* 81:113–9.
- Balcells I, Cirera S and Busk PK (2011) Specific and sensitive quantitative RT-PCR of miRNAs with DNA primers. *BMC Biotechnol* 11:70.
- Bartel DP, Lee R and Feinbaum R (2004) MicroRNAs: genomics, biogenesis, mechanism, and function. *Cell* 116:281–97.
- Bernstein E, Caudy AA, Hammond SM and Hannon GJ (2001) Role for a bidentate ribonuclease in the initiation step of RNA interference. *Nature* 409:363–366.
- Bookout AL, Cummins CL, Kramer MF, Pesola JM, J.Mangelsdorf D, Mangelsdorf DJ, Pesola JM and Kramer MF (2006) High-Throughput Real-Time Quantitative Reverse Transcription PCR. *Curr Protoc Mol Biol Chapter 15:15.8.1-15.8.28*.
- Camacho C, Coulouris G, Avagyan V, Ma N, Papadopoulos J, Bealer K and Madden TL (2009) BLAST+: architecture and applications. *BMC Bioinformatics* 10:421.
- Chen R, Jiang N, Jiang Q, Sun X, Wang Y, Zhang H and Hu Z (2014) Exploring microRNA-like small RNAs in the filamentous fungus *Fusarium oxysporum*. *PLoS One* 9:e104956.
- Chiba M, Kimura M and Saya A (2012) Exosomes secreted from human colorectal cancer cell lines contain mRNAs, microRNAs and natural antisense RNAs, that can transfer into the human hepatoma HepG2 and lung cancer A549 cell lines. *Oncol Rep* 28:1551–1558.
- Dix A, Czakai K, Leonhardt I, Schäferhoff K, Bonin M, Guthke R, Einsele H, Kurzai O, Löffler J, Linde J. 2017 Specific and novel microRNAs are regulated as response to fungal infection in human dendritic cells. *Frontiers in Microbiology*, v. 8,1.11.
- Croston TL, Nayak AP, Lemons AR, Goldsmith WT, Gu JK, Germolec DR, Beezhold DH, Green BJ (2016) Influence of *Aspergillus fumigatus* conidia viability on murine pulmonary.

microRNA and mRNA expression following subchronic inhalation exposure. 46: 1315–1327.

Croston TL, Lemons AR, Beezhold DH, Green BJ(2018) MicroRNA Regulation of Host Immune Responses following Fungal Exposure. *Front Immunol.* 9:1-10.

Dahlmann TA and Kück U (2015) Dicer-Dependent Biogenesis of Small RNAs and Evidence for MicroRNA-Like RNAs in the Penicillin Producing Fungus *Penicillium chrysogenum*. *PLoS One* 10:e0125989.

Dehury B, Panda D, Sahu J, Sahu M, Sarma K, Barooah M, Sen P and Modi MK (2013) *In silico* identification and characterization of conserved miRNAs and their target genes in sweet potato (*Ipomoea batatas* L.) Expressed Sequence Tags (ESTs). *Plant Signal Behav* 8:1–13.

Dlakić M (2006) DUF283 domain of Dicer proteins has a double-stranded RNA-binding fold. *Bioinformatics* 22:2711–2714.

Drinnenberg IA, Weinberg DE, Xie KT, Mower JP, Wolfe KH, Fink GR and Bartel DP (2009) RNAi in budding yeast. *Science* 326:544–550.

Finn RD, Coghill P, Eberhardt RY, Eddy SR, Mistry J, Mitchell AL, Potter SC, Punta M, Qureshi M, Sangrador-Vegas A et al. (2015) The Pfam protein families database: towards a more sustainable future. *Nucleic Acids Res* 44:279-285.

Galagan JE, Calvo SE, Borkovich KA, Selker EU, Read ND, Jaffe D, FitzHugh W, Ma L-J, Smirnov S, Purcell S et al. (2003) The genome sequence of the filamentous fungus *Neurospora crassa*. *Nature* 422:859–868.

Grimson A, Srivastava M, Fahey B, Woodcroft BJ, Chiang HR, King N, Degenan BM, Rokhsar DS and Bartel DP (2008) Early origins and evolution of microRNAs and Piwi-interacting RNAs in animals. *Nature* 455:1193–1197.

He H, Jazdzewski K, Li W, Liyanarachchi S, Nagy R, Volinia S, Calin GA, Liu C -g., Franssila K, Suster S et al. (2005) The role of microRNA genes in papillary thyroid carcinoma. *Proc Natl Acad Sci* 102:19075–19080.

Janbon G, Maeng S, Yang D-H, Ko Y, Jung K-W, Moyrand F, Floyd A, Heitman J and Bahn Y-S (2010) Characterizing the role of RNA silencing components in *Cryptococcus neoformans*. *Fungal Genet Biol* 47:1070–80.

Jiang N, Yang Y, Janbon G, Pan J and Zhu X (2012) Identification and functional demonstration of miRNAs in the fungus *Cryptococcus neoformans*. *PLoS One* 7:e52734.

Joshua-Tor L (2006) The Argonautes. *Cold Spring Harb Symp Quant Biol* 71:67–72.

Kang K, Zhong J, Jiang L, Liu G, Gou CY, Wu Q, Wang Y, Luo J and Gou D (2013) Identification of microRNA-Like RNAs in the Filamentous Fungus *Trichoderma reesei* by Solexa Sequencing. *PLoS One* 8:1–7.

Larkin MA, Blackshields G, Brown NP, Chenna R, Mcgettigan PA, McWilliam H, Valentin F, Wallace IM, Wilm A, Lopez R et al. (2007) Clustal W and Clustal X version 2.0. *Bioinformatics* 23:2947–2948.

Lau SKP, Chow W-N, Wong AYP, Yeung JMY, Bao J, Zhang N, Lok S, Woo PCY and Yuen K-Y (2013) Identification of microRNA-like RNAs in mycelial and yeast phases of the thermal dimorphic fungus *Penicillium marneffeii*. *PLoS Negl Trop Dis* 7:e2398.

Lee H-CC, Li L, Gu W, Xue Z, Crosthwaite SK, Pertsemlidis A, Lewis ZA, Freitag M, Selker EU, Mello CC et al. (2010) Diverse pathways generate microRNA-like RNAs and Dicer-independent small interfering RNAs in fungi. *Mol Cell* 38:803–14.

Lee RC, Feinbaum RL and Ambros V (1993) The *C. elegans* heterochronic gene *lin-4* encodes small RNAs with antisense complementarity to *lin-14*. *Cell* 75:843–854.

Lingel A, Simon B, Izaurralde E and Sattler M (2003) Structure and nucleic-acid binding of the *Drosophila* Argonaute 2 PAZ domain. *Nature* 426:465–9.

Lorenz R, Bernhart SH, Höner zu Siederdisen C, Tafer H, Flamm C, Stadler PF and Hofacker IL (2011) ViennaRNA Package 2.0. *Algorithms Mol Biol* 6:26.

Lorenz R, Wolfinger MT, Tanzer A and Hofacker IL (2016) Predicting RNA secondary

- structures from sequence and probing data. *Methods* 103:86–98.
- Martinez, R. 2017 New Trends in Paracoccidioidomycosis Epidemiology. *Journal of Fungi*, v. 3, n. 1, p. 1-5.
- Mishra AK, Duraisamy GS, Týcová A and Matoušek J (2015) Computational exploration of microRNAs from expressed sequence tags of *Humulus lupulus*, target predictions and expression analysis. *Comput Biol Chem* 59:131–141.
- Nakayashiki H (2005) RNA silencing in fungi: mechanisms and applications. *FEBS Lett* 579:5950–7.
- Nakayashiki H, Kadotani N and Mayama S (2006) Evolution and diversification of RNA silencing proteins in fungi. *J Mol Evol* 63:127–35.
- Page RD (1996) TreeView: an application to display phylogenetic trees on personal computers. *Comput Appl Biosci* 12:357–8.
- Panda D, Dehury B, Sahu J, Barooah M, Sen P and Modi MK (2014) Computational identification and characterization of conserved miRNAs and their target genes in garlic (*Allium sativum* L.) expressed sequence tags. *Gene* 537:333–342.
- Peres da Silva R, Puccia R, Rodrigues ML, Oliveira DL, Joffe LS, César G V, Nimrichter L, Goldenberg S and Alves LR (2015) Extracellular vesicle-mediated export of fungal RNA. *Sci Rep* 5:7763.
- Quinlan AR and Hall IM (2010) BEDTools: a flexible suite of utilities for comparing genomic features. *Bioinformatics* 26:841–842.
- Restrepo A (1985) The ecology of *Paracoccidioides brasiliensis*: a puzzle still unsolved. *Sabouraudia* 23:323–34.
- Saitou N and Nei M (1987) The neighbor-joining method: a new method for reconstructing phylogenetic trees. *Mol Biol Evol* 4:406–25.
- Sharma S, Kar S, Sahu SK, Samal B, Mallick A, Das S, Sharma S, Kar S, Sahu SK, Samal B

et al. (2010) Is inclusion of Sabouraud dextrose agar essential for the laboratory diagnosis of fungal keratitis? *Indian J Ophthalmol* 58:281–6.

Shikanai-Yasuda MA, Telles Filho F de Q, Mendes RP, Colombo AL, Moretti ML, Kono A, Tresoldi AT, Wanke B, Carvalho CR, Benard G et al. (2006) Consenso em paracoccidioidomicose. *Rev Soc Bras Med Trop* 39:297–310.

Silva-Bailão MG, Bailão EFLC, Lechner BE, Gauthier GM, Lindner H, Bailão AM, Haas H and Soares CMDA (2014) Hydroxamate production as a high affinity iron acquisition mechanism in *Paracoccidioides* spp. *PLoS One* 9:

Singulani J, Da Silva J, Gullo F, Costa M, Fusco-Almeida AM, Enguita F and Mendes-

Giannini MJ (2017) Preliminary evaluation of circulating microRNAs as potential biomarkers in paracoccidioidomycosis. *Biomed Reports* 6:353–357.

Song J-J, Smith SK, Hannon GJ and Joshua-Tor L (2004) Crystal structure of Argonaute and its implications for RISC slicer activity. *Science* 305:1434–7.

Restrepo A. 1985. The ecology of *Paracoccidioides brasiliensis*: a puzzle still unsolved.v.23, p. 323-34,.

Thompson JD, Gibson TJ, Plewniak F, Jeanmougin F and Higgins DG (1997) The CLUSTAL X windows interface: Flexible strategies for multiple sequence alignment aided by quality analysis tools. *Nucleic Acids Res* 25:4876–4882.

Tsutsumi A, Kawamata T, Izumi N, Seitz H and Tomari Y (2011) Recognition of the pre-miRNA structure by *Drosophila* Dicer-1. *Nat Struct Mol Biol* 18:1153–1158.

Marioto TG, Navarro dos Santos Ferraro AC, Goulart de Andrade F, Barros Oliveira M, Itano EN, Petrofeza S, Venancio EJ, Turini Gonzales Marioto D, Navarro dos Santos Ferraro AC, Goulart de Andrade F et al. (2017) Study of differential expression of miRNAs in lung tissue of mice submitted to experimental infection by *Paracoccidioides brasiliensis*. *Med Mycol* 7:774-784.

Zhang BH, Pan XP, Cox SB, Cobb GP and Anderson TA (2006) Evidence that miRNAs are different from other RNAs. *Cell Mol Life Sci* 63:246–254.

Zhang H, Kolb FA, Jaskiewicz L, Westhof E and Filipowicz W (2004) Single processing center models for human Dicer and bacterial RNase III. *Cell* 118:57–68.

Zhao T, Li G, Mi S, Li S, Hannon GJ, Wang XJ and Qi Y (2007) A complex system of small RNAs in the unicellular green alga. *Genes Dev* 1190–1203.

Zhou J, Fu Y, Xie J, Li B, Jiang D, Li G and Cheng J (2012) Identification of microRNA-like RNAs in a plant pathogenic fungus *Sclerotinia sclerotiorum* by high-throughput sequencing. *Mol Genet Genomics* 287:275–282.

Zhou Q, Wang Z, Zhang J, Meng H and Huang B (2012) Genome-wide identification and profiling of microRNA-like RNAs from *Metarhizium anisopliae* during development. *Fungal Biol* 116:1156–62.

Internet Resources

Uniprot database, (<http://www.uniprot.org/>);

NCBI database, (<http://blast.ncbi.nlm.nih.gov/Blast.cgi?PAGE=Proteins>);

PFAM database, (<http://pfam.xfam.org/>).

Supplementary material

The following online material is available for this article:

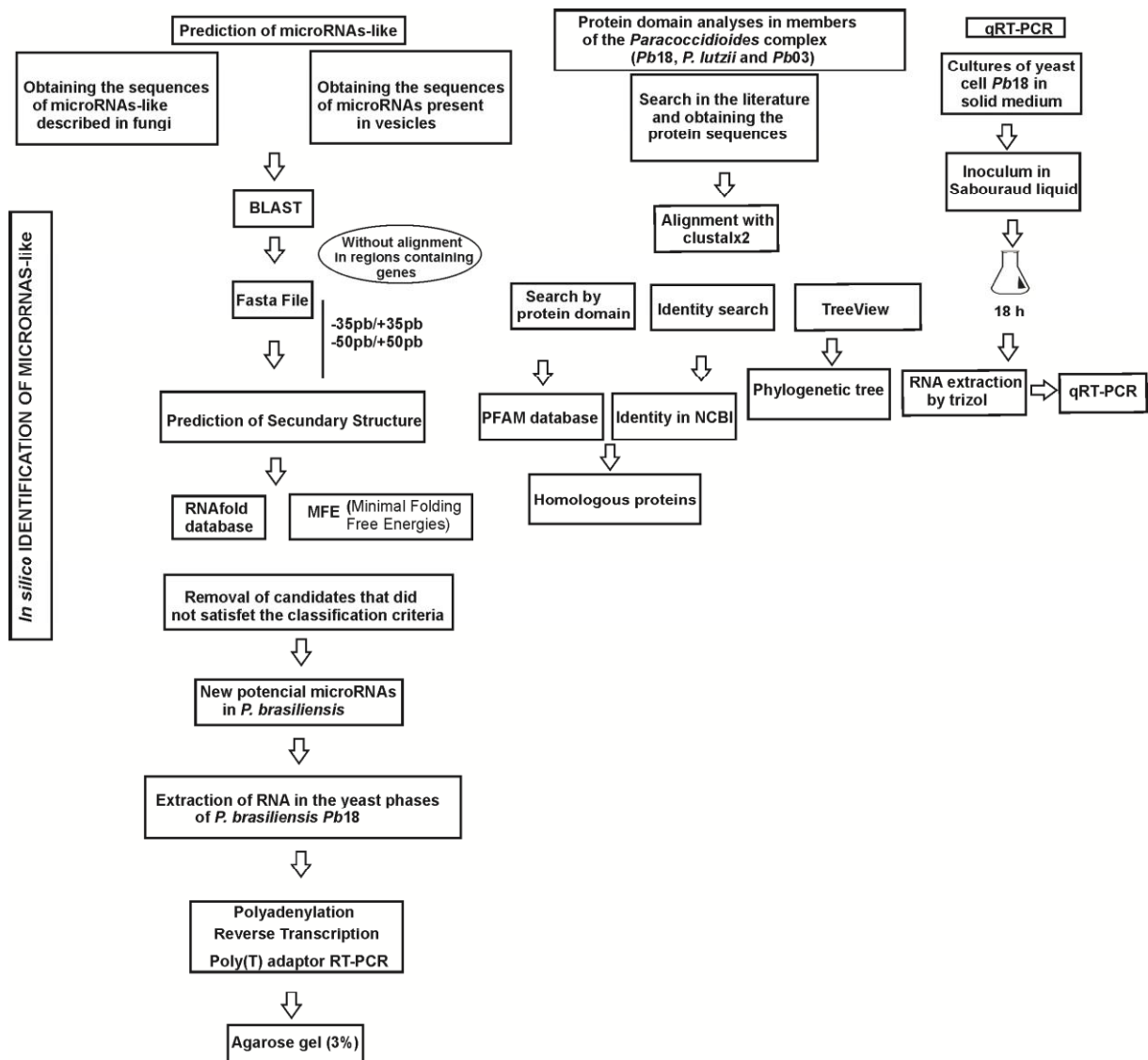
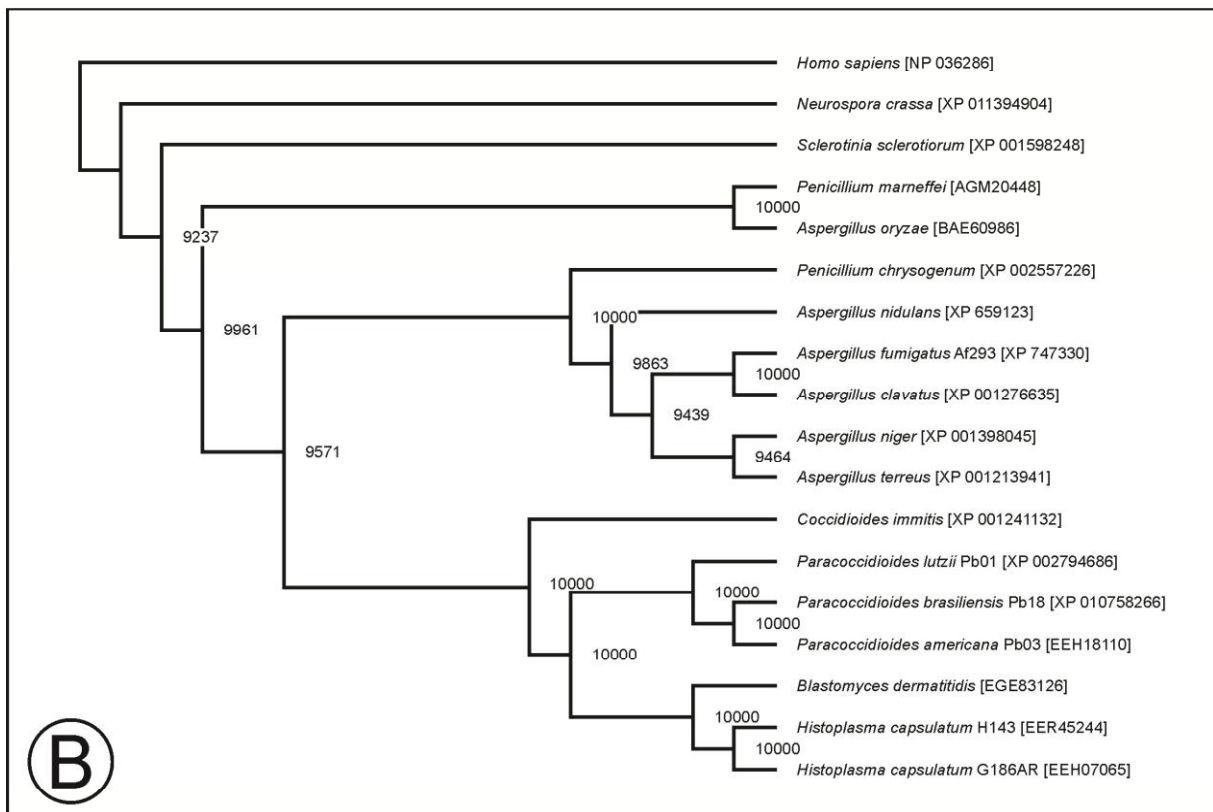
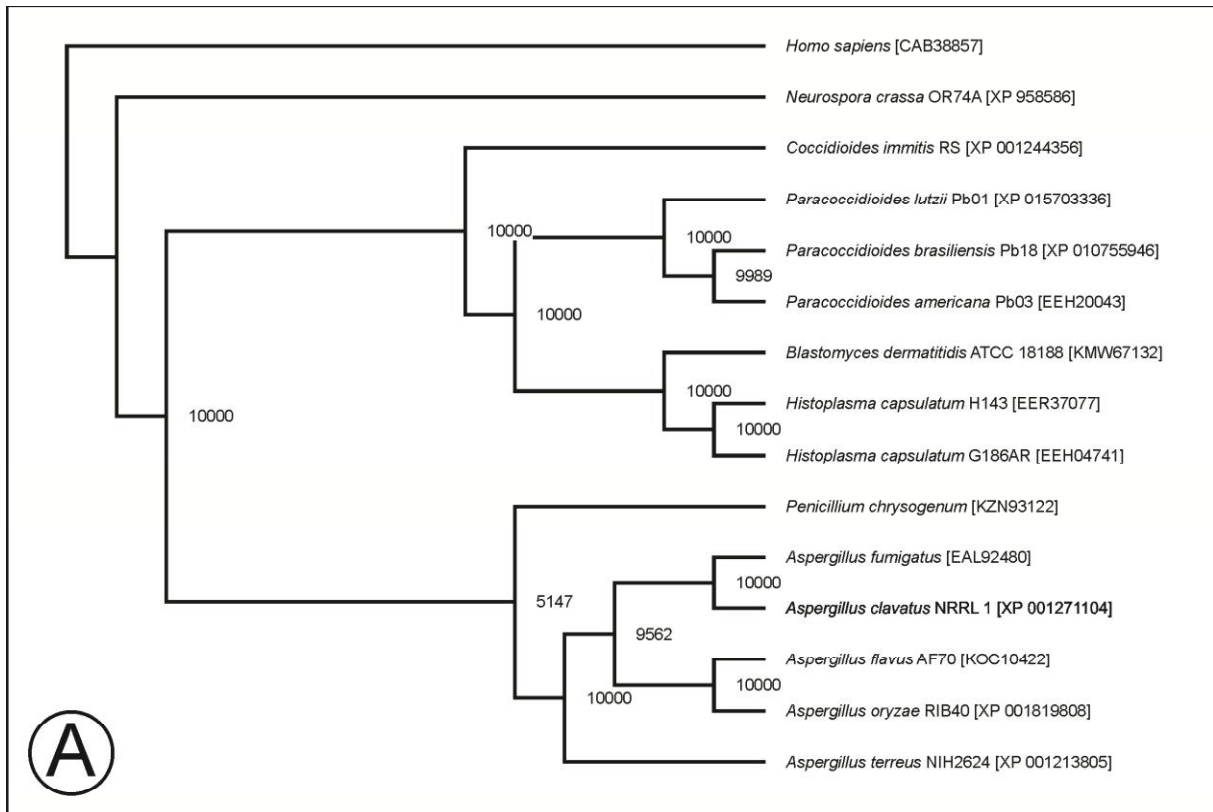


Figure S1- Flowchart of study design used for the prediction of miRNAs-like in the genome of *P. brasiliensis*.



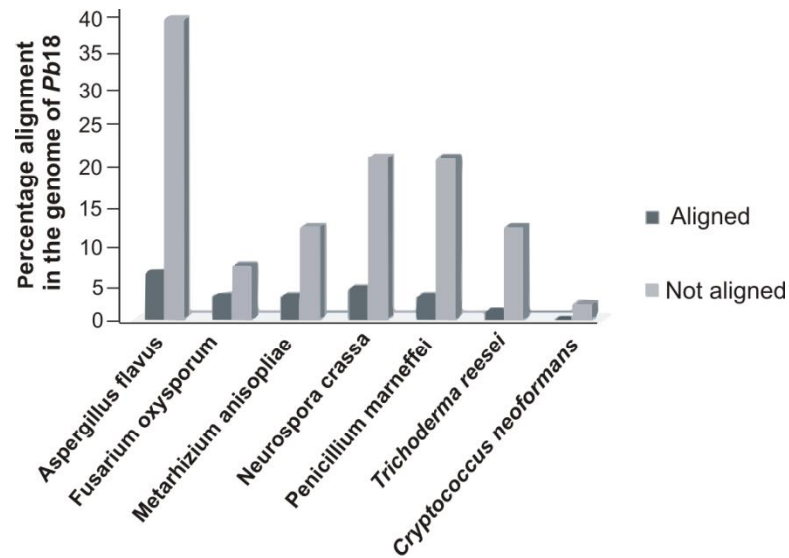


Figure S3- Alignment analysis of miRNAs-like in the genome of *P. brasilensis*. MiRNAs-like described in fungi demonstrated identity to regions of the *P. brasilensis* Pb18 genome. The dark gray bars represent the percentage of miRNAs-like aligned in the genome of *P. brasilensis* and light gray bars demonstrate the percentage of miRNAs-like that did not align to the Pb18 genome.

Supplementary table 1-Access number of the proteins used to construct the phylogenetic trees.

	Accession number			
	Argonaute 1	Argonaute 2	Dicer 1	Dicer 2
<i>Aspergillus clavatus</i> NRRL1	-	ACLA_058710	ACLA_014840	ACLA_055980
<i>Aspergillus flavus</i> AF70	-	-	KC686608	AFLA_066400
<i>Aspergillus fumigatus</i>	AFUA_3G11010	AFUA_8G05280	AFUA_5G11790	AFUA_4G02930
<i>Aspergillus kawachii</i>	-	-	-	AKAW_05119
<i>Aspergillus nidulans</i>	-	ANIA_01519	ANIA_00119	PDIP_77770
<i>Aspergillus niger</i>	-	ANI_1_1958144	ANI_1_424164	-
<i>Aspergillus oryzae</i> RIB40	AO090003000654	AO090012000881	AO090120000355	AO3042_00077
<i>Aspergillus terreus</i> NIH2624	ATEG_04627	ATEG_04763	ATEG_02092	ATEG_07902
<i>Blastomyces dermatitidis</i> ATCC	BDDG_11934	BDDG_06070	BDCG_08125	BDCG_02544
<i>Coccidioides immitis</i> RS	CIMG_03797	CIMG_08296	-	CIMG_05654
<i>Cryptococcus neoformans</i> H99	-	-	CNAG_02745	-
<i>Histoplasma capsulatum</i> G186AR	HCBG_06692	HCBG_03944	HCBG_01751	HCBG_01136
<i>Histoplasma capsulatum</i> H143	HCDG_08528	HCDG_00823	HCDG_06891	-
<i>Magnaporthe oryzae</i> 70-15	-	-	MGG_01541	MGG_12357
<i>Neurospora crassa</i> OR74A	NCU06838	NCU08389	NCU08270	NCU06766
<i>Paracoccidioides brasiliensis</i> Pb01	PAAG_11422	PAAG_03231	PAAG_11489	PAAG_00072
<i>Paracoccidioides brasiliensis</i> Pb03	PADG_02302	PABG_00673	PABG_04917	PABG_05105
<i>Paracoccidioides brasiliensis</i> Pb18	PADG_00716	PADG_03108	PADG_11946	PADG_07189
<i>Penicillium chrysogenum</i>	EN45_032900	PC12G03410	-	-
<i>Penicillium marneffeii</i>	-	AGM20448	-	-
<i>Sclerotinia sclerotiorum</i>	-	SS1G_00384	SS1G_13747	SS1G_10419
<i>Schizosaccharomyces pombe</i> 972h	-	-	SPCC188.13c	-
<i>Sporothrix schenckii</i>	-	-	C8CK81_SPOSC	-

Supplementary table 2. Oligonucleotide sequences used in the present study.

Genes	Forward sequences	Reverse sequence
<i>dcr 1</i>	GGAGATTGAAGCTACTGAGAC	TCTGGCAGACACTATTTACAAC
<i>dcr 2</i>	GAGGGAGGCAACCAACTATC	TTAGAAACCACCTCGTCCTTG
<i>ago-1</i>	CCATGGCTGCAGTGTCAGTA	AAACACCATCGCGGAAGTAGT
<i>ago-2</i>	CGACTATTTTCAGACGCACATAT	GGGTAAAGCTTAGCATTGTC
<i>Act</i>	CGTCCTCGCCATCATGGTAT	TCTCCATATCATCCCAGTTCG
Super.:2.3:1128222-1128358(-)	GCAGTGTGCATGTGCAT	GGTCCAGTTTTTTTTTTTTTTTCAC
Super.:2.5:587199-587317(+)	CGCAGAAATCACCTTCAC	GGTCCAGTTTTTTTTTTTTTTGAAG
Super.:2.6:955763-955879(+)	GGCGGACGCGATG	GTCCAGTTTTTTTTTTTTTTCCAC
Super.:2.12:21200-21275(-)	CAGCGCAGTAGGATTAGGAT	GGTCCAGTTTTTTTTTTTTTTTCT
Super.:2.14:171583-171670(+)	GGAGAGGGGGCCG	GGTCCAGTTTTTTTTTTTTTTCAAC

(*) all primers described in table S2 were constructed for this work, except the actin primer.

Supplementary table 3. Identified miRNAs-like homologues to other fungi species, in the genome of *P. brasiliensis* Pb18.

Query id ^a	Sequence ^b	Subject id ^c	Identity (%) ^d	Alignment length ^e	Mismatches ^f	Gap opens ^g	Evalue ^h	Bit score ⁱ	Organism ^j	Reference ^k
Afl-miR-13	CUUUCUGGUUGAUGGCGUCGGA	Supercontig_2.7	100	16	0	0	0.048	32.2	<i>A.flavus</i>	Bai et al., 2015
Afl-miR-23	GAGGGGAGAGGGGCGGUUG	Supercontig_2.14	100	17	0	0	0.009	34.2	<i>A.flavus</i>	
Afl-miR-23	GAGGGGAGAGGGGCGGUUG	Supercontig_2.1	95	20	1	0	0.036	32.2	<i>A.flavus</i>	
Afl-miR-33	GGCGAGAUGGCCGAGCGGUC	Supercontig_2.3	100	16	0	0	0.036	32.2	<i>A.flavus</i>	
Afl-miR-33	GGCGAGAUGGCCGAGCGGUC	Supercontig_2.9	100	17	0	0	0.009	34.2	<i>A.flavus</i>	
Afl-miR-6	GAGGGCGAGAGGGUGGAA	Supercontig_2.14	100	16	0	0	0.036	32.2	<i>A.flavus</i>	
Afl-miR-7	GUGGGAGGUUGAGUGGGUGGUA	Supercontig_2.3	100	16	0	0	0.048	32.2	<i>A.flavus</i>	
Afl-miR-9	GGCGAGAUGGCCGAGCGGUCC	Supercontig_2.3	100	17	0	0	0.011	34.2	<i>A.flavus</i>	
Afl-miR-9	GGCGAGAUGGCCGAGCGGUCC	Supercontig_2.9	100	18	0	0	0.003	36.2	<i>A.flavus</i>	
fox_miRNA_2	GACAACGUGGCCGAGUGGUUAAGGC	Supercontig_2.2	100	18	0	0	0.004	36.2	<i>F. oxysporum</i>	Chen et al., 2014
fox_miRNA_2	GACAACGUGGCCGAGUGGUUAAGGC	Supercontig_2.6	100	18	0	0	0.004	36.2	<i>F. oxysporum</i>	
fox_miRNA_4	UGGAUGAAUCAAGCGUGGUUAUGA	Supercontig_2.9	100	16	0	0	0.054	32.2	<i>F. oxysporum</i>	
fox_miRNA_8	CUUGAGACCCGGUUCAAUUCGCCGC	Supercontig_2.8	95.65	23	1	0	0.001	38.2	<i>F. oxysporum</i>	
man-miR-10	AGGGAUCUAGAAAAGAAAGGCUU	Supercontig_2.8	100	16	0	0	0.048	32.2	<i>M. anisopliae</i>	Zhou et al., 2012
man-miR-14	UAAAAGAUGUGGAAAAGAAGGC	Supercontig_2.3	100	17	0	0	0.012	34.2	<i>M. anisopliae</i>	
man-miR-5	UUAACAAGGCGUCGAGGGUAU	Supercontig_2.1	100	16	0	0	0.042	32.2	<i>M. anisopliae</i>	
miR-18	TTGGCAGGAATGTGGTGACGAACA	Supercontig_2.3	100	17	0	0	0.017	34.2	<i>N. crassa</i>	Yang et al., 2013
miR-1	TAAGCCGCGAGTACGCTCCGACT	Supercontig_2.3	100	16	0	0	0.066	32.2	<i>N. crassa</i>	
miR-4	TTCCCAAATCACCTTCACCTTACC	Supercontig_2.12	100	17	0	0	0.017	34.2	<i>N. crassa</i>	
miR-4	TTCCCAAATCACCTTCACCTTACC	Supercontig_2.5	100	18	0	0	0.004	36.2	<i>N. crassa</i>	
miR-6	GGCCGATTTCTCGTCAGTCA	Supercontig_2.1	100	16	0	0	0.042	32.2	<i>N. crassa</i>	
PM-miR-MC17	UGGCGGACGCGAUGGUGGAGG	Supercontig_2.6	100	16	0	0	0.042	32.2	<i>P. marneffei</i>	Lau et al., 2013
PM-miR-MC7	UAGGAUUAGGAUUAGGAUUA	Supercontig_2.1	100	16	0	0	0.036	32.2	<i>P. marneffei</i>	

PM-miR-MC7	UAGGAUUAGGAUUAGGAUUA	Supercontig_2.12	100	16	0	0	0.036	32.2	<i>P. marneffe</i>	
PM-miR-MC7	UAGGAUUAGGAUUAGGAUUA	Supercontig_2.12	100	16	0	0	0.036	32.2	<i>P. marneffe</i>	
PM-miR-MC7	UAGGAUUAGGAUUAGGAUUA	Supercontig_2.12	100	17	0	0	0.009	34.2	<i>P. marneffe</i>	
PM-miR-MC7	UAGGAUUAGGAUUAGGAUUA	Supercontig_2.2	95	20	1	0	0.036	32.2	<i>P. marneffe</i>	
PM-miR-MC7	UAGGAUUAGGAUUAGGAUUA	Supercontig_2.4	100	17	0	0	0.009	34.2	<i>P. marneffe</i>	
PM-miR-MC7	UAGGAUUAGGAUUAGGAUUA	Supercontig_2.5	100	16	0	0	0.036	32.2	<i>P. marneffe</i>	
PM-miR-MC7	UAGGAUUAGGAUUAGGAUUA	Supercontig_2.5	100	17	0	0	0.009	34.2	<i>P. marneffe</i>	
PM-miR-MC7	UAGGAUUAGGAUUAGGAUUA	Supercontig_2.5	95	20	1	0	0.036	32.2	<i>P. marneffe</i>	
PM-miR-YC1	UGCCAUUGCUAAGUCAAGG	Supercontig_2.3	100	17	0	0	0.008	34.2	<i>P. marneffe</i>	
Tre-miR-2	TCTCTGTTGGAGTTGAGGGGG	Supercontig_2.2	100	16	0	0	0.042	32.2	<i>T. reesei</i>	Kang et al., 2013
miR1	TCCTGAACCTTGATCACCATTGA	-	-	-	-	-	-	-	<i>Cryptococcus neoformans</i>	Jiang et al., 2012
miR2	TCGACACCTTCATCGTAA	-	-	-	-	-	-	-	<i>Cryptococcus neoformans</i>	
Afl-miR-4	GUGGAGGAUUGGGACGGGGU	-	-	-	-	-	-	-	<i>Aflavus</i>	
Afl-miR-5	CUUUGGAGGGAUUGGUGGGA	-	-	-	-	-	-	-	<i>Aflavus</i>	
Afl-miR-8	UUUUGUGGAAUCUGCCUCGCGCU	-	-	-	-	-	-	-	<i>Aflavus</i>	
Afl-miR-10	CUGGAUUCGUCCCGGAACCC	-	-	-	-	-	-	-	<i>Aflavus</i>	
Afl-miR-11	AGCGGCUAAGGCGCACGGUUA	-	-	-	-	-	-	-	<i>Aflavus</i>	
Afl-miR-12	CUUCUAUCUCGUCGGGGUCA	-	-	-	-	-	-	-	<i>Aflavus</i>	
Afl-miR-14	AAAGGGCAUGGGUAGUAUGA	-	-	-	-	-	-	-	<i>Aflavus</i>	
Afl-miR-15	CUGGUCGGGUUGAUGAUGGA	-	-	-	-	-	-	-	<i>Aflavus</i>	
Afl-miR-16	AUUGCUUGCAUGUUCGUUCUGGA	-	-	-	-	-	-	-	<i>Aflavus</i>	
Afl-miR-17	CUUUCUAUAUACGUCGGAA	-	-	-	-	-	-	-	<i>Aflavus</i>	
Afl-miR-18	CCAUGAUACUUGUUGGUCGGA	-	-	-	-	-	-	-	<i>Aflavus</i>	
Afl-miR-19	AGCGAGACGACCUGCCUGGCA	-	-	-	-	-	-	-	<i>Aflavus</i>	
Afl-miR-20	CAUCUCUUGUCGGUUCGAGA	-	-	-	-	-	-	-	<i>Aflavus</i>	
Afl-miR-21	AUGGGGUCUGUAUGUGAUGGA	-	-	-	-	-	-	-	<i>Aflavus</i>	

Afl-miR-22	GGAAGUUGAUCUUGAUUGUUGGA	-	-	-	-	-	-	-	<i>A.flavus</i>
Afl-miR-24	UGGCUAUCGAUCGAUCGUCGGA	-	-	-	-	-	-	-	<i>A.flavus</i>
Afl-miR-25	GUGUAGGGUGUGGUAGUCUC	-	-	-	-	-	-	-	<i>A.flavus</i>
Afl-miR-26	CCUGUCUAUCGAGGAUUGUUGGA	-	-	-	-	-	-	-	<i>A.flavus</i>
Afl-miR-27	GGAUGAUAGGUCGGGAUGAGA	-	-	-	-	-	-	-	<i>A.flavus</i>
Afl-miR-28	UAGCUAUCUCGUGACAGACAAU	-	-	-	-	-	-	-	<i>A.flavus</i>
Afl-miR-29	ACUCCUUGGGCGCAUCGUUGGA	-	-	-	-	-	-	-	<i>A.flavus</i>
Afl-miR-30	UUACUGUACAAAGCUAGACA	-	-	-	-	-	-	-	<i>A.flavus</i>
Afl-miR-31	CAAGGAUUGUGAUUGUUCUGGA	-	-	-	-	-	-	-	<i>A.flavus</i>
Afl-miR-32	CUUGUUCGUCGGGGGAUGGCA	-	-	-	-	-	-	-	<i>A.flavus</i>
Afl-miR-34	AAGGCGGACGUUGGCGGCUAUA	-	-	-	-	-	-	-	<i>A.flavus</i>
Afl-miR-35	GGCGGACUGCUUCAACGACGGA	-	-	-	-	-	-	-	<i>A.flavus</i>
Afl-miR-36	ACUUUAGAUGGUCGUGUUGGGGA	-	-	-	-	-	-	-	<i>A.flavus</i>
Afl-miR-37	CAUUGUUUAAGCGUCGUUGGAA	-	-	-	-	-	-	-	<i>A.flavus</i>
Afl-miR-38	CCAUGGGAUUCUAAUCGUCGGA	-	-	-	-	-	-	-	<i>A.flavus</i>
Afl-miR-39	GGUUUUGAUGAUCGUGUCGGA	-	-	-	-	-	-	-	<i>A.flavus</i>
Afl-miR-40	CCUAUCGGCAUUGGAGACGGA	-	-	-	-	-	-	-	<i>A.flavus</i>
Afl-miR-41	GUCGUGGUAAGUGGCGUCGGA	-	-	-	-	-	-	-	<i>A.flavus</i>
Afl-miR-42	GUUCUCAGCAGAUUCGGCCGGA	-	-	-	-	-	-	-	<i>A.flavus</i>
Afl-miR-43	CCUAGGACAAGGGCGCACAGAGU	-	-	-	-	-	-	-	<i>A.flavus</i>
Afl-miR-44	GUAUCAAUGACAGAUUGAAGGA	-	-	-	-	-	-	-	<i>A.flavus</i>
Afl-miR-45	AGGCGACUGGUACAUGUAUGG	-	-	-	-	-	-	-	<i>A.flavus</i>
Afl-miR-46	AUGGCAUUGAAUCGGUCGGGA	-	-	-	-	-	-	-	<i>A.flavus</i>
Afl-miR-47	AUGUAGUACUGCAUCGUUCUGGA	-	-	-	-	-	-	-	<i>A.flavus</i>
Afl-miR-48	UGGGUGGUGGGUGGCGAUGGCU	-	-	-	-	-	-	-	<i>A.flavus</i>
fox_milRNA_1	UGCUAGGGUAGAGAAUUUUGCAGGC	-	-	-	-	-	-	-	<i>F.oxysporum</i>

fox_milRNA_2	GGCAUUGUGUUCGCACGCGUAGGUUCG	-	-	-	-	-	-	-	-	<i>F. oxysporum</i>
fox_milRNA_3a	GGUGUGGUGUAUCGGUUUAUCAUCCGC	-	-	-	-	-	-	-	-	<i>F. oxysporum</i>
fox_milRNA_3b	CCGGUGUGGUGUAUCGGUUUAUCAUCCGC	-	-	-	-	-	-	-	-	<i>F. oxysporum</i>
fox_milRNA_5	UCCGGUAUGGUGUAGUGGC	-	-	-	-	-	-	-	-	<i>F. oxysporum</i>
fox_milRNA_6	GUUCCGUGGUCUAGUUGGUUAUGGCAUCU	-	-	-	-	-	-	-	-	<i>F. oxysporum</i>
fox_milRNA_7	CUUCCGUAGUAUAGUGGUCAGUAUGCA	-	-	-	-	-	-	-	-	<i>F. oxysporum</i>
man-miR-1	UAUCUUGUGGACUAAUAGGUA	-	-	-	-	-	-	-	-	<i>M. anisopliae</i>
man-miR-2	UACAAGGCACGAGCAAGGU	-	-	-	-	-	-	-	-	<i>M. anisopliae</i>
man-miR-3	UUGUCGAGGCAUACCACUAAU	-	-	-	-	-	-	-	-	<i>M. anisopliae</i>
man-miR-4	UCGAGGAGCAGAAGCUGAUCUU	-	-	-	-	-	-	-	-	<i>M. anisopliae</i>
man-miR-6	UUUGGAGAGGUCUGUGUUU	-	-	-	-	-	-	-	-	<i>M. anisopliae</i>
man-miR-7	GCGGGUGCUGAGAAAAGCGUUUA	-	-	-	-	-	-	-	-	<i>M. anisopliae</i>
man-miR-8	UUGCAUGAUGAGACUUUUU	-	-	-	-	-	-	-	-	<i>M. anisopliae</i>
man-miR-9	UGCCUAGGCAGGGUAGAUCAG	-	-	-	-	-	-	-	-	<i>M. anisopliae</i>
man-miR-11	UGCAGGGGAGCAUCGUCGUUG	-	-	-	-	-	-	-	-	<i>M. anisopliae</i>
man-miR-12	AGACCUCGUUGAUGCUGGCAUU	-	-	-	-	-	-	-	-	<i>M. anisopliae</i>
man-miR-13	CGACGACUCUGGCGAGGACAA	-	-	-	-	-	-	-	-	<i>M. anisopliae</i>
man-miR-15	GAUGUCGAAUCGUGCCGGGCUC	-	-	-	-	-	-	-	-	<i>M. anisopliae</i>
milR-2	TGTCTGGTACTTTCATCCGGCTGT	-	-	-	-	-	-	-	-	<i>N. crassa</i>
milR-3	TGAACGAGCGGTTGTTGT	-	-	-	-	-	-	-	-	<i>N. crassa</i>
milR-5	AAGCAAGATCCGGACATTC	-	-	-	-	-	-	-	-	<i>N. crassa</i>
milR-7	TGCGGTGCTTTCCTTGCCCT	-	-	-	-	-	-	-	-	<i>N. crassa</i>
milR-8	AAACGCTCTACCGGTTGCTGTTAGA	-	-	-	-	-	-	-	-	<i>N. crassa</i>
milR-9	GAGCTTGTCGCCTTCAA	-	-	-	-	-	-	-	-	<i>N. crassa</i>
milR-10	CACTCGTGTGCTGTAGCGGACTA	-	-	-	-	-	-	-	-	<i>N. crassa</i>
milR-11	TGACCGGGCGTTGTTGTT	-	-	-	-	-	-	-	-	<i>N. crassa</i>

milR-12	TCATCCGATCATGTCACATTGTC	-	-	-	-	-	-	-	<i>N. crassa</i>
milR-13	TGGGAATGTGAGGCGTTTG	-	-	-	-	-	-	-	<i>N. crassa</i>
milR-14	TGCCGTGTCGTAGCATCGAAGTCAA	-	-	-	-	-	-	-	<i>N. crassa</i>
milR-15	TTATTTGCCAAATCAACACTCGG	-	-	-	-	-	-	-	<i>N. crassa</i>
milR-16	TACTTGATTACAGCGTCTATAC	-	-	-	-	-	-	-	<i>N. crassa</i>
milR-17	CGGCATCAGCGTGTCA	-	-	-	-	-	-	-	<i>N. crassa</i>
milR-19	GATACACGCTAGATGTCCCT	-	-	-	-	-	-	-	<i>N. crassa</i>
milR-20	TACTCTGTGTCTCGGTGTGGTT	-	-	-	-	-	-	-	<i>N. crassa</i>
milR-21	ATCCTGGCTTCCTTGCCTG	-	-	-	-	-	-	-	<i>N. crassa</i>
milR-22	TGGAGGGTGATATATGGTTTGCCAG	-	-	-	-	-	-	-	<i>N. crassa</i>
milR-23	TGCAATCTAGTCGCGTCCCTCTT	-	-	-	-	-	-	-	<i>N. crassa</i>
milR-24	TGCGGGCATTGAGTGGTCGACG	-	-	-	-	-	-	-	<i>N. crassa</i>
milR-25	CGACGCGAGAAGAAGGGGATTG	-	-	-	-	-	-	-	<i>N. crassa</i>
PM-milR-M1	GAGAAACGCCUUAUGAUCGAC	-	-	-	-	-	-	-	<i>P. marneffe</i>
PM-milR-M1*	UGACUCGAAGAGCCUCUA	-	-	-	-	-	-	-	<i>P. marneffe</i>
PM-milR-M2	GUCCUAUAGUAAAGCCAGUC	-	-	-	-	-	-	-	<i>P. marneffe</i>
PM-milR-M2*	AUUUCUAGGCUAUA AAAAGCUU	-	-	-	-	-	-	-	<i>P. marneffe</i>
PM-milR-MC3	UGAUUCAAAAGUGGGCUAUC	-	-	-	-	-	-	-	<i>P. marneffe</i>
PM-milR-MC4	UCAAGUCAACCCUUACUC	-	-	-	-	-	-	-	<i>P. marneffe</i>
PM-milR-MC5	UUGCUAUGAUGAAAGCUGAGCA	-	-	-	-	-	-	-	<i>P. marneffe</i>
PM-milR-MC6	AACGUUUAAAUUCCGAUACAAUU	-	-	-	-	-	-	-	<i>P. marneffe</i>
PM-milR-MC8	UUUCUACAGCUGCUGAACGUC	-	-	-	-	-	-	-	<i>P. marneffe</i>
PM-milR-MC9	UUGGCGUUGGUGUAAUUG	-	-	-	-	-	-	-	<i>P. marneffe</i>
PM-milR-MC10	UCGACUGGCUCACCUGAUGCC	-	-	-	-	-	-	-	<i>P. marneffe</i>
PM-milR-MC11	UCGAUGUACUCCUUGUGGA	-	-	-	-	-	-	-	<i>P. marneffe</i>
PM-milR-MC12	UGUUCAUCGAUCUGCUGUAGA	-	-	-	-	-	-	-	<i>P. marneffe</i>

PM-milR-MC13	UGCCACUCGAUCAUCUUGGG	-	-	-	-	-	-	-	<i>P. marneffe</i>
PM-milR-MC14	UAAGAGCUGUACAUAUGUAAG	-	-	-	-	-	-	-	<i>P. marneffe</i>
PM-milR-MC15	AUCCGGAUCGAGUUUUCAC	-	-	-	-	-	-	-	<i>P. marneffe</i>
PM-milR-MC16	CAUAAGGUCGAGAGUCUGCA	-	-	-	-	-	-	-	<i>P. marneffe</i>
PM-milR-YC2	CAGCGGUGAUGACAACC	-	-	-	-	-	-	-	<i>P. marneffe</i>
PM-milR-YC3	CCGUUCUAAAAUUGCUAGAGC	-	-	-	-	-	-	-	<i>P. marneffe</i>
PM-milR-YC4	UUGCUAUGAUGAAAGCUGAGCA	-	-	-	-	-	-	-	<i>P. marneffe</i>
PM-milR-YC5	UUUCUUGUCUACCUUUCGAGU	-	-	-	-	-	-	-	<i>P. marneffe</i>
PM-milR-YC6	UUCUCGGUGGCGAUGUCCAUI	-	-	-	-	-	-	-	<i>P. marneffe</i>
PM-milR-YC7	CCUUCAGAUCUGGGCUAUGCCC	-	-	-	-	-	-	-	<i>P. marneffe</i>
Tre-milR-1	AGCCGGCTGTTGACGTAGGTGA	-	-	-	-	-	-	-	<i>T. reesei</i>
Tre-milR-3	GGGAGAATGCGCCGTGATTGT	-	-	-	-	-	-	-	<i>T. reesei</i>
Tre-milR-4	AGCAGCGACGGCGAACTCTGC	-	-	-	-	-	-	-	<i>T. reesei</i>
Tre-milR-5	CCCGTTTATCTGATCAACGCCG	-	-	-	-	-	-	-	<i>T. reesei</i>
Tre-milR-6	CGGAGCTGGAGGAGGACTGCGA	-	-	-	-	-	-	-	<i>T. reesei</i>
Tre-milR-7	TCAAGGGGAATCTGAGGCAG	-	-	-	-	-	-	-	<i>T. reesei</i>
Tre-milR-8	CTCAGGGGAAGTGGAGATGGA	-	-	-	-	-	-	-	<i>T. reesei</i>
Tre-milR-9	TGGCATGTTAGACAAGTTGCG	-	-	-	-	-	-	-	<i>T. reesei</i>
Tre-milR-10	AGGCTGTACTGTAGGCGAG	-	-	-	-	-	-	-	<i>T. reesei</i>
Tre-milR-11	TGGAGACGTGGAGCCGGA	-	-	-	-	-	-	-	<i>T. reesei</i>
Tre-milR-12	GGTGCGGGCTGGCGGCGG	-	-	-	-	-	-	-	<i>T. reesei</i>
Tre-milR-13	CCAGCAGGACTATGACGACG	-	-	-	-	-	-	-	<i>T. reesei</i>

- a) Identifier of the miRNAs-like;
b) Sequence;
c) Alignment region;
d) Percent of the identity between the sequences;
e) Size of alignment between the sequences of miRNAs-like and the genome region of *P. brasiliensis* (*Pb18*);
f) Number of different bases between the aligned sequences;
g) Absence of complementary bases between the sequences;

h) Likelihood sequence analyzed to align randomly to other sequences in the database. false positive rate;

i) Normalized score obtained using the following formula: $S' = (I S - \ln K) / \ln 2$;

j) Microorganism which miRNA-like have been described;

k) Articles describing miRNAs-like in fungus;

(-) Absence of alignment in genome of *P. brasiliensis* (Pb18);

(*) microRNA star.

Supplementary table 4. Identification of miRNAs-like described in fungi vesicles with identity in the genome of *P. brasiliensis* Pb18.

Query id ^a	Subject id ^b	% Identity ^c	Alignment length ^d	Mismatches ^e	Gap opens ^f	Evalue ^g	Bit score ^h	Fungi vesicle ⁱ	Reference ^j
aae-miR-309b-5p	Supercontig_2.3	100	16	0	0	0.054	32.2	<i>S. cerevisiae</i>	Silva et.al. 2015
aca-miR-1388-5p	Supercontig_2.4	95	20	1	0	0.048	32.2	<i>S. cerevisiae</i> / <i>C. albicans</i>	
aca-miR-20a-5p	Supercontig_2.3	100	17	0	0	0.012	34.2	<i>C. albicans</i>	
aca-miR-5419	Supercontig_2.1	100	16	0	0	0.042	32.2	<i>C. neoformans</i> / <i>S. cerevisiae</i>	
aly-miR166g-5p	Supercontig_2.4	100	16	0	0	0.042	32.2	<i>C. neoformans</i>	
aly-miR166g-5p	Supercontig_2.9	100	16	0	0	0.042	32.2	<i>C. neoformans</i>	
aly-miR167b-3p*	Supercontig_2.8	100	16	0	0	0.054	32.2	<i>S. cerevisiae</i>	
aly-miR4233	Supercontig_2.1	100	17	0	0	0.011	34.2	<i>C. albicans</i>	
aly-miR4233	Supercontig_2.2	100	16	0	0	0.042	32.2	<i>C. albicans</i>	
aly-miR4233	Supercontig_2.29	100	16	0	0	0.042	32.2	<i>C. albicans</i>	
aly-miR4233	Supercontig_2.4	100	16	0	0	0.042	32.2	<i>C. albicans</i>	
aly-miR4233	Supercontig_2.8	100	16	0	0	0.042	32.2	<i>C. albicans</i>	
ame-miR-3754	Supercontig_2.2	100	16	0	0	0.054	32.2	<i>P. brasiliensis</i>	
ame-miR-3772	Supercontig_2.2	100	16	0	0	0.054	32.2	<i>C. albicans</i> / <i>C. neoformans</i>	
ath-miR2938	Supercontig_2.7	100	16	0	0	0.042	32.2	<i>C. albicans</i>	
ath-miR414	Supercontig_2.10	100	17	0	0	0.011	34.2	<i>C. albicans</i> / <i>P. brasiliensis</i>	
ath-miR414	Supercontig_2.1	100	16	0	0	0.042	32.2	<i>C. albicans</i> / <i>P. brasiliensis</i>	
ath-miR414	Supercontig_2.11	95.24	21	1	0	0.011	34.2	<i>C. albicans</i> / <i>P. brasiliensis</i>	
ath-miR414	Supercontig_2.11	95.24	21	1	0	0.011	34.2	<i>C. albicans</i> / <i>P. brasiliensis</i>	

bmo-miR-2768-5p	Supercontig_2.3	100	17	0	0	0.012	34.2	<i>C. albicans</i>
bmo-miR-3250	Supercontig_2.3	100	17	0	0	0.011	34.2	<i>C. albicans/ P. brasiliensis</i>
bmo-miR-3250	Supercontig_2.3	100	18	0	0	0.003	36.2	<i>C. albicans/ P. brasiliensis</i>
bmo-miR-3250	Supercontig_2.6	100	16	0	0	0.042	32.2	<i>C. albicans/ P. brasiliensis</i>
bmo-miR-3306	Supercontig_2.7	100	16	0	0	0.06	32.2	<i>C.neoformans</i>
bmo-miR-3382-3p*	Supercontig_2.1	100	16	0	0	0.066	32.2	<i>P. brasiliensis</i>
bmo-miR-3425	Supercontig_2.2	100	16	0	0	0.066	32.2	<i>C. albicans</i>
bmo-miR-3430	Supercontig_2.1	95.24	21	1	0	0.017	34.2	<i>C. albicans</i>
bta-miR-1284	Supercontig_2.3	100	16	0	0	0.048	32.2	<i>C. albicans</i>
bta-miR-2304	Supercontig_2.10	100	16	0	0	0.036	32.2	<i>C.neoformans</i>
bta-miR-2304	Supercontig_2.4	100	16	0	0	0.036	32.2	<i>C.neoformans</i>
bta-miR-2437	Supercontig_2.8	100	16	0	0	0.042	32.2	<i>C. albicans</i>
cfa-miR-214	Supercontig_2.6	100	17	0	0	0.012	34.2	<i>C.neoformans</i>
cin-miR-367-5p	Supercontig_2.2	100	17	0	0	0.009	34.2	<i>C.neoformans/C. albicans</i>
cin-miR-4171-5p	Supercontig_2.11	100	16	0	0	0.036	32.2	<i>C.neoformans/C. albicans/S. cerevisiae</i>
cin-miR-4171-5p	Supercontig_2.32	95	20	1	0	0.036	32.2	<i>C.neoformans/C. albicans/S. cerevisiae</i>
cin-miR-4171-5p	Supercontig_2.32	95	20	1	0	0.036	32.2	<i>C.neoformans/C. albicans/S. cerevisiae</i>
cin-miR-4171-5p	Supercontig_2.32	95	20	1	0	0.036	32.2	<i>C.neoformans/C. albicans/S. cerevisiae</i>
cin-miR-4171-5p	Supercontig_2.32	95	20	1	0	0.036	32.2	<i>C.neoformans/C. albicans/S. cerevisiae</i>
cin-miR-4171-5p	Supercontig_2.32	95	20	1	0	0.036	32.2	<i>C.neoformans/C. albicans/S. cerevisiae</i>
cin-miR-4171-5p	Supercontig_2.32	95	20	1	0	0.036	32.2	<i>C.neoformans/C. albicans/S. cerevisiae</i>
cin-miR-4171-5p	Supercontig_2.8	95	20	1	0	0.036	32.2	<i>C.neoformans/C. albicans/S. cerevisiae</i>
cin-miR-4171-5p	Supercontig_2.8	95	20	1	0	0.036	32.2	<i>C.neoformans/C. albicans/S. cerevisiae</i>
cin-miR-4171-5p	Supercontig_2.8	95	20	1	0	0.036	32.2	<i>C.neoformans/C. albicans/S. cerevisiae</i>
csi-miR3946	Supercontig_2.13	100	16	0	0	0.06	32.2	<i>C.neoformans/S. cerevisiae</i>
csi-miR3946	Supercontig_2.2	100	16	0	0	0.06	32.2	<i>C.neoformans/S. cerevisiae</i>
csi-miR3946	Supercontig_2.3	100	16	0	0	0.06	32.2	<i>C.neoformans/S. cerevisiae</i>
csi-miR3946	Supercontig_2.6	100	16	0	0	0.06	32.2	<i>C.neoformans/S. cerevisiae</i>
csi-miR3946	Supercontig_2.6	100	16	0	0	0.06	32.2	<i>C.neoformans/S. cerevisiae</i>

csi-miR3946	Supercontig_2.8	100	16	0	0	0.06	32.2	<i>C.neoformans/S. cerevisiae</i>
csi-miR3946	Supercontig_2.8	100	17	0	0	0.015	34.2	<i>C.neoformans/S. cerevisiae</i>
der-miR-13b	Supercontig_2.11	100	16	0	0	0.048	32.2	<i>P.brasiliensis/C.neoformans/S. cerevisiae</i>
dme-miR-2491-3p*	Supercontig_2.10	100	17	0	0	0.008	34.2	<i>S. cerevisiae</i>
dme-miR-2491-3p*	Supercontig_2.10	100	17	0	0	0.008	34.2	<i>S. cerevisiae</i>
dme-miR-2491-3p*	Supercontig_2.10	100	18	0	0	0.002	36.2	<i>S. cerevisiae</i>
dme-miR-2491-3p*	Supercontig_2.1	100	16	0	0	0.03	32.2	<i>S. cerevisiae</i>
dme-miR-2491-3p*	Supercontig_2.1	100	17	0	0	0.008	34.2	<i>S. cerevisiae</i>
dme-miR-2491-3p*	Supercontig_2.1	100	17	0	0	0.008	34.2	<i>S. cerevisiae</i>
dme-miR-2491-3p*	Supercontig_2.1	100	18	0	0	0.002	36.2	<i>S. cerevisiae</i>
dme-miR-2491-3p*	Supercontig_2.1	100	18	0	0	0.002	36.2	<i>S. cerevisiae</i>
dme-miR-2491-3p*	Supercontig_2.11	100	17	0	0	0.008	34.2	<i>S. cerevisiae</i>
dme-miR-2491-3p*	Supercontig_2.12	100	17	0	0	0.008	34.2	<i>S. cerevisiae</i>
dme-miR-4968-3p*	Supercontig_2.10	100	16	0	0	0.048	32.2	<i>C.neoformans/S. cerevisiae</i>
dme-miR-4968-3p*	Supercontig_2.10	100	16	0	0	0.048	32.2	<i>C.neoformans/S. cerevisiae</i>
dme-miR-4968-3p*	Supercontig_2.10	100	17	0	0	0.012	34.2	<i>C.neoformans/S. cerevisiae</i>
dme-miR-4968-3p*	Supercontig_2.10	100	17	0	0	0.012	34.2	<i>C.neoformans/S. cerevisiae</i>
dme-miR-4968-3p*	Supercontig_2.10	100	17	0	0	0.012	34.2	<i>C.neoformans/S. cerevisiae</i>
dme-miR-4968-3p*	Supercontig_2.10	100	18	0	0	0.003	36.2	<i>C.neoformans/S. cerevisiae</i>
dme-miR-4968-3p*	Supercontig_2.10	100	21	0	0	5.00E-05	42.1	<i>C.neoformans/S. cerevisiae</i>
dme-miR-4968-3p*	Supercontig_2.10	100	21	0	0	5.00E-05	42.1	<i>C.neoformans/S. cerevisiae</i>
dme-miR-4968-3p*	Supercontig_2.10	95	20	1	0	0.048	32.2	<i>C.neoformans/S. cerevisiae</i>
dme-miR-4968-3p*	Supercontig_2.10	95	20	1	0	0.048	32.2	<i>C.neoformans/S. cerevisiae</i>
dme-miR-4968-3p*	Supercontig_2.10	95	20	1	0	0.048	32.2	<i>C.neoformans/S. cerevisiae</i>
dme-miR-4968-3p*	Supercontig_2.10	95	20	1	0	0.048	32.2	<i>C.neoformans/S. cerevisiae</i>
dme-miR-4968-3p*	Supercontig_2.10	95	20	1	0	0.048	32.2	<i>C.neoformans/S. cerevisiae</i>
dme-miR-4968-3p*	Supercontig_2.10	95	20	1	0	0.048	32.2	<i>C.neoformans/S. cerevisiae</i>
dme-miR-4968-3p*	Supercontig_2.10	95.24	21	1	0	0.012	34.2	<i>C.neoformans/S. cerevisiae</i>
dme-miR-4968-3p*	Supercontig_2.10	95.24	21	1	0	0.012	34.2	<i>C.neoformans/S. cerevisiae</i>
dme-miR-4968-3p*	Supercontig_2.10	95.24	21	1	0	0.012	34.2	<i>C.neoformans/S. cerevisiae</i>

dme-miR-4968-3p*	Supercontig_2.12	95.24	21	1	0	1.20E-02	34.2	<i>C.neoformans/S. cerevisiae</i>
dme-miR-4968-3p*	Supercontig_2.13	100	16	0	0	4.80E-02	32.2	<i>C.neoformans/S. cerevisiae</i>
dme-miR-4968-3p*	Supercontig_2.13	100	16	0	0	4.80E-02	32.2	<i>C.neoformans/S. cerevisiae</i>
dme-miR-4968-3p*	Supercontig_2.13	100	16	0	0	0.048	32.2	<i>C.neoformans/S. cerevisiae</i>
dme-miR-4968-3p*	Supercontig_2.13	100	16	0	0	0.048	32.2	<i>C.neoformans/S. cerevisiae</i>
dme-miR-4968-3p*	Supercontig_2.13	100	16	0	0	0.048	32.2	<i>C.neoformans/S. cerevisiae</i>
dme-miR-4968-3p*	Supercontig_2.13	100	17	0	0	0.012	34.2	<i>C.neoformans/S. cerevisiae</i>
dme-miR-4968-3p*	Supercontig_2.13	100	18	0	0	0.003	36.2	<i>C.neoformans/S. cerevisiae</i>
dme-miR-4968-3p*	Supercontig_2.13	100	18	0	0	0.003	36.2	<i>C.neoformans/S. cerevisiae</i>
dme-miR-4968-3p*	Supercontig_2.13	100	19	0	0	8.00E-04	38.2	<i>C.neoformans/S. cerevisiae</i>
dme-miR-4968-3p*	Supercontig_2.13	95	20	1	0	0.048	32.2	<i>C.neoformans/S. cerevisiae</i>
dme-miR-4968-3p*	Supercontig_2.13	95	20	1	0	0.048	32.2	<i>C.neoformans/S. cerevisiae</i>
dme-miR-4968-3p*	Supercontig_2.13	95	20	1	0	0.048	32.2	<i>C.neoformans/S. cerevisiae</i>
dme-miR-4968-3p*	Supercontig_2.13	95	20	1	0	0.048	32.2	<i>C.neoformans/S. cerevisiae</i>
dme-miR-4968-3p*	Supercontig_2.13	95.24	21	1	0	0.012	34.2	<i>C.neoformans/S. cerevisiae</i>
dme-miR-4968-3p*	Supercontig_2.13	95.24	21	1	0	0.012	34.2	<i>C.neoformans/S. cerevisiae</i>
dme-miR-4968-3p*	Supercontig_2.13	95.24	21	1	0	0.012	34.2	<i>C.neoformans/S. cerevisiae</i>
dme-miR-4968-3p*	Supercontig_2.13	95.24	21	1	0	0.012	34.2	<i>C.neoformans/S. cerevisiae</i>
dme-miR-4968-3p*	Supercontig_2.13	95.24	21	1	0	0.012	34.2	<i>C.neoformans/S. cerevisiae</i>
dme-miR-4968-3p*	Supercontig_2.13	95.24	21	1	0	0.012	34.2	<i>C.neoformans/S. cerevisiae</i>
dme-miR-4968-3p*	Supercontig_2.13	95.24	21	1	0	0.012	34.2	<i>C.neoformans/S. cerevisiae</i>
dme-miR-4968-3p*	Supercontig_2.13	95.24	21	1	0	0.012	34.2	<i>C.neoformans/S. cerevisiae</i>
dme-miR-4968-3p*	Supercontig_2.13	95.24	21	1	0	0.012	34.2	<i>C.neoformans/S. cerevisiae</i>
dme-miR-4968-3p*	Supercontig_2.14	100	17	0	0	0.012	34.2	<i>C.neoformans/S. cerevisiae</i>
dme-miR-4968-3p*	Supercontig_2.14	95	20	1	0	0.048	32.2	<i>C.neoformans/S. cerevisiae</i>
dme-miR-4968-3p*	Supercontig_2.15	100	16	0	0	0.048	32.2	<i>C.neoformans/S. cerevisiae</i>
dme-miR-4968-3p*	Supercontig_2.17	100	17	0	0	0.012	34.2	<i>C.neoformans/S. cerevisiae</i>
dme-miR-4968-3p*	Supercontig_2.17	100	17	0	0	0.012	34.2	<i>C.neoformans/S. cerevisiae</i>
dme-miR-4968-3p*	Supercontig_2.17	100	18	0	0	0.003	36.2	<i>C.neoformans/S. cerevisiae</i>

dpe-miR-13a	Supercontig_2.11	100	16	0	0	0.048	32.2	<i>C.neoformans</i>
dps-miR-2565-5p	Supercontig_2.3	100	16	0	0	0.048	32.2	<i>S.cerevisiae</i>
dps-miR-968-3p*	Supercontig_2.3	100	16	0	0	0.06	32.2	<i>C.albicans</i>
dre-miR-216a	Supercontig_2.18	100	17	0	0	0.012	34.2	<i>C.albicans</i>
dwi-miR-13a	Supercontig_2.11	100	16	0	0	0.048	32.2	<i>C.albicans</i>
gga-miR-1457	Supercontig_2.2	100	16	0	0	0.048	32.2	<i>C.albicans</i>
gga-miR-1458	Supercontig_2.1	100	16	0	0	0.042	32.2	<i>S.cerevisiae</i>
gga-miR-1692	Supercontig_2.1	100	17	0	0	0.009	34.2	<i>C.albicans/S.cerevisiae/C.neoformans</i>
gga-miR-1692	Supercontig_2.2	100	17	0	0	0.009	34.2	<i>C.albicans/S.cerevisiae/C.neoformans</i>
gga-miR-1814	Supercontig_2.12	100	16	0	0	0.036	32.2	<i>C.neoformans</i>
gga-miR-29a-5p	Supercontig_2.4	100	17	0	0	0.012	34.2	<i>C.albicans</i>
gga-miR-3540	Supercontig_2.5	100	16	0	0	0.048	32.2	<i>S.cerevisiae</i>
gga-miR-466	Supercontig_2.1	100	17	0	0	0.014	34.2	<i>C.neoformans</i>
gga-miR-466	Supercontig_2.11	100	16	0	0	0.054	32.2	<i>C.neoformans</i>
gga-miR-466	Supercontig_2.17	100	16	0	0	0.054	32.2	<i>C.neoformans</i>
gga-miR-466	Supercontig_2.3	100	16	0	0	0.054	32.2	<i>C.neoformans</i>
gga-miR-466	Supercontig_2.8	100	16	0	0	0.054	32.2	<i>C.neoformans</i>
gra-miR482	Supercontig_2.6	95	20	1	0	0.048	32.2	<i>C.neoformans</i>
hsa-miR-320a	Supercontig_2.9	100	16	0	0	0.048	32.2	<i>C.albicans</i>
hsa-miR-3620-5p	Supercontig_2.10	100	18	0	0	0.003	36.2	<i>C.neoformans/S.cerevisiae</i>
hsa-miR-3620-5p	Supercontig_2.10	100	19	0	0	8.00E-04	38.2	<i>C.neoformans/S.cerevisiae</i>
hsa-miR-3620-5p	Supercontig_2.10	100	20	0	0	2.00E-04	40.1	<i>C.neoformans/S.cerevisiae</i>
hsa-miR-3620-5p	Supercontig_2.1	100	17	0	0	0.012	34.2	<i>C.neoformans/S.cerevisiae</i>
hsa-miR-3620-5p	Supercontig_2.3	100	16	0	0	0.048	32.2	<i>C.neoformans/S.cerevisiae</i>
hsa-miR-3620-5p	Supercontig_2.4	100	17	0	0	0.012	34.2	<i>C.neoformans/S.cerevisiae</i>
hsa-miR-3620-5p	Supercontig_2.4	95.24	21	1	0	0.012	34.2	<i>C.neoformans/S.cerevisiae</i>
hsa-miR-3620-5p	Supercontig_2.6	100	18	0	0	0.003	36.2	<i>C.neoformans/S.cerevisiae</i>
hsa-miR-3620-5p	Supercontig_2.6	100	19	0	0	8.00E-04	38.2	<i>C.neoformans/S.cerevisiae</i>
hsa-miR-3925-5p	Supercontig_2.2	100	16	0	0	0.048	32.2	<i>C.albicans</i>
hsa-miR-3976	Supercontig_2.31	100	16	0	0	0.06	32.2	<i>C.neoformans</i>

hsa-miR-4507	Supercontig_2.10	95	20	1	0	0.036	32.2	<i>C.neoformans/S. cerevisiae</i>
hsa-miR-4507	Supercontig_2.10	95	20	1	0	0.036	32.2	<i>C.neoformans/S. cerevisiae</i>
hsa-miR-4507	Supercontig_2.3	100	16	0	0	0.036	32.2	<i>C.neoformans/S. cerevisiae</i>
hsa-miR-4507	Supercontig_2.4	100	17	0	0	0.009	34.2	<i>C.neoformans/S. cerevisiae</i>
hsa-miR-4507	Supercontig_2.6	95	20	1	0	0.036	32.2	<i>C.neoformans/S. cerevisiae</i>
hsa-miR-4539	Supercontig_2.6	100	16	0	0	0.048	32.2	<i>C. albicans</i>
hsa-miR-5194	Supercontig_2.11	100	16	0	0	0.048	32.2	<i>S. cerevisiae</i>
hsa-miR-5195-3p*	Supercontig_2.4	100	17	0	0	0.011	34.2	<i>S. cerevisiae</i>
hsv2-miR-H13	Supercontig_2.12	100	16	0	0	0.048	32.2	<i>S. cerevisiae</i>
mml-miR-938	Supercontig_2.31	100	16	0	0	0.048	32.2	<i>C. neoformans</i>
mml-miR-938	Supercontig_2.31	100	16	0	0	0.048	32.2	<i>C. neoformans</i>
mmu-let-7c-3p*	Supercontig_2.2	100	16	0	0	0.048	32.2	<i>C. albicans/C. neoformans</i>
mmu-miR-1895	Supercontig_2.10	95.24	21	1	0	0.012	34.2	<i>S. cerevisiae</i>
mmu-miR-1903	Supercontig_2.12	100	16	0	0	0.048	32.2	<i>S. cerevisiae</i>
mmu-miR-1903	Supercontig_2.2	100	16	0	0	0.048	32.2	<i>S. cerevisiae</i>
mmu-miR-1903	Supercontig_2.3	100	16	0	0	0.048	32.2	<i>S. cerevisiae</i>
mmu-miR-1903	Supercontig_2.3	100	16	0	0	0.048	32.2	<i>S. cerevisiae</i>
mmu-miR-1903	Supercontig_2.4	100	17	0	0	0.012	34.2	<i>S. cerevisiae</i>
mmu-miR-1903	Supercontig_2.7	100	16	0	0	0.048	32.2	<i>S. cerevisiae</i>
mmu-miR-297a-5p	Supercontig_2.2	95.24	21	1	0	0.012	34.2	<i>C. albicans</i>
mmu-miR-297a-5p	Supercontig_2.3	100	16	0	0	4.80E-02	32.2	<i>C. albicans</i>
mmu-miR-297a-5p	Supercontig_2.3	100	17	0	0	1.20E-02	34.2	<i>C. albicans</i>
mmu-miR-339-5p	Supercontig_2.3	100	16	0	0	5.40E-02	32.2	<i>C. albicans</i>
mmu-miR-383-3p*	Supercontig_2.32	100	16	0	0	4.20E-02	32.2	<i>S. cerevisiae</i>
mmu-miR-383-3p*	Supercontig_2.32	100	16	0	0	4.20E-02	32.2	<i>S. cerevisiae</i>
mmu-miR-383-3p*	Supercontig_2.32	100	16	0	0	4.20E-02	32.2	<i>S. cerevisiae</i>
mmu-miR-383-3p*	Supercontig_2.32	100	16	0	0	4.20E-02	32.2	<i>S. cerevisiae</i>
mmu-miR-383-3p*	Supercontig_2.32	100	16	0	0	0.042	32.2	<i>S. cerevisiae</i>
mmu-miR-383-3p*	Supercontig_2.8	100	16	0	0	0.042	32.2	<i>S. cerevisiae</i>

mmu-miR-383-3p*	Supercontig_2.8	100	16	0	0	0.042	32.2	<i>S. cerevisiae</i>
mmu-miR-383-3p*	Supercontig_2.8	100	16	0	0	0.042	32.2	<i>S. cerevisiae</i>
mmu-miR-466f-5p	Supercontig_2.3	100	18	0	0	0.003	36.2	<i>C. albicans</i>
mmu-miR-466h-3p*	Supercontig_2.1	100	17	0	0	0.008	34.2	<i>C. neoformans</i>
mmu-miR-466h-3p*	Supercontig_2.11	100	18	0	0	0.002	36.2	<i>C. neoformans</i>
mmu-miR-466h-3p*	Supercontig_2.2	100	16	0	0	0.03	32.2	<i>C. neoformans</i>
mmu-miR-466h-3p*	Supercontig_2.3	100	16	0	0	0.03	32.2	<i>C. neoformans</i>
mmu-miR-466h-3p*	Supercontig_2.3	100	18	0	0	0.002	36.2	<i>C. neoformans</i>
mmu-miR-466h-3p*	Supercontig_2.6	100	17	0	0	0.008	34.2	<i>C. neoformans</i>
mmu-miR-466h-5p	Supercontig_2.3	95	20	1	0	0.048	32.2	<i>C. neoformans</i>
mmu-miR-466h-5p	Supercontig_2.6	100	16	0	0	0.048	32.2	<i>C. neoformans</i>
mmu-miR-466j	Supercontig_2.1	100	19	0	0	9.00E-04	38.2	<i>S. cerevisiae</i>
mmu-miR-466j	Supercontig_2.11	100	16	0	0	0.054	32.2	<i>S. cerevisiae</i>
mmu-miR-466j	Supercontig_2.11	100	16	0	0	0.054	32.2	<i>S. cerevisiae</i>
mmu-miR-466j	Supercontig_2.2	100	17	0	0	0.014	34.2	<i>S. cerevisiae</i>
mmu-miR-466j	Supercontig_2.3	100	16	0	0	0.054	32.2	<i>S. cerevisiae</i>
mmu-miR-466j	Supercontig_2.3	100	16	0	0	0.054	32.2	<i>S. cerevisiae</i>
mmu-miR-466j	Supercontig_2.3	100	16	0	0	0.054	32.2	<i>S. cerevisiae</i>
mmu-miR-466j	Supercontig_2.3	100	17	0	0	0.014	34.2	<i>S. cerevisiae</i>
mmu-miR-466j	Supercontig_2.3	100	18	0	0	0.003	36.2	<i>S. cerevisiae</i>
mmu-miR-466j	Supercontig_2.3	100	20	0	0	2.00E-04	40.1	<i>S. cerevisiae</i>
mmu-miR-466j	Supercontig_2.3	95.24	21	1	0	0.014	34.2	<i>S. cerevisiae</i>
mmu-miR-466k	Supercontig_2.6	100	16	0	0	0.054	32.2	<i>C. neoformans/S. cerevisiae</i>
mmu-miR-466k	Supercontig_2.8	100	16	0	0	0.054	32.2	<i>C. neoformans/S. cerevisiae</i>
mmu-miR-466k	Supercontig_2.18	100	16	0	0	0.054	32.2	<i>C. neoformans/S. cerevisiae</i>
mmu-miR-466k	Supercontig_2.3	100	16	0	0	0.054	32.2	<i>C. neoformans/S. cerevisiae</i>
mmu-miR-466k	Supercontig_2.3	100	16	0	0	0.054	32.2	<i>C. neoformans/S. cerevisiae</i>
mmu-miR-466k	Supercontig_2.3	100	16	0	0	0.054	32.2	<i>C. neoformans/S. cerevisiae</i>
mmu-miR-466k	Supercontig_2.4	100	16	0	0	0.054	32.2	<i>C. neoformans/S. cerevisiae</i>

mmu-miR-466k	Supercontig_2.4	100	16	0	0	0.054	32.2	<i>C.neoformans/S. cerevisiae</i>
mmu-miR-466k	Supercontig_2.5	100	16	0	0	0.054	32.2	<i>C.neoformans/S. cerevisiae</i>
mmu-miR-467a-3p*	Supercontig_2.22	100	16	0	0	0.048	32.2	<i>S. cerevisiae</i>
mmu-miR-467a-3p*	Supercontig_2.4	100	16	0	0	0.048	32.2	<i>S. cerevisiae</i>
mmu-miR-467a-3p*	Supercontig_2.9	100	16	0	0	0.048	32.2	<i>S. cerevisiae</i>
mmu-miR-467g	Supercontig_2.10	100	18	0	0	0.003	36.2	<i>C. albicans/ P. brasiliensis</i>
mmu-miR-467g	Supercontig_2.12	100	17	0	0	1.10E-02	34.2	<i>C. albicans/ P. brasiliensis</i>
mmu-miR-467g	Supercontig_2.16	100	16	0	0	4.20E-02	32.2	<i>C. albicans/ P. brasiliensis</i>
mmu-miR-467g	Supercontig_2.27	100	16	0	0	0.042	32.2	<i>C. albicans/ P. brasiliensis</i>
mmu-miR-467g	Supercontig_2.3	95	20	1	0	0.042	32.2	<i>C. albicans/ P. brasiliensis</i>
mmu-miR-467g	Supercontig_2.4	100	16	0	0	0.042	32.2	<i>C. albicans/ P. brasiliensis</i>
mmu-miR-467g	Supercontig_2.5	100	18	0	0	0.003	36.2	<i>C. albicans/ P. brasiliensis</i>
mmu-miR-467g	Supercontig_2.7	100	17	0	0	0.011	34.2	<i>C. albicans/ P. brasiliensis</i>
mmu-miR-669f-3p*	Supercontig_2.10	100	16	0	0	0.054	32.2	<i>S. cerevisiae</i>
mmu-miR-669f-3p*	Supercontig_2.13	100	16	0	0	0.054	32.2	<i>S. cerevisiae</i>
mmu-miR-669f-3p*	Supercontig_2.16	100	17	0	0	0.014	34.2	<i>S. cerevisiae</i>
mmu-miR-669f-3p*	Supercontig_2.2	100	16	0	0	0.054	32.2	<i>S. cerevisiae</i>
mmu-miR-669f-3p*	Supercontig_2.22	100	16	0	0	0.054	32.2	<i>S. cerevisiae</i>
mmu-miR-669f-3p*	Supercontig_2.3	95	20	1	0	0.054	32.2	<i>S. cerevisiae</i>
mmu-miR-669f-3p*	Supercontig_2.4	100	16	0	0	0.054	32.2	<i>S. cerevisiae</i>
mmu-miR-669f-3p*	Supercontig_2.4	100	18	0	0	0.003	36.2	<i>S. cerevisiae</i>
mmu-miR-669f-3p*	Supercontig_2.7	100	16	0	0	0.054	32.2	<i>S. cerevisiae</i>
mmu-miR-669f-3p*	Supercontig_2.9	100	16	0	0	0.054	32.2	<i>S. cerevisiae</i>
mmu-miR-669f-3p*	Supercontig_2.9	100	16	0	0	0.054	32.2	<i>S. cerevisiae</i>
mmu-miR-669f-5p	Supercontig_2.11	100	16	0	0	0.06	32.2	<i>S. cerevisiae</i>
mmu-miR-669f-5p	Supercontig_2.2	100	17	0	0	0.015	34.2	<i>S. cerevisiae</i>
mmu-miR-669f-5p	Supercontig_2.3	100	16	0	0	0.06	32.2	<i>S. cerevisiae</i>
mmu-miR-669f-5p	Supercontig_2.3	100	16	0	0	0.06	32.2	<i>S. cerevisiae</i>
mmu-miR-669f-5p	Supercontig_2.3	100	16	0	0	0.06	32.2	<i>S. cerevisiae</i>
mmu-miR-669f-5p	Supercontig_2.3	100	16	0	0	0.06	32.2	<i>S. cerevisiae</i>

mmu-miR-669f-5p	Supercontig_2.3	100	17	0	0	0.015	34.2	<i>S. cerevisiae</i>
mmu-miR-669f-5p	Supercontig_2.3	100	17	0	0	0.015	34.2	<i>S. cerevisiae</i>
mmu-miR-669f-5p	Supercontig_2.3	100	20	0	0	2.00E-04	40.1	<i>S. cerevisiae</i>
mmu-miR-669f-5p	Supercontig_2.6	100	16	0	0	6.00E-02	32.2	<i>S. cerevisiae</i>
mtr-miR5227	Supercontig_2.1	100	16	0	0	0.048	32.2	<i>C. albicans</i>
oan-miR-1346	Supercontig_2.10	100	16	0	0	0.03	32.2	<i>C. neoformans</i>
oan-miR-1351-3p*	Supercontig_2.1	100	16	0	0	0.042	32.2	<i>S. cerevisiae/C. albicans/C. neoformans</i>
oan-miR-1418-5p	Supercontig_2.3	100	16	0	0	0.042	32.2	<i>C. neoformans</i>
oan-miR-1420e-5p	Supercontig_2.3	100	17	0	0	0.014	34.2	<i>P. brasiliensis</i>
oan-miR-1421n-2-5p	Supercontig_2.1	100	17	0	0	0.012	34.2	<i>P. brasiliensis</i>
oan-miR-1422q-5p	Supercontig_2.7	100	16	0	0	0.048	32.2	<i>S. cerevisiae</i>
osa-miR1438	Supercontig_2.1	100	16	0	0	4.80E-02	32.2	<i>C. albicans</i>
osa-miR1438	Supercontig_2.1	100	16	0	0	4.80E-02	32.2	<i>C. albicans</i>
osa-miR1438	Supercontig_2.5	100	16	0	0	4.80E-02	32.2	<i>C. albicans</i>
osa-miR1438	Supercontig_2.9	100	16	0	0	4.80E-02	32.2	<i>C. albicans</i>
osa-miR1438	Supercontig_2.9	100	17	0	0	0.012	34.2	<i>C. albicans</i>
osa-miR156k	Supercontig_2.1	100	16	0	0	0.042	32.2	<i>S. cerevisiae</i>
osa-miR156k	Supercontig_2.8	100	16	0	0	0.042	32.2	<i>S. cerevisiae</i>
osa-miR2921	Supercontig_2.14	100	16	0	0	0.06	32.2	<i>C. neoformans</i>
osa-miR2921	Supercontig_2.46	100	16	0	0	0.06	32.2	<i>C. neoformans</i>
osa-miR399c	Supercontig_2.3	100	16	0	0	0.042	32.2	<i>C. neoformans</i>
osa-miR5144-5p	Supercontig_2.17	100	16	0	0	0.042	32.2	<i>C. neoformans/S. cerevisiae</i>
osa-miR821c	Supercontig_2.12	95	20	1	0	0.06	32.2	<i>P. brasiliensis</i>
osa-miR821c	Supercontig_2.4	100	16	0	0	0.06	32.2	<i>P. brasiliensis</i>
pab-miR482d	Supercontig_2.1	100	16	0	0	0.042	32.2	<i>S. cerevisiae</i>
pma-miR-130e	Supercontig_2.3	100	16	0	0	0.054	32.2	<i>P. brasiliensis</i>
pma-miR-20a-5p	Supercontig_2.3	100	17	0	0	0.014	34.2	<i>C. albicans/C. neoformans</i>
ppt-miR1047-5p	Supercontig_2.10	100	16	0	0	0.042	32.2	<i>P. brasiliensis</i>
ppy-miR-1228	Supercontig_2.7	100	16	0	0	0.036	32.2	<i>S. cerevisiae</i>
rno-let-7e-3p*	Supercontig_2.2	100	16	0	0	0.048	32.2	<i>C. albicans/C. neoformans</i>

mo-miR-483-5p	Supercontig_2.13	100	16	0	0	0.048	32.2	<i>C.neoformans</i>
mo-miR-483-5p	Supercontig_2.2	100	16	0	0	0.048	32.2	<i>C.neoformans</i>
mo-miR-483-5p	Supercontig_2.6	95.24	21	1	0	0.012	34.2	<i>C.neoformans</i>
mo-miR-487b-5p	Supercontig_2.3	100	16	0	0	0.054	32.2	<i>S.cerevisiae</i>
sbi-miR821e	Supercontig_2.4	100	18	0	0	0.003	36.2	<i>C.neoformans</i>
sha-miR-23b	Supercontig_2.11	100	16	0	0	0.03	32.2	<i>C.albicans</i>
sme-miR-2149-5p	Supercontig_2.2	100	16	0	0	0.042	32.2	<i>C.neoformans</i>
smo-miR1097	Supercontig_2.2	100	16	0	0	0.042	32.2	<i>C.albicans</i>
ssc-miR-664-5p	Supercontig_2.2	100	16	0	0	0.054	32.2	<i>P.brasiliensis</i>
tgu-miR-200a-5p	Supercontig_2.26	95	20	1	0	0.042	32.2	<i>C.albicans/S.cerevisiae</i>
tgu-miR-2976	Supercontig_2.11	100	16	0	0	0.042	32.2	<i>C.albicans/C.neoformans/ P.brasiliensis</i>
vvi-miR3631c	Supercontig_2.7	100	17	0	0	0.012	34.2	<i>C.neoformans/S.cerevisiae</i>
vvi-miR3631d	Supercontig_2.7	100	17	0	0	0.012	34.2	<i>S.cerevisiae/ P.brasiliensis</i>

- a) Identifier of the microRNAs;
b) Sequence;
c) Percent of the identity between the sequences;
d) Size of alignment between the sequences of microRNAs and the genome region of *P. brasiliensis* (Pb18);
e) Number of different bases between the aligned sequences;
f) Absence of complementary bases between the sequences;
g) Likelihood sequence analyzed to align randomly to other sequences in the database. false positive rate;
h) Normalized score obtained using the following formula: $S' = (I S - \ln K) / \ln 2$;
i) Microorganism which microRNAs have been described;
j) Article describing microRNAs in fungi vesicles; (*) microRNA star.



Capítulo 3

Regulation of the morphogenesis, cell wall synthesis and energy production, mediated by microRNAs-like produced in yeast, mycelium and during the dimorphic transition in *Paracoccidioides brasiliensis*.

Juliana S. de Curcio^{1,2}; Juliano D. Paccez¹; Evandro Novaes³; Célia Maria de Almeida Soares^{1*}.

1-Laboratório de Biologia Molecular, Instituto de Ciências Biológicas, Universidade Federal de Goiás, Brasil, Campus II Samambaia, CEP: 74690-900.

2-Programa de Pós-Graduação em Patologia Molecular, Faculdade de Medicina, Universidade de Brasília, Brasil, CEP: 70910-900.

3-Universidade Federal de Goiás, Escola de Agronomia, Setor de Melhoramento de Plantas, Campus II Samambaia, Rodovia Goiânia a Nova Veneza, CEP: 74.690-900.

* author for correspondence: cmasoares@gmail.com

Abstract

MicroRNAs are molecules involved in the mechanism of post transcriptional gene regulation. Several studies have demonstrated that these molecules play determining role during the infection process. In pathogenic fungi microRNAs-like have been described at different morphological stages and such molecules regulate targets involved in morphogenesis, energy production mechanism of DNA repair. *Paracoccidioides* spp. are the etiological agents of the main systemic mycosis in Latin America. Fungi of the *Paracoccidioides* complex present a plasticity to colonize different niches. In fact those fungi remodel pathways involved in cellular metabolism, production of structural cell wall components. However, the mechanisms that regulate the expression of genes and proteins in those pathogens are not fully elucidated. Therefore, the present work characterizes the microRNAs-like produced by *P. brasiliensis*, Pb18 in yeast cells, mycelium and during the dimorphic transition, through high performance sequencing and bioinformatics analyzes. Here we demonstrate that transcripts encoding proteins involved in microRNA-like biogenesis are differentially expressed between each morphological stage. In addition, new generation sequencing data allowed the description of 48 microRNAs-like present in the cDNA libraries, and of the total, 44 were differentially regulated among the libraries. Differential expression data revealed a similar profile of regulated microRNAs-like between the mycelial and dimorphic transition phases (22 hs), however in the parasitic yeast phase occurs a complete remodeling of the expression of these small RNAs. Analyzes of the targets of the microRNAs-like, with higher expression in yeast cells, revealed differentially regulated cellular processes. Data demonstrate that microRNAs-like presumably regulate the polysaccharide present in the yeast cell wall, by the repression of proteins involved in the β -glucan synthesis and chitin degradation. Also, repressing oxidative phosphorylation in yeast cells is presumed, since this metabolic step is preferentially used in the mycelial phase. Proteins involved in oxidative stress response present in mitochondria, hyphae production and cell division were also repressed by yeast-cells induced microRNAs-like; meantime these proteins were not regulated by microRNAs-like present in the cDNA libraries of mycelium and mycelium-to-yeast transition. Therefore, this work describes potential post-transcriptional regulation mediated by microRNAs-like in *P. brasiliensis* and its influence on the adaptive processes of this thermal dimorphic fungus.

Keywords: *Paracoccidioides*, microRNAs-like, PCM, cell wall, mycosis.

Introduction

MicroRNAs are small RNAs ranging in size from 21 to 24 nt, which action is regulate the expression of target genes involved on different processes such as cell proliferation and tumorigenesis. Regulation of gene expression by microRNAs is an evolutionarily conserved mechanism. Several studies have demonstrated the importance of those molecules during the development of infection by pathogens, in the human host (He et al., 2018; Pires et al., 2017; Sharbati et al., 2011). In fungi microRNAs-like are regulated in conditions, such as changes in environmental temperature (Bai et al., 2015), growth as different morphologies (Lau et al., 2013; Zhou et al., 2012).

In *Penicillium chrysogenum*, the miR-21 was predicted to bind to at least three mRNA targets that are involved in DNA-repair mechanisms. The targets of other microRNAs-like produced by this fungus include cytochrome P450 protein, putative proline-rich cell wall protein, PLC-like phosphodiesterase and many hypothetical proteins (Dahlmann and Kück, 2015). In *Aspergillus fumigatus* microRNAs-like have as target proteins involved in control of metabolism, transport, signal transduction, as well as one protein which is responsible for ustiloxin B biosynthesis (Bai et al., 2015). MicroRNA-like produced by *Metarhizium anisopliae* have as targets proteins involved in sporulation and probably, microRNAs-like may influence the process of conidia formation (Zhou et al., 2012). The thermal dimorphic fungus *Penicillium marneffeii* microRNAs-like target proteins such as benzoate 4-monooxygenase, cytochrome P450 and the protein RanBP10 involved in the process of cellular mitosis (Lau et al., 2013).

Species of the *Paracoccidioides* complex (Bocca et al., 2013; Carrero et al., 2008; Matute et al., 2006; Teixeira et al., 2009; Turissini et al., 2017), are thermodimorphic fungi that cause systemic mycosis with the highest prevalence in Latin America. Countries such as Brazil, Ecuador and Venezuela have high incidence of the disease, mainly in rural workers, causing health problems with high mortality rates and often leaving sequels on the patients (Bocca et al., 2013; Coutinho et al., 2002; do Valle et al., 2017; Shikanai-Yasuda et al., 2006, 2017). Several studies have demonstrated the plasticity that species belonging to the *Paracoccidioides* complex possess in adapting to different niches including the human host.

Transcriptional studies in members of the *Paracoccidioides* complex revealed remodeling of genes during the dimorphic transition event, a process that precedes

colonization in the host. In fact during this event there is a remodeling of polysaccharides present in the cell wall, with induction of chitin and α -glucan biosynthesis genes (Bastos et al., 2007). In addition proteins involved in cellular signaling pathways such as MAPK and calmodulin are induced (Nunes et al., 2005). Specific genes have also been described as essential during the dimorphic transition including histidine kinase *drk1* (Chaves et al., 2016), *Ras-1* and 2 (Fernandes et al., 2008) and blocking the function of these genes and proteins by specific inhibitors impairs the dimorphic transition process. In addition, cyclic AMP levels also influence the morphogenesis of those fungi (Chen et al., 2007).

In addition to the cellular changes triggered by temperature in species of the *Paracoccidioides* complex, transcriptional data also demonstrated genes that are expressed at each specific stage of these pathogens. The metabolism between the mycelium and yeast phases is also different, since mycelium has a metabolism preferably aerobic, in contrast to yeast cells that present higher expression of genes such that one encoding for alcohol dehydrogenase I, involved in anaerobic metabolism. Genes encoding enzymes of the glyoxylate cycle such as isocitrate lyase, were also preferentially expressed in yeast cells (Felipe et al., 2005). Proteomic data comparing mycelium, dimorphic transition from mycelium to yeast and yeast cells, corroborate the data obtained from the transcriptome analysis of members of the *Paracoccidioides* complex. In general, the data point to a higher expression genes encoding to glycolytic pathway enzymes, to glyoxylate cycle enzymes and enzymes of lipid metabolism in the yeast phase. In the mycelium phase, the induced proteins are related to aerobic energy production, in addition to proteins involved in cell defense against oxidizing agents such as mitochondrial peroxiredoxin and superoxide dismutase dependent on manganese. After 22 hours of dimorphic transition from mycelium to yeast cells, occurs induction of the pentose phosphate pathway proteins, possibly to produce substrate for the glycolysis that is induced in the yeast phase, in addition to the induction of heat shock response proteins (Rezende et al., 2011). Although, transcriptional and proteomic data reveal a fine regulation of genes and proteins in the specific morphological stages and during the dimorphic transition, the mechanisms regulating the expression of these genes and proteins are not fully elucidated

In *Paracoccidioides* spp. proteins involved in biogenesis of microRNAs-like and silencing of target genes are conserved, being similar to those of other fungi. In addition, the transcripts encoding those proteins are produced in the yeast phase of this

pathogen. Based on analyzes of sequence similarity we described the presence of microRNAs-like, homologues to those produced by other fungi, conserved in the genome of this pathogen (Curcio et al., 2018 submitted) . Considering the relevance of the knowledge of mechanisms developed by members of the *Paracoccidioides* complex, for survival and regulation of biological processes, the study of microRNAs-like is of relevance. Therefore, the objective of this study was characterize the presence and differential expression of microRNAs-like in *Paracoccidioides brasiliensis*. in different stages of development, as well as, biological processes regulated by microRNAs-like. This study can open doors for future investigations of the function of those molecules in the process of infection in the host.

Material and Methods

Fungus strain and developmental phases

Paracoccidioides brasiliensis *Pb18* (ATCC 32069) in the yeast and mycelium phases was cultivated and maintained in solid Sabouraud medium (Das et al., 2010) temperatures of 36°C and 22°C respectively. The components of Sabouraud dextrose agar medium (HIMEDIA) are as follows: Peptone 10% (w/v), dextrose 4% (w/v), 1.5% (w/v) agar. After, five days of culture in solid medium, *Pb18* yeast cells were inoculated in Sabouraud liquid medium at 36° C for 18 h, under agitation (150 rpm). After maintenance for 15 days in solid medium, the mycelium of *Pb18* was inoculated in Sabouraud liquid medium for 18 h under agitation at 150 rpm, at 22°C. For the transition experiments, the mycelium of *Pb18*, grown in solid Sabouraud medium for 15 days, was inoculated into Sabouraud liquid medium for 96 h at 22°C. The transition from mycelium to yeast was performed by changing the temperature from 22°C to 36°C. The definition of the transition time for the subsequent experiments was obtained by counting the yeast appearing cells in a Neubauer's Chamber. Cultures were evaluated at 0, 22, 48, 72 and 96 h after the temperature change.

RNA extraction and analysis of the expression of transcripts by quantitative real-time PCR (qRT-PCR)

The mycelial and yeast forms inoculated on Sabouraud for 18 h and during the dimorphic transition (22 h) were centrifuged at 12 000 x g for 10 min at 4 °C, with the supernatant being discarded. The cells were lysed with glass beads in the presence of

TRIzol (TRI Reagent, Sigma-Aldrich, St. Louis, MO) and RNA extraction was performed according to the manufacturer's specifications.

RNA samples collected, as described above, were used for gene expression and for high-performance sequencing data. Oligonucleotide primers for dicers and argonaunts (Curcio et al., 2018, submitted) were used in the analysis of transcripts. Total RNA was incubated with DNase (RQ1 RNase-free DNase, Promega) and subsequently subjected to reverse transcription *in vitro* (SuperScript III First-Strand Synthesis SuperMix; Invitrogen, Life Technologies). Synthesized cDNAs were used in the RT-PCRq reaction using Step OnePlus platform (Applied Biosystems) with a mixture of SYBR green PCR master mix (Applied Biosystems, Foster City, CA). Normalization of the values was performed using the gene encoding the actin protein (GenBank XP_010761942). The standard curves were generated by dilution at 1: 5 of the cDNA and the relative expression levels of the transcripts were calculated using the standard curve method for relative quantification (Fernandes et al., 2008). Statistical comparisons were performed using the STUDENT's t-test; $p \leq 0.05$ values were considered statistically significant.

RNAs integrity, small RNA libraries construction and next-generation sequencing (NGS)

The integrity and quality of the RNA samples were evaluated using 1% (w/v) agarose gel electrophoresis, Nanodrop (Life Technologies) to check for RNA purity (OD260/ OD280), Qubit ® 2.0 (Life Technologies) for quantification and the 2100 BioAnalyzer (Agilent) system for determination of RNA integrity. Subsequently the RNAs were stored in a chemically inert matrix GenTegra™ RNA (GenOne Biotechnologies) and sent for sequencing. Mycelial, transition and yeast libraries were constructed with the NEBNext® Multiplex Small RNA Library Prep Set for Illumina (Illumina KIT). Initially adapters were ligated into the 3' and 5'-regions of the RNA molecules, then cDNAs were synthesized, amplified, purified and size selected from an agarose gel. The sequencing of the samples was performed by a company, GenOne Biotechnologies, using the Illumina HiSeq 2500 platform.

Sequence analyses for prediction of microRNA-like

Sequences in FASTQ format were obtained for each library: mycelium, mycelia transition to yeast cells and yeast cells phases. Initially, the quality of the sequences was evaluated with the FastQC program. Poor quality sequences, as well as the adapters

used for library preparation, were removed with the Trimmomatic program (Bolger et al., 2014). After processing the sequences, they were submitted to BLASTx (States and Gish, 1994) against the nr database (<https://blast.ncbi.nlm.nih.gov/>) in order to confirm that the sequences of the RNAseq were from *P. brasiliensis* Pb18. The processed sequences were then mapped into the reference genome of *P. brasiliensis* present in NCBI (https://www.ncbi.nlm.nih.gov/genome/334?genome_assembly_id=212342) with the mapper.pl script of the mirDeep2 program (Friedländer et al., 2012). The output mapping file was analyzed by the miRDeep2.pl script to search for pre-miRNA structure in the Pb18 genome. Basically, mirDeep2 searches for genome locations with many reads mapped and with self-complementary, hairpin structure characteristic of the pre-microRNA (Friedländer et al., 2012). When a pre-microRNA is predicted, mirDeep2 outputs its sequence, including the predicted mature and star sequences in FASTA format.

miRNAs-like differential expression analyses with RNA-Seq and prediction of target genes

The numbers of reads mapped to each miRNA-like were evaluated with the quantifier.pl script of mirDeep2. The result was a counting matrix, with each miRNA-like in the rows and libraries (mycelium, transition and yeast phases). This count matrix was used for statistical tests of differential expression among libraries using DESeq2 (Love et al., 2014), a package of the R/Bioconductor. A likelihood ratio test (LRT) was performed to compare the full model (including all the phases) against the reduced model (only intercept). This LRT was used to find any difference among the phases. In addition, Negative Binomial Wald Tests were performed to compare all the three phases in a pairwise manner. The potential targets of miRNA-like candidates were predicted using 3' UTR sequences from all *P. brasiliensis* Pb18 genes. The 3' UTR sequences were obtained with a custom Perl script that retrieved the first 200 bp sequences from all the Pb18 transcripts downloaded from the NCBI database (https://www.ncbi.nlm.nih.gov/genome/334?genome_assembly_id=212342) (Brown et al., 2015). The search for homology between the miRNAs and the 3' UTR of all genes was performed by the RNAhybrid program (Rehmsmeier et al., 2004), with the following parameters: -f 2,7 for requiring complete complementary at the seed region (positions 2-7 of the microRNA); -e -20 requiring a minimum free energy of the predicted hybridization below -20 kcal/mol; -p 0.05 for a 5% p-value cutoff (Lewis et

al., 2005). The functional classification of the targets was performed through the Blast2GO (Conesa et al., 2005) and Funct2 programs.

Results

RNA extraction and regulation of the genes encoding proteins involved in the processing of microRNAs-like.

The steps used in this work for prediction of microRNAs-like in *P. brasiliensis Pb18* are shown in the workflow chart (Supplementary Figure 1). The procedure of extracting RNAs of the different phases of *P. brasiliensis Pb18* was carried out with the purpose of identifying microRNAs-like produced by this pathogen. The time of extraction of RNA in the transition phase from mycelium to yeast cells was determined by counting yeast cells at 0, 22, 48, 72, 96 h after temperature shift. Based on this time course analysis, the time of 22 h of transition was selected for the experiments of gene expression and sequencing of microRNAs-like. It was verified that at 22 h after the temperature shift, yeast cells were detected (Supplementary Figure 2). After determination of RNA extraction time, expression levels of transcripts coding for dicers and argonats were evaluated among the different morphological stages. The transcript coding for *dcr-1* depicted similar expression in the transition event and in yeast cells. *dcr2* depicted similar expression in mycelium and yeast cells, although a decrease in expression was observed during mycelium to yeast transition (Figure 1 A-D). The transcripts coding for *ago-1* and *ago-2* have decreased expression during the dimorphic transition. It is noteworthy, that the expression of *dcr-1* and *ago-1* predominates in yeast cells; *ago-2* is predominant in mycelium, whereas *dcr-2* has similar expression in mycelium and yeast cells.

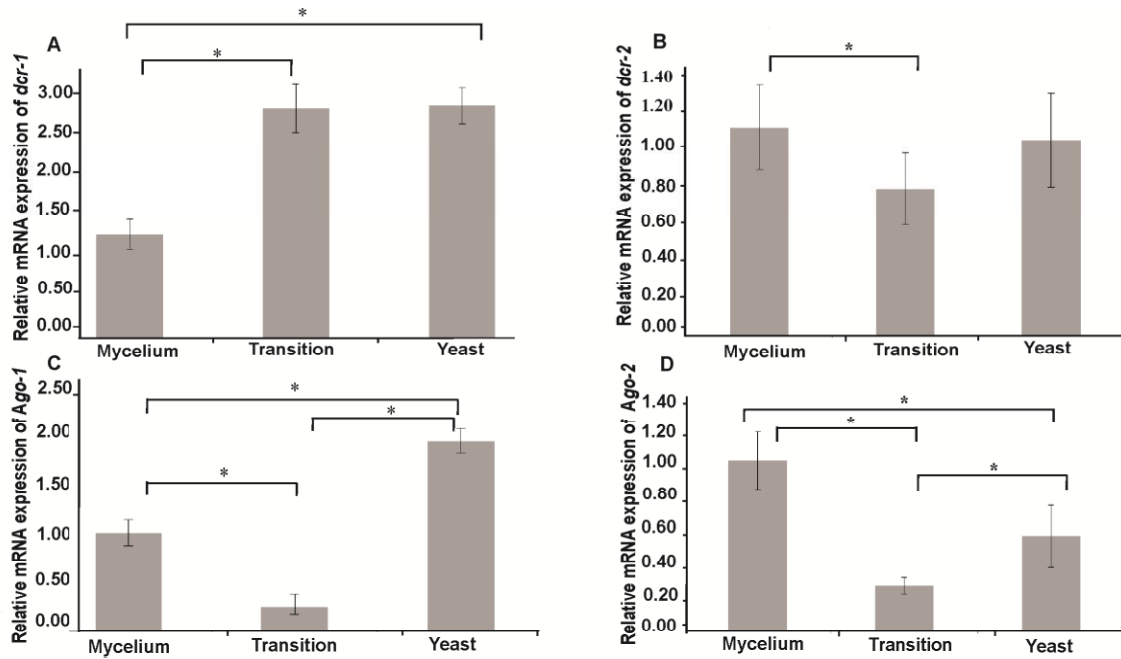


Figure 1- Analysis of expression of genes involved in post-transcriptional gene silencing (A) *dcr 1*, (B) *dcr 2* (*dicer*), (C) *Ago 1*, (D) *Ago 2* (*Argonaut*) in mycelium, transition from mycelium to yeast and yeast cells of *Pb18* by real time PCR. The data were normalized with the transcript encoding actin. The T-test was used for statistical comparisons. Error bars represent standard deviation of three biological replicates. (*) Represents $p \leq 0,05$.

Processing of data from RNA sequencing

Due to differential regulation of the genes encoding proteins involved in processing of microRNAs-like (dicers and argonauts) we constructed the small-RNA libraries at the times: 22 hours of transition from mycelium to yeast and 18 hours of growth in liquid sabouraud medium for mycelium and yeast cells. The cDNAs were sequenced with the Hiseq2500 Illumina platform in biological triplicates. The number of raw small-RNA sequences obtained ranges from 18.205.091 to 22.443.544 among libraries (Supplementary table 1). All cDNA libraries generated sequences of high quality with the vast majority of the bases having PHRED Score above 30, indicating an average of one sequencing error per 1000 base pairs. In supplemental figure S3, the quality data of one of the mycelial libraries is presented. Although the RNAseq data presented high quality, additional processing was performed with the Trimmomatic mainly to remove adapters' sequences present in the libraries. The number of sequences for the different conditions before and after processing is presented in Supplementary Table 1.

Identification of *P. brasiliensis* putative microRNAs-like by deep sequencing and differential expression analyzes

After obtaining the RNAseq data and processing the sequences, they were mapped in the genome of *P. brasiliensis* employing the mirDeep2 program. The number of reads mapped between libraries ranged from 1.203.138 at 1.782.745 (data not shown). The mapped sequences were also analyzed by miRDeep2 in order to evaluate the presence of sequences with potential to be precursors of microRNAs-like and generate mature microRNAs-like. Table 1 shows the precursor, mature and star sequences of the microRNAs among the three conditions. Among the libraries, 48 microRNAs-like were identified with a mirDeep2 score above 5, recommended to increase the likelihood of true positive predictions. In fact, 3 microRNAs-like described in the *in silico* analyzes demonstrate high similarity with sequences of the microRNA-like identified in libraries (data not show). The sequences of all the precursors presented characteristics of hairpin with minimum free folding energy values similar to those described in other microorganisms (Figure Supplementary 4) (Jiang et al., 2012; Lau et al., 2013).

Analyses with DESeq2/R indicated that the vast majority of the predicted microRNAs-like were differentially expressed among developmental phases of the fungus (mycelial, transition and yeast). Among the 48 predicted microRNAs-like, 44 were differentially expressed between the conditions, with a false discovery rate of 5% (FDR <0.05). Between the mycelial and transition libraries 16 microRNAs-like were differentially expressed, with seven induced in the mycelium library and nine in the transition library (Table supplementary 2). Comparisons between mycelial and yeast cells libraries identified 39 microRNAs-like differentially regulated, with 19 induced in the yeast cells and 20 in mycelium (Table supplementary 3). Between yeast and transition libraries, 38 microRNAs-like were differentially expressed, with 18 induced during transition and 20 in yeast cells (Table supplementary 4). Figure 2 shows a heat-map with the expression profile of the differentially regulated microRNAs-like among libraries. In general, microRNAs-like expression profiles were similar between mycelium and dimorphic transition (22 h) phases, explaining why only 16 microRNAs were differentially regulated between these two libraries. However in the parasitic, yeast phase occurs a complete remodeling of the expression profile of the microRNAs-like, possibly to assist in the process of adaptation to this new morphological stage.

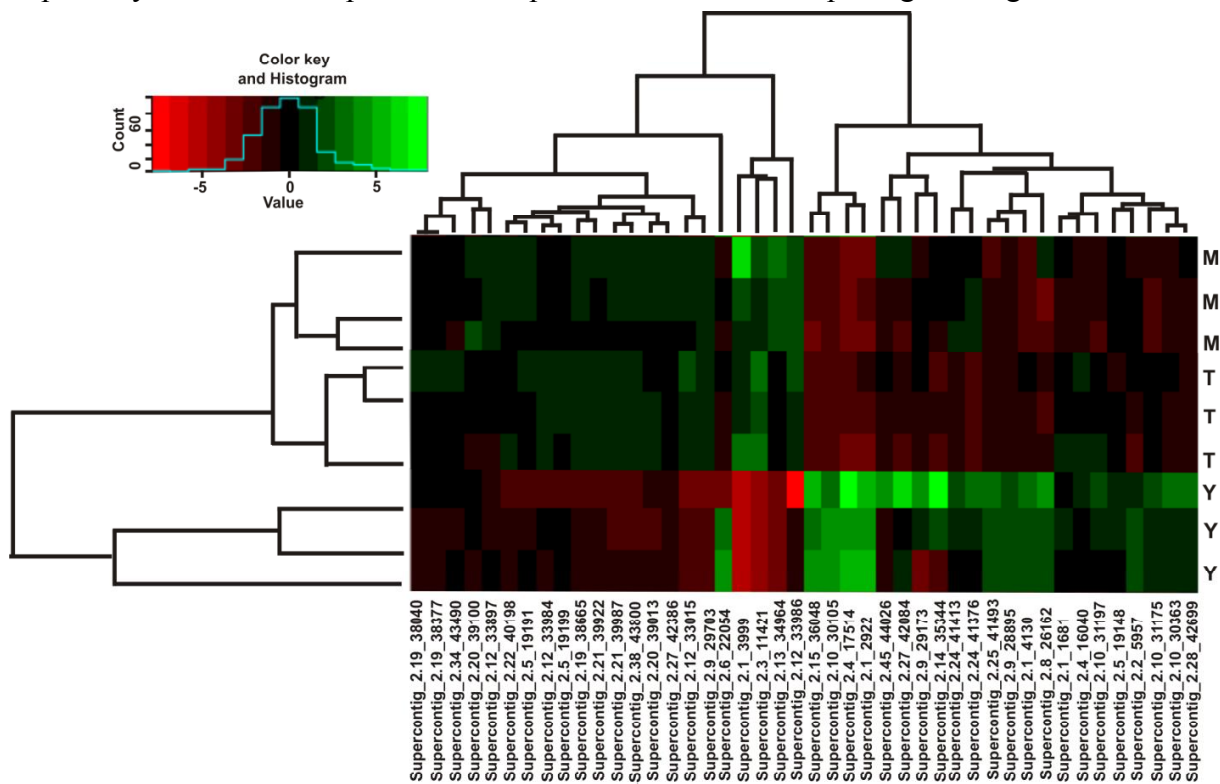


Figure 2- Heat map of differentially expressed microRNAs-like. The differentially expressed miRNAs-like are those with values of $p_{adj} < 0.05$. Changes in the level of microRNAs-like between the different morphological stages are demonstrating in the heat map. For each library, biological triplicates were constructed, down-regulated microRNAs-like are shown in red in the heat map and up-regulated microRNAs-like are shown in green (Y)-Yeast cells (M)-Mycelium, (T)-Transition.

MicroRNAs-like with higher differential expression in the yeast cells were chosen for analysis of biological processes regulated by those molecules. The choice of microRNAs-like with higher expression values between mycelial versus yeast cells and transition versus yeast cells libraries considers the $P_{adj} < 0.00001$ and $\log^2\text{FoldChange} > 4$. Table 2 shows the microRNAs-like that showed all the criteria described above.

Table 2- MicroRNAs-like with the highest values in the yeast libraries.

Supercontig	$\log^2\text{foldchange}$	P-value	Padj	Up-regulated	Down-regulated
Supercontig_2.15_36048	-6.203401859	2.31E-50	5.67E-49	Yeast	Mycelium/Transition
Supercontig_2.25_41493	-4.130461472	6.59E-43	8.07E-42	Yeast	Mycelium/Transition
Supercontig_2.4_17514	-8.946602967	3.34E-71	1.64E-69	Yeast	Mycelium/Transition
Supercontig_2.1_4130	-4.639213062	7.57E-29	7.42E-28	Yeast	Mycelium/Transition
Supercontig_2.1_2922	-7.651258173	2.32E-16	1.26E-15	Yeast	Mycelium/Transition
Supercontig_2.10_30105	-9.782396983	1.09E-14	5.34E-14	Yeast	Mycelium/Transition
Supercontig_2.6_22054	-4.685124996	9.82E-10	2.83E-09	Yeast	Mycelium/Transition
Supercontig_2.14_35344	-8.405374165	4.35E-07	1.12E-06	Yeast	Mycelium/Transition

Biological processes regulated by microRNAs-like

Some microRNAs-like had more than 700 targets, such as the microRNA present in the Supercontig_2.25_41493, Supercontig_2.1_2922 and Supercontig_2.15_36048. It is known that microRNAs have several targets. Curiously the microRNA-like (Supercontig_2.10_30105) presented only a single target, annotated as involved in protein fate (folding and transport) similar to the results found in *P. chrysogenum* (Dahlmann and Kück, 2015) (Figure S5). However, most of the microRNAs-like presented around 18 to 150 targets (data not shown).

The predicted targets silenced by microRNAs-like induced in the yeast phase are involved in biogenesis of cellular components such as the cell wall, including chitinase 3, cell wall glucanase (Scw4p), 42 kDa endochitinases, in addition to having target proteins present in the respiratory chain such as mitochondrial ATP synthase, NADH dehydrogenases, cytochrome c oxidase. Proteins of the oxidative stress response including, thioredoxin, Mn superoxide dismutase mitochondrial (SOD5) and SOD2 were predicted to be silenced by microRNAs-like induced in the yeast phase. MicroRNAs-like that exhibited as predicted targets proteins involved in the development of hyphae, cell division and morphogenesis such as Gpa2p and hydrophobin were repressed in the mycelial library and during the 22 h dimorphic

transition (Table 3). In this way, the broad extent of differentially expressed microRNAs-like in the parasitic phase of this fungus is relevant as it can point to a potential involvement of microRNAs-like in the infection process of the fungus for disease establishment.

Table 3-Biological process regulated by microRNAs-like induced in yeast cells.

BIOGENESIS OF CELLULAR COMPONENTS			
MicroRNA-like	up-regulated	down-regulated	Target
Supercontig_2.1_2922	Yeast	Mycelium/Transition	PADG_07744/42 kDa endochitinase
Supercontig_2.14_35344	Yeast	Mycelium/Transition	PADG_04922/cell wall glucanase (Scw4)
Supercontig_2.25_41493	Yeast	Mycelium/Transition	PADG_05303/beta-1,6-glucan boisynthesis protein (Knh1),
Supercontig_2.15_36048	Yeast	Mycelium/Transition	PADG_02143/cell wall biogenesis Mhp1
Supercontig_2.15_36048	Yeast	Mycelium/Transition	PADG_06374/chitinase 3
CELL RESCUE, DEFENSE AND VIRULENCE			
Supercontig_2.1_2922	Yeast	Transition/Mycelium	PADG_01755_Fe/Mn Superoxide dismutase (SOD2)
Supercontig_2.1_2922	Yeast	Transition/Mycelium	PADG_06322_Cytochrome c peroxidase
Supercontig_2.1_2922	Yeast	Transition/Mycelium	PADG_06887_Thioredoxin
Supercontig_2.4_17514	Yeast	Mycelium/Transition	PADG_01954_Fe/Mn superoxide dismutase mitochondrial(SOD5)
Supercontig_2.14_35344	Yeast	Mycelium/Transition	PADG_04912_Thioredoxin-dependent peroxidase
Supercontig_2.25_41493	Yeast	Mycelium/Transition	PADG_01755_FE/Mn Superoxide dismutase (SOD2)
Supercontig_2.25_41493	Yeast	Mycelium/Transition	PADG_04587/peroxiredoxin HYR1
Supercontig_2.25_41493	Yeast	Mycelium/Transition	PADG_06887/thioredoxin
Supercontig_2.15_36048+	Yeast	Mycelium/Transition	PADG_01755_Fe/Mn Superoxide dismutase (SOD2)
CELL FATE			
Supercontig_2.1_2922	Yeast	Mycelium/Transition	PADG_07875/hydrophobin 1
CELLULAR COMMUNICATION/SIGNAL TRANSDUCTION MECHANISM			

Supercontig_2.15_36048+	Yeast	Mycelium/Transition	PADG_04598/small G- GPA2
METABOLISM			
Supercontig_2.25_41493	Yeast	Mycelium/Transition	PADG_04274/polysaccharide synthase Cps1p
ENERGY			
Supercontig_2.1_2922	Yeast	Mycelium/Transition	PADG_00288/NADH-ubiquinone oxidoreductase 21 kDa subunit
Supercontig_2.1_2922	Yeast	Mycelium/Transition	PADG_00577/electrontransfer flavoprotein-ubiquinone oxidoreductase
Supercontig_2.1_2922	Yeast	Mycelium/Transition	PADG_01941/mitochondrial hypoxia responsive domain-containing protein
Supercontig_2.1_2922	Yeast	Mycelium/Transition	PADG_02454/NADH-ubiquinone oxidoreductase 178 kDa subunit
Supercontig_2.1_2922	Yeast	Mycelium/Transition	PADG_03039/MICOS complex subunit MIC60
Supercontig_2.1_2922	Yeast	Mycelium/Transition	PADG_03516/NADH dehydrogenase iron-sulfur protein
Supercontig_2.1_2922	Yeast	Mycelium/Transition	PADG_04397/cytochrome c subunit Vb
Supercontig_2.1_2922	Yeast	Mycelium/Transition	PADG_11513/NADH-ubiquinone oxidoreductase 19 kDa subunit
Supercontig_2.4_17514	Yeast	Mycelium/Transition	PADG_02454/NADH-ubiquinone oxidoreductase 178 kDa subunit
Supercontig_2.4_17514	Yeast	Mycelium/Transition	PADG_08052/cytochrome P450
Supercontig_2.4_17514	Yeast	Mycelium/Transition	PADG_11807/ferric reductase transmembrane component 3
Supercontig_2.15_36048+	Yeast	Mycelium/Transition	PADG_00399/short-chain dehydrogenase
Supercontig_2.15_36048+	Yeast	Mycelium/Transition	PADG_00492/NADH dehydrogenase (ubiquinone) Fe-S protein 5
Supercontig_2.15_36048+	Yeast	Micellium/Transition	PADG_01433/isoflavone reductase family protein
Supercontig_2.15_36048+	Yeast	Micellium/Transition	PADG_02623/NADH-ubiquinone oxidoreductase B12 subunit
Supercontig_2.15_36048+	Yeast	Micellium/Transition	PADG_04699/NADH-ubiquinone oxidoreductase subunit

Supercontig_2.15_36048+	Yeast	Micellium/Transition	PADG_04729/ATP synthase subunit mitochondrial
Supercontig_2.15_36048+	Yeast	Micellium/Transition	PADG_05343/NADH dehydrogenase
Supercontig_2.15_36048+	Yeast	Micellium/Transition	PADG_05402/mitochondrial F1F0 ATP synthase subunit F
Supercontig_2.15_36048+	Yeast	Micellium/Transition	PADG_05750/cytochrome c oxidase polypeptide VI
Supercontig_2.15_36048+	Yeast	Micellium/Transition	PADG_06116/cytochrome c oxidase subunit 6a
Supercontig_2.15_36048+	Yeast	Micellium/Transition	PADG_07481/H /K ATPase alpha subunit
Supercontig_2.15_36048+	Yeast	Micellium/Transition	PADG_07789/ATP synthase subunit mitochondrial
Supercontig_2.15_36048+	Yeast	Micellium/Transition	PADG_08054/malate NAD-dependent
Supercontig_2.15_36048+	Yeast	Micellium/Transition	PADG_12182/ATP NAD kinase
Supercontig_2.25_41493	Yeast	Mycelium/Transition	PADG_00316/short chain dehydrogenase/reductase
Supercontig_2.25_41493	Yeast	Mycelium/Transition	PADG_00492/NADH:ubiquinone oxidoreductase 11.5kD subunit
Supercontig_2.25_41493	Yeast	Mycelium/Transition	PADG_00577/electron transfer flavoprotein-ubiquinone oxidoreductase
Supercontig_2.25_41493	Yeast	Mycelium/Transition	PADG_00968/mitochondrial protein Fmp25
Supercontig_2.25_41493	Yeast	Mycelium/Transition	PADG_01569/oxidoreductase
Supercontig_2.25_41493	Yeast	Mycelium/Transition	PADG_02048/nitroreductase family protein
Supercontig_2.25_41493	Yeast	Mycelium/Transition	PADG_02817/short chain dehydrogenase (AtsC)
Supercontig_2.25_41493	Yeast	Mycelium/Transition	PADG_04248/NADH-ubiquinone oxidoreductase subunit GRIM-19
Supercontig_2.25_41493	Yeast	Mycelium/Transition	PADG_04729/ATP synthase D chain, mitochondrial
Supercontig_2.25_41493	Yeast	Mycelium/Transition	PADG_04878/NADH-ubiquinone oxidoreductase 40 kDa subunit
Supercontig_2.25_41493	Yeast	Mycelium/Transition	PADG_05006/dehydrogenase with different specificities
Supercontig_2.25_41493	Yeast	Mycelium/Transition	PADG_05403/NADH-ubiquinone oxidoreductase 21 kDa subunit

Supercontig_2.25_41493	Yeast	Mycelium/Transition	PADG_05407/external NADH-ubiquinone oxidoreductase
Supercontig_2.25_41493	Yeast	Mycelium/Transition	PADG_05436/ubiquinol-cytochrome c reductase iron-sulfur subunit
Supercontig_2.25_41493	Yeast	Mycelium/Transition	PADG_05750/cytochrome c oxidase subunit Va
Supercontig_2.25_41493	Yeast	Mycelium/Transition	PADG_06494/dihydrolipoyl dehydrogenase
Supercontig_2.25_41493	Yeast	Mycelium/Transition	PADG_07081/electron transfer flavoprotein subunit alpha
Supercontig_2.25_41493	Yeast	Mycelium/Transition	PADG_07210/malate dehydrogenase
Supercontig_2.25_41493	Yeast	Mycelium/Transition	PADG_11426/cytochrome P450
Supercontig_2.25_41493	Yeast	Mycelium/Transition	PADG_11806/metalloreductase
Supercontig_2.25_41493	Yeast	Mycelium/Transition	PADG_12403/short chain oxidoreductase/dehydrogenase
Supercontig_2.25_41493	Yeast	Mycelium/Transition	PADG_12404/short-chain dehydrogenase/reductase SDR

Discussion

Differential expression of biogenic machinery of small RNAs

Proteins involved in the processing of microRNAs are conserved in different kingdoms. In *P. marneffei*, human thermotolerant pathogenic fungus, analyzes of the expression of the mRNA coding for *ago-2* revealed a significant increase in the expression of this gene in the mycelium phase in relation to yeast, the same results were obtained for *dcr2* (Lau et al., 2013). In contrast, *dcr-1* mRNA expression was induced in yeast compared to mycelium. In the present work the gene expression data of *ago-2*, *dcr-1* and *dcr-2* are similar to that described in *P. marneffei* (Figure 1). In general, the data point to induction of the expression of genes coding for dicers and argonaunts among the different morphological phases. Furthermore in *N. crassa* (Lee et al., 2010) and *P. marneffei* (Lau et al., 2013) different protein dicers are involved in the processing of microRNAs-like. For example the PM-milR-M1 and PM-milR-M2 from *P. marneffei* produced only in the filamentous phase, were dependent on dicer 2 protein for their biogenesis, the dicer 1 protein is not essential. Possibly in *P. brasiliensis* this mechanism also happens, what means, this differential expression could be due to the use of different proteins in the processing of microRNAs-like.

Remodeling of the cell wall in the parasitic phase, mediated by microRNAs-like.

During the infection process in the host, species of the *Paracoccidioides* complex change the composition of polysaccharide in the cell wall. In this sense, the cell wall of the yeast phase is composed mainly of chitin and α -1,3-glucan (Kanetsuna and Carbonell, 1970). Several microRNAs-like induced in the yeast phase had target proteins involved in biogenesis, integrity and remodeling of the cell wall (Table-3). For example, the microRNA-like present in the supercontig_2.1_2922 possess as target the 42 kda endochitinase protein. In fact in, *P.lutzii*, the CTS1p endochitinase was induced in the transition from yeast to mycelium, in order to remove chitin from the cell wall, to favor the budding of hyphae in the filamentous phase of this fungus (Bonfim et al., 2006). The chitinase 3 was also regulated by microRNAs-like induced in the yeast cell (Table 3). In *P. lutzii* the chitinase 3 was identified only in the cell wall of mycelium in proteomic studies (Araújo et al., 2017). In *Candida albicans*, to the activity of chitinases was higher in the hypha and the synthesis and hydrolysis of chitin were induced during

yeast-hypha morphogenesis (Selvaggini et al., 2004). As chitinases are involved in the degradation of chitin, possibly the induction of this microRNA-like in the parasitic phase is related to the fact that chitin is present in a higher concentration in this stage and therefore, the induction of the protein that degrades this component is not necessary.

Other microRNAs-like induced in the yeast phase had as targets, proteins involved in cell wall integrity and morphogenesis, such as cell wall glucanase (Scw4p). This protein presented similarities with the cell wall glucanase (Scw4p) and glycosyl hydrolase 17 family from *A. fumigatus* and *Saccharomyces cerevisiae* respectively. In the pathogenic fungus *A. fumigatus* mutation in the gene encoding the Scw4p protein, results in a decrease of the β -glucan in the cell wall, reduction of filamentous growth and higher sensitivity to cell wall stressors, possibly due to the alteration in the constitution of the cell wall polymer (Millet et al., 2018). Similar results have also been found in *S. cerevisiae* (Cortés et al., 2002). In *P. lutzii*, β -1,3-glucanosyltransferase (GEL3p) transcript and protein expression levels were increased in the mycelium phase in comparison to the yeast phase (Castro et al., 2009). Moreover, the Gel1p protein was associated with the argonaute protein in this fungus, as detected by two-hybrid assays (De Sousa Lima et al., 2012).

Moreover, β -1,6-glucan biosynthesis (Knh1) and cell wall biogenesis (Mhp1) proteins were also regulated by microRNAs-like induced in the yeast phase. In *S. cerevisiae* the Mhp1 protein is involved in synthesis of β -1-6-glucans (Lai et al., 1997); this polymer is present in the cell wall in the yeast phase in small amounts (Puccia et al., 2011). In the fission yeast *S. pombe*, Bgs1p/Cps1p protein was identified as a putative beta 1,3-glucan synthase; phenotypic analyzes demonstrated that the protein encoded by this gene is involved in the synthesis of β 1,3 glucan, polarized growth and germination of spores. In the present work this protein was probably down-regulated by microRNA-like produced in the yeast phase (Table 3). As β -1,3-glucan is the main polysaccharide of the mycelia phase, the induction of proteins involved in the biosynthesis of this polymer is not necessary for yeast cells, since β -1,3 glucan is a polysaccharide with higher immunogenic potential (Kanetsuna and Carbonell, 1970; Mendes et al., 2017). In this sense, microRNAs-like can regulate the polymer present in the cell wall at each morphological stage by the induction or repression of proteins involved in its biosynthesis.

Regulation of processes involved in energy production by microRNA-like and response to oxidizing agents

The mycelial phase uses preferentially aerobic metabolism for energy production, compared to cells in the yeast phase (Nunes et al., 2005). Several proteins involved in the production of energy through the respiratory chain, including NADH-dehydrogenase, flavoproteins and ATP-synthase mitochondrial were predicted to be silenced by microRNAs-like induced in the yeast phase. During the respiration process, occurs the formation of reactive oxygen species (ROS). In this sense, microRNAs-like predicted to target RNAs encoding proteins involved in the maintenance of intracellular redox potential and action against oxidizing agents including Mn/Fe superoxide dismutase (SOD2), thioredoxins, Fe/Mn mitochondrial superoxide dismutase (SOD5), peroxiredoxin and aldehyde dehydrogenase, were repressed in the mycelium phase and during the dimorphic transition. In *Paracoccidioides* spp., some proteins such as peroxiredoxin (PRX) and Mn/Fe superoxide dismutase (SOD2), were induced in the mycelial phase (Rezende et al., 2011) in different points of the dimorphic transition from mycelium to yeast, and genes involved in response to oxidative stress and maintenance of intracellular redox potential were also induced (Nunes et al., 2005).

In fact, growth under metabolic conditions that favor the production of reactive oxygen species and the dimorphic transition process are stressful conditions to which these pathogens must adapt. In this way, the microRNAs-like that had these proteins as targets were down-regulated during the dimorphic transition and in the mycelial phase. On the other hand, in yeast cells that suffer less from the action of reactive oxygen species (Rezende et al., 2011) the expression of proteins to respond to oxidative stress is not a demanding requirement. Therefore, the differential expression of microRNAs-like in *P. brasiliensis* in the mycelium, dimorphic transition and yeast phases may be part of a mechanism of post-transcriptional regulation that controls the amount of proteins involved in the response to oxidative stress and energy production at each morphological stage.

Cell growth and morphogenesis

Several induced microRNAs-like in the parasitic form have as targets proteins involved in morphogenesis and cell growth (Figure 3 and Table 3). Hydrophobins are small hydrophobic proteins, involved in different cellular processes in fungi such as cell

growth and development. In *A. fumigatus* (RodA) hydrophobin is involved in the permeability, hydrophobicity, and immune-inertia of the cell (Valsecchi et al., 2017). In *Paracoccidioides* spp. the mRNA from hydrophobins 1 and 2 were detected only in mycelial phase and during the first 24 h of mycelium to yeast transition (Albuquerque et al., 2004; Goldman et al., 2003). Interestingly, the microRNA-like which has hydrophobin 1 as the target, was repressed in the mycelial and dimorphic transition cDNA libraries.

The mechanism of formation of pseudohifas in *S. cerevisiae* during nitrogen deprivation involves the Ras2p protein, which activates adenylyl cyclase to produce cyclic adenosine monophosphate. In addition to Ras2p, another Gpa2p protein, which belongs to the G-protein family is involved in the development of pseudohifas in *S. cerevisiae*, and mutations in this gene blocked the formation of pseudohifas and reduced levels of intracellular cyclic AMP (Kübler et al., 1997; Lorenz, 1997). In *P. brasiliensis* the microRNAs-like having Gpa2p as target, were induced in the parasitic phase, however in the filamentous phase and during the dimorphic transition such microRNAs-like were repressed, preventing hypha development.

Figure 3 summarizes the pathways potentially regulated by microRNAs like. In general, the microRNAs-like induced in the yeast phase, regulate the polymer present in the cell wall, by the repression of proteins involved in the degradation of chitin and synthesis of β -1,3 glucan and β -1,6 glucan. Furthermore, these microRNAs-like are predicted in yeast cells, to repress oxidative phosphorylation, in addition to proteins involved in the response oxidizing agents generated by the electron transport chain (Figure 3). Therefore *P. brasiliensis* possibly produces microRNAs-like as a mechanism of post-transcriptional gene regulation that favors the morphological, metabolic and adaptive changes carried out by this fungus in order to promote infection.

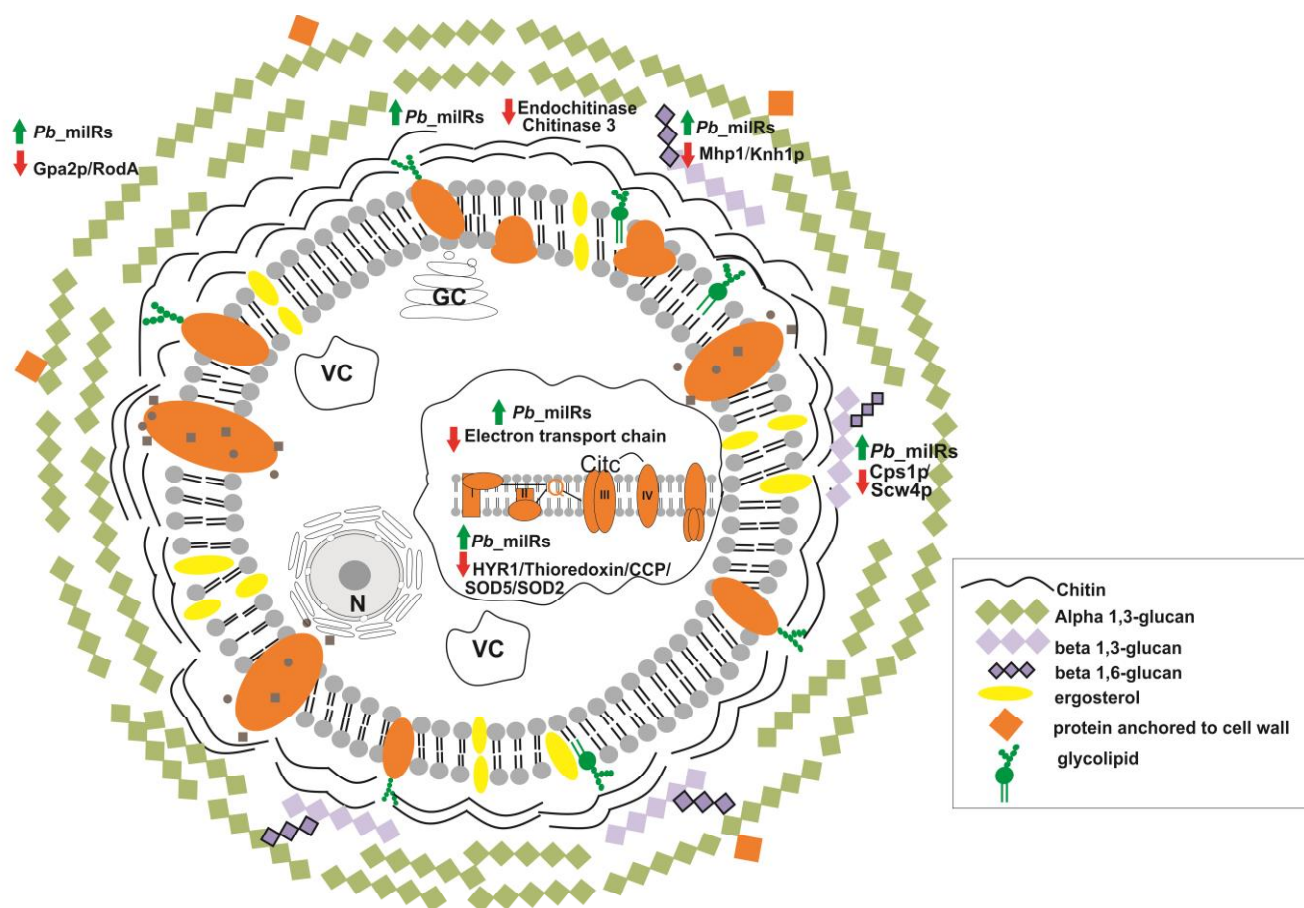


Figure 3-Predicted targets for microRNAs-like, that were induced in the yeast phase. Cell wall constitution, morphogenesis, formation of hyphae and response to oxidizing agents, are some of the processes regulated by microRNAs-like. Green arrows indicate up-regulated microRNAs-like and red arrows indicate down-regulated proteins and biological processes by microRNAs-like in yeast cells. N=cell nucleus; VC=vacuole; GC=Golgi complex.

Acknowledgments

This work was supported by grants from Conselho Nacional de Desenvolvimento Científico e Tecnológico (CNPq) and Fundação de Amparo à Pesquisa do Estado de Goiás (FAPEG)- Instituto Nacional de Ciência e Tecnologia (INCT) de Estratégias de Interação Patógeno Hospedeiro and Fundo Newton. JSC is fellow from Coordenação de Aperfeiçoamento de Pessoal de Nível Superior.

Author contributions

CMA Soares and JS de Curcio conceived and designed the experiments. JS de Curcio, performed the experiments. JS de Curcio, JD Pancez, E Novaes and CMA Soares analyzed and/or interpreted the data. CMA Soares contributed to reagents and materials. JS de Curcio, JD Pancez, E Novaes and CMA Soares wrote the manuscript.

References

- Albuquerque, P., Kyaw, C. M., Saldanha, R. R., Brigido, M. M., Felipe, M. S. S., and Silva-Pereira, I. (2004). Pbhyd1 and Pbhyd2: Two mycelium-specific hydrophobin genes from the dimorphic fungus *Paracoccidioides brasiliensis*. *Fungal Genet. Biol.* 41, 510–520. doi:10.1016/j.fgb.2004.01.001.
- Araújo, D. S., de Sousa Lima, P., Baeza, L. C., Parente, A. F. A., Melo Bailão, A., Borges, C. L., et al. (2017). Employing proteomic analysis to compare *Paracoccidioides lutzii* yeast and mycelium cell wall proteins. *Biochim. Biophys. Acta - Proteins Proteomics* 1865, 1304–1314. doi:10.1016/j.bbapap.2017.08.016.
- Bai, Y., Lan, F., Yang, W., Zhang, F., Yang, K., Li, Z., et al. (2015). SRNA profiling in *Aspergillus flavus* reveals differentially expressed miRNA-like RNAs response to water activity and temperature. *Fungal Genet. Biol.* 81, 113–119. doi:10.1016/j.fgb.2015.03.004.
- Bastos, K. P., Bailão, A. M., Borges, C. L., Faria, F. P., Felipe, M. S. S., Silva, M. G., et al. (2007). The transcriptome analysis of early morphogenesis in *Paracoccidioides brasiliensis* mycelium reveals novel and induced genes potentially associated to the dimorphic process. *BMC Microbiol.* 7, 29. doi:10.1186/1471-2180-7-29.
- Bocca, A. L., Amaral, A. C., Teixeira, M. M., Sato, P. K., Sato, P. K., Shikanai-Yasuda, M. A., et al. (2013). Paracoccidioidomycosis: eco-epidemiology, taxonomy and clinical and therapeutic issues. *Future Microbiol.* 8, 1177–1191. doi:10.2217/fmb.13.68.
- Bolger, A. M., Lohse, M., and Usadel, B. (2014). Trimmomatic: A flexible trimmer for Illumina sequence data. *Bioinformatics* 30, 2114–2120. doi:10.1093/bioinformatics/btu170.
- Bonfim, S. M. R. C., Cruz, A. H. S., Jesuino, R. S. A., Ulhoa, C. J., Molinari-Madlum, E. E. W. I., Soares, C. M. A., et al. (2006). Chitinase from *Paracoccidioides brasiliensis*: Molecular cloning, structural, phylogenetic, expression and activity analysis. *FEMS Immunol. Med. Microbiol.* 46, 269–283. doi:10.1111/j.1574-695X.2005.00036.x.
- Brown, G. R., Hem, V., Katz, K. S., Ovetsky, M., Wallin, C., Ermolaeva, O., et al.

- (2015). Gene: A gene-centered information resource at NCBI. *Nucleic Acids Res.* 43, D36–D42. doi:10.1093/nar/gku1055.
- Carrero, L. L., Niño-Vega, G., Teixeira, M. M., Carvalho, M. J. A., Soares, C. M. A., Pereira, M., et al. (2008). New *Paracoccidioides brasiliensis* isolate reveals unexpected genomic variability in this human pathogen. *Fungal Genet. Biol.* 45, 605–612. doi:10.1016/j.fgb.2008.02.002.
- Castro, N. D. S., de Castro, K. P., Orlandi, I., Feitosa, L. D. S., Rosa e Silva, L. K., Vainstein, M. H., et al. (2009). Characterization and functional analysis of the beta-1,3-glucanosyltransferase 3 of the human pathogenic fungus *Paracoccidioides brasiliensis*. *FEMS Yeast Res.* 9, 103–14. doi:10.1111/j.1567-1364.2008.00463.x.
- Cortés, J.C., Ishiguro, J., Durán, A., Ribas, J.C. (2002) Localization of the (1,3)beta-D-glucan synthase catalytic subunit homologue Bgs1p/Cps1p from fission yeast suggests that it is involved in septation, polarized growth, mating, spore wall formation and spore germination. *J Cell Sci.* 21 4081-96.
- Chaves, A. F. A., Navarro, M. V, Castilho, D. G., Calado, J. C. P., Conceição, P. M., and Batista, W. L. (2016). A conserved dimorphism-regulating histidine kinase controls the dimorphic switching in *Paracoccidioides brasiliensis*. *FEMS Yeast Res.* 16, 1–30. doi:10.1093/femsyr/fow047.
- Chen, D., Janganan, T. K., Chen, G., Marques, E. R., Kress, M. R., Goldman, G. H., et al. (2007). The cAMP pathway is important for controlling the morphological switch to the pathogenic yeast form of *Paracoccidioides brasiliensis*. *Mol. Microbiol.* 65, 761–779. doi:10.1111/j.1365-2958.2007.05824.x.
- Conesa, A., Götz, S., García-Gómez, J. M., Terol, J., Talón, M., and Robles, M. (2005). Blast2GO: A universal tool for annotation, visualization and analysis in functional genomics research. *Bioinformatics* 21, 3674–3676. doi:10.1093/bioinformatics/bti610.
- Coutinho, Z. F., Silva, D. da, Lazera, M., Petri, V., Oliveira, R. M. de, Sabroza, P. C., et al. (2002). Paracoccidioidomycosis mortality in Brazil (1980-1995). *Cad. Saude Publica* 18, 1441–54.
- Curcio, J. S. de, Batista, M. P., Paccez, J. D., Novaes, E., and Soares, C. M. de A.

- (2018). In silico characterization of microRNAs-like sequences in the genome of *Paracoccidioides brasiliensis* Pb18. *Submitted*.
- Dahlmann, T. A., and Kück, U. (2015). Dicer-dependent biogenesis of small RNAs and evidence for microRNA-like RNAs in the penicillin producing fungus *Penicillium chrysogenum*. *PLoS One* 10, 1–22. doi:10.1371/journal.pone.0125989.
- Das, S., Sharma, S., Kar, S., Sahu, S. K., Samal, B., and Mallick, A. (2010). Is inclusion of Sabouraud dextrose agar essential for the laboratory diagnosis of fungal keratitis? *Indian J. Ophthalmol.* 58, 281–6. doi:10.4103/0301-4738.64122.
- De Sousa Lima, P., Bailão, E. F. L. C., Silva, M. G., Castro, N. D. S., Bão, S. N., Orlandi, I., et al. (2012). Characterization of the *Paracoccidioides* beta-1,3-glucanosyltransferase family. *FEMS Yeast Res.* 12, 685–702. doi:10.1111/j.1567-1364.2012.00819.x.
- do Valle, A. C. F., Marques de Macedo, P., Almeida-Paes, R., Romão, A. R., Lazéra, M. dos S., and Wanke, B. (2017). Paracoccidioidomycosis after Highway Construction, Rio de Janeiro, Brazil. *Emerg. Infect. Dis.* 23, 1917–1919. doi:10.3201/eid2311.170934.
- Felipe, M. S. S., Andrade, R. V., Arraes, F. B. M., Nicola, A. M., Maranhão, A. Q., Torres, F. A. G., et al. (2005). Transcriptional profiles of the human pathogenic fungus *Paracoccidioides brasiliensis* in mycelium and yeast cells. *J. Biol. Chem.* 280, 24706–24714. doi:10.1074/jbc.M500625200.
- Fernandes, L., Paes, H. C., Tavares, A. H., Silva, S. S., Dantas, A., Soares, C. M. A., et al. (2008). Transcriptional profile of *ras1* and *ras2* and the potential role of farnesylation in the dimorphism of the human pathogen *Paracoccidioides brasiliensis*. *FEMS Yeast Res.* 8, 300–310. doi:10.1111/j.1567-1364.2007.00317.x.
- Friedländer, M. R., MacKowiak, S. D., Li, N., Chen, W., and Rajewsky, N. (2012). MiRDeep2 accurately identifies known and hundreds of novel microRNA genes in seven animal clades. *Nucleic Acids Res.* 40, 37–52. doi:10.1093/nar/gkr688.
- Goldman, G. H., Savoldi, M., Semighini, C. P., Oliveira, R. C. De, Nunes, L. R., Travassos, L. R., et al. (2003). Expressed Sequence Tag Analysis of the Human Pathogen. *Society* 2, 34–48. doi:10.1128/EC.2.1.34.

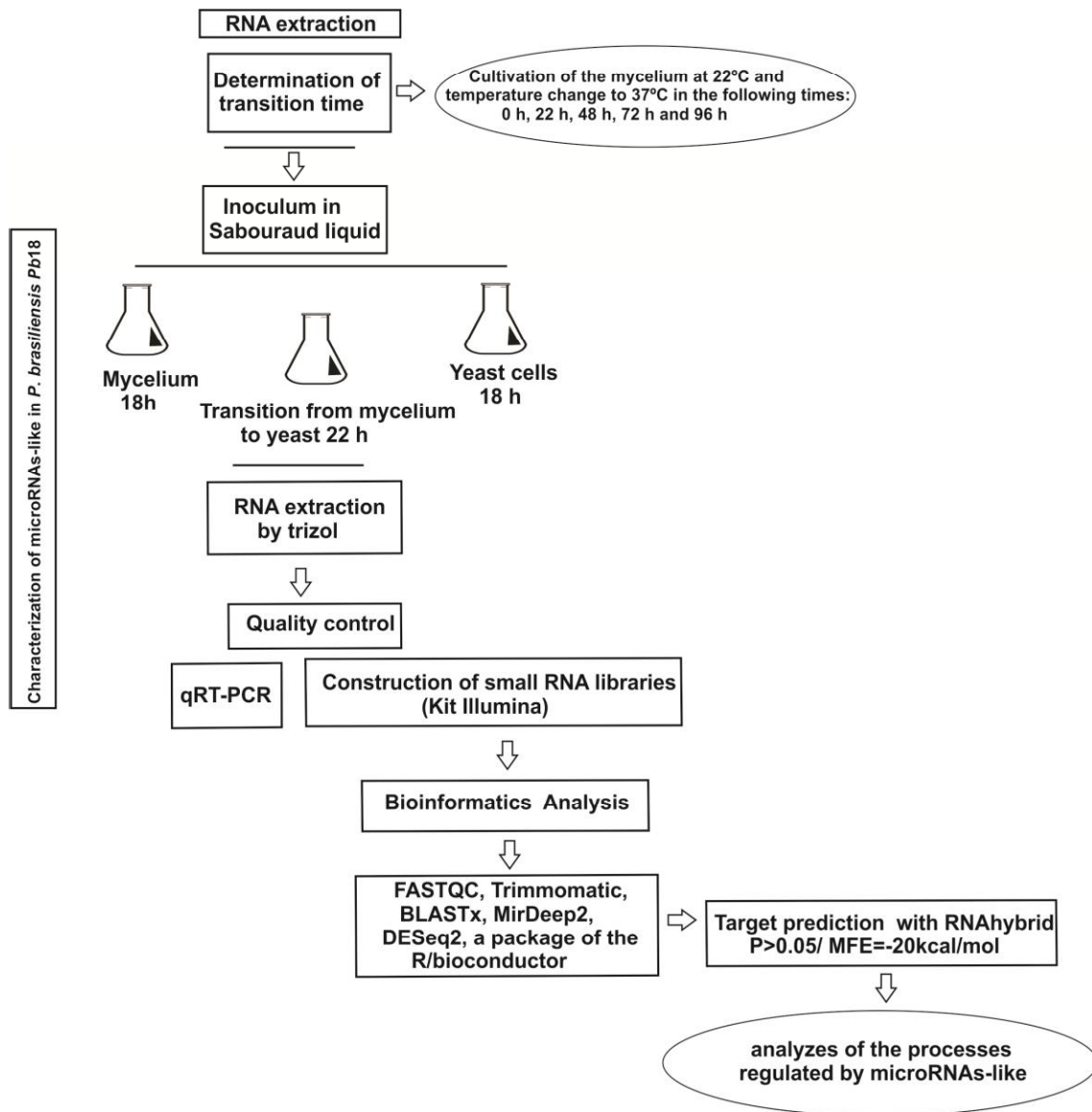
- He, X., Sun, Y., Lei, N., Fan, X., Zhang, C., Wang, Y., et al. (2018). MicroRNA-351 promotes schistosomiasis-induced hepatic fibrosis by targeting the vitamin D receptor. *Proc. Natl. Acad. Sci.* 115, 180–185. doi:10.1073/pnas.1715965115.
- Jiang, N., Yang, Y., Janbon, G., Pan, J., and Zhu, X. (2012). Identification and Functional Demonstration of miRNAs in the Fungus *Cryptococcus neoformans*. *PLoS One* 7, 20–25. doi:10.1371/journal.pone.0052734.
- Kanetsuna, F., and Carbonell, L. M. (1970). Cell wall glucans of the yeast and mycelial forms of *Paracoccidioides brasiliensis*. *J. Bacteriol.* 101, 675–80.
- Kübler, E., Mösch, H. U., Rupp, S., and Lisanti, M. P. (1997). Gpa2p, a G-protein α -subunit, regulates growth and pseudohyphal development in *Saccharomyces cerevisiae* via a cAMP-dependent mechanism. *J. Biol. Chem.* 272, 20321–20323. doi:10.1074/jbc.272.33.20321.
- Lai, M. H., Silverman, S. J., Gaughran, J. P., and Kirsch, D. R. (1997). Multiple copies of PBS2, MHP1 or LRE1 produce glucanase resistance and other cell wall effects in *Saccharomyces cerevisiae*. *Yeast* 13, 199–213. doi:10.1002/(SICI)1097-0061(19970315)13:3<199::AID-YEA76>3.0.CO;2-Z.
- Lau, S. K. P., Chow, W.-N., Wong, A. Y. P., Yeung, J. M. Y., Bao, J., Zhang, N., et al. (2013). Identification of microRNA-like RNAs in mycelial and yeast phases of the thermal dimorphic fungus *Penicillium marneffei*. *PLoS Negl. Trop. Dis.* 7, e2398. doi:10.1371/journal.pntd.0002398.
- Lee, H.-C. C., Li, L., Gu, W., Xue, Z., Crosthwaite, S. K., Pertsemliadis, A., et al. (2010). Diverse pathways generate microRNA-like RNAs and Dicer-independent small interfering RNAs in fungi. *Mol. Cell* 38, 803–14. doi:10.1016/j.molcel.2010.04.005.
- Lewis, B. P., Burge, C. B., and Bartel, D. P. (2005). Conserved seed pairing, often flanked by adenosines, indicates that thousands of human genes are microRNA targets. *Cell* 120, 15–20. doi:10.1016/j.cell.2004.12.035.
- Lorenz, M. C. (1997). Yeast pseudohyphal growth is regulated by GPA2, a G protein alpha homolog. *EMBO J.* 16, 7008–7018. doi:10.1093/emboj/16.23.7008.

- Love, M. I., Huber, W., and Anders, S. (2014). Moderated estimation of fold change and dispersion for RNA-seq data with DESeq2. *Genome Biol.* 15, 1–21. doi:10.1186/s13059-014-0550-8.
- Matute, D. R., McEwen, J. G., Puccia, R., Montes, B. A., San-Blas, G., Bagagli, E., et al. (2006). Cryptic speciation and recombination in the fungus *Paracoccidioides brasiliensis* as revealed by gene genealogies. *Mol. Biol. Evol.* 23, 65–73. doi:10.1093/molbev/msj008.
- Mendes, R. P., Cavalcante, R. de S., Marques, S. A., Marques, M. E. A., Venturini, J., Sylvestre, T. F., et al. (2017). *Paracoccidioidomycosis: Current Perspectives from Brazil*. doi:10.2174/1874285801711010224.
- Millet, N., Latgé, J.-P., and Mouyna, I. (2018). Members of Glycosyl-Hydrolase Family 17 of *A. fumigatus* Differentially Affect Morphogenesis. *J. fungi (Basel, Switzerland)* 4, 18. doi:10.3390/jof4010018.
- Nunes, L. R., Oliveira, R. C. De, Batista, D., Schmidt, V., Marques, R., Eliana, M., et al. (2005). Transcriptome Analysis of *Paracoccidioides brasiliensis* Cells Undergoing Mycelium-to-Yeast Transition Transcriptome Analysis of *Paracoccidioides brasiliensis* Cells Undergoing Mycelium-to-Yeast Transition. *Eukaryot. Cell* 4, 2115–2128. doi:10.1128/EC.4.12.2115.
- Pires, D., Bernard, E. M., Pombo, J. P., Carmo, N., Fialho, C., Gutierrez, M. G., et al. (2017). *Mycobacterium tuberculosis* modulates miR-106b-5p to control Cathepsin S expression resulting in higher pathogen survival and poor T-cell activation. *Front. Immunol.* 8, 1–13. doi:10.3389/fimmu.2017.01819.
- Puccia, R., Vallejo, M. C., Matsuo, A. L., and Longo, L. V. G. (2011). The *Paracoccidioides* cell wall: Past and present layers toward understanding interaction with the host. *Front. Microbiol.* 2, 1–7. doi:10.3389/fmicb.2011.00257.
- Rehmsmeier, M., Steffen, P., Höchsmann, M., Giegerich, R., and Ho, M. (2004). Fast and effective prediction of microRNA / target duplexes. *Spring*, 1507–1517. doi:10.1261/rna.5248604.and.
- Rezende, T. C. V, Borges, C. L., Magalhães, A. D., de Sousa, M. V., Ricart, C. A. O., Bailão, A. M., et al. (2011). A quantitative view of the morphological phases of

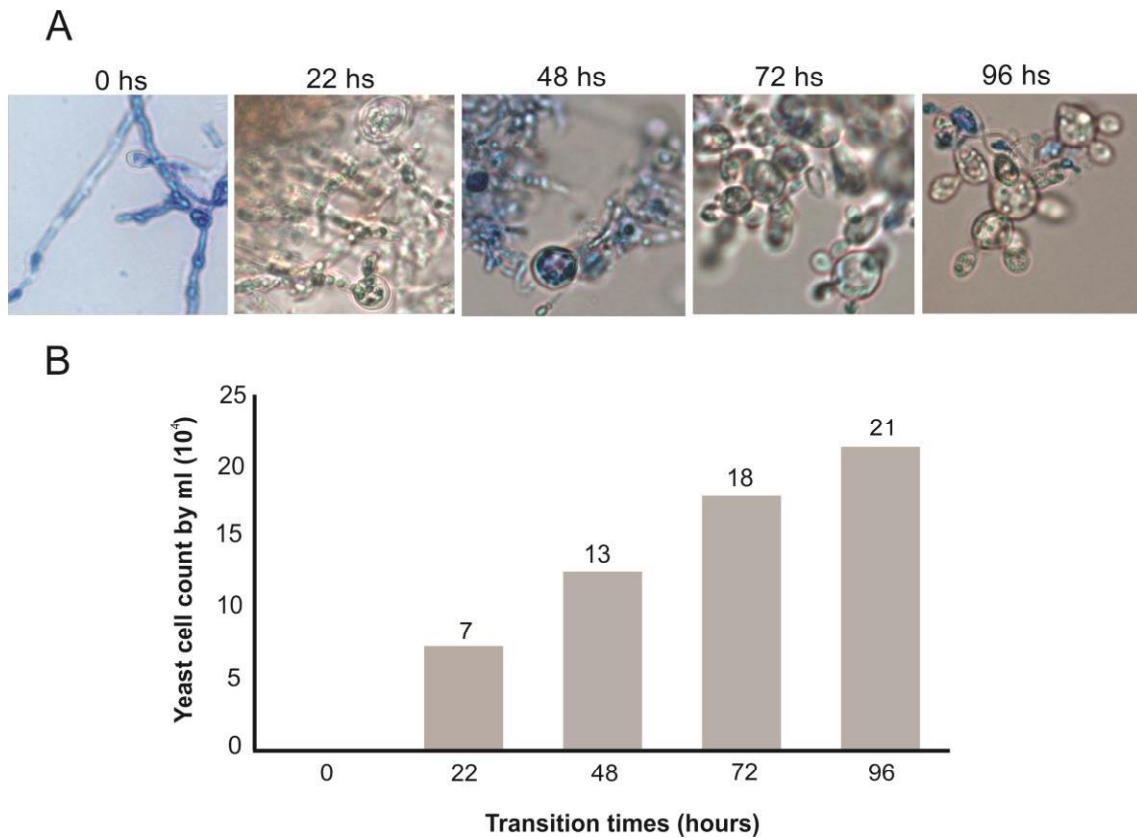
- Paracoccidioides brasiliensis* using proteomics. *J. Proteomics* 75, 572–587. doi:10.1016/j.jprot.2011.08.020.
- Selvaggini, S., Munro, C. A., Paschoud, S., Sanglard, D., and Gow, N. A. R. (2004). Independent regulation of chitin synthase and chitinase activity in *Candida albicans* and *Saccharomyces cerevisiae*. *Microbiology* 150, 921–928. doi:10.1099/mic.0.26661-0.
- Sharbati, J., Lewin, A., Kutz-Lohroff, B., Kamal, E., Einspanier, R., and Sharbati, S. (2011). Integrated microrna-mrna-analysis of human monocyte derived macrophages upon *Mycobacterium avium* subsp. *hominissuis* infection. *PLoS One* 6, e20258. doi:10.1371/journal.pone.0020258.
- Shikanai-Yasuda, M. A., Mendes, R. P., Colombo, A. L., de Queiroz-Telles, F., Kono, A. S. G., Paniago, A. M. M., et al. (2017). Brazilian guidelines for the clinical management of paracoccidioidomycosis. *Rev. Soc. Bras. Med. Trop.* 50, 715–740. doi:10.1590/0037-8682-0230-2017.
- Shikanai-Yasuda, M. A., Telles, F. D., Mendes, R. P., Colombo, A. L., Moretti, M. L., and Paracocci, G. C. C. (2006). Guidelines in paracoccidioidomycosis. *Rev. Soc. Bras. Med. Trop.* 39, 297–310. doi:10.1590/S0037-86822006000300017.
- States, D. J., and Gish, W. (1994). Combined use of sequence similarity and codon bias for coding region identification. *J. Comput. Biol.* 1, 39–50. doi:10.1089/cmb.1994.1.39.
- Teixeira, M. M., Theodoro, R. C., de Carvalho, M. J. A. A., Fernandes, L., Paes, H. C., Hahn, R. C., et al. (2009). Phylogenetic analysis reveals a high level of speciation in the *Paracoccidioides* genus. *Mol. Phylogenet. Evol.* 52, 273–283. doi:10.1016/j.ympev.2009.04.005.
- Turissini, D. A., Gomez, O. M., Teixeira, M. M., McEwen, J. G., and Matute, D. R. (2017). Species boundaries in the human pathogen *Paracoccidioides*. *Fungal Genet. Biol.* 106, 9–25. doi:10.1016/j.fgb.2017.05.007.
- Valsecchi, I., Dupres, V., Stephen-Victor, E., Guijarro, J., Gibbons, J., Beau, R., et al. (2017). Role of Hydrophobins in *Aspergillus fumigatus*. *J. Fungi* 4, 2. doi:10.3390/jof4010002.

Zhou, Q., Wang, Z., Zhang, J., Meng, H., and Huang, B. (2012). Genome-wide identification and profiling of microRNA-like RNAs from *Metarhizium anisopliae* during development. *Fungal Biol.* 116, 1156–62. doi:10.1016/j.funbio.2012.09.001.

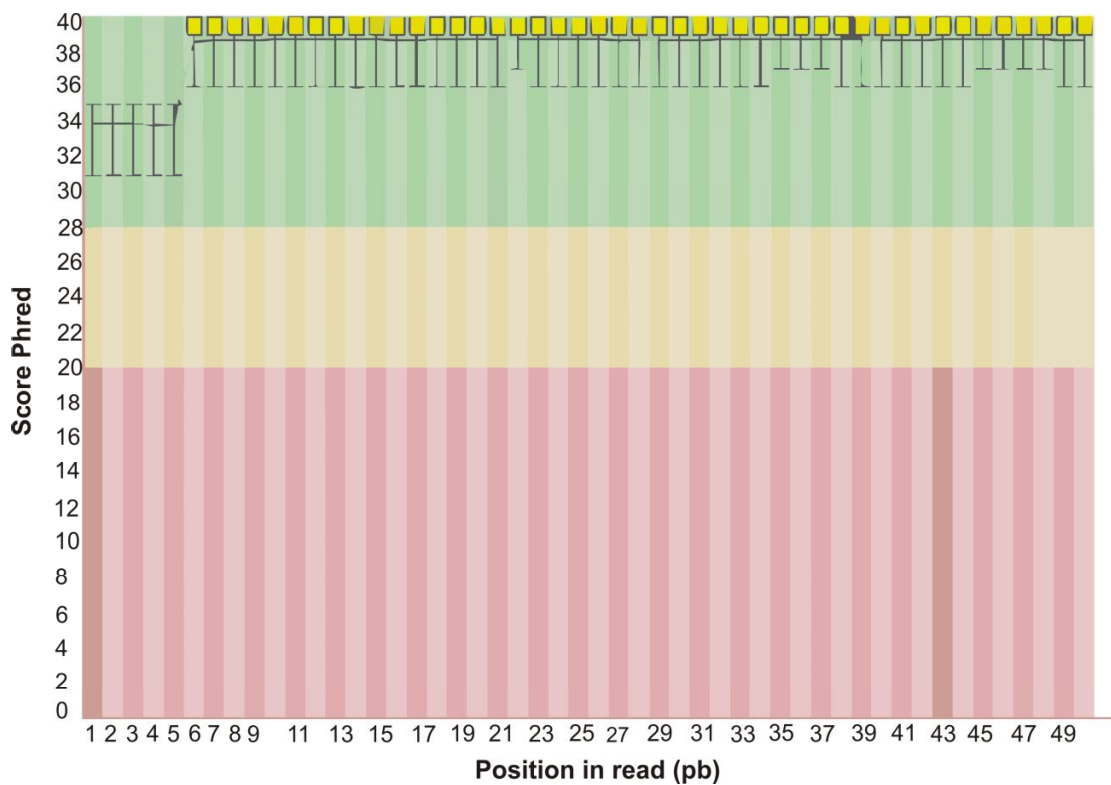
Supplementary material



Supplementary Figure 1- Work flow chart. Stages for characterization of microRNAs-like in mycelial, dimorphic transition and yeast cDNA libraries.

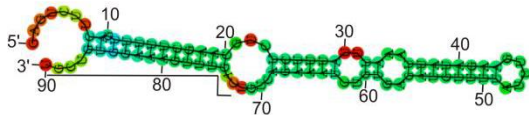


Supplementary Figure 2- Yeast cells appearing at the transitional times of *Paracoccidioides brasiliensis* Pb18 Mycelia was transferred from 22°C to 36°C and aliquots were taken at different times to count the number of yeast cells in the culture. (A)-Cellular morphology obtained at different times of the temperature shift (Increase of 100X). (B)-The number of yeast cells appearing in the culture after temperature shift.



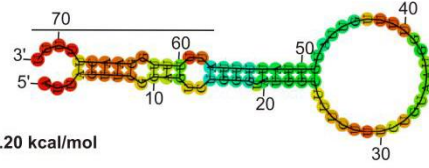
Supplementary figure 3- Distribution of Phred quality score of sequences from the library M1_raw.fg. The majority of the sequences presented Phred score > 30.

1)Supercontig_2.45_44026-



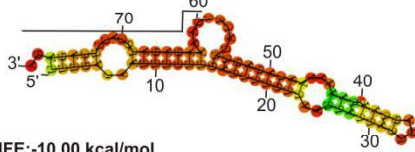
MFE:-15.60 kcal/mol

2)Supercontig_2.10_30105+



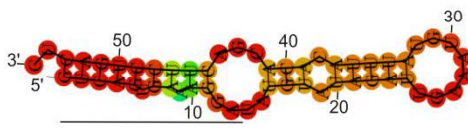
MFE:-7.20 kcal/mol

3)Supercontig_2.10_30363+



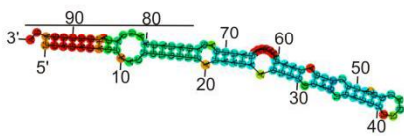
MFE:-10.00 kcal/mol

4)Supercontig_2.14_35344+



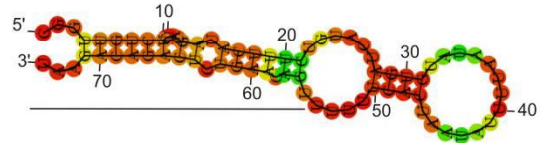
MFE:-10.80 kcal/mol

5)Supercontig_2.34_43474+



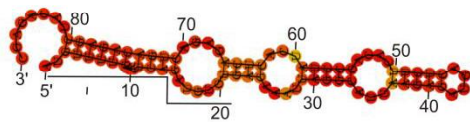
MFE:-19.20 kcal/mol

6)Supercontig_2.9_29173-



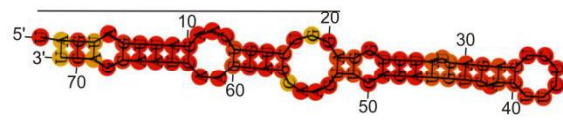
MFE:-10.00 kcal/mol

7)Supercontig_2.27_42084+



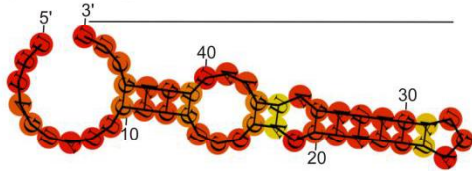
MFE:-22.00 kcal/mol

8)Supercontig_2.24_41376-



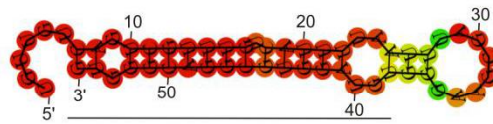
MFE:-18.80 kcal/mol

9)Supercontig_2.6_22054+



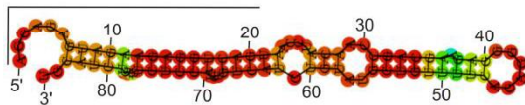
MFE:-9.10 kcal/mol

10)Supercontig_2.1_2922-



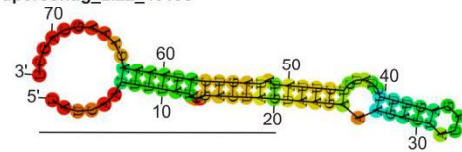
MFE:-14.30 kcal/mol

11)Supercontig_2.2_8815-



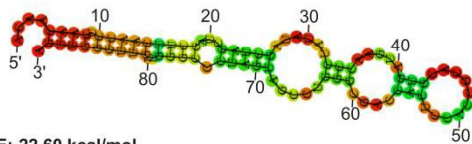
MFE:-25.40 kcal/mol

12)Supercontig_2.22_40198+



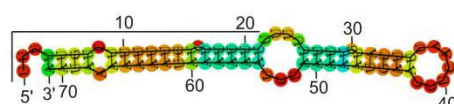
MFE:-9.90 kcal/mol

13)Supercontig_2.28_42699-



MFE:-22.60 kcal/mol

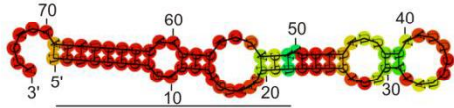
14)Supercontig_2.13_34964-



MFE:-5.30 kcal/mol

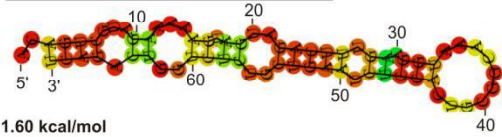


15) Supercontig_2.25_41493+



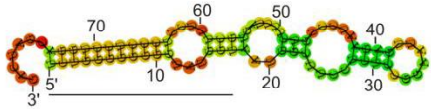
MFE: -18.30 kcal/mol

16) Supercontig_2.4_17514-



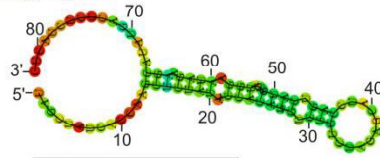
MFE: -11.60 kcal/mol

17) Supercontig_2.15_36048+



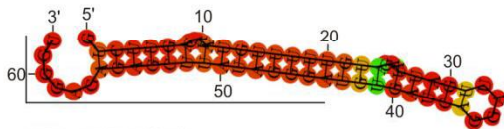
MFE: -22.60 kcal/mol

18) Supercontig_2.3_11421+



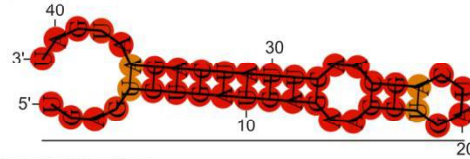
MFE: -14.70 kcal/mol

19) Supercontig_2.4_16040-



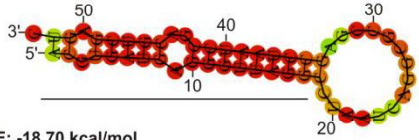
MFE: -12.50 kcal/mol

20) Supercontig_2.34_43490+



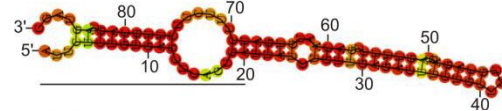
MFE: -13.70 kcal/mol

21) Supercontig_2.1_1681+



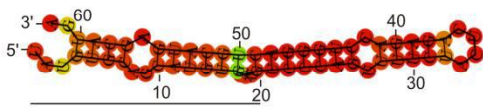
MFE: -18.70 kcal/mol

22) Supercontig_2.20_39100+



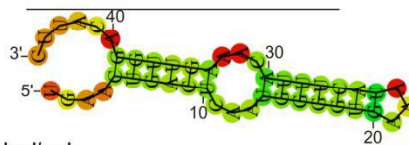
MFE: -25.20 kcal/mol

23) Supercontig_2.12_33015+



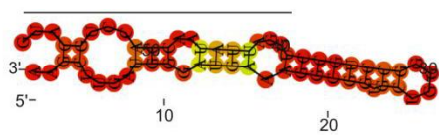
MFE: -24.20 kcal/mol

24) Supercontig_2.27_42386+



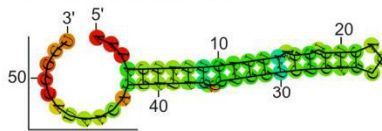
MFE: -6.50 kcal/mol

25) Supercontig_2.9_28895+



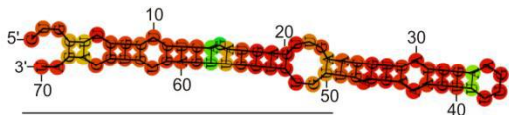
MFE: -15.90 kcal/mol

26) Supercontig_2.5_20695-



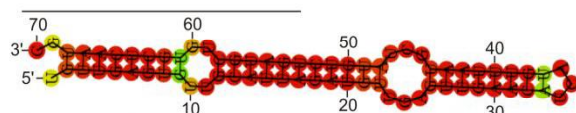
MFE: -6.90 kcal/mol

27) Supercontig_2.1_3999-



MFE: 19.30 kcal/mol

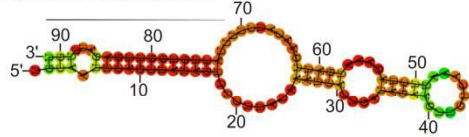
28) Supercontig_2.5_19148+



MFE: -27.90 kcal/mol

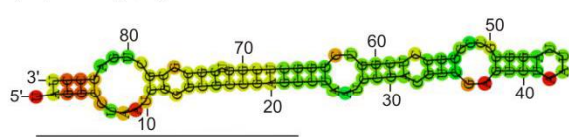


29) Supercontig_2.5_19199+



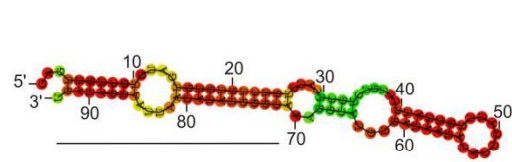
MFE: -19.10 kcal/mol

30) Supercontig_2.2_5957+



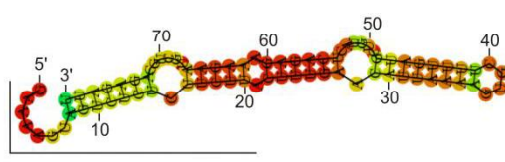
MFE: -42.00 kcal/mol

31) Supercontig_2.19_38665-



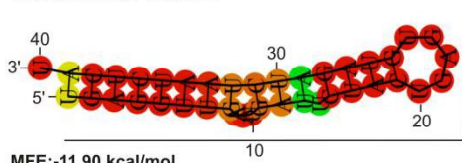
MFE: -26.20 kcal/mol

32) Supercontig_2.12_33897-



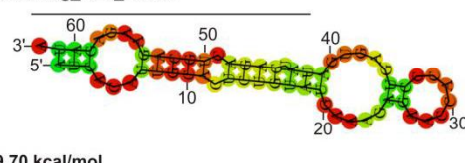
MFE: -15.10 kcal/mol

33) Supercontig_2.19_38040+



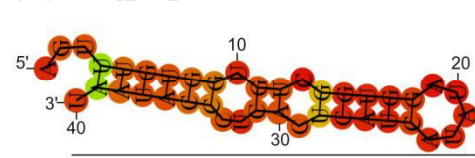
MFE: -11.90 kcal/mol

34) Supercontig_2.20_39013+



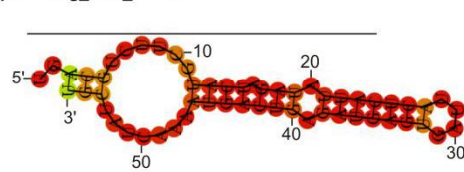
MFE: -9.70 kcal/mol

35) Supercontig_2.10_31175-



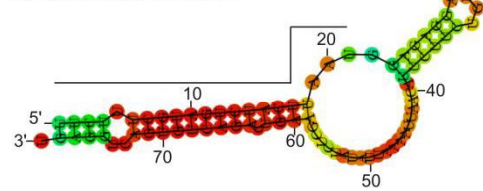
MFE: -9.80 kcal/mol

36) Supercontig_2.24_41413-



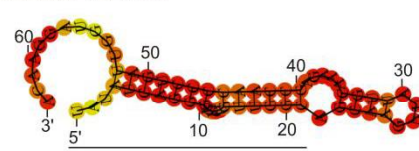
MFE: -14.40 kcal/mol

37) Supercontig_2.38_43800-



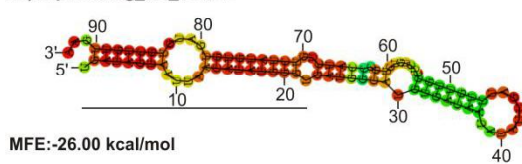
MFE: -16.40 kcal/mol

38) Supercontig_2.10_31197-



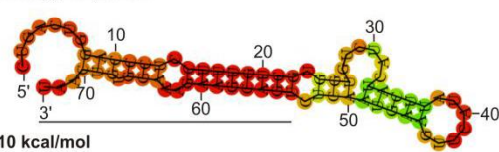
MFE: -19.80 kcal/mol

39) Supercontig_2.5_19191+



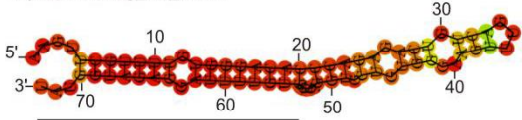
MFE: -26.00 kcal/mol

40) Supercontig_2.12_33986-



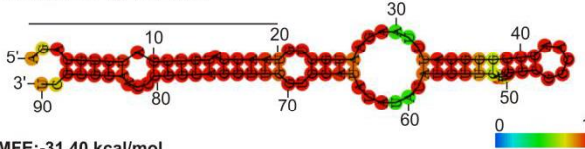
MFE: -19.10 kcal/mol

41) Supercontig_2.9_29703-

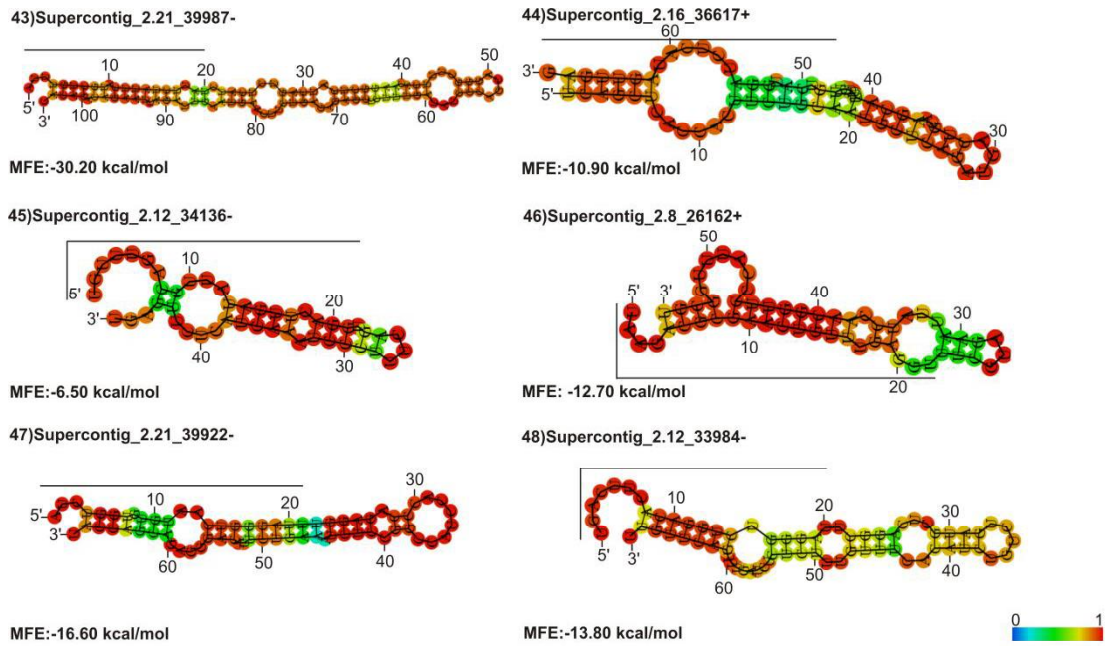


MFE: -20.50 kcal/mol

42) Supercontig_2.1_4130-

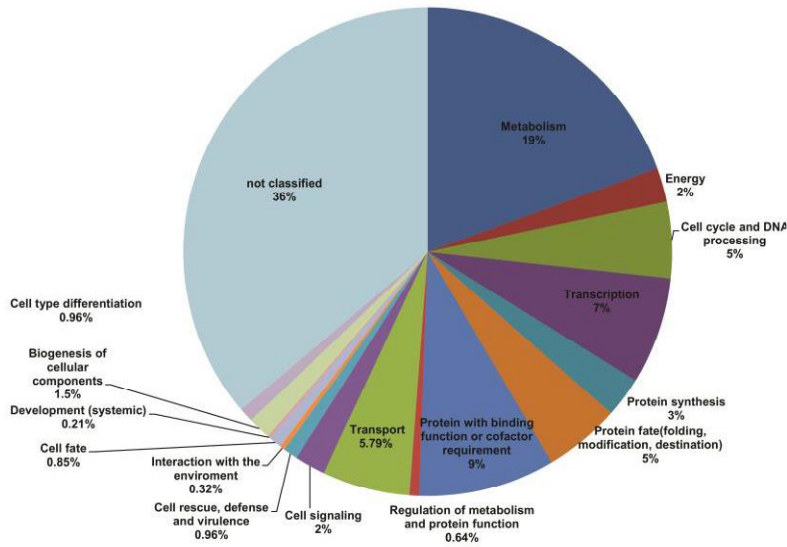


MFE: -31.40 kcal/mol

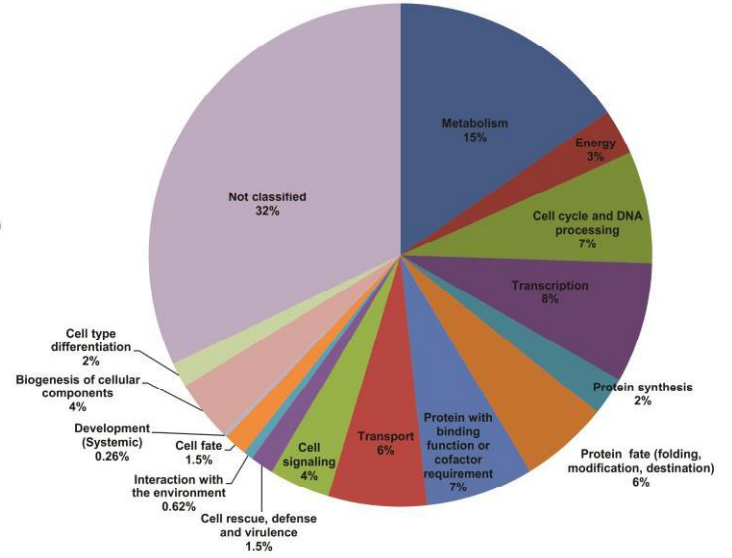


Supplementary Figure 4- Secondary structure of microRNAs-like identified. The secondary structure of the microRNAs-like and the negative free energy values were predicted using the RNA fold tool. The structure in form of hairpin were common to all pre-microRNAs-like. Besides, the predicted values of MFE for pre-microRNAs of *P. brasiliensis* were similar to those already described for other pre-microRNAs present in fungi. The color scale indicates the likelihood of matching between the bases.

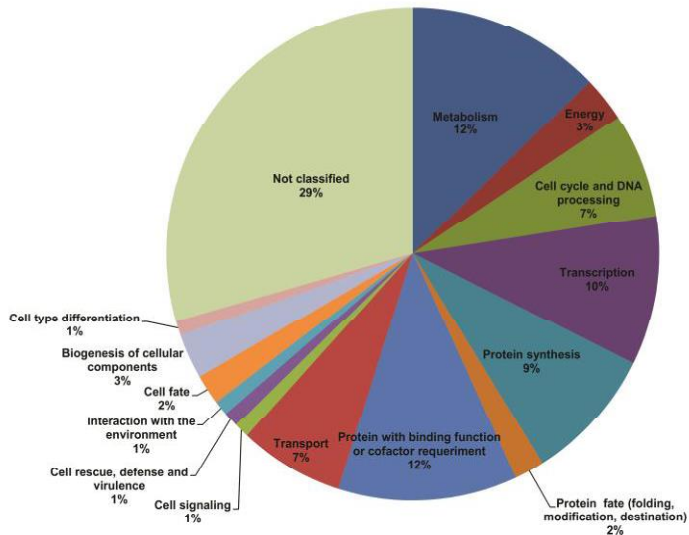
Supercontig_2.15_36048



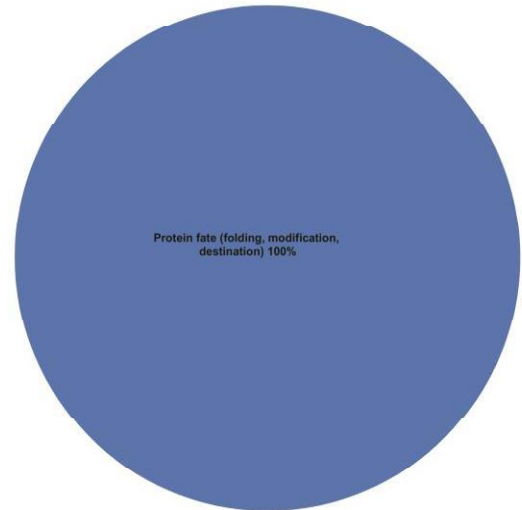
Supercontig_2.25_41493



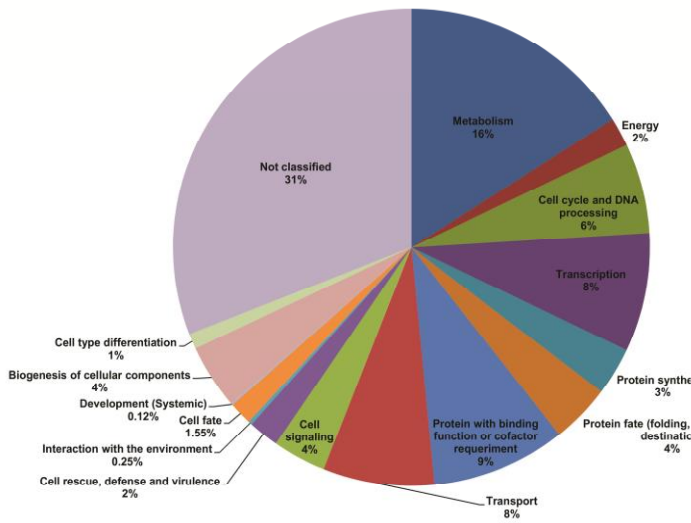
Supercontig_2.4_17514



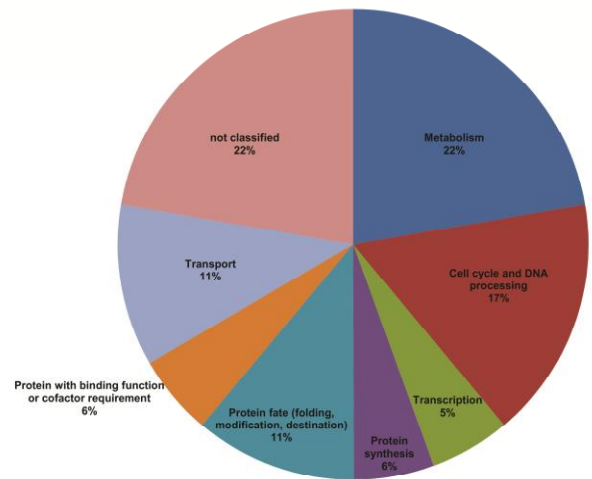
Supercontig_2.10_30105



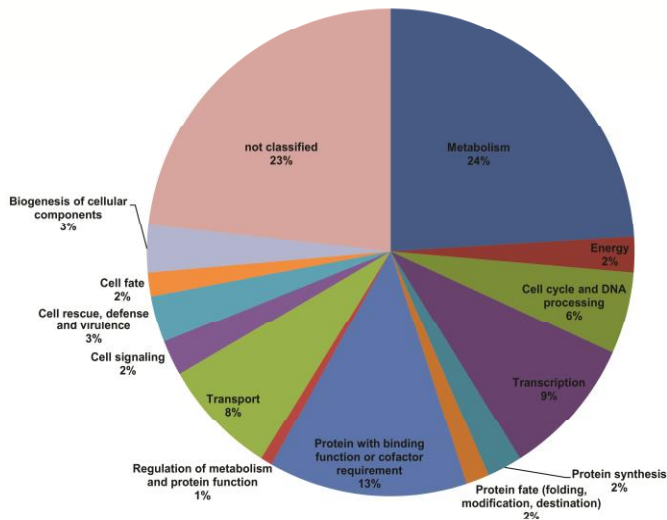
Supercontig_2.1_2922



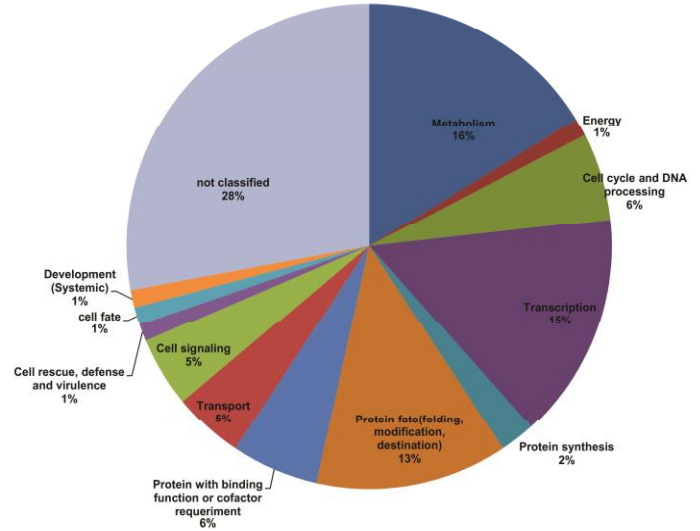
Supercontig_2.6_22054



Supercontig_2.14_35344



Supercontig_2.1_4130



Supplementary Figure 5- Biological processes regulated by microRNAs-like of *P. brasiliensis* Pb18. Biological processes regulated by microRNAs-like induced in yeast cells, include metabolism, energy, biogenesis of cellular components among others.

Supplementary Table 1- Number of sequences obtained and percentage of sequences eliminated after removal of the adapters with the Trimmomatic program.

Files ^a	# Raw reads ^b	reads processed ^c	% processed ^d
Mycelium-1_raw.fq	22.324.904	22.319.687	0.02%
Mycelium-2_raw.fq	22.443.544	22.434.973	0.04%
Mycelium-3_raw.fq	21.041.055	21.012.106	0.14%
Transition-1_raw.fq	22.243.452	22.194.102	0.22%
Transition-2_raw.fq	25.225.653	25.146.729	0.31%
Transition-3_raw.fq	25.256.164	25.198.165	0.23%
Yeast-1_raw.fq	18.205.091	18.191.337	0.08%
Yeast-2_raw.fq	19.110.427	19.092.755	0.09%
Yeast-3_raw.fq	19.580.516	19.566.999	0.07%

^a) Sequence files obtained after RNAseq;

^b) Total number of sequences obtained;

^c) Number of sequences remaining after removal of adapters;

^d) % of sequences removed with the Trimmomatic program.

Supplementary table 2- Differentially expressed microRNAs-like between the mycelial and transition libraries.

MicroRNA	log ² FoldChange	P-value	Padj	Mycelium	Transition
Supercontig_2.24_41376	3.68526619	5.39E-08	1.32E-06	up-regulated	down-regulated
Supercontig_2.13_34964	2.742853216	4.42E-05	0.000360582	up-regulated	down-regulated
Supercontig_2.24_41413	1.877923863	1.69E-05	0.000275626	up-regulated	down-regulated
Supercontig_2.20_39100	1.52208736	0.000395761	0.002154701	up-regulated	down-regulated
Supercontig_2.12_33897	1.467721833	8.99E-09	4.41E-07	up-regulated	down-regulated
Supercontig_2.27_42386	0.758278151	0.004103583	0.013405039	up-regulated	down-regulated
Supercontig_2.12_33986	0.724459365	0.002162186	0.008264669	up-regulated	down-regulated
Supercontig_2.34_43490	-0.884522917	0.015466832	0.044580869	down-regulated	up-regulated
Supercontig_2.21_39922	-1.052103515	0.002192667	0.008264669	down-regulated	up-regulated
Supercontig_2.12_33015	-1.071172378	0.000376871	0.002154701	down-regulated	up-regulated
Supercontig_2.1_1681	-1.289143579	0.000694309	0.003402113	down-regulated	up-regulated
Supercontig_2.1_4130	-1.297792105	0.001737498	0.007739762	down-regulated	up-regulated
Supercontig_2.10_31197	-1.397530425	0.000323701	0.002154701	down-regulated	up-regulated
Supercontig_2.4_16040	-1.415804598	3.56E-05	0.000348634	down-regulated	up-regulated
Supercontig_2.3_11421	-1.484382105	0.00324939	0.011372864	down-regulated	up-regulated
Supercontig_2.10_31175	-1.52396594	3.52E-05	0.000348634	down-regulated	up-regulated

Supplementary table 3- Differentially expressed microRNAs-like between the mycelium and yeast libraries

MicroRNAs	log ² Fold Change	P-value	Padj	Mycelium	Yeast
Supercontig_2.1_3999	7.105539883	3.90E-06	9.09E-06	up-regulated	down-regulated
Supercontig_2.13_34964	3.766658482	0.001721	0.002635	up-regulated	down-regulated
Supercontig_2.12_33986	3.595863626	1.55E-20	1.26E-19	up-regulated	down-regulated
Supercontig_2.3_11421	3.358609866	0.002898	0.004303	up-regulated	down-regulated
Supercontig_2.9_29703	3.328281386	2.09E-17	1.28E-16	up-regulated	down-regulated
Supercontig_2.38_43800	2.873597128	1.15E-13	5.14E-13	up-regulated	down-regulated
Supercontig_2.12_33015	2.488816656	8.61E-11	2.81E-10	up-regulated	down-regulated

Supercontig_2.21_39987	2.292888588	3.79E-12	1.55E-11	up-regulated	down-regulated
Supercontig_2.12_33897	2.235612998	1.09E-11	3.82E-11	up-regulated	down-regulated
Supercontig_2.20_39013	2.165306965	3.65E-08	9.93E-08	up-regulated	down-regulated
Supercontig_2.27_42386	2.136995738	3.12E-10	9.54E-10	up-regulated	down-regulated
Supercontig_2.19_38665	1.748336489	1.35E-07	3.48E-07	up-regulated	down-regulated
Supercontig_2.21_39922	1.581192154	1.46E-05	3.25E-05	up-regulated	down-regulated
Supercontig_2.22_40198	1.515221863	5.61E-05	0.000119	up-regulated	down-regulated
Supercontig_2.20_39100	1.27630446	0.022857	0.028717	up-regulated	down-regulated
Supercontig_2.5_19191	1.182651353	9.40E-05	0.000177	up-regulated	down-regulated
Supercontig_2.12_33984	0.998962297	0.013267	0.01757	up-regulated	down-regulated
Supercontig_2.19_38040	0.947519019	0.001028	0.00168	up-regulated	down-regulated
Supercontig_2.19_38377	0.947519019	0.001028	0.00168	up-regulated	down-regulated
Supercontig_2.5_19199	0.85284238	0.00506	0.007084	up-regulated	down-regulated
Supercontig_2.4_16040	-1.034768702	0.018781	0.024218	down-regulated	up-regulated
Supercontig_2.5_19148	-1.357115575	6.05E-05	0.000119	down-regulated	up-regulated
Supercontig_2.1_1681	-1.746689046	5.94E-05	0.000119	down-regulated	up-regulated
Supercontig_2.10_31197	-2.085442673	1.46E-07	3.57E-07	down-regulated	up-regulated
Supercontig_2.28_42699	-2.155123246	0.000248	0.00045	down-regulated	up-regulated
Supercontig_2.2_5957	-2.403349581	1.03E-11	3.82E-11	down-regulated	up-regulated
Supercontig_2.10_30363	-2.764054592	0.00417	0.006009	down-regulated	up-regulated
Supercontig_2.8_26162	-3.322413362	0.001303	0.002059	down-regulated	up-regulated
Supercontig_2.10_31175	-3.323271785	6.99E-19	4.89E-18	down-regulated	up-regulated
Supercontig_2.9_28895	-3.519352138	9.74E-44	1.59E-42	down-regulated	up-regulated
Supercontig_2.27_42084	-3.876847871	0.006697	0.009115	down-regulated	up-regulated
Supercontig_2.25_41493	-4.130461472	6.59E-43	8.07E-42	down-regulated	up-regulated
Supercontig_2.1_4130	-4.639213062	7.57E-29	7.42E-28	down-regulated	up-regulated
Supercontig_2.6_22054	-4.685124996	9.82E-10	2.83E-09	down-regulated	up-regulated
Supercontig_2.14_35344	-5.592115216	0.000433	0.000759	down-regulated	up-regulated
Supercontig_2.15_36048	-6.203401859	2.31E-50	5.67E-49	down-regulated	up-regulated
Supercontig_2.1_2922	-7.651258173	2.32E-16	1.26E-15	down-regulated	up-regulated
Supercontig_2.4_17514	-8.946602967	3.34E-71	1.64E-69	down-regulated	up-regulated
Supercontig_2.10_30105	-9.782396983	1.09E-14	5.34E-14	down-regulated	up-regulated

Supplementary table 4- Differentially expressed microRNAs-like between the transition and yeast libraries

MicroRNAs	log ² FoldChange	P-value	Padj	Transition	Yeast
Supercontig_2.3_11421	4.842991972	1.71E-05	3.50E-05	up-regulated	down-regulated
Supercontig_2.1_3999	4.586334264	0.002885831	0.004159	up-regulated	down-regulated
Supercontig_2.9_29703	3.56892224	8.78E-20	7.17E-19	up-regulated	down-regulated
Supercontig_2.12_33015	3.559989034	1.60E-20	1.57E-19	up-regulated	down-regulated
Supercontig_2.12_33986	2.871404261	1.21E-13	5.37E-13	up-regulated	down-regulated
Supercontig_2.38_43800	2.673060952	5.05E-12	1.77E-11	up-regulated	down-regulated
Supercontig_2.21_39922	2.633295669	5.17E-13	2.11E-12	up-regulated	down-regulated
Supercontig_2.21_39987	2.491237442	4.46E-14	2.43E-13	up-regulated	down-regulated
Supercontig_2.19_38665	2.151157228	8.65E-11	2.82E-10	up-regulated	down-regulated
Supercontig_2.20_39013	1.884230016	1.65E-06	3.85E-06	up-regulated	down-regulated

Supercontig_2.12_33984	1.814350811	6.85E-06	1.46E-05	up-regulated	down-regulated
Supercontig_2.27_42386	1.378717587	4.94E-05	8.65E-05	up-regulated	down-regulated
Supercontig_2.22_40198	1.342383031	0.000358179	0.000532	up-regulated	down-regulated
Supercontig_2.5_19199	1.281489704	2.50E-05	4.71E-05	up-regulated	down-regulated
Supercontig_2.5_19191	1.088019598	0.000326243	0.0005	up-regulated	down-regulated
Supercontig_2.19_38040	1.048697659	0.000279322	0.000442	up-regulated	down-regulated
Supercontig_2.19_38377	1.048697659	0.000279322	0.000442	up-regulated	down-regulated
Supercontig_2.12_33897	0.767891165	0.019761828	0.025482	up-regulated	down-regulated
Supercontig_2.5_19148	-1.379826126	4.50E-05	8.16E-05	down-regulated	up-regulated
Supercontig_2.10_31175	-1.799305845	1.49E-06	3.66E-06	down-regulated	up-regulated
Supercontig_2.24_41413	-2.258741535	3.54E-07	9.64E-07	down-regulated	up-regulated
Supercontig_2.2_5957	-2.506802813	1.29E-12	4.85E-12	down-regulated	up-regulated
Supercontig_2.9_29173	-2.624338846	0.005765853	0.007848	down-regulated	up-regulated
Supercontig_2.28_42699	-2.65450368	6.80E-06	1.46E-05	down-regulated	up-regulated
Supercontig_2.10_30363	-2.768651883	0.003964359	0.00555	down-regulated	up-regulated
Supercontig_2.45_44026	-2.963340515	0.037644752	0.047297	down-regulated	up-regulated
Supercontig_2.1_4130	-3.341420956	9.37E-16	6.56E-15	down-regulated	up-regulated
Supercontig_2.9_28895	-3.413511419	1.81E-41	2.96E-40	down-regulated	up-regulated
Supercontig_2.25_41493	-3.954881202	6.78E-40	8.31E-39	down-regulated	up-regulated
Supercontig_2.24_41376	-4.360254307	3.22E-07	9.27E-07	down-regulated	up-regulated
Supercontig_2.8_26162	-4.412715167	1.95E-05	3.82E-05	down-regulated	up-regulated
Supercontig_2.6_22054	-4.588081284	1.52E-09	4.65E-09	down-regulated	up-regulated
Supercontig_2.27_42084	-5.653748698	8.79E-05	0.000148	down-regulated	up-regulated
Supercontig_2.15_36048	-6.025314084	8.27E-48	2.03E-46	down-regulated	up-regulated
Supercontig_2.1_2922	-6.840924204	8.47E-14	4.15E-13	down-regulated	up-regulated
Supercontig_2.10_30105	-8.005471413	1.12E-14	6.84E-14	down-regulated	up-regulated
Supercontig_2.4_17514	-8.053057542	3.08E-61	1.51E-59	down-regulated	up-regulated
Supercontig_2.14_35344	-8.405374165	4.35E-07	1.12E-06	down-regulated	up-regulated



Capítulo 4

1.DISCUSSÃO

MicroRNAs são parte de um mecanismo de regulação gênica pós transcricional e tais moléculas fazem um fino ajuste da expressão protéica. Sabe-se que microRNAs possuem diferentes alvos, além de organizarem-se em agrupamentos para promover o silenciamento de um conjunto específico de genes (LAU et al., 2001). Após a descoberta de microRNA em *C. elegans* (LEE et al., 1993), tais moléculas foram caracterizadas em diferentes reinos, incluindo os fungos. Alguns trabalhos na literatura tem demonstrado que fungos patogênicos como *C. neoformans* (JIANG et al., 2012) e *P. marneffei* (LAU et al., 2013) produzem microRNAs-like em diferentes estágios morfológicos e tais moléculas são capazes de promover o silenciamento de genes alvos. Espécies do complexo *Paracoccidioides* são fungos termodimórficos (RESTREPO, 1985), que causam a principal micose sistêmica na América Latina com altas taxas de incidência no Brasil (SHIKANAI-YASUDA et al., 2006, SHIKANAI-YASUDA et al., 2017). Vários estudos têm caracterizado as mudanças na expressão de genes e proteínas durante a transição dimórfica, micélio e levedura (NUNES et al., 2005, BASTOS et al., 2007, REZENDE et al., 2011). Entretanto, os mecanismos que controlam a expressão de genes e proteínas entre cada fase deste patógeno ainda não são totalmente esclarecidos. Portanto este trabalho, emprega diferentes abordagens para caracterizar sequências preditas de microRNAs-like neste importante patógeno.

No **Capítulo 2** foi apresentada uma descrição das proteínas envolvidas no processamento de microRNAs-like entre diferentes espécies do complexo *Paracoccidioides*, além da descrição de microRNAs-like presentes no genoma deste patógeno. Proteínas dicers e argonautas envolvidas na maquinaria de silenciamento genético pós-transcricional são conservadas em fungos de diferentes Filos, incluindo Ascomycota, Basidiomycota e Zygomycota (DRINNENBERG et al., 2009). Análises de predição *in silico* demonstraram que o número de proteínas envolvidas na via de silenciamento gênico pós-transcricional em espécies do complexo *Paracoccidioides* estão de acordo com os dados descritos na literatura para outros fungos como, *C. neoformans*, *A. fumigatus* e *N. crassa*. Tais microorganismos apresentam dois genes parálogos para dicers e argonautas em seu genoma (GALAGAN et al., 2003, NAKAYASHIKI; KADOTANI; MAYAMA; 2006, JANBON et al., 2010. Em *Paracoccidioides* spp. essas proteínas conservam domínios, já descritos em proteínas de outros fungos, nos quais microRNA-like foram caracterizados (LEE et al., 2010, JIANG

et al., 2012). Análises filogenéticas das proteínas envolvidas no processamento de microRNAs-like em *Paracoccidioides* spp. revelaram que essas proteínas são filogeneticamente conservadas entre fungos dimórficos como *B. dermatitidis* e *P. Marneffei*. Os dados de expressão gênica reforçam a informação que, além de conservar a maquinaria de silenciamento gênico pós-transcricional, os transcritos que codificam estas proteínas são induzidas na forma parasitária deste patógeno.

Após a etapa de descrição das proteínas envolvidas no processamento de microRNAs-like e análises de expressão dos transcritos, análises *in silico* foram realizadas com intuito de caracterizar microRNAs-like presentes no genoma de *P. brasiliensis*. Trabalhos anteriores, já descreveram a identificação de miRNAs presentes em vesículas secretórias, com base em similaridade de sequência entre diferentes organismos (DEHURY et al., 2013, PANDA et al., 2014). Neste presente trabalho, foram preditas sequências de possíveis microRNA-like no genoma de *P. brasiliensis*, usando sequências de microRNAs-like já caracterizados em outros fungos ou presentes em vesículas secretadas por estes microorganismos. Do total de sequências analisadas, 18 foram preditas para serem sequências de potenciais microRNA-like. Desta forma os dados sugerem que este fungo retém regiões no genoma responsáveis pela gênese de microRNAs-like. Como descrito na literatura, sequências maduras de miRNAs são conservadas entre diferentes reinos, demonstrando a importância desse mecanismo de regulação de gênica pós-transcricional (LEE et al., 1993, CHEN et al., 2014). De fato, Peres da Silva e colaboradores (2015), predisseram possíveis sequências de microRNAs-like em vesículas segregadas por *P. brasiliensis* (Pb18), usando uma estratégia baseado em similaridade de sequências. Além disso, 22 sequências de potenciais microRNAs foram identificadas no genoma de *Humulus lupulus* empregando predição *in silico* de miRNAs baseado em sequências similares presentes no banco de dados miRBase (MISHRA et al., 2015).

Potenciais microRNA-like preditos neste trabalho originaram-se de precursores que formam estruturas semelhantes a um grampo (hairpin). De fato, durante a formação de um microRNA maduro, os precursores de microRNAs, adquirem uma estrutura em forma de grampo que é posteriormente processada por enzimas dicers para formar o duplex miRNA/miRNA* (BARTEL; LEE; FEINBAUM, et al., 2004). Trabalhos anteriores, demonstraram que valores de energia livre mínima (MFE) dos precursores de microRNAs-like em *P.marneffei* variam entre -17,86 kcal/mol e -23,88 kcal/mol (LAU et al., 2013). Em *A. flavus* os valores variam entre -19.4 kcal/mol e 140.2 kcal/mol e em

M. anisopliae os valores ficaram entre -20 kcal/mol e -105.32 kcal/mol (BAI et al., 2015, ZHOU et al., 2012). Desta forma os valores de energia livre de dobramento descritas neste presente trabalho estão de acordo com os descritos para outros fungos.. Além disso, obtivemos sequências de pre-microRNAs variando de 57 a 118 nucleotídeos com um tamanho médio de 71 nt. Trabalhos anteriores descrevem pre-microRNAs com um tamanho médio entre 68 a 208 nt em fungos (ZHOU et al., 2012). Por exemplo, em *C. neoformans* os tamanhos dos precursores de miR1 e miR2 foram aproximadamente 70 nt (JIANG et al., 2012).

Além dessas características, os valores de AMFE (ajuste de energia livre de dobramento, MFEI (índice mínimo de energia livre de dobramento) (ZHANG et al., 2006) e a porcentagem de uracila/adenina na sequência pré-microRNA foram analisados. Conforme observado em nossos dados, encontramos valores de MFEI baixos e AMFE similares a sequências de precursores de microRNA-like descritos em plantas (ZHANG et al., 2006). Possivelmente essas diferenças sejam resultado de uma menor complementaridade de bases entre as sequências precursoras de microRNAs em fungos quando comparado ao pre-microRNAs de plantas, onde a complementaridade das bases poderia ser maior (MISHRA et al., 2015). Os dados também demonstram uma maior quantidade de uracila em precursores de microRNAs-like, como já descrito na literatura (ZHANG et al., 2006).

Após a predição *in silico* de microRNAs-like por ferramentas de bioinformática, foram realizadas análises confirmatórias por RT-PCR qualitativa de alguns microRNAs-like preditos. Empregando esta estratégia detectou-se microRNAs-like maduros, com tamanhos entre 26 até 57 pares de base, confirmando as análises *in silico*. Em outros fungos, como *N. crassa*, (LEE et al., 2010) *C. neoformans* (JIANG et al., 2012) e *P. marneffei* (LAU et al., 2013) tamanhos menores de microRNAs-like maduros foram caracterizados empregando a técnica de *Northern blot*. Possivelmente esta diferença seja relacionada ao fato que, neste trabalho, o método para identificação de microRNAs-like, adiciona adeninas na molécula de RNA e este processo confere um tamanho maior aos microRNAs-like maduros.

Portanto, os dados apresentados neste trabalho demonstraram que as proteínas envolvidas na via de processamento de miRNAs são conservadas em *Paracoccidioides* spp. e relacionadas filogeneticamente com outros fungos dimórficos. Além disso, foi demonstrado que os transcritos que codificam essas proteínas são expressos na forma parasitaria de *Paracoccidioides* spp. As análises de bioinformática permitiram prever 18

moléculas de microRNA-like presentes no genoma de *P. brasiliensis* e os dados de predição de bioinformática foram validados experimentalmente. Em resumo, os dados descritos neste trabalho contribuem para adição de informações sobre moléculas presumivelmente envolvidas na regulação de gênica pós-transcricional e abre portas para a investigação de como essas moléculas funcionam em estádios específicos desse patógeno e durante a interação com o hospedeiro.

No **Capítulo 3** foram apresentadas as análises de microRNAs-like presentes em diferentes estágios morfológicos de *P. brasiliensis*, através da construção de bibliotecas de pequenos RNAs e sequenciamento de alta performance. Inicialmente foram realizadas análises da expressão de genes que codificam proteínas envolvidas na biogênese de microRNAs-like. Proteínas envolvidas no processamento de microRNAs são conservadas em diferentes reinos. No fungo patogênico termodimórfico *P. marneffei* análises da expressão do gene codificante de *ago-2* revelaram um aumento significativo na expressão deste transcrito na fase de micélio em relação à levedura, os mesmos resultados foram obtidos para *dcr-2* (LAU et al., 2013). Em contraste, a expressão do mRNA de *dcr-1* foi mais induzida em levedura em comparação com o micélio. No presente trabalho, os dados de expressão gênica de *ago-2*, *dcr-1* e *dcr-2* são semelhantes aos descritos em *P. marneffei*. Em geral, os dados apontam para a indução da expressão de genes que codificam para dicers e argonautas entre as diferentes fases morfológicas. Além disso, em *N. crassa* (LEE et al., 2010) e *P. marneffei* (LAU et al., 2013), diferentes proteínas dicers são envolvidas no processamento de microRNAs-like. Por exemplo, PM-milR-M1 e PM-milR-M2 de *P. marneffei* produzidos apenas na fase de micélio, são dependentes da proteína dicer-2 para sua biogênese, enquanto a proteína dicer-1 não é envolvida na biogênese destes dois microRNAs-like. Possivelmente em *P. brasiliensis*, este mecanismo também ocorra e essa expressão diferencial dos transcritos poderia ser atribuída ao emprego de diferentes proteínas no processamento de microRNAs-like.

Vários estudos sobre o processo de dimorfismo térmico e desenvolvimento em estádios morfológicos específicos dos fungos pertencentes ao complexo *Paracoccidioides* spp. demonstram uma plasticidade destes fungos patogênicos para adaptar-se e sobreviver sobre diferentes condições ambientais (NUNES et al., 2005, BASTOS et al., 2007, REZENDE et al., 2011). Neste sentido o presente trabalho focou nos possíveis alvos silenciados por microRNAs-like induzidos na fase de levedura, visto que esta é a fase parasitaria do hospedeiro. Sabe-se que durante o processo de infecção

no hospedeiro, as espécies do complexo *Paracoccidioides* alteram a composição do polissacarídeo presente na parede celular. Nesse sentido, a parede celular da fase leveduriforme é composta principalmente por quitina e α -1,3-glucana (KANETSUNA et al., 1970, PUCCIA et al., 2011). Vários microRNAs-like induzidos na fase de levedura tiveram como alvos proteínas envolvidas na biogênese, integridade e remodelamento da parede celular. Por exemplo, o microRNA-like presente no supercontig_2.1_2922 possui como alvo a proteína endoquitinase de 42 kda. *P. lutzii* induz a expressão da endoquitinase (CTS1p) durante a transição de levedura para micélio, com o intuito de remover a quitina da parede celular, favorecendo o surgimento de hifas na fase filamentosa deste fungo (BONFIM et al., 2006).

A quitinase 3 também foi regulada por microRNAs-like induzidos na biblioteca de levedura. Em *P. lutzii*, a proteína quitinase foi identificada apenas no proteoma da parede celular do micélio (ARAÚJO et al., 2017). Em *C. albicans* a atividade de quitinases foi maior na hifa, do que em leveduras e a síntese e hidrólise de quitina foram induzidas durante a morfogênese de levedura para hifa (SELVAGGINI et al., 2004). À medida que as quitinases estão envolvidas na degradação da quitina, possivelmente a indução desses microRNAs-like na fase parasitária esteja relacionada ao fato de que a quitina está presente em maior concentração nesse estágio e portanto, a presença de proteínas que degradam esse componente não é necessário.

Outros microRNAs-like induzidos na fase leveduriforme tem presumivelmente, como alvos, proteínas envolvidas na integridade da parede celular e morfogênese, como uma glucanase de parede celular (Scw4p). Esta proteína em *P. brasiliensis* é homóloga à glucanase de parede celular (Scw4p) e à proteína da família 17 glicosil- hidrolase de *A. fumigatus* e *S. cerevisiae*, respectivamente. No fungo patogênico *A. fumigatus*, a mutação no gene que codifica a proteína Scw4p, resulta em uma diminuição de β -glucana na parede celular, além de reduzir o crescimento filamentoso e promover maior sensibilidade aos agentes estressores de parede celular, possivelmente devido à alteração na constituição do polímero presente na parede celular (MILLET et al., 2018), Resultados semelhantes também foram encontrados em *S. cerevisiae* (SESTAK et al., 2004).

Além disso, a proteína de biossíntese de β -1,6-glucana (Knh1) e a proteína de biogênese da parede celular (Mhp1) são também reguladas, presumivelmente, por microRNAs-like induzidos na fase leveduriforme. Em *S. cerevisiae*, a proteína Mhp1 é relacionada à síntese de β -1-6-glucana (LAI et al., 1997) sendo que este polímero está

presente na parede celular na fase parasitária de *P. brasiliensis*, em pequenas quantidades (revisito em PUCCIA et al., 2011). Na levedura de fissão *S. pombe* a proteína Bgs1p/Cps1p foi identificada como uma putativa beta1,3-glucana sintase e análises fenotípicas demonstraram que a proteína codificada por este gene é envolvida na síntese de β -1,3 glucana e germinação de esporos (CORTÉS et al., 2002). No presente trabalho esta proteína também foi predita para ser reprimida por microRNA-like induzidos na fase de levedura. Como a β -1,3-glucana é o principal polissacarídeo da fase miceliana, a indução de proteínas envolvidas na biossíntese deste polímero não é necessária para células de levedura, uma vez que a β -1,3-glucana é o polissacarídeo com maior potencial imunogênico (KANETSUNA, CARBONELL, 1970, MENDES et al., 2017). Nesse sentido, os microRNAs-like poderiam regular o polímero presente na parede celular em cada estágio morfológico, pela indução ou repressão de proteínas envolvidas em sua biossíntese ou degradação.

Diversos microRNAs-like induzidos na forma parasitária, foram preditos para terem como alvos proteínas envolvidas na morfogênese e no crescimento celular. As hidrofobinas são pequenas proteínas hidrofóbicas, envolvidas em diferentes processos, como crescimento celular e desenvolvimento. Em *A. fumigatus*, a hidrofobina (RodAp) está envolvida na permeabilidade e hidrofobicidade da célula (VALSECCHI et al., 2017). Em *Paracoccidioides* spp. o mRNA das hidrofobinas 1 e 2 foi detectado apenas na fase filamentosa e durante as primeiras 24 h de transição de micélio para levedura (GOLDMAN et al., 2003, ALBUQUERQUE et al., 2004). Interessante, o microRNA-like que tem hidrofobina 1 como alvo, foi reprimido na biblioteca micélio e transição dimórfica.

O mecanismo de formação de pseudohifas em *S. cerevisiae* durante a privação de nitrogênio envolve a proteína Ras2p, que ativa adenilil ciclase para produzir adenosina monofosfato cíclico. A presença desta molécula é essencial para a ativação de proteínas envolvidas nas vias de sinalização que regulam a morfogênese deste fungo como, por exemplo, a via da MAPK. Além de Ras2p, outra proteína Gpa2p, que pertence à família das proteínas G é envolvida no desenvolvimento de pseudohifas em *S. cerevisiae* e mutações neste gene bloquearam a formação de pseudohifas e reduziram os níveis de AMP cíclico intracelular (KÜBLER et al., 1997, LORENZ, 1997). Em *P. brasiliensis* o microRNAs-like que possui Gpa2p como alvo foi induzido na fase parasitária, entretanto na fase de filamentosa e durante a transição dimórfica tal microRNAs-like foi reprimido. Muito provavelmente porque na fase parasitária em que

as células adquirem a morfologia de levedura, o processo de formação de hifas é bloqueado.

A fase miceliana, utiliza preferencialmente o metabolismo aeróbio para a produção de energia, em comparação com as células na fase de levedura (NUNES et al., 2005, FELIPE et al., 2005). Várias transcritos codificantes de proteínas envolvidas na produção de energia através da cadeia respiratória, incluindo NADH-desidrogenases, flavoproteínas e ATP-sintase mitocondrial foram preditos para serem silenciados por microRNAs-like induzidos na fase de levedura. A fosforilação oxidativa começa com a entrada de elétrons na cadeia respiratória, as desidrogenases captam estes elétrons provenientes das reações catabólicas e os canalizam para aceptores universais de elétrons o NAD⁺ ou NADP⁺ e FMN ou FAD (nucleotídeos de nicotinamida ou nucleotídeos de flavina, respectivamente). Os elétrons passam por uma série de carregadores ligados à membrana mitocondrial, que agem sequencialmente aceitando ou doando elétrons. Proteínas carregadores de elétrons presentes na cadeia respiratória são ubiquinonas, citocromos e proteínas ferro-enxofre. ATP-sintase mitocondrial é uma enzima localizada na membrana interna da mitocôndria, sendo responsável por catalisar a síntese de ATP através da fosforilação oxidativa, utilizando o NADH ou FADH₂ para fosforilação do ADP para ATP (NELSON; COX, 2014).

Entretanto durante o processo de respiração, ocorre a formação de espécies reativas de oxigênio (EROS). Neste sentido, microRNAs-like que foram preditos para terem como alvos proteínas envolvidas na manutenção do potencial redox intracelular e ação contra agentes oxidantes incluindo, superóxido dismutase de Mn/Fe (SOD2), tiorredoxinas, superóxido dismutase mitocondrial de Fe/Mn (SOD5), peroxirredoxina e aldeído desidrogenase foram reprimidos na fase de micélio e durante a transição dimórfica. Em *Paracoccidioides* spp., algumas proteínas como a peroxirredoxina (PRX) e a superóxido dismutase de Mn/Fe (SOD2), foram induzidas na fase de micélio (REZENDE et al., 2011) e em diferentes pontos da transição dimórfica de micélio para levedura. Genes envolvidos na resposta ao estresse oxidativo e manutenção do potencial redox intracelular também foram induzidos (NUNES et al., 2005). Portanto possivelmente na fase de levedura onde as espécies reativas de oxigênio, gerados pela cadeia transportadora de elétrons estejam em menor quantidade nas células, as proteínas de resposta a estes agentes sejam silenciados, devido a menor necessidade de combater agentes oxidantes.

2.CONCLUSÃO

Durante o processo de infecção no hospedeiro, microorganismos adquiriam mecanismos capazes de colonizar os tecidos infectados e promover o desenvolvimento da doença. Em fungos patogênicos o dimorfismo térmico é um fator de virulência que demonstrada à plasticidade destes organismos em sobreviver e adaptar-se ao crescimento sobre diferentes temperaturas e em ambientes hostis. Dentre desta classe encontra-se os fungos pertencentes ao complexo *Paracoccidioides*. Tais fungos são os agentes etiológicos da principal micose sistêmica da América latina, embora a micose causada por estes fungos seja caracterizada como um problema de saúde pública os mecanismos adaptativos para a sobrevivência deste patógeno ainda não são totalmente elucidados.

Neste sentido a análise e compreensão dos mecanismos moleculares empregados por estes patógenos durante seus estágios morfológicos, agregam conhecimento sobre o processo de infecção no hospedeiro assim como durante a fase saprofítica e transição dimórfica. O presente trabalho caracteriza pela primeira vez a presença de microRNAs-like em *P. brasiliensis*, através de ferramentas de bioinformática microRNAs-like descritos em outros fungos, foram conservados em regiões do genoma deste patógeno, além disso, proteínas envolvidos no processamento de microRNAs-like são conservadas entre as espécies deste complexo, demonstrando que tais fungos conservam toda maquinaria de silenciamento gênico pós-transcricional. Análises de expressão diferencial de microRNAs-like entre os diferentes estágios morfológicos corroboram com os dados de expressão gênica e proteica já descrito por outros pesquisadores. Os processos regulados por microRNAs-like incluem alteração dos polímeros presentes na parede celular, etapa essencial para escape das respostas imunológicas do hospedeiro, produção de energia através de vias anaeróbicas e aeróbicas nas fases de levedura e micélio respectivamente, combate a espécies reativas de oxigênio gerados pela fosforilação oxidativa, ativação de proteínas envolvidas no ciclo, morfogênese e formação de hifas. Desta forma, os dados do presente trabalho agregam mais informações sobre os mecanismos de regulação pós-transcricional empregados por estes patógenos para sua sobrevivência.

3. PERSPECTIVAS

As perspectivas que surgiram a partir dos resultados deste trabalho são:

- Avaliar os possíveis alvos nos microRNAs-like com maiores valores de expressão diferencial entre os estágios de micélio e transição dimórfica;
- Avaliar os possíveis alvos em humanos dos microRNAs-like produzidos por este patógeno;
- Analisar o perfil de expressão destes microRNA-like, durante a infecção em pneumócitos;
- Obter linhagens silenciadas para o genes codificadores de microRNAs-like e avaliar o impacto deste silenciamento no crescimento em diferentes estágios morfológicos;
- Realizar ensaios de virulência em modelo murino de infecção com as linhagens silenciadas para genes codificadores de microRNAs-like;

4. REFERÊNCIAS

- ALBUQUERQUE, P. et al. Pbhyd1 and Pbhyd2: Two mycelium-specific hydrophobin genes from the dimorphic fungus *Paracoccidioides brasiliensis*. **Fungal Genetics and Biology**, v. 41, n. 5, p. 510–520, 2004.
- ALBUQUERQUE, P. et al. *Paracoccidioides brasiliensis* RNA biogenesis apparatus revealed by functional genome analysis. **Genetics and molecular research : GMR**, v. 4, n. 2, p. 251–72, 2005.
- ANDRADE, R. V. et al. Cell organisation, sulphur metabolism and ion transport-related genes are differentially expressed in *Paracoccidioides brasiliensis* mycelium and yeast cells. **BMC Genomics**, v. 7, p. 1–13, 2006.
- ARANTES, T. D. et al. Environmental Mapping of *Paracoccidioides* spp. in Brazil Reveals New Clues into Genetic Diversity, Biogeography and Wild Host Association. **PLoS Neglected Tropical Diseases**, v. 10, n. 4, p. 1–18, 2016.
- ARAÚJO, D. S. et al. Employing proteomic analysis to compare *Paracoccidioides lutzii* yeast and mycelium cell wall proteins. **Biochimica et Biophysica Acta - Proteins and Proteomics**, v. 1865, n. 11, p. 1304–1314, 2017.
- ARISTIZABAL, B. H. et al. Morphological transition of *Paracoccidioides brasiliensis* conidia to yeast cells : *In vivo* inhibition in females. **Infection and Immunity**, v. 66, n. 11, p. 5587–5591, 1998.
- BAGAGLI, E. et al. *Paracoccidioides brasiliensis*: Phylogenetic and ecological aspects. **Mycopathologia**, v. 165, n. 4–5, p. 197–207, 2008.
- BAI, Y. et al. sRNA profiling in *Aspergillus flavus* reveals differentially expressed miRNA-like RNAs response to water activity and temperature. **Fungal genetics and biology : FG & B**, v. 81, p. 113–9, 2015.
- BARTEL, D. P.; LEE, R.; FEINBAUM, R. MicroRNAs : Genomics , Biogenesis , Mechanism , and Function Genomics : The miRNA Genes. v. 116, p. 281–297, 2004.
- BASTOS, K. P. et al. The transcriptome analysis of early morphogenesis in *Paracoccidioides brasiliensis* mycelium reveals novel and induced genes potentially associated to the dimorphic process. **BMC Microbiology**, v. 7, p. 1–14, 2007.
- BRUMMER, E; CASTANEDA, E; RESTREPO, A; Paracoccidioidomycosis: an update. **Clin. Microbiol. Revista**, v.6, p-90-103, 1993.
- BAUMBERGER, N.; BAULCOMBE, D. C. Arabidopsis ARGONAUTE1 is an RNA Slicer that selectively recruits microRNAs and short interfering RNAs. **Proceedings of the National Academy of Sciences**, v. 102, n. 33, p. 11928–11933, 2005.

- BELITARDO, D. R. et al. *Paracoccidioides brasiliensis* infection in domestic rabbits (*Oryctolagus cuniculus*). **Mycoses**, v. 57, n. 4, p. 222–227, 2014.
- BOCCA, A. L. et al. Paracoccidioidomycosis: eco-epidemiology, taxonomy and clinical and therapeutic issues. **Future Microbiology**, v. 8, n. 9, p. 1177–1191, 2013.
- BONFIM, S. M. R. C. et al. Chitinase from *Paracoccidioides brasiliensis*: Molecular cloning, structural, phylogenetic, expression and activity analysis. **FEMS Immunology and Medical Microbiology**, v. 46, n. 2, p. 269–283, 2006.
- CAPELLA MACHADO, G. et al. Cryptic species of *Paracoccidioides brasiliensis*: Impact on paracoccidioidomycosis immunodiagnosis. **Memorias do Instituto Oswaldo Cruz**, v. 108, n. 5, p. 637–643, 2013.
- CARRERO, L. L. et al. New *Paracoccidioides brasiliensis* isolate reveals unexpected genomic variability in this human pathogen. **Fungal Genetics and Biology**, v. 45, n. 5, p. 605–612, 2008.
- CATAN, J. C.; MORALES, M. Images in clinical tropical medicine cutaneous paracoccidioidomycosis. **American Journal of Tropical Medicine and Hygiene**, v. 93, n. 3, p. 433–434, 2015.
- CASADEVALL, A. PIROFSKI, L.A. Virulence factors and their mechanisms of action: the view from a damage-response framework. **J Water Health**, v.7, 2009.
- CORTÉS, J.C. et al. Localization of the (1,3)beta-D-glucan synthase catalytic subunit homologue Bgs1p/Cps1p from fission yeast suggests that it is involved in septation, polarized growth, mating, spore wall formation and spore germination. **J Cell Sci**, v. 21, p. 4081-96, 2002.
- CHAVES, A. F. A. et al. A conserved dimorphism-regulating histidine kinase controls the dimorphic switching in *Paracoccidioides brasiliensis*. **FEMS Yeast Research**, v. 16, n. 5, p. 1–10, 2016.
- CHEN, D. et al. The cAMP pathway is important for controlling the morphological switch to the pathogenic yeast form of *Paracoccidioides brasiliensis*. **Molecular Microbiology**, v. 65, n. 3, p. 761–779, 2007.
- CHEN, R. et al. Exploring microRNA-like small RNAs in the filamentous fungus *Fusarium oxysporum*. **PloS one**, v. 9, n. 8, 2014.
- DAHLMANN, T. A.; KÜCK, U. Dicer-Dependent Biogenesis of Small RNAs and Evidence for MicroRNA-Like RNAs in the Penicillin Producing Fungus *Penicillium chrysogenum*. **PloS one**, v. 10, n. 5, 2015.
- DEHURY, B. et al. *In silico* identification and characterization of conserved miRNAs

and their target genes in sweet potato (*Ipomoea batatas* L.) Expressed Sequence Tags (ESTs). **Plant signaling & behavior**, v. 8, n. 12, p. 1–13, 2013.

de CURCIO, et al. *In silico* characterization of microRNAs-like sequences in the genome of *Paracoccidioides brasiliensis* Pb18. **GMB**, 2018, submetido.

DIX, A. et al. Specific and novel microRNAs are regulated as response to fungal infection in human dendritic cells. **Frontiers in Microbiology**, v. 8, n. FEB, 2017.

DRINNENBERG, I. A. et al. RNAi in budding yeast. **Science (New York, N.Y.)**, v. 326, n. 5952, p. 544–550, out. 2009.

DUKIK, K. et al. Novel taxa of thermally dimorphic systemic pathogens in the Ajellomycetaceae (Onygenales). **Mycoses**, v. 60, n. 5, p. 296–309, 2017.

FELIPE, M. S. S. et al. Transcriptome characterization of the dimorphic and pathogenic fungus *Paracoccidioides brasiliensis* by EST analysis. **Yeast**, v. 20, n. 3, p. 263–271, 2003.

FELIPE, M. S. S. et al. Transcriptional Profiles of the Human Pathogenic Fungus *Paracoccidioides brasiliensis* in Mycelium and Yeast Cells. **Journal of Biological Chemistry**, v. 280, n. 26, p. 24706–24714, 2005.

FERNANDES, L. et al. Transcriptional profile of *ras1* and *ras2* and the potential role of farnesylation in the dimorphism of the human pathogen *Paracoccidioides brasiliensis*. **FEMS Yeast Research**, v. 8, n. 2, p. 300–310, 2008.

FRANCO, M. et al. Paracoccidioidomycosis: A Recently Proposed Classification of Its Clinical Forms. **Revista da Sociedade Brasileira de Medicina Tropical**, v. 20, n. 2, p. 129–132, 1987.

GALAGAN, J. E. et al. The genome sequence of the filamentous fungus *Neurospora crassa*. **Nature**, v. 422, n. 6934, p. 859–868, 2003.

GHOSH, J. et al. *Leishmania donovani* targets *dicer1* to downregulate miR-122, lower serum cholesterol, and facilitate murine liver infection. **Cell Host and Microbe**, v. 13, n. 3, p. 277–288, 2013.

GOLDMAN, G. H. et al. Expressed Sequence Tag Analysis of the Human Pathogen. **Society**, v. 2, n. 1, p. 34–48, 2003.

GRIMSON, A. et al. Early origins and evolution of microRNAs and Piwi-interacting RNAs in animals. **Nature**, v. 455, n. 7217, p. 1193–1197, out. 2008.

GROSSHAN, H.; FILIPOWICZ, W. The expanding world of small RNAs. **Nature**, v. 451, 2008.

HE, L.; HANNON, G. J. MicroRNAs: small RNAs with a big role in gene regulation.

- Nature reviews. Genetics**, v. 5, n. 7, p. 522–531, 2004.
- HE, X. et al. MicroRNA-351 promotes schistosomiasis-induced hepatic fibrosis by targeting the vitamin D receptor. **Proceedings of the National Academy of Sciences**, v. 115, n. 1, 2018.
- HERNÁNDEZ, O. et al. Kinetic analysis of gene expression during mycelium to yeast transition and yeast to mycelium germination in *Paracoccidioides brasiliensis*. **Biomédica : revista del Instituto Nacional de Salud**, v. 31, n. 4, p. 570–9, 2011.
- HERNÁNDEZ, O. et al. Alternative oxidase plays an important role in *Paracoccidioides brasiliensis* cellular homeostasis and morphological transition. **Medical Mycology**, v. 53, n. 3, p. 205–214, 2015.
- JANBON, G. et al. Characterizing the role of RNA silencing components in *Cryptococcus neoformans*. **Fungal genetics and biology : FG & B**, v. 47, n. 12, p. 1070–80, dez. 2010.
- JIANG, N. et al. Identification and functional demonstration of miRNAs in the fungus *Cryptococcus neoformans*. **PloS one**, v. 7, n. 12, p. e52734, 2012.
- KANETSUNA, F.; CARBONELL, L. M. Cell wall glucans of the yeast and mycelial forms of *Paracoccidioides brasiliensis*. **Journal of Bacteriology**, v. 101, n. 3, p. 675–680, 1970.
- KANG, K. et al. Identification of microRNA-Like RNAs in the Filamentous Fungus *Trichoderma reesei* by Solexa Sequencing. **PLoS ONE**, v. 8, n. 10, p. 1–7, 2013.
- KÜBLER, E. et al. Gpa2p, a G-protein α -subunit, regulates growth and pseudohyphal development in *Saccharomyces cerevisiae* via a cAMP-dependent mechanism. **Journal of Biological Chemistry**, v. 272, n. 33, p. 20321–20323, 1997.
- LAGOS-QUINTANA, M. et al. Identification of Novel Genes Coding for Small Expressed RNAs. v. 853, n. 2001, 2001.
- LAI, M. H. et al. Multiple copies of PBS2, MHP1 or LRE1 produce glucanase resistance and other cell wall effects in *Saccharomyces cerevisiae*. **Yeast**, v. 13, n. 3, p. 199–213, 1997.
- LAU, N. C. et al. An abundant class of tiny RNAs with probable regulatory roles in *Caenorhabditis elegans*. **Science**, v. 294, n. 5543, p. 858–862, 2001.
- LAU, S. K. P. et al. Identification of microRNA-like RNAs in mycelial and yeast phases of the thermal dimorphic fungus *Penicillium marneffei*. **PLoS neglected tropical diseases**, v. 7, n. 8, 2013.
- LEE, H.-C. C. et al. Diverse pathways generate microRNA-like RNAs and Dicer-

independent small interfering RNAs in fungi. **Molecular cell**, v. 38, n. 6, p. 803–14, jun. 2010.

LEE, R. C.; FEINBAUM, R. L.; AMBROS, V. The *C. elegans* heterochronic gene *lin-4* encodes small RNAs with antisense complementarity to *lin-14*. **Cell**, v. 75, n. 5, p. 843–854, dez. 1993.

LORENZ, M. C. Yeast pseudohyphal growth is regulated by GPA2, a G protein alpha homolog. **The EMBO Journal**, v. 16, n. 23, p. 7008–7018, 1997.

MARQUES, S. A. Paracoccidioidomycosis: epidemiological, clinical, diagnostic and treatment up-dating. **Anais brasileiros de dermatologia**, v. 88, n. 5, p. 700–11, 2013.

MARTINEZ, R. Epidemiology of Paracoccidioidomycosis. **Revista do Instituto de Medicina Tropical de São Paulo**, v. 57, p. 11–20, 2015.

MARTINEZ, R. New Trends in Paracoccidioidomycosis Epidemiology. **Journal of Fungi**, v. 3, n. 1, p. 1, 2017.

MARIOTO, T.G.D. et al. Study of differential expression of miRNAs in lung tissue of mice submitted to experimental infection by *Paracoccidioides brasiliensis*. **Med Mycol**, v.55, p- 774-784, 2017.

MATOS, T. G. F.; MORAIS, F. V.; CAMPOS, C. B. L. Hsp90 regulates *Paracoccidioides brasiliensis* proliferation and ROS levels under thermal stress and cooperates with calcineurin to control yeast to mycelium dimorphism. **Medical Mycology**, v. 51, n. 4, p. 413–421, 2013.

MATUTE, D. R. et al. Cryptic speciation and recombination in the fungus *Paracoccidioides brasiliensis* as revealed by gene genealogies. **Molecular Biology and Evolution**, v. 23, n. 1, p. 65–73, 2006.

MENDES, J. F. et al. Paracoccidioidomycosis infection in domestic and wild mammals by *Paracoccidioides lutzii*. **Mycoses**, v. 60, n. 6, p. 402–406, 2017

MENDES, R. P. et al. **Paracoccidioidomycosis: Current Perspectives from Brazil**. v.11,p. 224-282, 2017.

MCEWEN, J.G. et al. Experimental murine paracoccidioidomycosis induced by the inhalation of conidia. **J Med Vet Mycol**. v. 25, p. 165-75, 1987.

NEMECEK, J.C. WÜTHRICH, M. KLEIN, B.S. Global control of dimorphism and virulence in fungi. **Science**. v.28, p.583-8, 2006.

MILLET N. et al. Members of Glycosyl-Hydrolase Family 17 of *A. fumigatus* Differentially Affect Morphogenesis. **Journal of Fungi**, v. 4, n. 1, p. 18, 2018.

MISHRA, A. K. et al. Computational exploration of microRNAs from expressed

sequence tags of *Humulus lupulus*, target predictions and expression analysis. **Computational Biology and Chemistry**, v. 59, p. 131–141, 2015.

NAKAYASHIKI, H.; KADOTANI, N.; MAYAMA, S. Evolution and diversification of RNA silencing proteins in fungi. **Journal of molecular evolution**, v. 63, n. 1, p. 127–35, 2006.

NELSON, D.L.; COX, M.M. Princípios de bioquímica de Lehninger. 6º edição, Rio de Janeiro, Artmed, 2014.

NICOLÁS, F. E. et al. The RNAi machinery controls distinct responses to environmental signals in the basal fungus *Mucor circinelloides*. **BMC Genomics**, v. 16, n. 1, p. 1–14, 2015.

NOZAWA, M.; MIURA, S.; NEI, M. Origins and evolution of microRNA genes in plant species. **Genome Biology and Evolution**, v. 4, n. 3, p. 230–239, 2011.

NUNES, L. R. et al. Transcriptome Analysis of *Paracoccidioides brasiliensis* Cells Undergoing Mycelium-to-Yeast Transition. **Eukaryotic cell**, v. 4, n. 12, p. 2115–2128, 2005.

OLIVEIRA, A. F. et al. Paracoccin distribution supports its role in *Paracoccidioides brasiliensis* growth and dimorphic transformation. **PLoS ONE**, v. 12, n. 8, p. 1–14, 2017.

PANDA, D. et al. Computational identification and characterization of conserved miRNAs and their target genes in garlic (*Allium sativum* L.) expressed sequence tags. **Gene**, v. 537, n. 2, p. 333–342, mar. 2014.

PARENTE, J. A. et al. Comparison of transcription of multiple genes during mycelia transition to yeast cells of *Paracoccidioides brasiliensis* reveals insights to fungal differentiation and pathogenesis. **Mycopathologia**, v. 165, n. 4–5, p. 259–273, 2008.

PARK, M. Y. et al. Nuclear processing and export of microRNAs in Arabidopsis. **Proceedings of the National Academy of Sciences**, v. 102, n. 10, p. 3691–3696, 2005.

PERES DA SILVA, R. et al. Extracellular vesicle-mediated export of fungal RNA. **Scientific Reports**, v. 5, n. 1, p. 7763. 2015.

PINZAN, C. F. et al. Immunological basis for the gender differences in murine *Paracoccidioides brasiliensis* infection. **PLoS ONE**, v. 5, n. 5, 2010.

PIRES, D. et al. *Mycobacterium tuberculosis* modulates miR-106b-5p to control Cathepsin S expression resulting in higher pathogen survival and poor T-cell activation. **Frontiers in Immunology**, v. 8, p. 1–13, 2017.

PUCCIA, R. et al. The *Paracoccidioides* cell wall: Past and present layers toward

understanding interaction with the host. **Frontiers in Microbiology**, v. 2, p. 1-7, 2011.

REINHART, B. J. et al. MicroRNAs in plants. **Plant signaling & behavior**, v. 16, p. 1616–1626, 2002.

REINHART, B. J. et al. The 21 nt nucleotide let-7 RNA regulates developmental timing in *C. elegans*. **Nature**, v.403, n.6772, p.901-906, 2000.

RESTREPO A. The ecology of *Paracoccidioides brasiliensis*: a puzzle still unsolved.v.23, p. 323-34, 1985.

REZENDE, T. C. V et al. A quantitative view of the morphological phases of *Paracoccidioides brasiliensis* using proteomics. **Journal of Proteomics**, v. 75, n. 2, p. 572–587, 2011.

SALAZAR, M. E.; RESTREPO, A.; STEVENS, D. A. Inhibition by estrogens of conidium-to-yeast conversion in the fungus *Paracoccidioides brasiliensis*. **Infection and Immunity**, v. 56, n. 3, p. 711–713, 1988.

SALGADO-SALAZAR, C. et al. The human fungal pathogen *Paracoccidioides brasiliensis* (Onygenales: Ajellomycetaceae) is a complex of two species: phylogenetic evidence from five mitochondrial. **Cladistics**, v. 26, p. 613–624, 2010.

SBEGHEN, M. R. et al. *Paracoccidioides brasiliensis* Infection in Small Wild Mammals. **Mycopathologia**, v. 180, n. 5–6, p. 435–440, 2015.

SCHNITGER, A. K. D. et al. *Listeria monocytogenes* infection in macrophages induces vacuolar-dependent host miRNA response. **PLoS ONE**, v. 6, n. 11, 2011.

SHEN, J.; HUNG, M.C. Signaling-mediated Regulation of MicroRNA Processing. **Cancer Res.** v. 75, n.5 p. 783–791, 2015.

SELVAGGINI, S. et al. Independent regulation of chitin synthase and chitinase activity in *Candida albicans* and *Saccharomyces cerevisiae*. **Microbiology**, v. 150, n. 4, p. 921–928, 2004.

SESTAK, S. et al. Scw10p, a cell-wall glucanase/transglucosidase important for cell-wall stability in *Saccharomyces cerevisiae*. **Microbiology**, v. 150, n. 10, p. 3197–3208, 2004.

SHANKAR, J. et al. Influence of 17 β -estradiol on gene expression of *Paracoccidioides* during mycelia-to-yeast transition. **PloS one**, v. 6, n. 12, 2011.

SHARBATI, J. et al. Integrated microrna-mrna-analysis of human monocyte derived macrophages upon *Mycobacterium avium* subsp. *hominissuis* infection. **PLoS ONE**, v. 6, n. 5, 2011.

SHIKANAI-YASUDA, M. A. et al. Consenso em paracoccidioidomicose. **Revista da**

- Sociedade Brasileira de Medicina Tropical**, v. 39, n. 3, p. 297–310, 2006.
- SHIKANAI-YASUDA, M. A. et al. Brazilian guidelines for the clinical management of paracoccidioidomycosis. **Revista da Sociedade Brasileira de Medicina Tropical**, v. 50, n. 5, p. 715–740, 2017.
- SINGULANI, J. et al. Preliminary evaluation of circulating microRNAs as potential biomarkers in paracoccidioidomycosis. **Biomedical Reports**, v. 6, n. 3, p. 353–357, 2017.
- TEIXEIRA, M. M. et al. Phylogenetic analysis reveals a high level of speciation in the *Paracoccidioides* genus. **Molecular Phylogenetics and Evolution**, v. 52, n. 2, p. 273–283, 2009.
- TEIXEIRA, M. M. et al. *Paracoccidioides* Species Complex: Ecology, Phylogeny, Sexual Reproduction, and Virulence. **PLoS Pathogens**, v. 10, n. 10, p. 4–7, 2014.
- THEODORO, R. C. et al. Genus *Paracoccidioides*: Species recognition and biogeographic aspects. **PLoS ONE**, v. 7, n. 5, 2012.
- THIND, S. K.; TABORDA, C. P.; NOSANCHUK, J. D. Dendritic cell interactions with *Histoplasma* and *Paracoccidioides*. **Virulence**, v. 6, n. 5, p. 424–432, 2015.
- TRIEU, T. A. et al. A Non-canonical RNA Silencing Pathway Promotes mRNA Degradation in Basal Fungi. **PLoS Genetics**, v. 11, n. 4, p. 1–32, 2015.
- TURISSINI, D. A. et al. Species boundaries in the human pathogen *Paracoccidioides*. **Fungal Genetics and Biology**, v. 106, p. 9–25, 2017.
- UNTEREINER, W. A. et al. The Ajellomycetaceae, a new family of vertebrate-associated Onygenales. **Mycologia**, v. 96, n. 4, p. 812–821, 2004.
- VALSECCHI, I. et al. Role of Hydrophobins in *Aspergillus fumigatus*. **Journal of Fungi**, v. 4, n. 1, p. 2, 2017.
- VALLE, A.C.F. et al., Paracoccidioidomycosis after Highway Construction, Rio de Janeiro, Brazil. **Emerging Infectious Diseases**, v. 23, n. 11, p. 1917–1919, 2017.
- VOINNET, O. Origin, Biogenesis, and Activity of Plant MicroRNAs. **Cell**, v. 136, n. 4, p. 669–687, 2009.
- WEIBERG, A. et al. Fungal small RNAs suppress plant immunity by hijacking host RNA interference pathways. **Science**, v. 342, n. 6154, p. 118–123, 2013.
- XIE, M. microRNA biogenesis, degradation and activity in plants. 2015.
- YAMAMOTO, N. et al. Particle-size distributions and seasonal diversity of allergenic and pathogenic fungi in outdoor air. **ISME Journal**, v. 6, n. 10, p. 1801–1811, 2012.
- YANG, Q. et al. Transcription of the Major *Neurospora crassa* microRNA-Like Small

RNAs Relies on RNA Polymerase III. **PLoS Genetics**, v. 9, n. 1, p. 1–12, 2013.

YI, R. et al. Overexpression of exportin 5 enhances RNA interference mediated by short hairpin RNAs and microRNAs. **RNA (New York, N.Y.)**, v. 11, n. 2, p. 220–226, 2005.


ZHANG, B. H. et al. Evidence that miRNAs are different from other RNAs. **Cellular and Molecular Life Sciences**, v. 63, n. 2, p. 246–254, 2006.

ZHAO, T. et al. A complex system of small RNAs in the unicellular green alga. **Genes & Development**, p. 1190–1203, 2007.

ZHOU, J. et al. Identification of microRNA-like RNAs in a plant pathogenic fungus *Sclerotinia sclerotiorum* by high-throughput sequencing. **Molecular Genetics and Genomics**, v. 287, n. 4, p. 275–282, 2012.

ZHOU, Q. et al. Genome-wide identification and profiling of microRNA-like RNAs from *Metarhizium anisopliae* during development. **Fungal biology**, v. 116, n. 11, p. 1156–62, nov. 2012.

ZHANG, Y. et al. Comparison of miRNA Evolution and Function in Plants and Animals. **Microrna**, v.7, n.1, 4-10, 2018.



Anexo
Contribuição em artigo

Identification of membrane proteome of *Paracoccidioides lutzii* and its regulation by zinc

Aim: During infection development in the host, *Paracoccidioides* spp. faces the deprivation of micronutrients, a mechanism called nutritional immunity. This condition induces the remodeling of proteins present in different metabolic pathways. Therefore, we attempted to identify membrane proteins and their regulation by zinc in *Paracoccidioides lutzii*. **Materials & methods:** Membranes enriched fraction of yeast cells of *P. lutzii* were isolated, purified and identified by 2D LC–MS/MS detection and database search. **Results & conclusion:** Zinc deprivation suppressed the expression of membrane proteins such as glycoproteins, those involved in cell wall synthesis and those related to oxidative phosphorylation. This is the first study describing membrane proteins and the effect of zinc deficiency in their regulation in one member of the genus *Paracoccidioides*.

Lay abstract: The methodology of protein identification allows the characterization of biological processes performed by those molecules. Therefore, we performed a membrane proteomic analysis of *Paracoccidioides lutzii* and further evaluated the responses of the fungus to zinc deprivation. The results obtained in the work allowed the characterization of membrane proteins present in organelles that are related to different cellular functions. Zinc deprivation changes processes related to cellular physiology and metabolism. These results help us to understand the process of pathogen–host interaction, since zinc deprivation is a condition present during infection.

First draft submitted: 6 April 2017; Accepted for publication: 21 June 2017; Published online: 25 July 2017

Keywords: membranes • nanoUPLC–MS^E • *Paracoccidioides lutzii* • proteome
 • zinc deprivation

The genus *Paracoccidioides* comprises the etiologic agents of paracoccidioidomycosis, the most widespread systemic mycosis in Latin America. As other thermodimorphic fungi, members of the genus *Paracoccidioides* grow as mycelia in the environment and as yeast cells at 36°C and in host tissues [1]. The infection occurs through the host respiratory route [2], in which inhalation of conidia or mycelial propagules allows these structures to reach the host pulmonary alveoli, in which they perform the dimorphic transition and

differentiate into yeast cells [3]. This mycosis represents an important public health problem due the quantity of premature deaths, particularly in certain segments of society, such as rural workers [4].

Zinc is a metal of importance for the development of microorganisms. It serves as a structural or catalytic cofactor for many proteins, participating in several processes, such as cell division and differentiation [5]. Zinc homeostasis, a critical process to cells, is maintained at both transcriptional and post-

Juliana Santana de Curcio^{1,1},
 Marielle Garcia Silva^{a,1},
 Mirelle Garcia Silva Bailão¹,
 Sônia Nair Bão³, Luciana
 Casaletti¹, Alexandre Mello
 Bailão¹ & Célia Maria de
 Almeida Soares^{*,1}

¹Laboratório de Biologia Molecular, Instituto de Ciências Biológicas, Universidade Federal de Goiás, Goiânia, Goiás, Brazil

²Unidade Acadêmica Especial Ciências da Saúde, Universidade Federal de Goiás, Jataí, Goiás, Brazil

³Laboratório de Microscopia, Universidade de Brasília, Brasília, Brazil

⁴Escola de Engenharia, Pontifícia Universidade Católica de Goiás, Goiás, Brazil

*Author for correspondence:

Tel.: +55 62 35211736

cmasoares@gmail.com

[†]Authors contributed equally

translational levels occurring in response to changes in intracellular zinc levels [6]. The uptake of zinc in *Saccharomyces cerevisiae* is mediated by two systems: the high-affinity uptake system, which is active in zinc-limited conditions [7]; and the low-affinity uptake system, which is active in the presence of sufficient zinc concentrations [8]. The expression and activity of the high-affinity zinc transporter (Zrt1) and low-affinity zinc transporter (Zrt2) are regulated by the transcription factor, *Zap1* [9,10]. During zinc limitation, *Zap1* induces the expression of *Zrt1* and *Zrt2* [11]. The regulation at post-translational level occurs when the cell, under low zinc concentration, is exposed to high extracellular levels of zinc. This exposure causes the internalization of Zrt1p protein via endocytosis and subsequent degradation in the vacuole [10]. Another mechanism of zinc uptake, at the intracellular level, includes the Msc2p and Zrg17p transporters, which are localized at the endoplasmic reticulum and induced under zinc deficiency [12,13]. The vacuole is the main site of zinc sequestration and detoxification in the yeast *S. cerevisiae* [14]. Two transporters of the cation diffusion facilitator family named Zrc1p and Cot1p are responsible for vacuole zinc accumulation [15]. Zrt3p is another transporter localized at vacuolar membrane, which is responsible for the release of zinc into the cytoplasm upon metal deficiency in *S. cerevisiae* [15,16].

In *Paracoccidioides* spp., *in silico* analyses identified zinc transporters homologs to those described in *S. cerevisiae* such as Zrt1p, Zrt2p, Zrc1p, Cot1p and Msc2p. Moreover, a homolog to the transcriptional factor *Zap1* is also present in the genome of *Paracoccidioides* spp. [17]. Studies demonstrated the induction of *Zrt1* and *Zrt2* expression in yeast cells upon zinc deprivation [18,19] and induction of *Zrt2* in neutral to alkaline pH during zinc deficiency, as described to *ZrfC* in *Aspergillus fumigatus* [18]. Moreover, studies on *Paracoccidioides* sp., after contact with human plasma and liver of mice revealed the induction of high-affinity zinc transporter under these conditions [20,21].

Plasma membrane plays an important role in cells, acting as a physical barrier, regulating the exchange of information, ions and metabolites between the cell and the environment [22]. Moreover, membranes are responsible for the intracellular compartmentalization of organelles [23]. Membrane proteins perform a variety of functions such as transport, cell adhesion, signal receptors and nutrient uptake. Zinc transporters (Zrt1p and Zrt2p) are located at the plasma membrane [9] on dependence of the concentration of zinc in the medium [10,23]. Around 30% of the open-reading frames in eukaryote genomes encode for integral membrane proteins [24]. However, analysis of membrane proteins is underrepresented in proteomic

analyses, owing to the heterogeneous nature of those molecules [23]. Insolubility in aqueous buffers, hindering the extraction steps of the lipid bilayer [25] and inhibition of the tryptic activity in the segments of the integral membrane proteins [26] make those molecules underrepresented in proteomic analysis. Therefore, the establishment of a methodology able to encompass all these characteristics is a challenge in proteomic sciences [27].

Although membrane proteins perform cellular processes essential to cell survival, the knowledge about this class of proteins is still limited in *Paracoccidioides* spp. To our knowledge, *Paracoccidioides* spp. membrane proteome has not been analyzed yet. Therefore, the current study is intended to investigate, using nanoU-PLC-MS^E and label-free approach, proteins in membranes of *Paracoccidioides lutzii* and their responses to zinc deprivation. This study allowed the identification of proteins belonging to the whole membrane system, comprising plasma membrane and membranes of cytoplasmic organelles, such as mitochondria, peroxisome, vacuole and endoplasmic reticulum. The biological processes performed by zinc-regulated proteins include composition of cell wall, vesicles traffic, oxidative phosphorylation, zinc uptake in the vacuole and glycosylation in the endoplasmic reticulum. Besides depicting the first large-scale depository of membrane proteins in the genus *Paracoccidioides*, this article highlights protein candidates potentially involved in the response to zinc limitation, a condition found in the host.

Materials & methods

Fungal strain, growth conditions & zinc deprivation experiments

The experiments were performed with *P. lutzii*, Pb01 (ATCC MYA-826). The yeast phase was maintained at 36°C in Fava Netto's medium (1% [w/v] peptone, 0.5% [w/v] yeast extract, 0.3% [w/v] proteose peptone, 0.5% [w/v] beef extract, 0.5% [w/v] NaCl, 4% [w/v] glucose, 1.2% [w/v] agar, pH 7.2) [28] supplemented with 4% (w/v) glucose. Yeast cells were inoculated in Fava Netto's liquid medium for 72 h at 36°C, 150 rpm, in order to obtain cells at the exponential growth phase. Afterward, the cells were centrifuged at 1200 × *g* for 10 min at 4°C and washed in phosphate-buffered saline (PBS 1X). The supernatant was discarded, the cells were resuspended in PBS 1x and inoculated at the concentration of 10⁶ cells/ml in McVeigh/Morton' liquid medium (MMcM) containing: 4% (w/v) glucose, 0.15% (w/v) KH₂PO₄, 0.05% (w/v) MgSO₄·7H₂O, 0.015% (w/v) CaCl₂·2H₂O, 0.2% (w/v) (NH₄)₂SO₄, 0.2% (w/v) L-asparagine, 0.02% (w/v) L-cystine, 1% (v/v) of vitamin supplement (0.006% [w/v] thiamine, 0.006% [w/v] niacin

B3, 0.006% [w/v] Ca²⁺ pantothenate, 0.001% [w/v] inositol B7, 0.0001% [w/v] biotin B8, 0.001% [w/v] riboflavin, 0.01% [w/v] folic acid B9, 0.01% [w/v] choline chloride, 0.01% [w/v] pyridoxine and 0.1% (v/v) of trace elements supplement (0.0057% [w/v] H₃BO₃, 0.0081% [w/v] MnSO₄·14H₂O, 0.0036% [w/v] (NH₄)₆MO₇O₂₄·4H₂O, 0.0157% [w/v] CuSO₄·H₂O, 0.1404% [w/v] Fe(NH₄)₂(SO₄)₂·6H₂O) [29], pH 7.0, for 24 h.

Following 24 h of cultivation in MMcM medium, 10⁶ cells/ml were transferred to the same medium containing 30 μM ZnSO₄·7H₂O, or depleted of zinc. The depleted medium was prepared with no addition of ZnSO₄ and was supplemented with the zinc chelator N,N,N,N-tetrakis(2-pyridyl-methyl) ethylenediamine (Sigma-Aldrich, MO, USA) at a concentration of 0.05 mM. The cultures were incubated with gentle shaking at 36°C for 24 h, 150 rpm, as previously described [19].

Extraction of membrane proteins

The protocol described by Vidakovic *et al.* [30] was used with some modifications. Experiments were performed in biological triplicates as three independent experiments. Yeast cells cultured in MMcM medium were centrifuged at 1200 × *g* for 10 min at 4°C, frozen in liquid nitrogen and disrupted by maceration using a gral and pestle until a fine powder was obtained [31]. After this step, the sample was transferred to a conical tube and resuspended in 50 mM Tris-HCl, pH 7.5. Glass beads were added to the conical tube and after agitation for 20 min at 4°C, the sample was subjected to centrifugation at 8000 × *g* for 10 min at 4°C. The supernatant was diluted in 10 ml of 0.1 M sodium carbonate (Na₂CO₃) pH 11 for 1 h. The carbonate treated sample was submitted to ultracentrifugation in a Beckman Coulter Optima L-90K centrifuge at 115,000 × *g* for 1 h, at 4°C. The supernatant was discarded and the pellet containing the membranes fraction was resuspended in 50 mM Tris-HCL pH 7.5 using a glass homogenizer (grinder) on ice, to solubilize the membranes fraction. The sample was submitted to another step of ultracentrifugation at 115,000 × *g* for 1 h at 4°C. An aliquot of the pellet was used for the transmission electron microscopy (TEM) analysis while the remainder was resuspended in 50 mM ammonium bicarbonate pH 8.0 and stored at -80°C.

Transmission electron microscopy

TEM was performed to evaluate the quality of the sample. TEM of the membranes fraction was performed according to standard protocols [32]. The samples of the membrane fraction and intact cells of *P. lutzii* were fixed in 2% (w/v) paraformaldehyde and 2% (v/v) glutaraldehyde in 0.1 M sodium cacodylate buffer, pH 7.2, for 2 h, at room temperature.

After washing in 0.1 M sodium cacodylate buffer pH 7.2, the samples were postfixed in 2% (w/v) osmium tetroxide, 1.6% (w/v) potassium fericyanide (1:1) and 5 mM CaCl₂ in sodium cacodylate buffer, pH 7.2, for 1 h, at room temperature, followed by washing in 0.1 M sodium cacodylate buffer, pH 7.2. The samples were maintained for 12 h in an aqueous solution of 0.5% (v/v) uranyl acetate at 4°C, washed in distilled water and dehydrated in an ascending series of acetone (v/v) (30, 50, 70, 90 and 100%). The material was embedded in a mixture of (3:1) acetone/Spurr resin (Electron Microscopy Sciences, Co.) for 6 h, (2:1) acetone/Spurr resin overnight, (1:1) acetone/Spurr resin for 6 h, (1:2) acetone/Spurr resin overnight and finally in pure resin for 6 h. The samples were imbedded in Spurr resin for 3 days in an incubator, at 60°C. The ultrathin sections were contrasted with 3% (v/v) aqueous uranyl acetate and 10% (v/v) lead citrate. The samples were analyzed in a TEM, JEM 1011 (Electron Microscopy Sciences, Co, Jeol, Tokyo, Japan.)

Preparation of membrane proteins for nanoUPLC-MS^E analysis

The amount of protein in the membrane extract was determined using the Bradford reagent (Sigma-Aldrich) [33]. The samples were analyzed using nanoscale LC-MS/MS. Sample aliquots (100 μg) were prepared for nanoUPLC-MS^E as previously described [34]. Briefly, ammonium bicarbonate pH 8.5 at 50 mM and 75 μl of 0.2% (v/v) RapiGEST (Waters Corp, MA, USA) were sequentially added to the samples. After, the solution was vortexed and incubated in dry bath for 15 min at 80°C. After incubation, the samples were centrifuged and the proteins reduced by adding 2.5 μl of a 100 mM DTT solution, followed by incubation for 30 min at 60°C. The alkylation of proteins was performed by addition of 2.5 μl of 300 mM iodoacetamide and incubation in a dark room for 30 min. An aliquot of 40 μl of trypsin (Promega, WI, USA) 50 ng/μl in 50 mM ammonium bicarbonate was added. The sample was vortexed slightly and digested at 37°C for 16 h. Following digestion, the hydrolysis of RapiGEST was performed by addition of 10 μl of 5% (v/v) trifluoroacetic acid and incubation at 37°C for 90 min. The sample was centrifuged at 20,000 × *g* at 6°C for 30 min, and the supernatant was transferred to microfuge tubes and dried in a speed vacuum. Peptides were solubilized in 30 μl of ultrapure water, submitted to purification and concentration using a pipette tip with a bed of chromatographic media (ZipTips® C18 Pipette Tips, MA, USA) and dried in a speed vacuum. The peptides were resuspended in a solution of 1 pmol/μl MassPREP Digestion Standard (rabbit phos-

phorilase B; Waters Corp) to prepare the final concentration of 200 fmol/ μ l of the rabbit phosphorilase B. The buffer solution of 20 mM ammonium formate was used to increase the pH. After solubilization, peptides were transferred to a Waters Total Recovery vial (Waters Corp).

NanoUPLC-MS^E analysis

The proteomic analysis was performed using a label-free nanoUPLC-MS^E technology. Briefly, tryptic peptides were separated by RP-RP-HPLC using a nano-ACQUITYTM system (Waters Corp), as described before [35]. The first column was loaded with 5 μ g digests and sequentially, separated in ten fractions in the mobile phase at pH 10. Each fraction was subjected to the second dimension of RP chromatography with a mobile phase at pH 2.5. Label-free data-independent scanning (MS^E) experiments were performed with a Synapt HDMS mass spectrometer (Waters, Manchester, UK), which switched between low collision energy (3 eV) and elevated collision energy (12–40 eV) applied to the trap ‘T-wave’ CID cell with argon gas, as described [36].

The protein identifications and quantitative packaging were generated using specific algorithms [37,38] and search was performed against an in-house *P. lutzii*-specific database. The ProteinLynx Global server v.2.5.2 (PLGS) was used to perform the spectral processing, database searching conditions and quantitative comparisons. The specific database was randomized in order to access the false-positive rate of identification (4%). The intensity measurements were typically adjusted for these components, in other words, the deisotoped and charge state-reduced exact mass-retention times that were replicated throughout the entire experiment for the analysis at the exact mass retention-time cluster level. Components were typically clustered with a 10 ppm mass precision and a 0.25 min time tolerance against the database-generated theoretical peptide ion masses with a minimum of one matched peptide. The alignment of elevated energy ions with low-energy precursor peptide ions was performed with an approximate precision of 0.05 min. The precursor and fragmentation tolerances were determined automatically. The search parameters used were: trypsin as digest reagent, 1 missed cleavage, carbamidomethyl as fixed modification and phosphorylation STY and oxidation M were used as variable modifications. The minimum fragment ion matches per peptide, the minimum fragment ion matches per protein and the minimum peptide matches per protein were, respectively, set as 2, 5 and 1. The mass variation tolerance was set to 50 ppm. A protein detected in all replicates, presenting a variance coefficient less than 10%

(PAAG_08059), was used to normalize the expression data to compare the protein levels between control and zinc-limiting conditions. Protein and peptides tables generated by PLGS were merged and the dynamic range of the experiments, peptides detection type and mass accuracy were determined for each condition [39]. Software FBAT [40], MassPivot (kindly provided by AM Murad), Spotfire[®] (© TIBCO Software Inc.) and Microsoft Office Excel (Microsoft[®]) were used.

In silico analysis

The data obtained after analysis by nanoUPLC-MS^E and identification in ProteinLynx were submitted to *in silico* search in database in order to determine proteins subcellular location and association with cell membranes. The subcellular location was determined by using WoLF PSORT (www.genscript.com/psort/wolf_psort.html) [41] and Gene Ontology (GO; <http://pedant.gsf.de/>) databases [42]. The protein association with membranes evaluated the presence of transmembrane domains and prenylation, myristoylation, palmitoylation and GPI anchor. The TMHMM program, version 2.0 (www.cbs.dtu.dk/services/TMHMM) [43] was used to predict transmembrane regions. The big-PI Fungal Predictor program (http://mendel.imp.ac.at/gpi/fungi_server.html) [44] was used to predict glycosylphosphatidylinositol anchors. The search for myristoylated proteins was performed using the programs, Myristoylator (<http://web.expasy.org/myristoylator/>) [45] and TerminiNator (www.isv.cnrs-gif.fr/terminator3/index.html) [26]. The last was also utilized for the prediction of palmitoylated proteins, while the prediction of prenylation was achieved with the PrePS-Prenylation Prediction Suite (<http://mendel.imp.ac.at/sat/PrePS/index.html>) software [46]. The search for signal peptide was performed using the SignalP program, version 4.1 (www.cbs.dtu.dk/services/SignalP/) [47]. Loctree program (<https://roslab.org/services/loctree2/>) [48] was employed in order to determine in which organelle membrane proteins were localized. The functional classification of proteins present in membranes fraction was accomplished using Funcat2 database (http://pedant.gsf.de/pedant3htmlview/pedant3view?Method=analysis&Db=p3_r48325_Par_brasi_Pb01).

Analysis of chitin amount in the cell wall of

P. lutzii

Calcofluor white (CFW, Sigma Biochemical) was utilized to stain *P. lutzii* (Pb01) yeast cells in order to evaluate the effect of zinc deprivation at the cell wall. *P. lutzii* yeast cells were grown under zinc deprivation or in presence of this metal for 24 h. For analysis of chitin amount, the cells were fixed in 100% methanol at -80°C for 20 min, at -20°C for additional 20 min

and subsequently washed by centrifugation. The cells were collected, stained with CFW (100 µg/ml in PBS 1×) for 30 min and washed with PBS 1×. The specimens were analyzed under a fluorescence microscope (Zeiss AxioCam MRc – Scope A1) [49]. CFW fluorescence intensity was measured using the AxioVision Software (Carl Zeiss AG, Germany). The minimum of 100 cells for each microscope slides, in triplicates, were used to evaluate fluorescence intensity of the cells upon zinc presence or deprivation, for 24 h. The software provided the fluorescence intensity (in pixels) and the standard error of each analysis. Statistical comparisons were performed using the Student's t test and p-values ≤0.05 were considered statistically significant.

Schiff periodic acid staining of proteins

The staining with Schiff periodic acid was performed in order to evaluate the profile of glycosylated proteins during zinc deficiency. After separation of membrane proteins by electrophoresis, the proteins were fixed in 10% (v/v) acetic acid and 25% (v/v) isopropanol by 18 h at 4°C. After this step, the polyacrylamide gel was washed twice during 15 min with 7.5% (v/v) acetic acid and immersed in a solution of 0.4% (v/v) periodic acid for 1 h at 4°C. Afterward, the gel was immersed in Schiff reagent for 1 h at 4°C in the dark, and subsequently washed three times, 10 min each, in 0.5% (v/v) potassium metabisulfite in the dark. The gel was washed with 7.5% (v/v) acetic acid for 5 min and stored in the same solution at 4°C [50].

Analysis of glycosylated proteins & glucans by fluorescence microscopy

The profile of glycosylated proteins during zinc deprivation was evaluated by staining with Concanavalin A (ConA) TYPE VI conjugated to FITC (Sigma, catalog n.C7642). The yeast cells cultured in the presence or absence of zinc were stained with ConA+FITC at a final concentration of 100 µg/ml [51]. ConA+FITC in a volume of 200 µl was incubated with yeast cells of *P. lutzii* at 37°C, for 30 min, under stirring. After, the cells were washed with PBS 1×, twice. The cells were incubated with aniline blue solution 100% (v/v) (Sigma, catalog n.B8563) for 5 min under stirring and subsequently washed twice with PBS 1× [52]. Both samples stained with ConA+FITC or aniline blue were visualized under a fluorescence microscope (Zeiss AxioCam MRc-Scope A1). Fluorescence intensity was calculated as described above, for both dyes.

Results

TEM of *Pb01* membranes fraction

The membrane proteins of *Pb01* were obtained according to the steps shown in the workflow chart

(Supplementary Figure 1). TEM was performed in order to confirm the enrichment of samples with cell membranes of *P. lutzii*. As shown in Figure 1, the membrane fragments detected in the electron micrograph corroborate the enrichment of the extract.

Proteomic data

NanoUPLC-MS^E is a method that improves protein and proteome coverage compared with the conventional LC-MS/MS approach [34]. The results presented here are from merged data of three replicates, leading to the identification of 746 proteins from the total membranes preparation of *P. lutzii*. Of the 746 proteins, 717 were identified with two or more peptides (data not shown). The resulting nanoUPLC-MS^E protein and peptide data generated by PLGS process are shown in Supplementary Figures 2 & 3. The experiments resulted in 2938 and 2237 identified peptides; 55 and 59% were obtained from peptide match-type data in the first pass to control and zinc deprivation conditions, respectively, and 16% were obtained in the second pass in both conditions (Supplementary Figure 2). A total of 14% of the peptides were identified by a missed trypsin cleavage in both experimental conditions, whereas in source fragmentation rates of 4 and 1% were obtained to control and zinc deprivation, respectively (Supplementary Figure 2). The results obtained from dynamic range detection are presented in Supplementary Figure 3. This graphic represents the concentration of proteins identified in their detection range.

Subcellular localization of *P. lutzii* membrane proteins

The identified proteins in the whole membrane system in number of 746 were evaluated regarding to the subcellular localization using the cellular component information of GO and WoLF PSORT softwares (Supplementary Table 1). The proteins were present in at least two replicates, to be included in the analysis (data not shown). *In silico* analysis revealed that 27.61% (206 proteins) of the identified proteins are presumably not present in membranes, but located in the cytoplasmic region; 25.2% (188 proteins) of the identified proteins were present in membranes, including plasma membrane, mitochondria, endoplasmic reticulum, Golgi complex, peroxisome and vacuole; 24.66% (184 proteins) were presumably inside mitochondria (Supplementary Figure 4).

Proteins in the whole membrane system of *P. lutzii*

The criteria for considering proteins as associated with membranes were the presence of transmem-

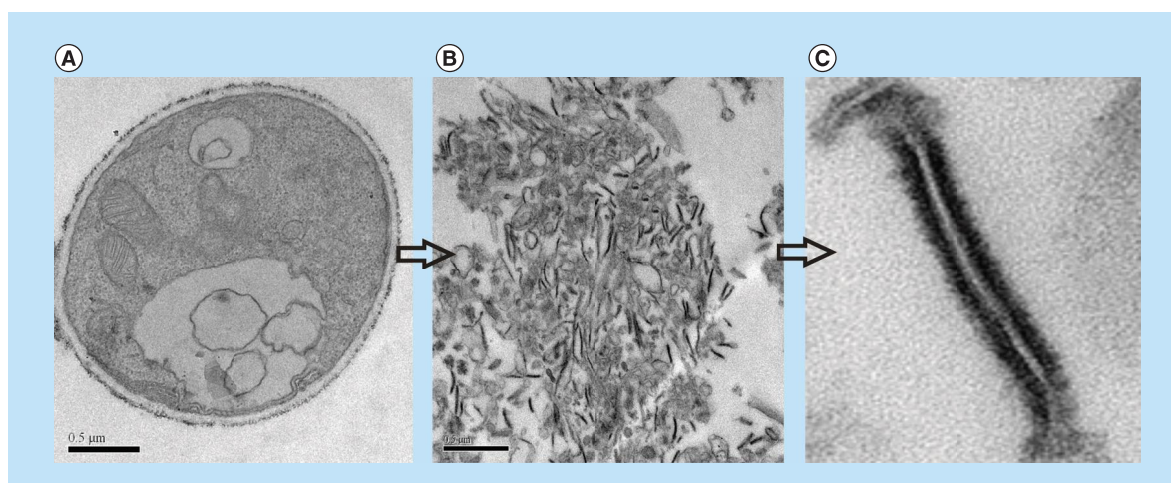


Figure 1. Transmission electron microscopy of *Paracoccidioides lutzii*, whole membranes system fraction. (A) Intact cells of *P. lutzii*. (B) Membranes extract. (C) Fragment of membrane, evidencing the lipid bilayer (increase of 40,000 times).

brane domains and post-transcriptional modifications (prenylation, myristoylation, palmitoylation and GPI anchor). In addition, proteins described in GO terms as belonging to cell membranes with score higher than 50 were classified as membrane proteins. From the total of 746 identified proteins (Supplementary Table 1), 25.2% (188 proteins) were classified as belonging to the membranes of *P. lutzii* (Supplementary Table 2).

Regarding to the 188 proteins identified as members of the membranes in yeast cells of *P. lutzii*, we analyzed the type of cellular membrane that they belong to. According to Loctree software annotations, the identified membrane proteins originated from various organelles, and this finding confirms the ability of the used method to access all cellular membranes. According to our data depicted in Supplementary Figure 5, from the whole membrane system, 38% (71 proteins) represent mitochondrial membrane proteins, 24% (46 proteins) and 16% (30 proteins) represent endoplasmic reticulum and plasma membrane proteins, respectively. Besides, Golgi complex membrane proteins represent 5% (10 proteins), vacuole membrane proteins comprise 3% (6 proteins) and nucleus membrane proteins represent 2% (4 proteins). Some proteins exhibited transmembrane domains or post-translational modifications such as prenylation and myristoylation, although they were not classified by the Loctree software. Table 1 depicts the ten most abundant membrane proteins in this study. Those proteins are present in membranes of different organelles such as mitochondria, peroxisome, endoplasmic reticulum and plasma membrane.

Supplementary Table 3 shows the cell membranes in which proteins are localized. Proteins present at the plasma membrane of yeast cells were represented by

those with known functions, such as plasma membrane ATPase (PAAG_08082), chitin synthase B (PAAG_03391), osmosensor protein (PAAG_04025), a zinc transporter (PAAG_00105) of the Zip family, as well as by proteins with unknown functions. The proteins associated with the endoplasmic reticulum comprise in high number enzymes of the protein glycosylation pathway. Nevertheless, proteins with known mitochondrial localization and functions were detected, such as those involved in import of proteins, enzymes of the electron transport chain and of ATP synthesis. Proteins involved in vesicles transport present in Golgi apparatus were identified, such as ADP ribosylation factor (PAAG_07702), SNARE Ykt6 (PAAG_01588). Furthermore, proteins involved in transport in vacuole and peroxisomes were also identified.

As summarized in Supplementary Table 3, eight proteins present in the endoplasmic reticulum and one Golgi membrane protein were involved in protein glycosylation. Oligosaccharyltransferase (PAAG_04719/PAAG_01037) represented with two subunits in the proteome of the endoplasmic reticulum membrane, catalyzes the initial step of N-glycosylation, with the transfer of N-glycan precursor to nascent polypeptide [53]. In addition, calnexin (PAAG_07037), a protein involved in the correct folding of glycoproteins in mammalian cells [54] and fungus [55], was identified as well. The addition of the outer chain to the N-linked core oligosaccharide at Golgi is performed by mannosyltransferases; two α -1,2-mannosyltransferases (PAAG_02462/PAAG_07238) were found in membranes of the endoplasmic reticulum and Golgi, as depicted in Supplementary Table 3. In addition, dolichol phosphate mannosyltransferases (PAAG_01874), which perform protein N-glycosylation/O-glyco-

Table 1. The most abundant membrane proteins.

Accession number [†]	Protein identification [*]	Score protein [§]	fmol	TMH [#]	PTM ^{††}	SignalP score ≥ 0.5 ^{**}
PAAG_08620	ADP ATP carrier protein 310 aa	28,165	1955.942	3	-	-
PAAG_08082	Plasma membrane ATPase 930 aa	27,274.75	1292.34	9	-	-
PAAG_07564	Outer mitochondrial membrane protein porin 285 aa ^{§§}	17,746.9	601.808	-	-	-
PAAG_00850	Glucosamine fructose 6 phosphate aminotransferase 489 aa ^{§§}	16,121.64	527.8133	-	-	-
PAAG_00481	Membrane biogenesis protein Yop1 171 aa	11,930.6	449.3233	3	-	-
PAAG_04838	ATP synthase subunit 4 245 aa ^{§§}	13,824.06	372.026	-	-	-
PAAG_04570	ATP synthase D chain mitochondrial 175 aa ^{§§}	3393.7	388.8589	-	-	-
PAAG_05350	Mitochondrial phosphate carrier protein 422 aa ^{§§}	5905.8	335.2175	-	-	-
PAAG_08028	GTP-binding protein ypt1 202 aa	25,168.0	448.6622	-	C:20	-
PAAG_02265	Mitochondrial F1F0 ATP synthase subunit 102 aa	14,358.8	295.1655	1	-	-

^{††}Accession number and description of protein according to database of *Paracoccidioides* spp. (www.broadinstitute.org/annotation/genome/paracoccidioides_brasiliensis/MultiHome.html).
[§]Protein score obtained from MS data using the PLGS.
^{||}Quantification of membrane proteins according to internal standard.
^{*}Represents the amount of transmembrane domains identified in proteins using the program TMHMM version 2.0 (www.cbs.dtu.dk/services/TMHMM/).
^{††}Indicates the presence of post-translational modification. The program Terminator (www.isv.cnrs.fr/terminator3/test.php) and Myristoylator (<http://web.expasy.org/myristoylator/>) were employed in search for myristoylated proteins. To search for palmitoylated proteins was performed with the program Terminator (www.isv.cnrs.fr/terminator3/test.php). For identification of prenylated proteins, the program was the PrePS (<http://mendel.imp.ac.at/sat/PrePS/index.html>). The prediction for GPI anchor was performed with the program big-PI fungi predictor (http://mendel.imp.ac.at/gpi/fungi_server.html). C:14 and C:16 indicate the presence of a myristoyl or palmitoyl group in the protein, respectively. C:15 indicates the presence of a recognition site to the addition of a farnesyl group by the enzyme FT and C:20 indicates the presence of a recognition site to addition of a geranyl group by the enzyme GGT1 or a site recognition for addition of a geranyl group by the enzyme GGT2. GPI represents the presence of a GPI anchor in protein.
^{**}The program SignalP version 4.0 (www.cbs.dtu.dk/services/SignalP/) was employed in the search for signal peptide. The values demonstrate the score protein with signal peptide. The D-Score must be higher or equal to the value of (0.05).
[#]In all cases, the symbol represents absence in the analyzed category.
[§]The functional classification was performed using the database of FunCat2 (http://pedant.gsf.de/pedant3htmlview/pedant3view?Method=analysis&Db=p3_48325_Par_brazi_Pb01). The database GO using the information relative to cellular component was employed to evaluate the possible localization of proteins in cell membranes of *Paracoccidioides* sp.
^{§§}Some proteins did not show any form of classical association with the lipid bilayer, but they presented the subcellular localization in GO as belonging to the membrane with score ≥ 50 .
[†]FT: Farnesyltransferase; GGT1: Geranylgeranyltransferase; GGT2: Rab Geranylgeranyltransferase; GO: Gene ontology; GPI: Lipid anchor modified; GTP: Guanosine triphosphate; PI: Big-PI fungi database; PLGS: ProteinLynx Global Server; PrePS: Prenylation Prediction Suite; PTM: Post-translational modification; TMH: Transmembrane helices.

sylation [56], and members of this family were also detected in this study. Proteins related to the glycosylation pathway, such as α -1,2-mannosyltransferase (*kre5p*, *ktr4*), mannosyltransferases (PMTs), *Stt3p* and calnexin [57], were also identified in the membrane proteome of *A. fumigatus*.

Regulation of *P. lutzii* membrane proteins by zinc

Proteomic membrane analyses revealed that whole membrane system proteins alter their abundance in response to different stress conditions [30,58]. Therefore, we investigated zinc regulation of membrane proteins in yeast cells grown upon zinc deficiency. Previous studies demonstrated a remodeling of *P. lutzii* metabolism in response to oxidative stress induced during zinc deprivation [19]. A 1.5-fold change was used as a threshold to determine the up- and down-regulated membrane proteins under zinc deprivation. A total of 115 proteins, corresponding to 60.85% of the classified membrane proteins, depicted in Supplementary Table 2, were downregulated upon zinc deprivation (Supplementary Table 4). Eighty one of those proteins were not detectable in the membranes of yeast cells deprived of zinc, only in the control. The functional classification of downregulated membrane proteins revealed that most of them in a percentage of 31% (36 proteins) were involved in transport events (Figure 2). Of special note, proteins of mitochondrial membrane functionally related to electron transport and oxidative phosphorylation were downregulated, suggesting that energy production by the respiratory chain was inhibited during zinc deprivation. Additionally, the glycosylation of proteins seems to be affected by zinc deprivation, as demonstrated by the downregulation of several enzymes/proteins involved in the process (Supplementary Table 4).

Eighteen proteins corresponding to 9.52% of those classified as belonging to membranes were upregulated upon zinc deprivation (Supplementary Table 5). Sixteen of those proteins were only identified upon zinc deprivation. A total of 56% (10 proteins) of the 18 proteins were involved in transport events and 6% (1 protein) was involved in protein fate (Figure 2).

The classification of regulated proteins, according to the predicted membranes they belong to, is presented in Supplementary Figure 6. It was observed that 43% (49 proteins) of the downregulated membrane proteins are predicted to be mitochondrial, followed by endoplasmic reticulum 30% (34 proteins) and plasma membrane 15% (17 proteins). Among the upregulated proteins, 28% (5 proteins) were predicted as belonging mainly to mitochondrial membrane and 22% (4 proteins) to plasma membrane.

Modification of *P. lutzii* yeast cell wall upon zinc deprivation

Chitin, glucans, lipids and proteins are the main constituents of the cell walls of mycelium and yeast forms of *Paracoccidioides* spp. [59,60]. Proteomic analysis revealed that proteins involved in the deposit of chitin in the cell wall, such as chitin synthase B (PAAG_03391) [61] and phosphoinositide phosphatase Sac1 (PAAG_03162) [62], were downregulated under zinc deprivation. Moreover, the enzyme 1-acyl-*sn*-glycerol-3-phosphate acyltransferase- β (1-AGPAT; PAAG_07503), involved in production of phospholipids, cell wall constituents of *Paracoccidioides* spp. [63], was also downregulated at zinc-limited conditions. Therefore, fluorescence microscopy was performed in order to investigate changes in the cell wall using the fluorophore CFW that binds specifically the chitin present in the cell wall. As shown in Figure 3A, fluorescence of cell wall in zinc-deprived cells decreased when compared with the control. Quantitative analyzes of the fluorescence intensity (in pixels) of cells growing in the presence and absence of zinc, demonstrated a significant decrease of the fluorescence in cells under zinc deprivation ($p < 0.05$; Figure 3B).

Zinc availability modulates glycosylation events

Several proteins of endoplasmic reticulum involved in events of glycosylation were downregulated during zinc deprivation. It includes dolichyl-phosphate-mannose-protein mannosyltransferase (PAAG_05910/PAAG_04725), α -1,2-mannosyltransferase KTR1 (PAAG_07238) and dolichyl-di-phosphooligosaccharide-protein glycotransferase (PAAG_04110). Staining with Schiff periodic acid allows the detection of glycoproteins, through the oxidation reaction between the periodic acid and the glycoproteins. Thus, the intensity of color depends on the number and the nature of sugar moieties bound to the glycoprotein [64]. Under zinc deficiency, the intensity of Schiff staining was lower when compared with the control, as depicted in Figure 4A. The use of ConA conjugated to FITC revealed a significant decrease in the fluorescence of *P. lutzii* cells after zinc deprivation, as depicted in Figure 4B & C. ConA is a lectin that specifically binds glucan and mannan moieties [65]. Additionally, the use of aniline blue which selectively stains cell β -(1,3) glucan [52], did not show any difference on fluorescence in cells cultured in the presence or absence of zinc (Figure 5). In this way, the reduction of protein glycosylation is probably a result of the stress caused by zinc deprivation and not a consequence of a reduced amount of glucans.

Discussion

In the whole membrane proteome of *P. lutzii*, obtained with the use of sodium carbonate pH 11

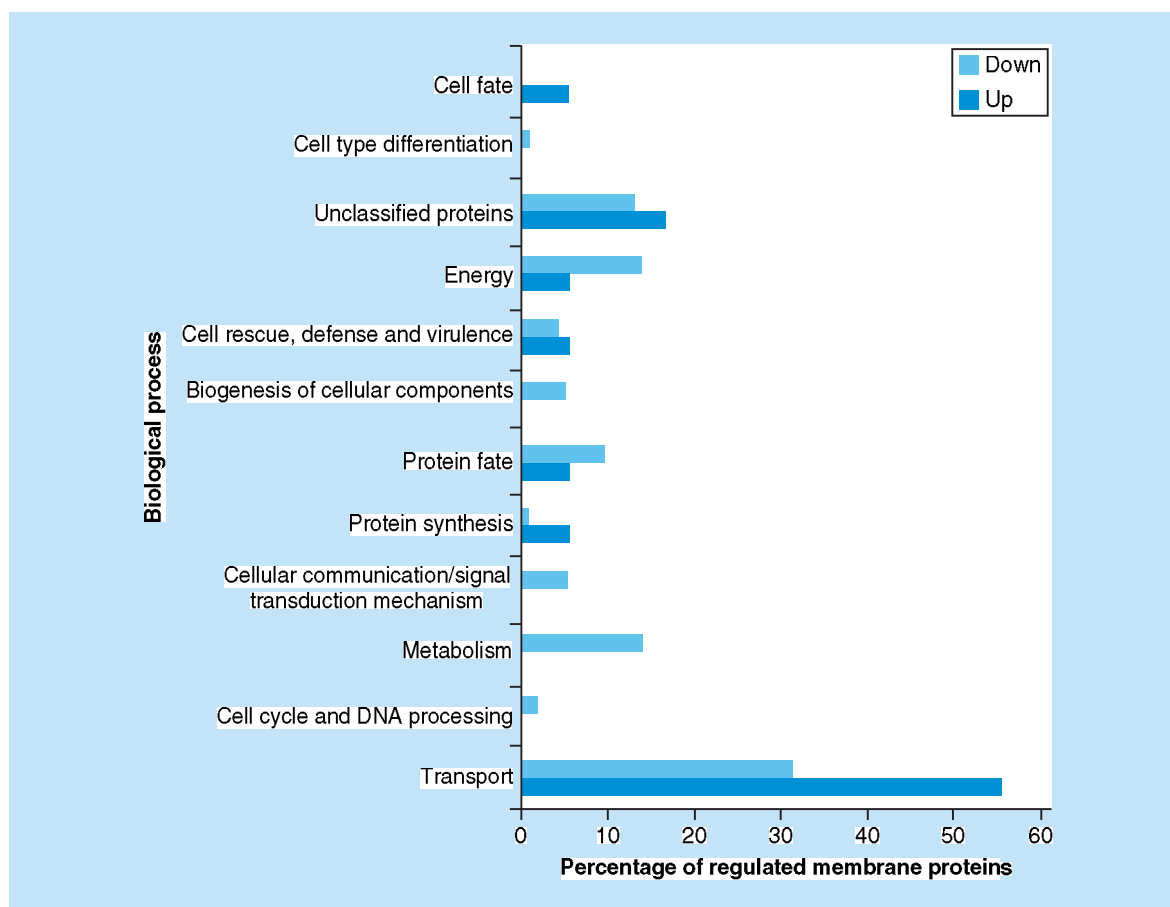


Figure 2. Functional classification of membrane proteins regulated by zinc availability. The database FunCat2 was used to perform this classification. Light gray bars represent downregulated proteins and dark gray bars represent upregulated proteins. Proteins upregulated: Transport – 56% (10 proteins), Cell cycle and DNA processing – 0% (0 protein), Metabolism – 0% (0 protein), Cellular communication – 0% (0 protein), Protein synthesis – 6% (1 protein), Protein fate – 6% (1 protein), Biogenesis of cellular components – 0% (0 protein), Cell rescue – 6% (1 protein), Energy – 6% (1 protein), Unclassified – 17% (3 proteins), Cell-type differentiation – 0% (0 protein), Cell fate – 6% (1 protein). Proteins downregulated: Transport – 31% (36 proteins), Cell cycle and DNA processing – 2% (2 proteins), Metabolism – 14% (16 proteins), Cellular communication – 5% (6 proteins), Protein synthesis – 1% (1 protein), Protein fate – 10% (11 proteins), Biogenesis of cellular components – 5% (6 proteins), Cell rescue – 4% (5 proteins), Energy – 14% (16 proteins), Unclassified – 13% (15 proteins), Cell-type differentiation – 1% (1 protein), Cell fate – 0% (0 protein).

and ultracentrifugation, 188 proteins were described (Supplementary Table 2). Literature search and *in silico* analyses revealed proteins associated with different cell membranes. When cells are lysed in an aqueous environment, the cell-limiting membrane and membranes of organelles may fragment and form vesicles that can be separated from the cytosol by partitioning or sedimentation. However, cytoplasmic proteins may be entrapped in vesicles formed after cell lysis. Thus, in order to get a true membrane protein extract, steps employing solutions, such as sodium carbonate, are used to remove proteins that do not show a strong association with membranes [25,30,66]. The use of sodium carbonate pH 11 has been described in the literature as a tool to obtain membrane proteins. Analysis of whole membrane system proteome of pathogenic and

nonpathogenic microorganisms, such as *Escherichia coli* [67], *Bordetella pertussis* [30] and *S. cerevisiae* [58], employing sodium carbonate pH 11 and steps of ultracentrifugation, allowed the identification of several membrane proteins. The success of the technique utilized for obtaining *P. lutzii* membrane proteins can be evaluated by comparing our data to those in the literature. In analyses of plasma membrane proteome of *S. cerevisiae* during salt stress, 24% of the identified proteins belong to the plasma membrane while 25 and 33% were represented by ribosomal proteins and proteins from the early secretory pathway belonging to endoplasmic reticulum and Golgi apparatus, respectively [58]. At this work, 25.2% (188 proteins) of the total of identified proteins were predicted as belonging to membranes (Supplementary Figure 4).

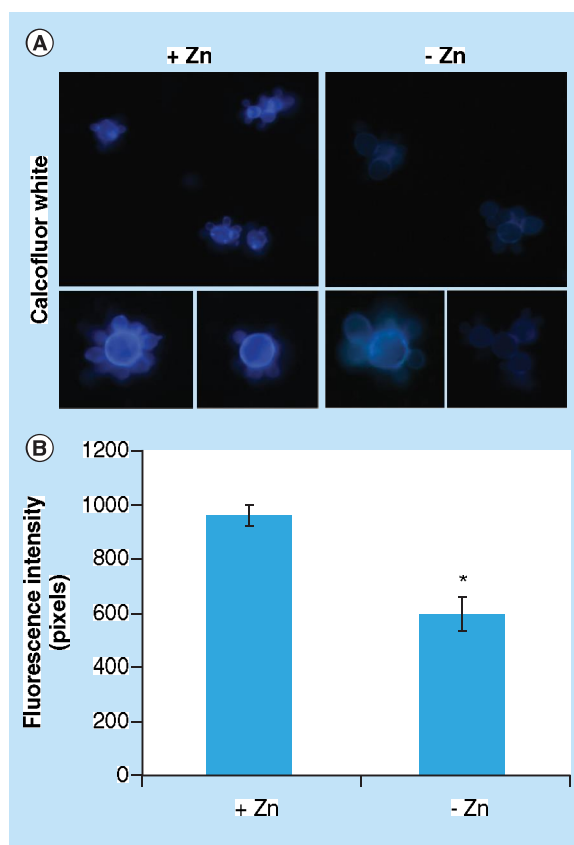


Figure 3. Effect of zinc deprivation in *Paracoccidioides lutzii* yeast cells wall. Yeast cells were cultivated in MMcM medium depleted or supplemented with zinc for 24 h. **(A)** The cells were fixed and stained with CFW (increase of 40 times). **(B)** Fluorescence intensity (in pixels) of the cells under zinc deprivation. The AxioVision Software (Carl Zeiss) was used to obtain the values of fluorescence intensity. The values of fluorescence intensity and the standard error of each analysis were used to plot the graph. Data are expressed as mean \pm standard error (represented using error bars). * $p \leq 0.05$. CFW: Calcofluor white; MMcM: McVeigh/Morton' liquid medium.

In this study we identified 188 proteins of membranes, and from those, 63.3% (119 proteins) presented at least one transmembrane domain, 9.04% (17 proteins) presented post-translational modifications such as prenylation, myristoylation, palmitoylation, GPI anchor and 9.57% (18 proteins) presented signal peptide (Supplementary Table 2). In *C. albicans*, from 214 identified proteins in a preparation of plasma membrane, 47.66% (102 proteins) showed at least one transmembrane domain and 13.55% (29 proteins) presented signal peptide [68]. Comparing the data, it is possible to see that the forms of association with cell membranes approximate to the number found in this work.

In this work, membrane proteins involved in synthesis or maintenance of cell wall, in glycosylation path-

ways and in the electron transport chain were identified (Supplementary Table 2), similarly to data described in *C. albicans* [68]. Also, the whole membrane proteome of *P. lutzii* includes proteins related to vesicle traffic, such as ADP ribosylation factor (PAAG_07702), SNARE (PAAG_01588). In addition, some proteins were described only in this work compared with *C. albicans* [68] and *A. fumigatus* [57], such as zinc transporter (PAAG_00105), sideroflexin-1 (PAAG_09064) and peroxin (PAAG_08209; Supplementary Table 2). Bioinformatics analyses allowed the identification and classification of membrane proteins, not yet described in some proteomic works.

Some studies with *Paracoccidioides* spp. under metals deprivation allowed the characterization of metabolic and adaptive responses to iron [69] and zinc [19]. Due to the importance of zinc in pathogens survival and in the development of diseases, we evaluated membrane proteins in yeast cells of *P. lutzii* upon deprivation of this metal. Analysis of whole membrane system proteome during zinc deprivation allowed identification of a probable alteration on glycerophospholipid metabolism, as predicted by the regulation of enzymes located in endoplasmic reticulum membrane, such as the 1-AGPAT (PAAG_07503). This enzyme catalyzes the formation of phosphatidic acid (PA) from lysophosphatidic acid by incorporating an acyl moiety at sn-2 position. The PA produced by the 1-AGPAT activity is a substrate of the pathway for production of phospholipids, such as phosphatidylserine (PS), phosphatidylinositol (PI), phosphatidylethanolamine (PE) and phosphatidylcholine (PC), which are present at the cell wall of *S. cerevisiae* [70] and *Paracoccidioides* spp. [63]. Similarly, in *S. cerevisiae*, the activities of the enzymes involved in PS, PE and PC pathways were decreased under zinc deficiency [71]. As PA is the upstream substrate in the synthesis of all those phospholipids, we may suggest that the decreased production of PA by repression of the 1-AGPAT can lead to the reduction in PS, PE and PC levels and possible alterations in cell wall composition. Additionally to the descriptions above, another protein of the endoplasmic reticulum membrane, named Sac1, is involved in structure of cell wall and was downregulated in *P. lutzii* upon zinc deprivation, strongly suggesting modifications in the cell wall structure. Studies in *C. albicans* demonstrated that Sac1-p is related to the cell wall integrity. The deletion of *Sac1* increases the sensitivity to stress of the cell wall and alters the content and distribution of chitin in the mutant [72]. Moreover, chitin synthase B (PAAG_03391), a plasma membrane protein, was also downregulated in this study in the absence of zinc. The reduced level of those proteins possibly alters the quantity of chitin at the cell wall, as depicted in Figure 3.

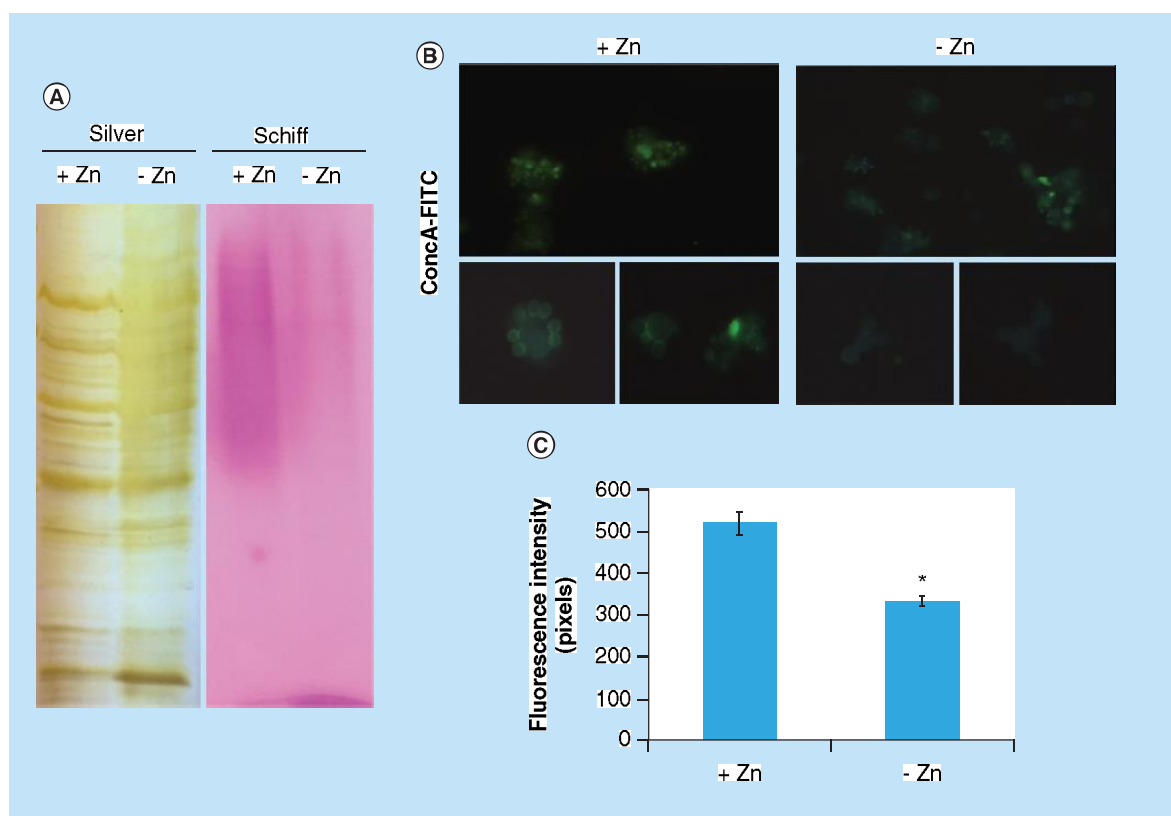


Figure 4. Zinc deprivation alters proteins glycosylation. (A) Protein extracts of membranes were fractionated by electrophoresis and stained with periodic acid Schiff. The same extracts were stained with silver. (B) Fluorescence microscopy of *P. lutzii* cells that were cultured in the presence or absence of zinc for 24 h and subsequently incubated with ConA conjugated to FITC (increase of 40 times). (C) Fluorescence intensity graph. The data for fluorescence intensity evaluation were obtained through the AxioVision Software (Carl Zeiss). The values of fluorescence intensity (in pixels) and the standard error of each analysis were used to plot the graph. Data are expressed as mean \pm standard error (represented using error bars), (*) represents $p \leq 0.05$. ConA: Concanavalin A; FITC: Fluorescein isothiocyanate.

Zinc deprivation repressed proteins present in membranes of organelles such as mitochondria and vacuole, as depicted in Supplementary Table 4. Studies performed with *S. cerevisiae* revealed that the transport of zinc into the vacuole has an ATP-dependent mechanism, requiring an H^+ gradient generated by the V-ATPase. Thus, changes in the proton gradient generated by V-ATPase inhibit zinc uptake by the vacuole [73]. In this work, a vacuolar ATP synthase of 98 kDa (PAAG_02679) was repressed during zinc deprivation. As the vacuole is the main organelle responsible for zinc storage [14], the cells possibly inhibit the storage of this micronutrient in order to try to overcome zinc deprivation, allowing this metal available in the cytoplasm.

Protein glycosylation is the most common post-translational modification in eukaryotic cells. This process occurs by connecting a saccharide unit to a protein and is involved in the maintenance of protein conformation and activity, in protein protection from proteolytic degradation, and in protein intracellular

trafficking and secretion [74]. In studies performed with *Candida albicans*, it was observed that the process of glycosylation is important for cell wall integrity and for host–fungus interactions [75,76]. Also, in *C. albicans*, Hall *et al.* [77] observed that the Mnn2 mannosyltransferase family is related in immune recognition, virulence and cell wall integrity. Based on these facts, the reduction in the level of glycosylated proteins may interfere in the success of infection. In this work, we described downregulated membrane proteins present at the endoplasmic reticulum and Golgi apparatus involved in the process of N-O-glycosylation [57], such as α -1,2 mannosyltransferase KTR1 (PAAG_07238), dolichyl-di-phosphooligosaccharide-protein glycotransferase (PAAG_04110), calnexin (PAAG_07037), oligosaccharyl transferases (PAAG_04719/PAAG_01037). The dolichol-phosphate mannose Dpm1p protein, localized at the endoplasmic reticulum membrane, was downregulated under zinc-limited conditions. Dpm1p synthesizes Dol-P-Man, a compound that serves as mannosyl donor for glycosylation reactions

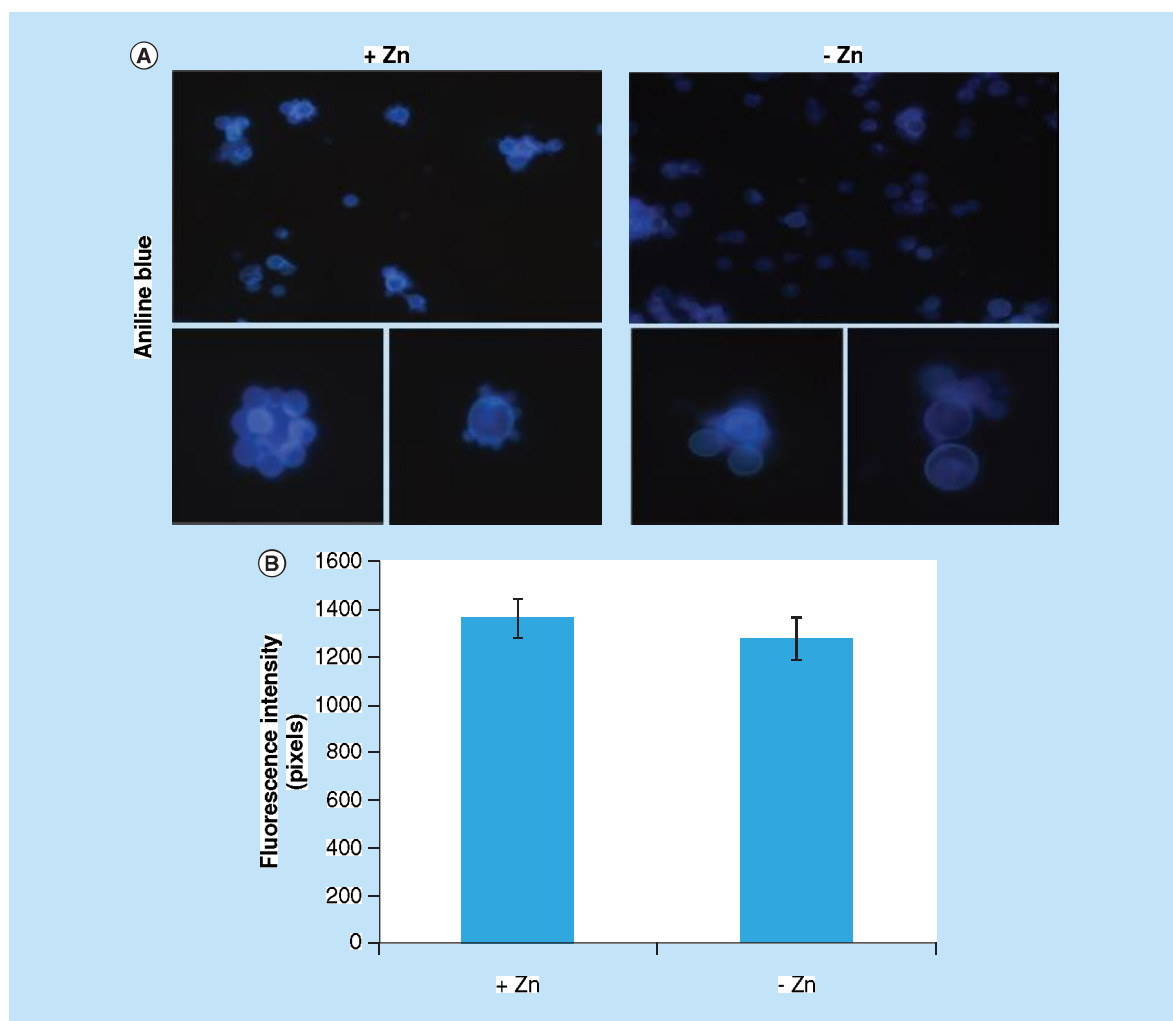


Figure 5. Evaluation of β -1,3 glucan quantities in the cell wall of *Paracoccidioides lutzii*. (A) Aniline blue was used to evaluate, by fluorescence microscopy, the presence of β -1,3 glucan in the cell wall of *P. lutzii* after growth in the presence and absence of zinc (increase of 40 times). (B) Fluorescence intensity graph. The values of fluorescence intensity (in pixels) and the standard error of each analysis were used to plot the graph. Data are expressed as mean \pm standard error (represented using error bars).

in the endoplasmic reticulum lumen [78]. We suggest that repression of those proteins upon zinc deprivation affects the glycosylation process in the endoplasmic reticulum in *P. lutzii* and, consequently, the profile of glycosylated proteins is less evident under zinc deprivation (Figure 4). Furthermore, the aniline blue staining confirmed that the reduction of protein glycosylation is not a consequence of a reduced amount of glucans (Figure 5), but probably a result of the stress caused by zinc deprivation. Furthermore, the deletion of genes encoding proteins of the N-glycosylation pathway, such as α -glucosidase-I and O-Mannosyltransferases, in *A. fumigatus* and *S. pombe* resulted in abnormalities in the cell wall [79–81]. We hypothesized that the repression of proteins involved in the glycosylation pathway in *P. lutzii* during zinc deprivation contributes to changes in the cell wall organization in this fungus.

Another response to zinc deprivation identified in this work was at the mitochondrial membrane level. Part of the energy used by cells is obtained during the process of oxidative phosphorylation that occurs in the inner mitochondrial membrane. Electrons generated in glycolysis and tricarboxylic acid cycle are used during energy achievement. A study with *S. cerevisiae* revealed that zinc deficiency leads to increased oxidative stress [82]. *Aspergillus niger* submitted to long-term oxidative stress reduces glucose uptake [83] and induces enzymes involved in the gluconeogenesis pathway. Parente *et al.* [19] observed that *P. lutzii* yeast cells cultivated for 24 h under zinc deprivation also induce gluconeogenesis. Furthermore, Gupta *et al.* [84] found that the tricarboxylic acid cycle had decreased activity when *Aspergillus parasiticus* is cultured in medium with zinc deficiency. In the present study, we observed that

proteins of oxidative phosphorylation were downregulated upon zinc deficiency (Supplementary Table 4). Additionally, the mitochondrial inner membrane Sco1 protein (PAAG_06668) [85], which is essential for cytochrome oxidase assembly [86], was also repressed during zinc deficiency in *P. lutzii*, corroborating previous data that pointed to a metabolism shift in *P. lutzii* upon zinc deficiency.

Proteins associated with traffic of vesicles were regulated by zinc, as well. GTP-binding proteins play a role in vesicle traffic through a cycle of GTP-binding and hydrolysis. GTP-binding proteins present at the surface of carrier vesicles are responsible for the delivery of these structures to the appropriate acceptor compartment. The presence of Rab-GTPases GTP-bound (active) and GDP-bound (inactive) form is mediated by interaction with regulatory proteins. The active form of Rabp proteins interacts with Rab effectors and GTPase-activating proteins and in inactive form, these proteins are recognized by guanine nucleotide exchange factors [87]. The Rab GDP-dissociation inhibitor protein (PAAG_06344) of *P. lutzii* was upregulated upon zinc deprivation (Supplementary Table 5). Its homolog Gdi1p, from *S. cerevisiae* induces the inhibition of GDP dissociation from Sec4p. A reversible modification of either Sec4p or Gdi1p would cause a dissociation of this complex, allowing attachment of Sec4p to a new vesicle [88]. The upregulation of Rab GDP-dissociation inhibitor in membrane proteome during zinc deprivation, here described, may induce the formation of a soluble inactive complex between Rabp and Sec4p proteins and, consequently, the presence of this complex could decrease the binding of Sec4 to new vesicles during zinc deprivation. The protein homolog to Sec4p, the GTP-binding protein SAS1 (PAAG_01500) was downregulated. The repression of those proteins may be associated with induction of Rab GDP-dissociation inhibitor protein and formation of complex Rabp/Sec4p, and consequently suppression on the traffic of vesicles under zinc limitation.

Upon microbial infection, the host sequesters zinc from either extra- and intracellular compartments [89,90] in order to limit microorganisms growth and proliferation. Considering this perspective, the use of zinc chelators during infection treatment may be suggested. Laskaris *et al.* [91] showed that mice infected with *A. fumigatus* had survival improved with administration of zinc-chelating agents in monotherapy and in combination with the antifungal caspofungin. Also, the use of metal chelators has been well documented in respect of iron [92–94]. As demonstrated here and also by Parente *et al.* [19], zinc plays a role in essential processes that contribute to the maintenance of *P. lutzii*

physiology. Taking this fact into account, the use of agents able to sequester this metal, alone or together with antifungals, may be an alternative in paracoccidioidomycosis treatment.

Conclusion & future perspective

The development and advance of strategies of treatment in the field of infectious diseases are based on the knowledge of a microorganism's physiology and metabolism. Information of pathogen behavior in situations that mimic conditions found in the host are valuable, since they can be used as guides in the definition of targets for treatment. To our knowledge, this is the first report that describes whole membrane system proteome and the response of *P. lutzii* to micronutrient starvation at the membrane proteome level. Identification of total membrane proteome of a member of the genus *Paracoccidioides* provides a starting point for future studies on functional analysis. Protein glycosylation and chitin content at the cell wall, both processes important in host–fungus interaction, were decreased under zinc deprivation, a condition found in the host. These and other metabolic changes described in this study may contribute to the arsenal of targets used in the development of new drugs in the future. Additionally, the establishment of a protocol for *Paracoccidioides* spp. membrane protein extraction opens new possibilities for the understanding of fungus biology.

Financial & competing interests disclosure

This work was supported by grants from Conselho Nacional de Desenvolvimento Científico e Tecnológico (CNPq) and Fundação de Amparo à Pesquisa do Estado de Goiás (FAPEG) – Instituto Nacional de Ciência e Tecnologia (INCT) de Estratégias de Interação Patógeno Hospedeiro (IPH) and Fundo Newton. JS de Curcio and MG Silva are fellows from Coordenação de Aperfeiçoamento de Pessoal de Nível Superior (CAPES) and CNPq, respectively. The authors have no other relevant affiliations or financial involvement with any organization or entity with a financial interest in or financial conflict with the subject matter or materials discussed in the manuscript apart from those disclosed.

No writing assistance was utilized in the production of this manuscript.

Author contributions

CMA Soares, JS de Curcio and MG Silva conceived and designed the experiments. JS de Curcio, MG Silva and L Casaletti performed the experiments. JS de Curcio, MG Silva, MGS Bailão, AM Bailão and CMA Soares analyzed and/or interpreted the data. SN Bão and CMA Soares contributed to reagents and materials. JS de Curcio, MG Silva and CMA Soares wrote the manuscript.

Open access

This work is licensed under the Creative Commons Attribution

4.0 License. To view a copy of this license, visit <http://creativecommons.org/licenses/by/4.0/>

Summary points

- This was the first work describing the whole membrane proteins of the pathogenic fungus *Paracoccidioides lutzii* and its regulation in a condition that mimics that found in the host.
- In this study, employing a methodology for extracting membrane proteins and nanoUPLC-MS^E, 188 proteins from the membrane system were identified.
- Under conditions of zinc deprivation, membrane proteins are regulated. In general, this stress alters several cellular processes carried out by proteins such as glycosylation, energy production, storage of zinc in vacuoles and vesicle traffic.
- Proteomic data revealed that membrane proteins involved in cell wall synthesis were repressed by zinc deprivation. This finding was confirmed by fluorescence microscopy. The cell wall is essential for the contact of the pathogen with the host.
- The data of this article allowed the characterization of the membrane proteins of *P. lutzii* in response to stress mediated by zinc deprivation.

References

Papers of special note have been highlighted as: • of interest;

•• of considerable interest

- 1 Restrepo AM. The ecology of *Paracoccidioides brasiliensis*: a puzzle still unsolved. *Sabouraudia J. Med. Vet. Mycol.* 23(5), 323–334 (1985).
- 2 San-Blas G, Niño-Vega G, Iturriaga T. *Paracoccidioides brasiliensis* and paracoccidioidomycosis: molecular approaches to morphogenesis, diagnosis, epidemiology, taxonomy and genetics. *Med. Mycol.* 40(3), 225–242 (2002).
- 3 McEwen JG, Bedoya V, Patino MM, Salazar ME, Restrepo A. Experimental murine paracoccidioidomycosis induced by the inhalation of conidia. *J. Med. Vet. Mycol.* 25(3), 165–175 (1987).
- 4 Shikanai-Yasuda MA, Telles FD, Mendes RP, Colombo AL, Moretti ML, Paracoccidioidomycose G. Guidelines in paracoccidioidomycosis. *Rev. Soc. Bras. Med. Trop.* 39(3), 297–310 (2006).
- 5 Van Ho A, Ward DM, Kaplan J. Transition metal transport in yeast. *Annu. Rev. Microbiol.* 56, 237–261 (2002).
- 6 Eide DJ. Multiple regulatory mechanisms maintain zinc homeostasis in *Saccharomyces cerevisiae*. *J. Nutr.* 133(5 Suppl. 1), S1532–S1535 (2003).
- **Reports the mechanisms of zinc uptake in different organelles and the importance of this metal in cell homeostasis.**
- 7 Zhao H, Eide D. The yeast *ZRT1* gene encodes the zinc transporter protein of a high-affinity uptake system induced by zinc limitation. *Proc. Natl Acad. Sci. USA* 93(6), 2454–2458 (1996).
- **Reports the high-affinity transporter induced during zinc deprivation.**
- 8 Zhao H, Eide D. The *ZRT2* gene encodes the low affinity zinc transporter in *Saccharomyces cerevisiae*. *J. Biol. Chem.* 271(38), 23203–23210 (1996).
- 9 Zhao H, Eide DJ. Zap1p, a metalloregulatory protein involved in zinc-responsive transcriptional regulation in *Saccharomyces cerevisiae*. *Mol. Cell. Biol.* 17(9), 5044–5052 (1997).
- 10 Gitan RS, Luo H, Rodgers J, Broderius M, Eide D. Zinc-induced inactivation of the yeast ZRT1 zinc transporter occurs through endocytosis and vacuolar degradation. *J. Biol. Chem.* 273(44), 28617–28624 (1998).
- 11 Rutherford JC, Bird AJ. Metal-responsive transcription factors that regulate iron, zinc, and copper homeostasis in eukaryotic cells. *Eukaryot. Cell* 3(1), 1–13 (2004).
- 12 Wu YH, Frey AG, Eide DJ. Regulation of the Zrg17 zinc transporter in the yeast secretory pathway. *Biochem. J.* 435(1), 259–266 (2011).
- 13 Ellis CD, Wang F, MacDiarmid CW, Clark S, Lyons T, Eide DJ. Zinc and the Msc2 zinc transporter protein are required for endoplasmic reticulum function. *J. Cell Biol.* 166(3), 325–335 (2004).
- 14 Ramsay LM, Gadd GM. Mutants of *Saccharomyces cerevisiae* defective in vacuolar function confirm a role for the vacuole in toxic metal ion detoxification. *FEMS Microbiol. Lett.* 152, 293–298 (1997).
- 15 MacDiarmid CW, Gaither LA, Eide D. Zinc transporters that regulate vacuolar zinc storage in *Saccharomyces cerevisiae*. *EMBO J.* 19(12), 2845–2855 (2000).
- 16 Eide DJ. Zinc transporters and the cellular trafficking of zinc. *Biochim. Biophys. Acta* 1763(7), 711–722 (2006).
- **Reports the trafficking of zinc and transporters involved in this process.**
- 17 Silva MG, Schrank A, Bailão EFLC *et al.* The homeostasis of iron, copper, and zinc in *Paracoccidioides brasiliensis*, *Cryptococcus neoformans var. Grubii*, and *Cryptococcus gattii*: a comparative analysis. *Front. Microbiol.* 2, 1–19 (2011).
- **Describes the genes involved in homeostasis of micronutrients in the fungi: *Paracoccidioides* spp. and *Cryptococcus* spp.**
- 18 Bailão EFLC, Parente AFA, Parente JA *et al.* Metal acquisition and homeostasis in fungi. *Curr. Fungal Infect. Rep.* 6(4), 257–266 (2012).
- **Describes the mechanisms of micronutrients acquisition in fungi and the iron sources in the host.**

- 19 Parente AFA, de Rezende TCV, de Castro KP *et al.* A proteomic view of the response of *Paracoccidioides* yeast cells to zinc deprivation. *Fungal Biol.* 117(6), 399–410 (2013).
- **Reports the regulation of expression of cytoplasmatic proteins during zinc deprivation in *Paracoccidioides*.**
- 20 Bailão AM, Schrank A, Luiz C *et al.* Differential gene expression by *Paracoccidioides brasiliensis* in host interaction conditions: representational difference analysis identifies candidate genes associated with fungal pathogenesis. *Microbes Infect.* 8(12-13), 2686–2697 (2006).
- 21 Bailão AM, Schrank A, Borges CL *et al.* The transcriptional profile of *Paracoccidioides brasiliensis* yeast cells is influenced by human plasma. *FEMS Immunol. Med. Microbiol.* 51(1), 43–57 (2007).
- **Reports the induction of high-affinity zinc transporter after incubation with human plasma.**
- 22 Ephritikhine G, Ferro M, Rolland N. Plant membrane proteomics. *Plant Physiol. Biochem.* 42(12), 943–962 (2004).
- 23 Tan S, Hwee TT, Chung MCM. Membrane proteins and membrane proteomics. *Proteomics* 8(19), 3924–3932 (2008).
- 24 Wallin E, von Heijne G. Genome-wide analysis of integral membrane proteins from eubacterial, archaean, and eukaryotic organisms. *Protein Sci.* 7(4), 1029–1038 (1998).
- 25 Santoni V, Molloy M, Rabilloud T. Membrane proteins and proteomics: an amour impossible? *Electrophoresis* 21(6), 1054–1070 (2000).
- 26 Hopff D, Wienkoop S, Lüthje S. The plasma membrane proteome of maize roots grown under low and high iron conditions. *J. Proteomics* 91, 605–618 (2013).
- 27 Rucevic M, Hixson D, Josic D. Mammalian plasma membrane proteins as potential biomarkers and drug targets. *Electrophoresis* 32(13), 1549–1564 (2011).
- 28 Fava-Netto C. Estudos quantitativos sobre fixação de complemento na blastomicose sul americana, com antígeno polissacarídico. *Arq. Cir. Clin. Exp.* 18, 197–254 (1955).
- 29 Restrepo A, Jimenez BE. Growth of *Paracoccidioides brasiliensis* yeast phase in a chemically defined culture medium. *J. Clin. Microbiol.* 12(2), 279–281 (1980).
- 30 Vidakovic MLP, Paba J, Lamberti Y, Andre C, De Sousa MV, Rodriguez ME. Profiling the *Bordetella pertussis* proteome during iron starvation research. *J. Proteome Res.* 6, 2518–2528 (2006).
- **Reports the methodology of membrane proteins extraction and their regulation by iron.**
- 31 Da Fonseca CA, Jesuino RSA, Felipe MS, Cunha DA, Brito WA, Soares CMA. Two-dimensional electrophoresis and characterization of antigens from *Paracoccidioides brasiliensis*. *Microbes Infect.* 3(7), 535–542 (2001).
- 32 Barbosa SM, Bão SN, Andreotti PF *et al.* Glyceraldehyde-3-phosphate dehydrogenase of *Paracoccidioides brasiliensis* is a cell surface protein involved in fungal adhesion to extracellular matrix proteins and interaction with cells. *Infect. Immun.* 74(1), 382–389 (2006).
- 33 Bradford M. A rapid and sensitive method for the quantification of microgram quantities of protein utilizing the principle of protein-dye binding. *Anal. Biochem.* 72, 248–254 (1976).
- 34 Murad AM, Souza GHMF, Garcia JS, Rech EL. Detection and expression analysis of recombinant proteins in plant-derived complex mixtures using nanoUPLC-MSE. *J. Sep. Sci.* 34(19), 2618–2630 (2011).
- 35 Geromanos SJ, Vissers JPC, Silva JC *et al.* The detection, correlation, and comparison of peptide precursor and products from data independent LC-MS with data dependant LC-MS/MS. *Proteomics* 9(6), 1683–1695 (2009).
- 36 Curty N, Kubitschek-Barreira PH, Neves GW *et al.* Discovering the infectome of human endothelial cells challenged with *Aspergillus fumigatus* applying a mass spectrometry label-free approach. *J. Proteomics* 97, 126–140 (2014).
- 37 Silva JC. Absolute quantification of proteins by LCMSE: a virtue of parallel MS acquisition. *Mol. Cell. Proteomics* 5(1), 144–156 (2006).
- 38 Silva JC, Denny R, Dorschel CA *et al.* Quantitative proteomic analysis by accurate mass retention time pairs. *Anal. Chem.* 77(7), 2187–2200 (2005).
- 39 Murad AM, Rech EL. NanoUPLC-MSE proteomic data assessment of soybean seeds using the Uniprot database. *BMC Biotechnol.* 12(1), 82 (2012).
- 40 Laird NM, Horvath S, Xu X. Implementing a unified approach to family-based tests of association. *Genet. Epidemiol.* 19(Suppl. 1), S36–S42 (2000).
- 41 Horton P, Park KJ, Obayashi T *et al.* WoLF PSORT: protein localization predictor. *Nucleic Acids Res.* 35(Suppl. 2), 585–587 (2007).
- 42 Frishman D, Mokrejs M, Kosykh D *et al.* The PEDANT genome database. *Nucleic Acids Res.* 31(1), 207–211 (2003).
- 43 Krogh A, Larsson B, von Heijne G, Sonnhammer ELL. Predicting transmembrane protein topology with a hidden Markov model: application to complete genomes. *J. Mol. Biol.* 305(3), 567–580 (2001).
- 44 Eisenhaber B, Schneider G, Wildpaner M, Eisenhaber F. A sensitive predictor for potential GPI lipid modification sites in fungal protein sequences and its application to genome-wide studies for *Aspergillus nidulans*, *Candida albicans*, *Neurospora crassa*, *Saccharomyces cerevisiae* and *Schizosaccharomyces*. *J. Mol. Biol.* 337(2), 243–253 (2004).
- 45 Bologna G, Yvon C, Duvaud S, Veuthey AL. N-terminal myristoylation predictions by ensembles of neural networks. *Proteomics* 4(6), 1626–1632 (2004).
- 46 Maurer-Stroh S, Eisenhaber F. Refinement and prediction of protein prenylation motifs. *Genome Biol.* 6(6), R55 (2005).
- 47 Petersen TN, Brunak S, von Heijne G, Nielsen H. SignalP 4.0: discriminating signal peptides from transmembrane regions. *Nat. Methods* 8(10), 785–786 (2011).
- 48 Goldberg T, Hecht M, Hamp T *et al.* LocTree3 prediction of localization. *Nucleic Acids Res.* 42(W1), 1–6 (2014).
- 49 Zambuzzi-Carvalho PF, Tomazett PK, Santos SC *et al.* Transcriptional profile of *Paracoccidioides* induced by oenothien B, a potential antifungal agent from the Brazilian Cerrado plant *Eugenia uniflora*. *BMC Microbiol.* 13, 227 (2013).

- 50 Maizels RM, Blaxter ML, Robertson BD, Selkirk ME. *Parasite Antigens, Parasite Genes: A Laboratory Manual for Molecular Parasitology*. Cambridge University Press, Cambridge, UK (1992).
- 51 Sagaram US, Shaw BD, Shim WB. *Fusarium verticillioides* *GAPI*, a gene encoding a putative glycolipid-anchored surface protein, participates in conidiation and cell wall structure but not virulence. *Microbiology* 153(9), 2850–2861 (2007).
- 52 Renshaw H, Vargas-Muñiz JM, Richards AD, Asfaw YG, Juvvadi PR, Steinbach WJ. Distinct roles of myosins in *Aspergillus fumigatus* hyphal growth and pathogenesis. *Infect. Immun.* 84, IAL.01190–IAL.01115 (2016).
- 53 Knauer R, Lehle L. The oligosaccharyltransferase complex from yeast. *Biochim. Biophys. Acta* 1426(2), 259–273 (1999).
- 54 Ruiz-Canada C, Kelleher DJ, Gilmore R. Cotranslational and posttranslational N-glycosylation of polypeptides by distinct mammalian OST isoforms. *Clin. Lymphoma.* 9(1), 19–22 (2009).
- 55 Wang N, Seko A, Takeda Y, Kikuma T, Ito Y. Cooperative role of calnexin and TigA in *Aspergillus oryzae* glycoprotein folding. *Glycobiology* 25(10), 1090–1099 (2015).
- 56 Goto M. Protein O-glycosylation in fungi: diverse structures and multiple functions. *Biosci. Biotechnol. Biochem.* 71(6), 1415–1427 (2007).
- 57 Ouyang H, Luo Y, Zhang L, Li Y, Jin C. Proteome analysis of *Aspergillus fumigatus* total membrane proteins identifies proteins associated with the glycoconjugates and cell wall biosynthesis using 2D LC-MS/MS. *Mol. Biotechnol.* 44(3), 177–189 (2010).
- 58 Szopinska A, Degand H, Hochstenbach JF, Nader J, Morsomme P. Rapid response of the yeast plasma membrane proteome to salt stress. *Mol. Cell. Proteomics* 10(11), M111.009589 (2011).
- 59 Kanetsuna F, Carbonell LM. Cell wall glucans of the yeast and mycelial forms of *Paracoccidioides brasiliensis*. *J. Bacteriol.* 101(3), 675–680 (1970).
- 60 San-blas G. The cell wall of fungal human pathogens: its possible role in host-parasite relationships dermatophytes. *Young* 184(Ivic), 159–184 (1982).
- 61 Preechasuth K, Anderson JC, Peck SC, Brown AJP, Gow NAR, Lenardon MD. Cell wall protection by the *Candida albicans* class I chitin synthases. *Fungal Genet. Biol.* 82, 264–276 (2015).
- 62 Whitters EA, Cleves AE, McGee TP, Skinner HB, Bankaitis VA. SAC1p is an integral membrane protein that influences the cellular requirement for phospholipid transfer protein function and inositol in yeast. *J. Cell Biol.* 122(1), 79–94 (1993).
- 63 Longo LVG, Nakayasu ES, Gazos-Lopes F *et al.* Characterization of cell wall lipids from the pathogenic phase of *Paracoccidioides brasiliensis* cultivated in the presence or absence of human plasma. *PLoS ONE* 8(5), e63372 (2013).
- 64 Matthieu JM, Quarles RH. Quantitative scanning of glycoproteins on polyacrylamide gels stained with periodic acid-schiff reagent (PAS). *Anal. Biochem.* 55(1), 313–316 (1973).
- 65 Shaw BD, Hoch HC. The pycnidiospore of *Phyllosticta ampellicida*: surface properties involved in substratum attachment and germination. *Mycol. Res.* 103(7), 915–924 (1999).
- 66 Fujiki Y, Hubbard AL, Fowler S, Lazarow PB. Isolation of intracellular membranes by means of sodium carbonate treatment: application to endoplasmic reticulum. *J. Cell Biol.* 93(1), 97–102 (1982).
- 67 Molloy M, Herbert B, Slade M. Proteomic analysis of the *Escherichia coli* outer membrane. *Eur. J.* 2881, 1–11 (2000).
- 68 Cabezón V, Llama-Palacios A, Nombela C, Monteoliva L, Gil C. Analysis of *Candida albicans* plasma membrane proteome. *Proteomics* 9(20), 4770–4786 (2009).
- 69 Parente AFA, Bailão AM, Borges CL *et al.* Proteomic analysis reveals that iron availability alters the metabolic status of the pathogenic fungus *Paracoccidioides brasiliensis*. *PLoS ONE* 6(7), e22810 (2011).
- 70 Carman GM, Han G-S. Regulation of phospholipid synthesis in *Saccharomyces cerevisiae* by zinc depletion. *Biochim. Biophys. Acta* 1771(3), 322–330 (2007).
- 71 Iwanyszyn WM, Han G-S, Carman GM. Regulation of phospholipid synthesis in *Saccharomyces cerevisiae* by zinc. *J. Biol. Chem.* 279(21), 21976–21983 (2004).
- 72 Zhang B, Yu Q, Jia C *et al.* The actin-related protein Sac1 is required for morphogenesis and cell wall integrity in *Candida albicans*. *Fungal Genet. Biol.* 81, 261–270 (2015).
- 73 MacDiarmid CW, Milanick MA, Eide DJ. Biochemical properties of vacuolar zinc transport systems of *Saccharomyces cerevisiae*. *J. Biol. Chem.* 277(42), 39187–39194 (2002).
- 74 Varki A. Biological roles of oligosaccharides: all of the theories are correct. *Glycobiology* 3(2), 97–130 (1993).
- 75 Albrecht A, Felk A, Pichova I *et al.* Glycosylphosphatidylinositol-anchored proteases of *Candida albicans* target proteins necessary for both cellular processes and host-pathogen interactions. *J. Biol. Chem.* 281(2), 688–694 (2006).
- 76 Mora-Montes HM, Bates S, Netea MG *et al.* Endoplasmic reticulum alpha-glycosidases of *Candida albicans* are required for N glycosylation, cell wall integrity, and normal host-fungus interaction. *Eukaryot. Cell* 6(12), 2184–2193 (2007).
- 77 Hall RA, Bates S, Lenardon MD *et al.* The Mnn2 mannosyltransferase family modulates mannoprotein fibril length, immune recognition and virulence of *Candida albicans*. *PLoS Pathog.* 9(4), 13–17 (2013).
- 78 Burda P, Aebi M. The dolichol pathway of N-linked glycosylation. *Biochim. Biophys. Acta* 1426(2), 239–257 (1999).
- 79 Willer T, Brandl M, Sipiczki M, Strahl S. Protein O-mannosylation is crucial for cell wall integrity, septation and viability in fission yeast. *Mol. Microbiol.* 57(1), 156–170 (2005).
- 80 Zhou H, Hu H, Zhang L *et al.* O-mannosyltransferase 1 in *Aspergillus fumigatus* (AfPmt1p) is crucial for cell wall integrity and conidium morphology, especially at an elevated temperature. *Eukaryot. Cell* 6(12), 2260–2268 (2007).

- 81 Zhang L, Feng D, Fang W *et al.* Comparative proteomic analysis of an *Aspergillus fumigatus* mutant deficient in glucosidase I (AfCwh41). *Microbiology* 155(7), 2157–2167 (2009).
- 82 Wu C, Bird AJ, Winge DR, Eide DJ. Regulation of the yeast TSA1 peroxiredoxin by ZAP1 is an adaptive response to the oxidative stress of zinc deficiency. *J. Biol. Chem.* 282(4), 2184–2195 (2007).
- 83 Li Q, Abrashev R, Harvey LM, McNeil B. Oxidative stress-associated impairment of glucose and ammonia metabolism in the filamentous fungus, *Aspergillus niger* B1-D. *Mycol. Res.* 112(9), 1049–1055 (2008).
- 84 Gupta SK, Maggon KK, Venkitasubramanian TA. Effect of Zinc on tricarboxylic acid cycle intermediates and enzymes in relation to aflatoxin biosynthesis. *J. Gen. Microbiol.* 99(1), 43–48 (1977).
- 85 Buchwald P, Krummeck G, Rödel G. Immunological identification of yeast SCO1 protein as a component of the inner mitochondrial membrane. *Mol. Gen. Genet.* 229(3), 413–420 (1991).
- 86 Glerum DM, Shtanko A, Tzagoloff A. SCO1 and SCO2 act as high copy suppressors of a mitochondrial copper recruitment defect in *Saccharomyces cerevisiae*. *J. Biol. Chem.* 271(34), 20531–20535 (1996).
- 87 Ignatev A, Kravchenko S, Rak A, Goody RS, Pylypenko O. A structural model of the GDP dissociation inhibitor Rab membrane extraction mechanism. *J. Biol. Chem.* 283(26), 18377–18384 (2008).
- 88 Garrett MD, Zahner JE, Cheney CM, Novick PJ. GDI1 encodes a GDP dissociation inhibitor that plays an essential role in the yeast secretory pathway. *EMBO J.* 13(7), 1718–1728 (1994).
- 89 Corbin BD, Seeley EH, Raab A *et al.* Metal chelation and inhibition of bacterial growth in tissue abscesses. *Science* 319(5865), 962–965 (2008).
- 90 Vignesh KS, Figueroa JAL, Porollo A, Caruso JA, Deepe GS Jr. Granulocyte macrophage-colony stimulating factor-induced Zn sequestration enhances macrophage superoxide and limits intracellular pathogen survival. *Immunity* 39(4), 697–710 (2013).
- 91 Laskaris P, Atrouni A, Calera JA, Enfer C. Administration of zinc chelators improves survival of mice infected with *Aspergillus fumigatus* both in monotherapy and in combination with caspofungin. *Antimicrob. Agents Chemother.* 60(10), 5631–5639 (2016).
- 92 Ibrahim AS, Gebremariam T, French SW, Edwards JE Jr, Spellberg B. The iron chelator deferasirox enhances liposomal amphotericin B efficacy in treating murine invasive pulmonary aspergillosis. *J. Antimicrob. Chemother.* 65(2), 289–292 (2009).
- 93 Leal SM, Roy S, Vareechon C *et al.* Targeting iron acquisition blocks infection with the fungal pathogens *Aspergillus fumigatus* and *Fusarium oxysporum*. *PLoS Pathog.* 9(7), 1–16 (2013).
- 94 Zarembek KA, Cruz AR, Yuang C-Y, Gallin JI. Antifungal activities of natural and synthetic iron chelators alone and in combination with azole and polyene antibiotics against *Aspergillus fumigatus*. *Antimicrob. Agents Chemother.* 53(6), 2654–2656 (2009).